

AD-A008 489

PROCEEDINGS (SUPPLEMENT), AFCRL  
SCIENTIFIC BALLOON SYMPOSIUM (8TH),  
30 SEPTEMBER TO 3 OCTOBER 1974

Andrew S. Carten, Jr.

Air Force Cambridge Research Laboratories  
Hanscom Air Force Base, Massachusetts

2 December 1974

DISTRIBUTED BY:

**NTIS**

National Technical Information Service  
U. S. DEPARTMENT OF COMMERCE

Unclassified

SECURITY CLASSIFICATION OF THIS PAGE (When Data Entered)

REPORT DOCUMENTATION PAGE		READ INSTRUCTIONS BEFORE COMPLETING FORM								
1. REPORT NUMBER AFCRL-TR-74-0596	2. GOVT ACCESSION NO.	3. RECIPIENT'S CATALOG NUMBER								
4. TITLE (and Subtitle) PROCEEDINGS (Supplement), EIGHTH AFCRL SCIENTIFIC BALLOON SYMPOSIUM, 30 SEPTEMBER TO 3 OCTOBER 1974		5. TYPE OF REPORT & PERIOD COVERED Scientific. Biennial.								
7. AUTHOR(s) Andrew S. Carten, Jr., Editor		6. PERFORMING ORG. REPORT NUMBER SR No. 185								
9. PERFORMING ORGANIZATION NAME AND ADDRESS Air Force Cambridge Research Laboratories (LC) Hanscom AFB Massachusetts 01731		8. CONTRACT OR GRANT NUMBER(s)								
11. CONTROLLING OFFICE NAME AND ADDRESS Air Force Cambridge Research Laboratories (LC) Hanscom AFB Massachusetts 01731		10. PROGRAM ELEMENT, PROJECT, TASK AREA & WORK UNIT NUMBERS 62101F 6665/BTS000001								
14. MONITORING AGENCY NAME & ADDRESS (if different from Controlling Office)		12. REPORT DATE 2 December 1974								
		13. NUMBER OF PAGES 286								
		15. SECURITY CLASS. (of this report) Unclassified								
		15a. DECLASSIFICATION/DOWNGRADING SCHEDULE								
16. DISTRIBUTION STATEMENT (of this Report)  Approved for public release; distribution unlimited.										
17. DISTRIBUTION STATEMENT (of the abstract entered in Block 20, if different from Report)										
18. SUPPLEMENTARY NOTES  Received for publication 29 November 1974 Conference held at Hyannis, Massachusetts										
19. KEY WORDS (Continue on reverse side if necessary and identify by block number)  <table border="0"> <tr> <td>Balloons</td> <td>Balloon-borne experiments</td> </tr> <tr> <td>Hot-air balloons</td> <td>Balloon design</td> </tr> <tr> <td>Tethered balloons</td> <td>Balloon materials</td> </tr> <tr> <td>Powered balloons</td> <td>Stratospheric measurements</td> </tr> </table>			Balloons	Balloon-borne experiments	Hot-air balloons	Balloon design	Tethered balloons	Balloon materials	Powered balloons	Stratospheric measurements
Balloons	Balloon-borne experiments									
Hot-air balloons	Balloon design									
Tethered balloons	Balloon materials									
Powered balloons	Stratospheric measurements									
20. ABSTRACT (Continue on reverse side if necessary and identify by block number)  <p>This publication, in conjunction with the main volume, AFCRL-TR-74-0393, dated 21 August 1974, contains the papers presented at the Eighth AFCRL Scientific Balloon Symposium, 30 September to 3 October 1974, held at Hyannis, MA. The papers are grouped in accordance with the five symposium sessions: Powered Balloons, Tethered Balloons, Free Balloon Technology, Balloon-Borne Experiments, and Special Applications.</p>										

PRICES SUBJECT TO CHANGE

DD FORM 1 JAN 73 1473

EDITH

Reproduced by  
NATIONAL TECHNICAL  
INFORMATION SERVICE  
US Department of Commerce  
Springfield, VA. 22151

Unclassified

SECURITY CLASSIFICATION OF THIS PAGE (When Data Entered)

## **Preface**

The AFCRL Scientific Balloon Symposia have over the years become established as the principal forum for the exchange of ideas and technical information within the wide community of balloon systems users and developers. With the Eighth Symposium, the main body of the Proceedings was, for the first time, published as preprints instead of after-the-fact documentation. The reader's attention is directed, therefore, to AFCRL TR 74-0393, dated 21 August 1974, which contains the bulk of the papers presented at the Eighth Symposium. This supplemental volume, dated 2 December 1974, contains the papers received too late for inclusion in the preprints. The circumstance of late receipt in no way affects the technical excellence of the papers contained herein and the publication of this supplement fulfills a clearly established dissemination need.

The cooperation and assistance provided by the individual authors whose papers appear in this supplement are acknowledged with grateful appreciation.

## Contents

### 1. POWERED BALLOONS

HIGH ALTITUDE SUPERPRESSURED POWERED AEROSTAT (HASPA) F.J. Peirone and P.R. Wessel	9
POBAL-S SUPERPRESSURE POWERED BALLOON J.D. Beemer	41

### 2. TETHERED BALLOONS

A SUMMARY OF TETHERED LIGHTER THAN AIR DEVELOPMENT CONDUCTED BY THE RANGE MEASURE- MENTS LABORATORY W. H. Manning, Jr.	59
CAPTIVE STRATOSPHERIC BALLOONS R. Regipa	83
THE INTERACTION OF TETHERED AEROSTATS WITH ATMOSPHERIC ELECTRICITY T.A. Hall	93
DESIGN TRENDS OF FUTURE AEROSTAT SYSTEMS E. L. Crosby, Jr. and T.H. Yon, Jr.	109

### 3. FREE-BALLOON TECHNOLOGY

FREE BALLOON CAPABILITIES: A CRITICAL PERSPECTIVE J. F. Dwyer	123
THERMAL ANALYSIS OF LONG DURATION FLIGHT PACKAGES L.A. Carlson and P. M. Brandeberry	163



## Contents

BALLOON DESIGN J. L. Rand	175
BALLOON SYSTEM STRENGTH AND FAILURE ANALYSIS L. D. Webb	191
MATERIAL SELECTION FOR HIGH-ALTITUDE FREE FLIGHT BALLOONS J. B. Munson	211
TWELVE YEARS AFTER THE FIRST LAUNCHING: OPERATIONAL ACTIVITIES OF CNES IN STRATOSPHERIC BALLOONS M. Rougeron	241
UPDATING FREE BALLOON TECHNOLOGY J. P. Nelson	259

### 4. BALLOON-BORNE EXPERIMENTS

Note: All papers from Session 4 are contained in the main volume,  
AFCRL-TR-74-0393, dated 21 August 1974.

### 5. SPECIAL APPLICATIONS

PRESSURE HOT AIRSHIP DESIGN AND PERFORMANCE J. B. Hebel and J. F. Hebel	273
--	-----

**Session 1**  
**Powered Balloons**

**Arthur O. Kern, Chairman**  
**Air Force Cambridge Research Laboratories**

#### Contents

1. Introduction	10
2. Baseline Configuration	11
3. Test Plans	31
4. Field Functional	34
5. Launch	35
6. Flight Plans	37

## High Altitude Superpressured Powered Aerostat (HASPA)\*

F.J. Petrone and P.R. Wessel  
Naval Ordnance Laboratory  
White Oak, Silver Spring, Maryland

### Abstract

A demonstration program is now underway in which the feasibility of a High Altitude Super-pressured Powered Aerostat (HASPA) will be determined. Basically the HASPA is an unmanned platform that would operate continuously at high-altitude for long periods of time and maintain an assigned station through powered maneuverability taking advantage of the low wind fields between the stratospheric and tropospheric winds. HASPA would serve as an extended duration airborne platform from which sensors or communication relay links can be operated. The present 32 month time frame of this program will include four demonstration flights (one unpowered and three powered) with expected flight durations of from a few days to over one month. This presentation will emphasize present flight objectives, vehicle design status, and potential problem areas with the proposed resolutions.

---

\*This program is sponsored by the Naval Electronic Systems Command.

## I. INTRODUCTION

The HASPA demonstration program is an experiment to determine the feasibility of using a High-Altitude Superpressured Powered Aerostat as an extended duration station-keeping platform.

Such vehicles face critical design requirements that are appreciably different than those encountered by the conventional low altitude airships. They also can provide capabilities not readily achieved by other systems. Operating at an altitude near 70,000 feet the mission capability of the system can be likened to that of a low altitude stationary satellite and many aspects of space technology are applicable.

The contractors for the development of HASPA are the Denver Division of the Martin Marietta Company and the G. T. Schjeldahl Company whose joint effort has played a major part in arriving at the present system baseline design.

The operating altitude of 70,000 feet is not purely a matter of choice. One of the most dominant features of the atmosphere is the existence of a minimum wind velocity near that altitude. It is purely fortuitous that the magnitude of the winds remains low enough at most times such that they can be overcome by realistic system designs. It is also fortunate that this altitude is well above that used for most aircraft operations. Information pertaining to the spatial and temporal extent of the minimum wind region and to the characteristics of the wind within that region is important to the success of the entire concept.

At 70,000 feet altitude the lift capability of either helium or hydrogen gas is approximately four pounds per thousand cubic feet. Thus any system designed for operation at such altitudes must accept weight constraints comparable to those faced in space. This requires hull materials with extremely high strength to weight ratios, power systems with very high energy densities, and command and control systems utilizing advanced concepts. It is evident that such vehicles must be unmanned, being unable to carry the weight of life support systems, which further implies the need for RPV (remotely piloted vehicle) technology.

The launch and recovery of vehicles of this nature will draw upon techniques common to high-altitude balloons. Once at altitude the vehicle will assume an aerodynamic shape as a result of excess

A thrust ring which supports the propulsion truss is laced to the aft of the hull. A two-motor system, which has increased reliability and efficiency over a single motor, will supply the necessary range of shaft horsepower to propel the HASPA in the required 15 to 25 knot regime.

The propeller will be a two (2) bladed configuration with a diameter about 30 feet and an estimated thrust conversion efficiency of 75 percent. Dynamic control in pitch and yaw will be achieved by gimbaling the propeller. The autopilot, actuators, and the gimbal system will respond to the inputs of the navigation computer or a remote command which will call for a desired heading. The mix of heading, airspeed, attitude, and altitude sensors is selected on the basis of Loran or Omega inputs to the navigation computer. This mix would be reduced if an inertial platform is incorporated since certain inputs to the computer could be achieved by the inertial system in lieu of the individual sensors.

The uncertainty in the drag coefficient, which ranges from 0.03 (theoretically derived on the basis of frontal area) to 0.06 (based on flight test data) produces a major uncertainty in the prime power requirement which can vary over a wide range as shown in Table 3.

Three different power sources will be used for the three scheduled powered flights -- AgO - Zn Primary Batteries, a ( $H_2 - O_2$ ) primary fuel cell and a secondary battery/solar array system. The selection of these power sources was based on cost, availability and flight requirements.

#### 2.1 Aerostat Envelope Material

The envelope material characteristics which are of primary importance in order that a HASPA will operate at a 70,000-foot altitude for a 30 day duration are:

- (1) Integrity - this property includes tensile strength, elastic modulus, tear strength, puncture resistance, shear stiffness and permeability.
- (2) Durability - exemplified by abrasion flexure resistance and weatherability.
- (3) Weight - the maximum material weight is dictated by the required payload weight, flight altitude, and maximum balloon volume.

Table 3. Prime Power Required As A Function Of  $C_D$  And Motor Type

Case #	Prime Power KW	Static Inverter Eff.	Motor Eff.	Motor Output HP	Speed Reducer Eff.	Shaft HP	Prop Eff.	Thrust HP	Air Speed (KTS)
1. $C_D = 0.03$	0.32	—	.80	0.35	.95	0.33	.75	0.25	15
1a.	1.56	—	—	1.68	—	1.6	—	1.2	25
1b.	0.44	.85	.7	0.35	.95	0.33	.75	0.25	15
	1.84	—	.8	1.68	—	1.6	—	1.2	25
2. $C_D = 0.044$	0.51	—	.80	0.55	.95	0.52	.75	0.39	15
2a.	2.3	—	—	2.47	—	2.35	—	1.76	25
2b.	0.70	.85	.7	0.55	.95	0.52	.75	0.39	15
	2.71	—	.8	2.47	—	2.35	—	1.76	25
3. $C_D = 0.06$	0.70	—	.8	0.75	.95	0.71	.75	0.53	15
3a.	3.14	—	—	3.37	—	3.2	—	2.4	25
3b.	0.94	.85	.7	0.75	.95	0.71	.75	0.53	15
	3.70	—	.8	3.37	—	3.2	—	2.4	25

NOTE: AT APPROXIMATELY 67,000 FEET

- a. DC Motor
- b. AC Motor

(4) Thermal surfaces - the absorptivity and emissivity properties of the material must be such that no significant temperature change occurs in the balloon skin, and hence, helium temperature such that the balloon super-pressure would drop below that required for structural integrity or exceed the allowable stress limits of the skin.

The candidate materials considered were Mylar and Emblem films, Mylar-Dacron and Mylar-Kevlar Biaxial Weave composite laminates, and Mylar-Kevlar Triaxial Weave composite laminates.

#### 2.1.1 MATERIAL INTEGRITY

In the preliminary structural analysis the maximum stress from static and dynamic forces expected in the hull is 60 lb/in. This analysis included a determination of loads, stresses, deflected shape, and other characteristics affecting the structural integrity of the aerostat system. The specific items investigated included internal pressure requirements, attachments for equipment bay and propulsion system, and hull material stresses. The selected material must withstand a long term dead load of  $1.5 \times 60$  lb/in or approximately 90 lb/in, where the total "safety factor" 1.5 has been proven valid on tethered aerostats such as the G. T. Schjeldahl Company 250 CBV. This total "safety factor" is the product of a number of strength degradation factors shown in Table 4. The ultimate strength of a number of candidate materials as a function of their weight per square yard is shown in Figure 2. Unfortunately, for long duration balloon flights the ultimate material strength is not a valid parameter for material selection because all plastic films show some degree of creep with long term loading. Therefore, the long

Table 4. Strength Degradation Factors

o Non-homogeneous material	1.05
o Seals	1.1
o Attachments and stress concentrations	1.1
o Fabrication errors	1.05
o Handling and Aging	<u>1.1</u>
Total Degradation Factor	1.5

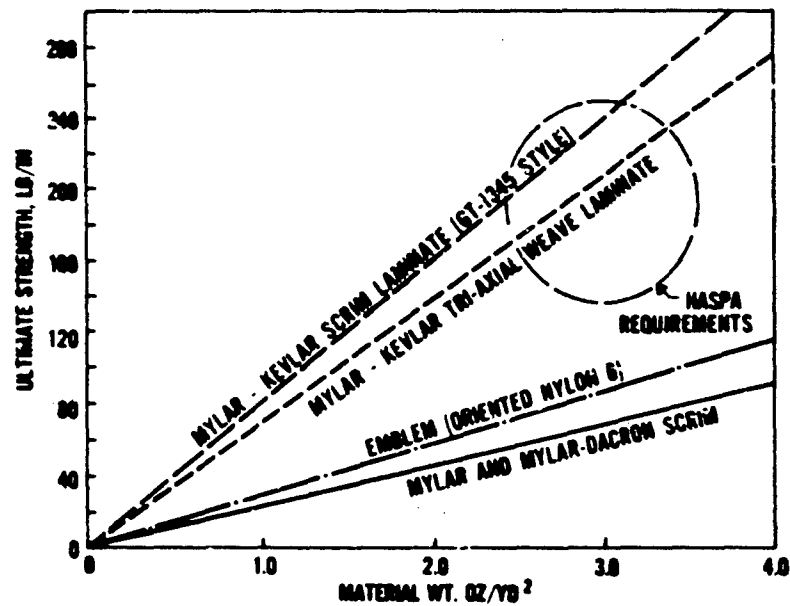


Figure 2. Ultimate Strength of Candidate Materials

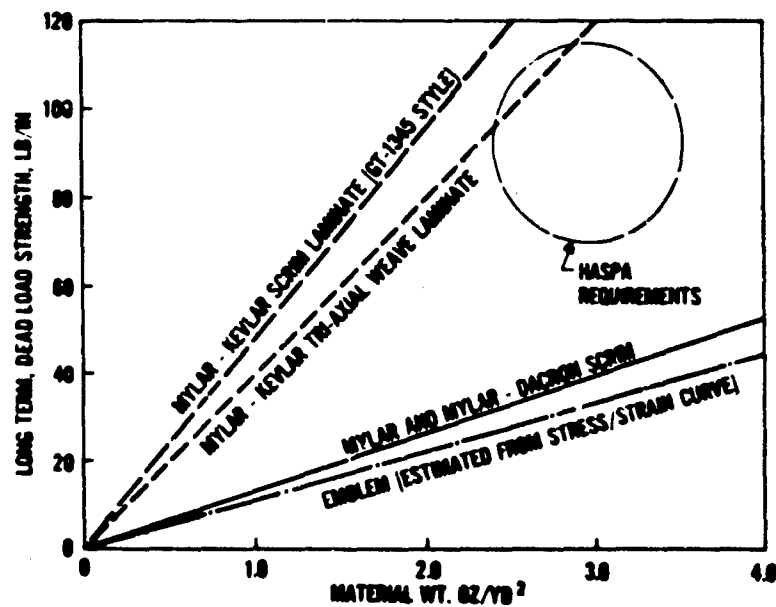


Figure 3. Dead Load Strength of Candidate Materials



term dead load strength, which is defined as the maximum dead load at which the material does not fail over the required duration, must be used as the valid parameter for selection of the aerostat material. These results are included in Figure 3 where the strengths shown for the Mylar-Kevlar laminate are derived from the strength to weight ratio of GT-1345 which is 56 percent Kevlar by weight. The effect of varying the percentage of Kevlar in the composite is shown in Figure 4. Since at least one mil of Mylar should be used to provide an adequate helium barrier, only composites above the dotted line are possibilities.

The results of tear testing are shown in Table 5. Although the materials used in these tests were not equivalent with respect to tensile strength and weights, the magnitude of the difference between unsupported films and scrim reinforced films is obvious. For an open weave scrim, the puncture resistance of the unsupported film and the composite is the same. However, the probability of tear propagation from a puncture is again a function of the tear strengths shown in Table 5.

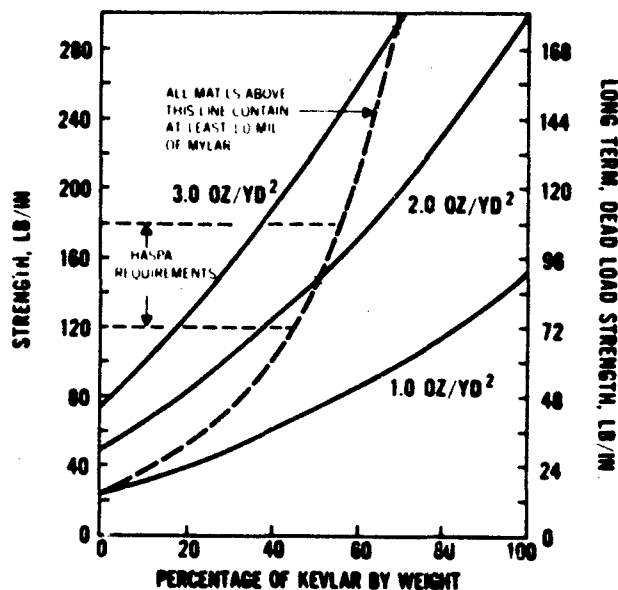


Figure 4. Kevlar-Mylar Composite Efficiency

Table 5. Tear Test Results

Material	Tear Strength (typical)
Mylar	0.033 lbs
Emblem	0.055 lbs
Mylar - Dacron Scrim	75.0 lbs
Mylar - Kevlar Scrim	110.0 lbs

Shear stiffness of the material is important. Material with low stiffness would permit large deflections in the hull under load. This deflection could show up as "swayback" in the hull due to the weight of the equipment bay. Even worse it could allow the hull to bend when steering loads are applied which would create problems with the control system. A number of shear tests have been conducted which indicate that any 0.5 mil or greater film or composite containing such a film will have sufficient shear stiffness. Tethered aerostats fabricated with two layers of 0.25 mil Mylar laminated to a loose plain weave fabric have been subjected to 80 knot winds at near sea level with no measurable deflections, which is over 100 times any loading anticipated in HASPA at 70,000 feet. Although tri-axial weave fabrics have in addition to shear stiffness a much higher shear strength than a regular orthogonal weave fabric, the hull is not exposed to shear stresses that threaten to fail the material in shear.

If at least 1.0 mil of any material such as mylar is used for the gas retention, the helium permeability is much less than 0.5 liter per square meter per day. Therefore, helium permeability should present no problems for the HASPA. Also, by laminating thin multiple layers of any gas retention material together to obtain the required thickness, the loss of gas because of "pinholes" is greatly reduced.

#### 2.1.2 MATERIAL DURABILITY

All of the candidate materials appear adequate in durability for the HASPA demonstration program. This is based on tests which determine the degradation of the material integrity properties when subjected to flexure and abrasion tests.

Weatherability over any specific duration can be definitely determined only by actual flight. Extensive data from superpressured Mylar balloon flights, which had an average life of over 100 days and some with durations of over two years, indicates that a 30-day life requirement is certainly feasible.

#### 2.1.3 MATERIAL WEIGHT

Since a restriction of  $1,000,000 \text{ ft}^3$  was placed on the volume of the demonstration HASPA, a maximum material weight is established. Thus, the maximum lift at 70,000 ft is 3800 lb from which the sub-systems weight (1640 lb) and the fin weight (~25 percent of the hull weight) must be subtracted to obtain the net weight available for material. This net weight is then divided by the calculated hull area (7700 square yards) to obtain the maximum possible material weight which is approximately  $3.5 \text{ oz/yd}^2$ .

#### 2.2 Thermal Surfaces

Superheat is defined to include the full temperature excursion of the aerostat. The superheat functions as the determinant of the superpressure only, within the limits that the pressure maintains the aerostat shape and does not exceed the burst strength of the hull material. Accurate prediction of the super temperature is a dominant factor in design since the minimum fabric hull strength required for the superheat could exceed that for all other imposed static or dynamic forces.

The prediction of the balloon temperature is subject to considerable uncertainty because of the complex interactions of direct solar radiation, reflected solar radiation and the earth's albedo. This analysis is further complicated due to the variation between the day and night environments. Figure 5 shows a typical heat transfer model demonstrating the complexity of the analysis as each of the heat flux values must be determined for each application.

As the HASPA design is developed, a computer program will provide balloon temperature estimates. Available data is adequate to provide the necessary computer inputs to predict mean values, extreme limits, and the probability of specific deviations from the mean values.

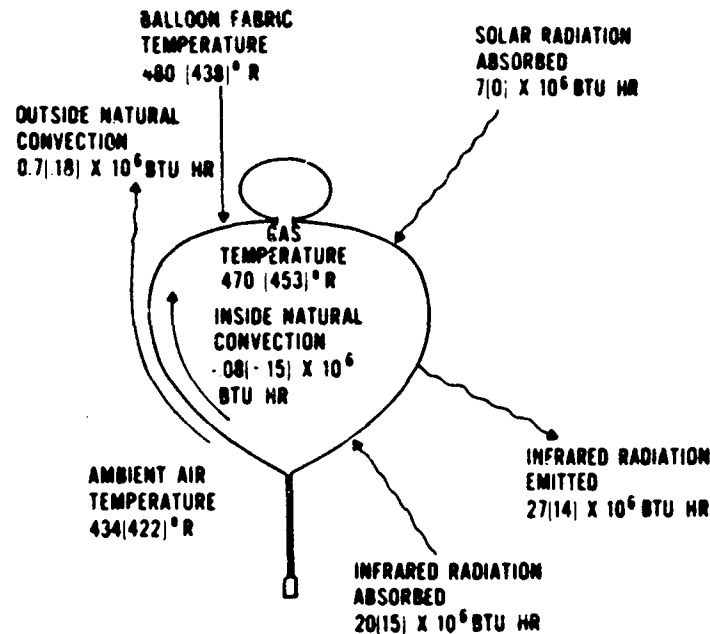
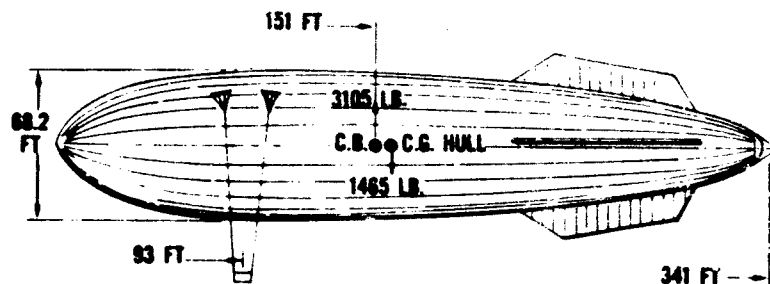


Figure 5. Heat Transfer Model of a Typical Floating Balloon System  
 XXX = Daylight Values, (XXX) = Nighttime Values

### 2.3 Aerostatics

The shape of HASPA will be that of a Navy Class C airship with a fineness ratio of 5:1. This shape has been previously extensively used and has been mathematically defined. Thus the volume, surface area, center of gravity (CG), center of buoyancy (CB), and inertia of the hull and enclosed gas can be accurately calculated with an existing computer program. The patterns used in the manufacture of the aerostat are defined using another existing computer program.

The aerostatic balance of the aerostat and attached components is critical to its free flight operation. For the system to float at a zero degree angle of attack the components must be located such that the system center of gravity is at the same longitudinal location as the CB. The theoretical CG and CB of the hull are shown in Figure 6. With a 1270 lb equipment bay located approximately as shown in the figure the system CG and CB are aligned. During the design and fabrication of the HASPA an accurate account of weights will be maintained in order that the attached component locations can be accurately determined for the first flight. Previous tethered



NOTE: VOLUME =  $8 \times 10^5$  CU FT

Figure 6. Configuration Parameters

aerostat experience has shown that this technique provides sufficient accuracy necessary to meet the flight requirements.

#### 2.4 Propulsion

The present baseline propulsion configuration consists of a large diameter propeller, gear train, electric motors, and a power control system. Thrust control, necessary to maintain the vehicle position, is accomplished by modulating the motor input. An inverter will convert the dc power to the necessary ac voltage and frequency required by the motor system. Two inverter designs are possible -- one capable of providing a continuously variable voltage and frequency, the other providing a discrete pair of voltages and frequencies for both top speed and cruise speed operation. At this time the latter design is selected on the basis of lower complexity and cost.

##### 2.4.1 PROPELLER DESIGN

Previous investigations have indicated that a propeller design with an efficiency of 75 percent is feasible in the required flight environment. The achievement of this high propeller efficiency is essential for the long endurance requirements where the available propulsion design must consider the aerodynamic qualities of blade sections at low Reynolds number. In this regime, high efficiencies are achieved with large diameter propellers according to the momentum theory. The necessity of a practical propeller weight places a constraint on the propeller size. When operating at an altitude of

70,000 feet, the density ratio is very low, 0.058. A large diameter propeller is necessary to achieve the required thrust for this very low density ratio. Coupled with a very low density ratio is a low coefficient of viscosity which together leads to extremely low values of Reynolds number. The Reynolds number for a propeller blade with a one foot chord is approximately  $1.4 \times 10^5$ . At this low Reynolds number, to achieve high lift/drag ratios, airfoils other than those employed with normal propeller sections are required. The available low Reynolds number data on airfoil sections indicates that lift/drag ratios of the order of 30 can be expected at the present time.

Preliminary investigations indicate that a 30 foot diameter, fixed pitch propeller with a blade chord of approximately 15 inches operating between 60 and 160 rpm can attain the required propeller efficiency under flight conditions. The estimated shaft power necessary to drive the propeller is shown in Figure 7 over the required range of altitudes and speeds and directly results from the thrust

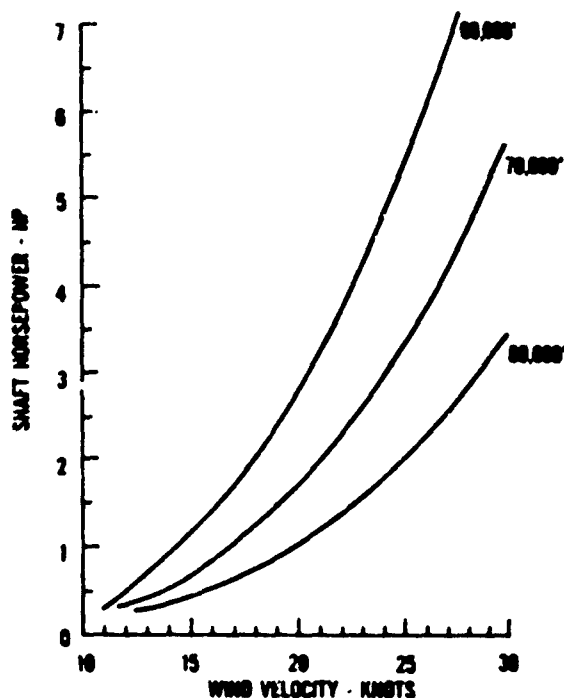


Figure 7. Estimated Propeller Power Requirements

requirements derived from the vehicle drag estimates shown in Figures 8, 9, 10 and 11.

Additional design requirements for the propeller are:

- lightweight
- impervious to cold to  $-70^{\circ}\text{F}$
- stable shape
- accurate contours and subtle progression of airfoils
- ideal twist, non-linear
- resistant to random damage
- good fatigue resistance
- ultra-violet resistance

The above requirements can be satisfied with blades made of a fiberglass shell with a rigid PVC foam plastic core. (See Figure 12.)

These materials are relatively non-sensitive to ultraviolet degradation. The solid foam core avoids all potential problems with moisture ingress and/or trapped air pockets with the great changes in ambient conditions.

A lightweight propeller hub using slim cross-section off the shelf bearings (Kaydon Reali-Slim), "G" diameter, could provide excellent support and low friction losses for the propeller. Bronze separators are used in these bearings and, with a light silicone lube, drag would be minimal at  $-70^{\circ}\text{F}$ .

Since performance data and test results on propellers to operate in the flight regime are not available, analytical studies are now being conducted to optimize the propeller design and performance. These studies include minimization of losses due to Reynolds number effects and further consideration of various hub and blade structural configurations in addition to the normal analytical determination of the propeller aerodynamic configuration. Performance and operational tests at the design temperature and density conditions will be conducted in an altitude test facility such as the 60-foot diameter Vacusphere at Langley.

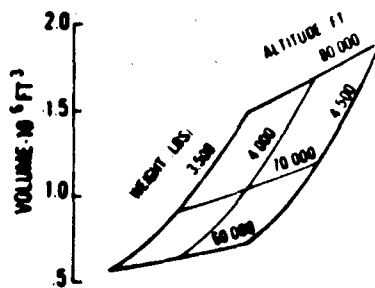


Figure 8. HASPA-Volume Determination

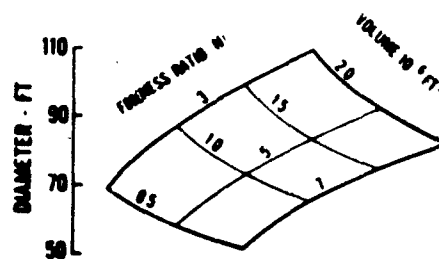


Figure 9. HASPA-Configuration Geometry

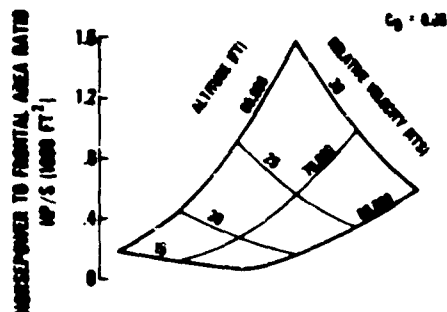


Figure 10. HASPA-Power/Frontal Area Ratio

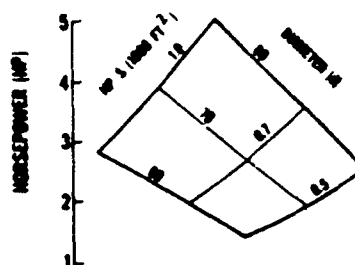


Figure 11. HASPA-Power Requirements

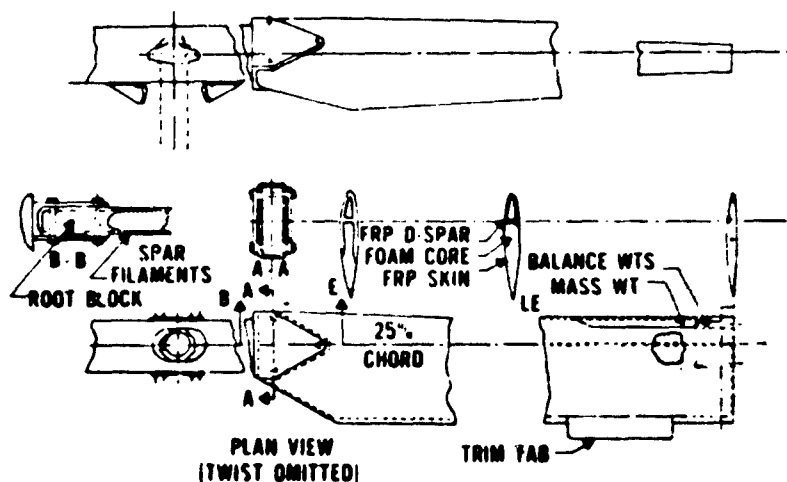


Figure 12. Typical Blade Structure

#### 2.4.2 ELECTRIC MOTORS

The baseline motors are alternating current, three phase, squirrel cage induction units. The primary characteristics of this type of motor are low starting torque, low starting current, and relatively constant speed from no load to full load. The primary consideration in the selection of an ac motor over a dc motor was to eliminate the use of brush/commutator action which can cause difficulties in the high altitude environment.

A highly reliable solid state inverter will convert the direct current primary supply voltage to the required alternating voltage



and frequency. The selected inverter design will either provide a continuously variable range of voltage and frequency or provide only pairs of voltage and frequency. The selection will be made at the end of the current conceptual design phase and will depend on operational considerations and cost.

Since the density at 70,000 feet is only 0.058 that at sea level, a thorough analysis must be made to determine if the motor and inverter will not exceed allowable operating temperature limits. Preliminary analysis indicates that the motor temperature can be kept within safe operating limits by simply increasing slightly the effective radiating area, but that the inverters which are located in the equipment bay would probably require a more complex heat rejection system.

#### 2.4.3 SPEED REDUCTION DRIVE - MOTOR TO PROPELLER

Off the shelf reduction drive candidates for a 5:1 speed reduction are: a chain and sprocket, a timing or "gear-belt" drive, and a planetary gear system. A V-belt drive is not as suitable because of erratic friction characteristics and excessive flex stresses at -70°F, and subsequent power losses. The chain drive would be slightly heavier and even with dry-lube, lubrication can be a problem. The timing belt has a low power to weight ratio, low profile, requires only torque bearing loading, has been used at -75°F satisfactorily, and, with the thin back steel or fiber glass reinforcement, has very low flexing power loss. Planetary systems are widely used in both space and aircraft applications and one has been selected for the base line design.

Additional trade-off studies are now being conducted to determine whether the drive belt/pulley or chain/sprocket drive would be preferable.

#### 2.4.4 BASELINE PROPULSION ASSEMBLY

The baseline propulsion assembly (Figure 13) is described as follows:

A fifteen (15) foot diameter tubular aluminum ring forms the base of the propulsion system truss. An intermediate (Figure 14) ring frame supports the two variable speed ac electric motor/reduction gear assemblies and the torque shaft. Tubular truss members support the propeller shaft gimbal assembly from the intermediate ring frame.

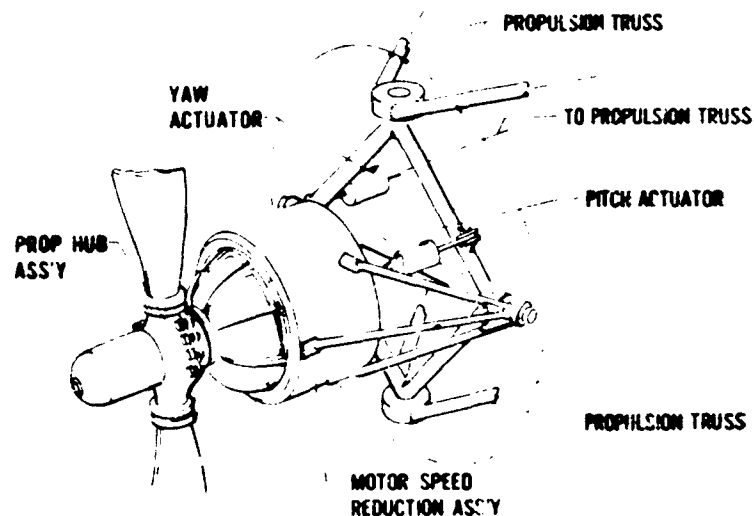


Figure 13. Propulsion System

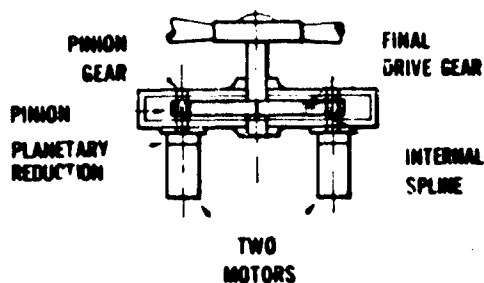


Figure 14. Speed Reducer

Torque is transmitted to the propeller shaft through a pair of pinion gears to a final drive gear. A propeller shaft bearing and thrust loads are provided for within the gimbal assembly. Screw-jack actuators controlling the pitch and yaw gimbaling of the propeller shaft are mounted to the gimbal support truss.

The thirty (30) foot diameter, two blade propeller may be gimballed  $\pm 20^\circ$  in pitch or yaw.

## 2.5 Autopilot and Flight Controls

Inputs to the control system will be generated by the HASPA Navigation System. This system will be based on any of three basic types (Loran-C, Inertial, or Omega) or combinations thereof and will be used to sense the HASPA drift rate and direction. Using this information and preprogrammed control laws, HASPA will be pointed into the wind and thrust will be applied to prevent HASPA from drifting down wind.

The control loops are visualized as being very slow (narrow bandwidth) because, if the maximum thrust vector deflection is 20 degrees the maximum control torque to inertia ratio about the pitch and yaw axes is in the range of 0.05 degrees per second<sup>2</sup> and the axial acceleration at full thrust is of the magnitude of .01G. The navigation and heading data will be supplied as sampled data at a frequency of one sample per second. Since the natural frequency of the vehicle in yaw will be about 0.02 hz, the sampling frequency of one sample per second or 50 samples per cycle should be very adequate from the standpoint of control dynamics. Simulations of the effect of sampling frequency are being conducted during the present Phase 0 study.

The requirement for pitch attitude control grows out of the fact that the thrust vector passes above the center of gravity and that as thrust is changed to assist in station keeping the moment of the thrust vector about the CG causes a change in pitch trim. This is compensated for in the control laws by commanding a change of the thrust vector in the pitch direction. The result will be that the thrust vector will slowly align itself through the center of rotation of the system. Therefore further changes in heading will only require small changes of thrust about the pitch axis. It may be possible that preflight prediction of the CG location and building a properly canted thrust vector into the design may permit elimination of the propeller pitch gimbal. This simplification would eliminate one source of mechanical failure and would thus tend to increase system reliability. On the other hand, eliminating the propeller degree of freedom about the pitch axis may require larger fins. This trade-off is the subject of another simulation program during Phase 0.

Preliminary design studies indicate that fins sized on the basis of the usual airship criteria of making their total exposed area equal to the maximum cross sectional area of the aerostat will provide

adequate damping and stability in roll. In our present configuration the maximum cross-sectional area is 3848 square feet. On the basis of 1/4 of this area per fin, each fin will be approximately 962 square feet. For a roll inertia of 218,000 slug feet squared, this fin size results in a damping coefficient of 0.1. This sampling, together with the system mass distribution, obviates the need for an active roll control system.

With regard to the altitude hold requirements, it is not anticipated that any active control will be required. This is possible because there is no consumable fuel exhausted overboard (including the product water from the fuel cells), no ballast, and the effects of diurnal variations in temperature result in changes of equilibrium of only about 200 feet.

In the design of the flight control system it will be necessary to carefully take into account the non-rigid characteristics of the HASPA. As the control laws call for deflection of the propeller gimbal there will be a tendency for the bag to deflect about the yaw and pitch axes. Thus the motion of the car (where the sensors are located) will tend to lag behind the gimbal deflection. In addition, other components of the relative motion between the car and the bag will have to be considered. Adequate computer simulations are necessary to be sure that the entire dynamic system is well integrated. Although the state-of-the-art in the airplane and missile autopilot field is well developed, this is not the case with lighter-than-air vehicles and so the control system design must be supported by analysis and simulation.

Computer simulation studies will include:

1. Steering Dynamics

A single plane simulation of the yaw control system will include the effects of data sampling. Existing simulation programs of Martin Marietta are available for this purpose. This simulation need not include the gyro instrument dynamics because the instruments have such high frequency response relative to the vehicle dynamics that the gyros will have no effect on system performance. The dynamics of the servo used to drive the propeller gimbal will be included.

2. Roll Control

A simulation of the roll dynamics is important since it will permit evaluation of roll damping as a function of fin area. This is important to choosing the minimum size fin area.

### 3. Three Axis "All-Up" Simulation

This simulation will include all three axes with appropriate cross coupling and is designed to confirm total system design before flight tests of the small scale vehicle are undertaken. The vehicle model will include structural feedback and the gyroscopic moment generated during rotation of the propeller around its gimbals. Disturbance inputs will include both winds and diurnal temperature cycles (the latter on a compressed time scale).

### 3. TEST PLANS

At this time only a preliminary development test program has been formulated. Early in the program a complete "Test Plan" will delineate all significant tests and will specifically include, on an individual test basis, objectives, methods and requirements.

Development tests primarily include engineering confidence level testing and debug integration testing. Flight test data are the correlated effects of many parameters which individually are of importance to the design engineer. For example the propulsion mechanism must be determined in a close to "in situ" environment in order that the inter-relationship between drag and propulsive efficiency can be determined in subsequent flight tests.

#### 3.1 Motor Tests

The motor configuration will be assembled and thoroughly tested in a controlled environment using a dynamometer in lieu of the actual propeller. These tests would include cooling, torque, speed control, and overall efficiency.

#### 3.2 Propeller Tests

The propeller will be tested in a controlled environment simulating its operating conditions. All up Qualification Tests in the normal sense of the word will not be conducted. The propeller will, however, be subjected to dynamic vibration and load tests at a level slightly ( $\sim 1.2$ ) higher than it will experience in the operational sense.

### 3.3 Materials and Aerostat Structure Tests

Only a minimum of material development testing is required because existing state-of-the-art material technology will be employed. Some testing will be required to optimize the characteristics of the final selected material. A scale model constructed of light-gauge Mylar will be fabricated to test the launch technique. This testing will be done indoors so that the model can be recovered and reused. No other development testing on the aerostat structure is anticipated.

### 3.4 Hot Bench Tests

Two series of Hot Bench Tests will take place. In the first, certain components will be tested under simulated environmental conditions such as pressure, temperature, and dynamic mechanical loads. At the completion of this series all components will be assembled and functionally tested.

### 3.5 Static Inflation Test (Indoors)

A static inflation test will be performed within a government supplied facility. This test is necessary to measure a number of critical aerostat properties. Some elements of this test are shown in Table 6.

The dimensional and geometry checks are to confirm the pattern designs and fabrication accuracy. The hull dimensions will be measured and used to calculate the actual volume of the hull to see if it deviates from the desired 800,000 ft<sup>3</sup>. Also the location of load supports and attachments will be verified. The hull growth with pressure will also be measured to correlate with the growth predicted by the structural analysis.

Table 6. Static Test Elements

- |   |
|---|
| <ul style="list-style-type: none"><li>o Dimension and geometry checks</li><li>o Leak check</li><li>o Structural (proof pressure) check</li><li>o Hardware interface check</li><li>o Possible weight and balance check</li></ul> |
|---|

Leak checking of a balloon of this size is not a straight forward process. If the hull is inflated to a fixed super-pressure and then monitored over a period of time, the changes in atmospheric pressure will cause changes in pressure much greater than those due to the maximum allowable leak rate. Therefore, it is almost impossible to detect a leakage component of the pressure changes. In past attempts to use this method on large balloons, temperature gradients were found both vertically and horizontally along the balloon making empirical corrections almost impossible.

The lift loss method used in tethered aerostats is not applicable as the HASPA cannot be filled with helium because the hull cannot handle the 60,000 lbs of buoyancy. Further, the cost of the 800,000 ft<sup>3</sup> of helium could most likely exceed the cost of the balloon.

The most likely leak check is the use of a helium or halogen leak detector. To use the helium leak detector, a small amount of helium is mixed with the air in the inflated hull. In a short period of time, the air and helium will stratify with the helium going to the top of the balloon. The top of the balloon can then be scanned with the leak detector by an operator on a "cherry picker". To check the whole balloon, it will be necessary to rotate the hull a few gores at a time until the full circumference has been checked. The halogen leak detector is used the same way except at the bottom of the balloon as the halogen gas (freon) is heavier than air.

The structural check will consist primarily of a proof pressure test to a level determined during the structural analysis. The hull will be held at this pressure long enough to verify that there is no material or seal creep. In addition to proof pressure testing, the hardware (primarily the equipment bay and propulsion system) will be attached to confirm fit and to verify that they do not cause unanticipated loading problems.

Since the center of buoyancy can only be located if the hull is full of a homogeneous lifting gas and to fill it with helium creates more lift than the hull can handle and an air-helium mixture will not be homogeneous, a weight and balance check during the static inflation test would not be successful. The center of gravity cannot be checked even if very sensitive scales are available; air currents in the hangar will create large enough forces on the aerostat to give erroneous results.

The most satisfactory method of weight and balance checks found to date consists of keeping meticulous records of all component weights and locations at time of assembly. The locations are verified during the dimensional checks. From this information the C.G. can be calculated to an estimated accuracy of six inches. The center of buoyancy will be recalculated using actual hull measurements to an estimated accuracy of six inches. If the worst combination of these errors occurs, it only changes the angle of attack of the aerostat by 1.5 degrees which can easily be overcome by the pitch control of the propulsion system.

At the time of design finalization there may be other secondary tests that become apparent and which will be incorporated into the static test plan at that time.

#### 1. FIELD FUNCTIONAL

The first time all elements of the system are grouped and tested as a system will be in the field. After completion of the Inflation test an all-up functional test will be conducted. This test will include a combined or marriage test of the entire system to the greatest degree possible and as such will include T/M, Tracking and control. Table 7 indicates the sequence of subtests that will be conducted.

Table 7. Test Sequence

- |   |
|---|
| <ul style="list-style-type: none"><li>o Wiring Ring-Out and Continuity</li><li>o Electric Power Checks</li><li>o Control Link Checks</li><li>o Beacon Verification</li><li>o T/M Verification</li><li>o Propulsion Verification</li><li>o Range/Mission Coordination Verification</li><li>o RFI/EMI Compatibility</li></ul> |
|---|



## 5. LAUNCH

To launch the HASPA in the limp state, the helium gas enters the end of the envelope away from the suspended load and other concentrated masses. This makes the envelope free to deploy as the gas expands during ascent.

The vertical motion of a free-flight balloon ascending under buoyant forces depends on the following:

Total System Weight - When in motion, this will include approximately one half the weight of the air displaced.

Free Lift - The difference between the system weight and the weight of the air displaced.

Aerodynamic Drag - The total effect of dynamic pressure acting over the projected area of the system plus frictional effects.

Thermodynamic "Drag" - The loss in lifting force due to the reduction in lifting gas temperature relative to the surrounding air due to expansion. The gas temperature depends on free and forced convective energy transfer, the solar and infrared radiation environment, and the thermal characteristics of the gas and balloon fabric.

For a balloon ascending in a limp-state, damage to the envelope fabric due to turbulent air flow sets the upper velocity limit. This limit depends on the envelope material strength approximately as follows:

Envelope Break Strength (lbs/in)	2-20	50-100
Maximum Ascent Velocity (fps)	15	30

Thermodynamic drag for a helium-filled balloon is small in the troposphere (below 40,000 feet) because the helium temperature drop is nearly matched by the natural atmospheric lapse rate. The relatively constant temperature in the stratosphere (40,000 to 80,000 feet) causes thermal drag forces on the ascending balloon to increase at a rate exceeding the decline in dynamic pressure. This has a damping effect on vertical motion.

The deployment sequence (Figure 15) would begin with layout of the hull, folded along its meridians, on a ground cloth at the launch site. The equipment bay and propulsion module would be locked together and mounted on the rear of the hull.

For the baseline balloon design with the equipment bay and propulsion module with a combined weight of 1565 pounds mounted at the rear of the hull, a minimum material break strength of 22 pounds per inch is required for an axially symmetric balloon envelope at launch which is about one third of the strength requirement estimated from pressure loading of the hull when fully deployed.

The lifting gas would be installed in the nose while the hull is restrained by a standard "launch arm" clutch in the same manner as a conventional free flight balloon.

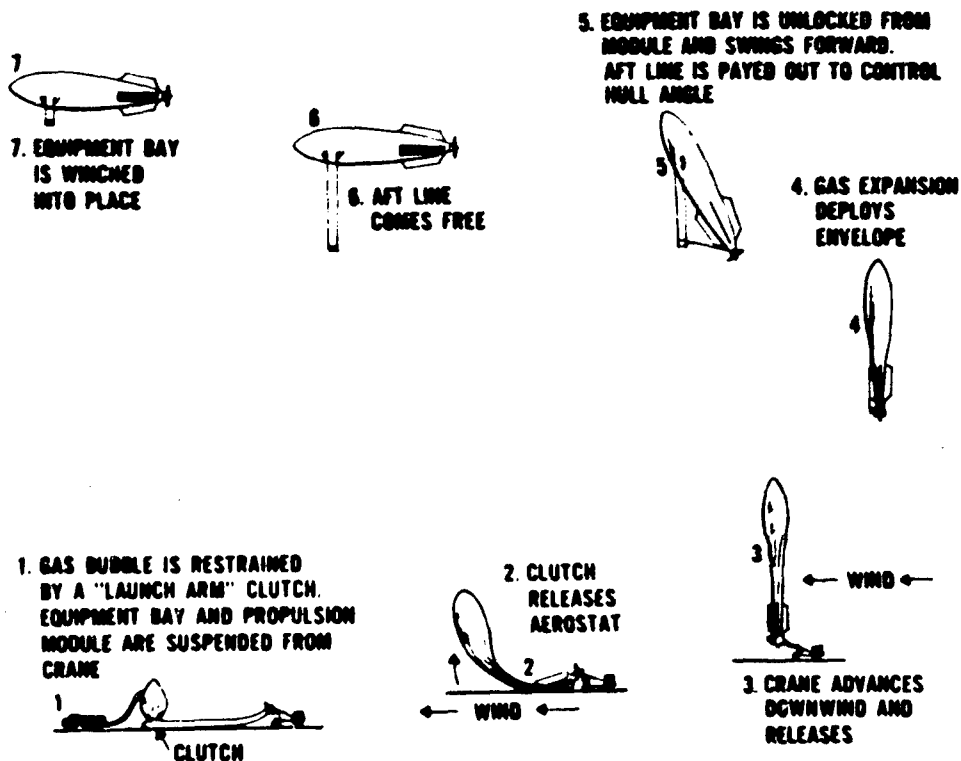


Figure 15. Launch Operation

The bay and propulsion module would be suspended from the boom of a mobile crane. After inflation and preflight checks are complete, the gas bubble would be released from the launch arm. The large projected area of the gas bubble prevents high accelerations as the balloon rises to a position over the suspended load. The payload would be positioned directly under the gas bubble by driving the crane downwind. At this point, the bay and module would be released and the system would accelerate to its terminal velocity of ascent. The operations are routine in winds up to 10 knots for free flight balloons carrying loads up to 3000 pounds. Total dynamic loading of the suspended load under this launch method is usually less than 2 g's.

As the balloon ascends, the lifting gas expands to fill the hull. Tension in the hull material would deploy the fins and fin guy lines to operating position. When the hull has become rigid, the equipment bay would be released from the propulsion module and winched toward the hull nose. A line extending back to the pod would control the hull rotation as the center of mass of the system is moved upward. When the equipment bay comes to rest at the confluence of the forward suspension lines, the system would be ready for operation.

## 6. FLIGHT PLANS

### 6.1 Unpowered Flight

Upon completion of the static test some of the equipment will be removed and replaced with mass and CG dummy hardware in preparation for the unpowered flight.

The purpose of the unpowered flight will be to verify the handling procedures, the launch technique, the ascent deployment sequence, the CG location, TM, tracking, command link, recovery system, and pilot/controller operations.

### 6.2 First Powered Flight

The objectives of the first powered test flight will be to substantiate the design of the propulsion and autopilot, measure uncertain aerodynamic design parameters, e.g., the drag coefficient, and evaluate the controller techniques. A primary battery power

Table 8. Primary Battery Power Source Characteristics

Weight:	830 lbs
Volume:	~9 cubic feet
Voltage:	30 volts
Amp. Hours:	2580

source whose characteristics are shown in Table 8 will be used which will allow a flight duration of at least 30 hours. At the conclusion of this test, the  $H_2-O_2$  fuel cell power source for the second flight will be interfaced in the recovered instrumentation bay.

#### 6.3 Second Powered Flight Test

The second powered test flight will confirm the station keeping ability and system structural integrity over a duration of ~7 days. This flight, which will be powered by an  $H_2-O_2$  fuel cell power source, will determine any environmental effects on the hull over a number of day/night cycles and demonstrate the feasibility of extended duration flight. Additional refinement in controller techniques will also be possible.

The fuel cell power system will utilize a 3 KW fuel cell stack, other related hardware, and cryogenic tanks which are residual from completed NASA programs. The General Electric Company will integrate the fuel cell power plant, designed from these components, with a suitable heat rejection system and product water container in a suitable recoverable equipment bay. The fuel cell power plant design parameters are shown in Table 9. At this time it appears that the heat rejection system will incorporate a heat exchanger with a fan to control the heat transfer rate. This method avoids the uncontrollable convection losses in a radiator which could result in freezing.

#### 6.4 Third Powered Flight

This test flight will use a solar cell array power source to support the maximum duration mission while maintaining the HASPA within the specified area of operation. Test objectives will include an evaluation of aging effects on the Aerostat material and long term leakage.

Table 9. Fuel Cell System Design Parameters

Nominal power rating:	1500 watts
Continuous overload:	100%
Design voltage:	28 volts nominal
Voltage range:	$\pm 10\%$ of nominal
Output control:	500 watts to 3000 watts
Fuel cell consumption	
at design point:	$\sim 0.95 \text{ lb/kWh}$
Maximum continuous load:	3000 watts
Minimum continuous load:	500 watts
Start-up time:	<15 minutes
Weight:	560 lb maximum including fuel cell module, control unit, coolant system, valves, regulators, plumbing, reactant system, heat rejection system, product water tank, and reactant supply

Wind and environmental variables will be monitored to determine the temporal extent of the minimum wind region and its characteristics.

Characteristics of the solar cell array/secondary battery power source are only preliminary at this time.

The weight of this power source is made up of two major components:

- a. The solar array panels which are appropriately distributed on the aerostat surface.
- b. The secondary battery pack and power conditioning which are contained in the recoverable instrumentation bay.

The weights estimated for a continuous 2100 watt power source which are conservatively based on estimates of solar panel efficiency and battery energy density would be as follows:

Solar Panels -  $\sim 170$  pounds - area  $\sim 1500$  square feet

Batteries and Power Conditioning -  $\sim 560$  pounds - volume  $\sim 7$  cubic feet.

#### **Contents**

1. Introduction	41
2. Parametric Analysis	43
3. System Design	51

## **POBAL-S Superpressure Powered Balloon**

**Jack D. Beemer  
Raven Industries, Inc.  
Sioux Falls, South Dakota 57101**

### **Abstract**

A fuel cell powered, high altitude, superpressure airship has been designed. Preliminary to designing this vehicle, a parametric analysis of various system concepts was performed. A discussion of the techniques used in the concept comparison analysis, of the results of the analysis, and of the system design is presented.

### **1. INTRODUCTION**

POBAL-S is a high altitude airship which has reached a preliminary design status. It was designed for the Air Force Cambridge Research Laboratories under a study contract which was awarded to Raven Industries, Inc. and included a review of power systems and system configurations, a parametric analysis to optimize the system design, and a preliminary design of a chosen concept. The goal was to arrive at a feasible and practical airship design which could meet the following performance requirements:

Duration - 7 days under continuous operation

Airspeed - constant at 8.2 m/s

Altitude\* - constant at 21,000 m

Payload Mass - 90 kg

Payload Power\*\* - continuous 500 W

The study was limited to aerodynamic superpressure balloons employing state of the art manufacturing technology. It was not limited to the performance goals, but was to cover a broader range of characteristics. Power sources which were reviewed were limited to solar cells, fuel cells, batteries, gas turbines, internal combustion engines, and advantageous wind fields. Other power sources were ruled out as not being practical.<sup>1</sup> The solar cell, fuel cell, gas turbine, and internal combustion engine concepts are depicted in Figure 1.

For the solar array powered concept the panels of cells, which are integrated to make the array, are placed on the surface of the balloon envelope and are located so that adequate power is delivered to the system for any conceivable sun angle.

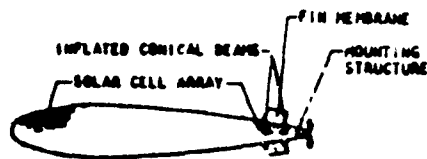
Major attention needs to be paid to the current/voltage characteristics of the cells at various angles to the sun. These characteristics are temperature dependent and under the configuration used here each panel would be operating at a different temperature because of radiation effects. The panels are connected either in series or parallel and are electrically integrated. Thus, they form an electrical energy source which will provide the required system power to operate the motor during the daylight hours and, at the same time, charge the batteries which are used for nighttime operation.<sup>2</sup>

The fuel cell powered concept is similar to the solar powered concept in that it provides electrical power to a gimbaled motor/propeller arrangement. The water generated by the fuel cell would be stored and not disposed of. Advantages of storing the water are that the fuel may be located at the point along the balloon axis which is required to attain horizontal equilibrium when the system is shut down and the system mass remains constant. The fuel cell concept also requires that the additional heat generated by the fuel cell be radiated. It may be possible to make use of this waste heat in controlling negative supertemperatures, but if one were to shut the system down at night then this heat would not be present. Thus, the system would have to be designed as if this capability were non-existent.

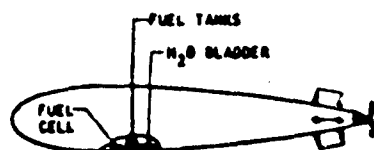
---

\*Originally the speed requirement was 10.3 m/s, but was changed during the course of the contract.

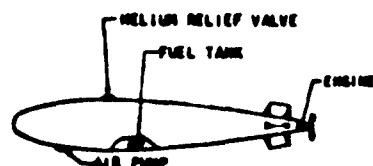
\*\*Originally there was no requirement for external electrical power to be furnished to the payload, but this was changed during the course of the contract.



**SOLAR ARRAY POWERED AIRSHIP**



**FUEL CELL POWERED AIRSHIP**



**GAS TURBINE OR INTERNAL COMBUSTION  
ENGINE POWERED AIRSHIP**

Figure 1. Vehicle Concepts

The gas turbine and internal combustion engine concepts are very similar. These power sources would actually be mounted on the gimbal arrangement and gimballed as with the electric motor for the electrical type systems. The fuel would be located beneath the center of buoyancy while the payload and electronics would be located near the front of the airship so that horizontal stability could be attained. It would not be possible to save the consumed fuel, and consequently a bailonet or pumping and valving scheme must be integrated into the system. One advantage of this type of system as compared to the fuel cell system is that the fuel can be stored in conventional type tanks. Considerations in final system design would have to be given to pumping the fuel from the storage area to the combustion chambers.

The concept of using only primary batteries for power, as anticipated, does not appear feasible except for very short duration missions. The advantages of such a concept lie in the simplicity of the design since all that is required is the batteries, mounted

somewhere in front of the system center of gravity, with power cables running back to an electric motor. This system then would be operating similar to the solar powered version during nighttime operation.

## 2. PARAMETRIC ANALYSIS

The parametric study was performed by using the HASKV (High Altitude Station Keeping Vehicle) computer program.<sup>3</sup> This program uses multiple iterative computer calculations which increase balloon size until buoyancy requirements, commensurate with hardware and propulsor mass requirements,



are met. The detail of the computer program is such as to account for weights of almost all components including such items as the electrical wiring, autopilot, propeller gimbaling mechanism, gore sealing tapes, number of adhesive layers in the gore film lamination, etc. The program capabilities include the following:

- (1) 57 input parameters (constants for parametric equations).
- (2) Natural shaped and class C shaped balloons.
- (3) Six different power sources.
  - (a) gas turbine
  - (b) Wankel engine
  - (c) diesel engine
  - (d) fuel cells
  - (e) solar cells
  - (f) batteries
- (4) Altitudes from 16,500 m to 30,000 m in 1500 m increments.
- (5) Altitude control for 1500 m or 3000 m excursions.
- (6) Wind speeds from 2.6 m/s to 15.4 m/s in 2.6 m/s increments.
- (7) Mission time variations.
- (8) Balloon diameters up to 100 m.

Figure 2 shows a simplified flow chart of the computer program.

A series of graphs have been developed which summarize the computer output of the parametric study.<sup>2,3</sup> By analyzing these graphs, comparisons can be made between power sources to determine the most optimum system for a given set of conditions. In addition to the power source comparisons, these graphs show the parameters a particular system is most sensitive to such as balloon material weight, coefficient of drag, and environmental parameters.

The graphs presented in Figure 3 compare the power and mass of basic systems. The mass versus duration and power versus duration curves appear similar because mass is proportional to (propulsion power)<sup>3/2</sup>.

Since system power and mass are excessively large for a solar cell system operating at 10.3 m/s true airspeed, it was decided to fly 5.1 m/s at night and 15.4 m/s during the day to give a 10.3 m/s average for 24 hours. Thus, solar cells are shown with  $V_N/V_D = 5.1/15.4 = .33$ . By flying at 5.1 m/s airspeed at night, the batteries (mass) required to operate the system, while the solar cells are inoperable, are reduced by a factor of 46, thus reducing the system mass considerably. The system mass crossover with the fuel cell system is between 5 and 6 days whereas on the power versus duration curve the crossover is at 18 days. This results because the power value furnished by the solar cell must be sufficient for 15.4 m/s operation whereas the other concepts operate continuously at 10.3 m/s.

On these base data curves the charge-discharge cycles for the batteries have been considered; and consequently, the solar cell power and mass requirements

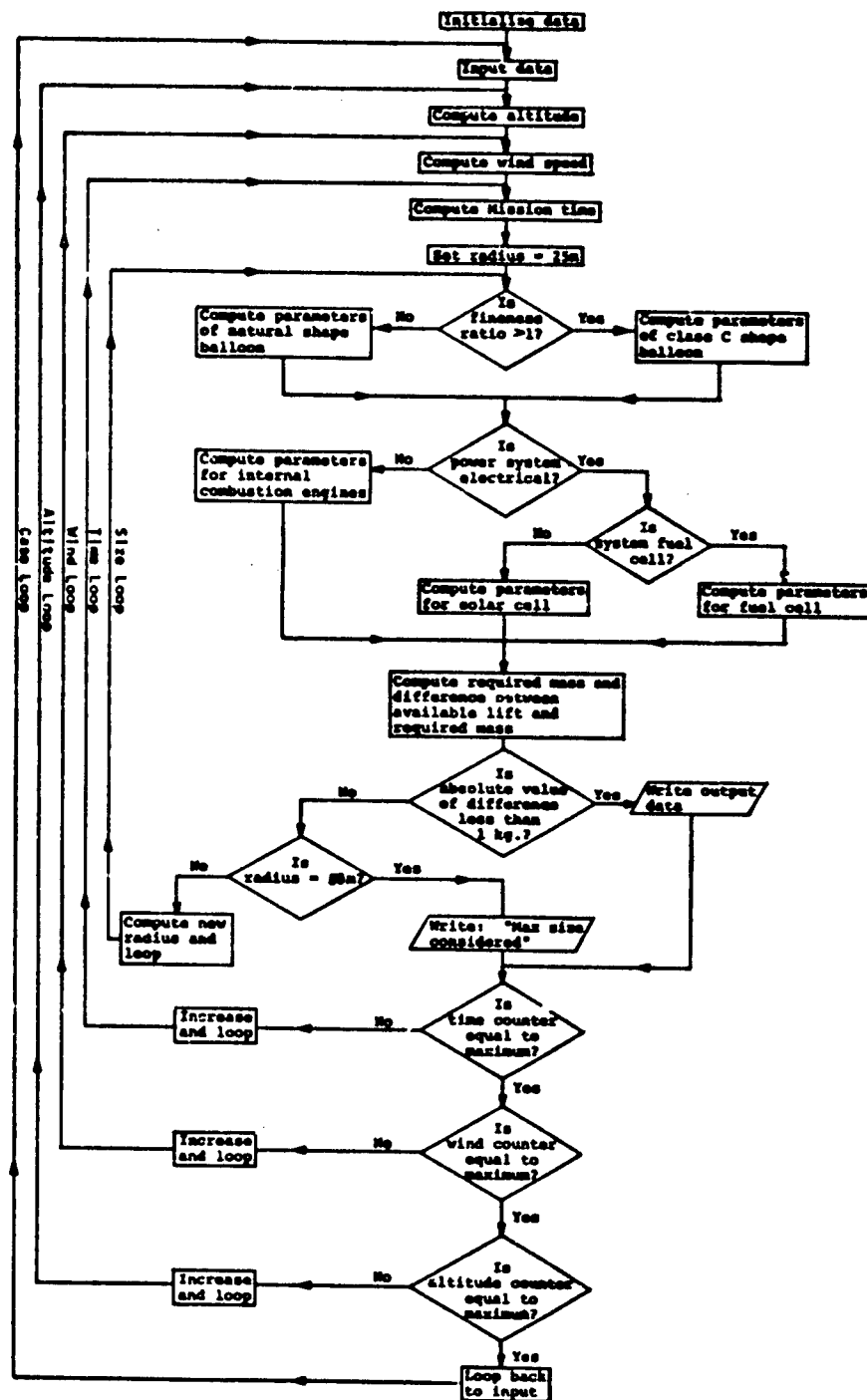
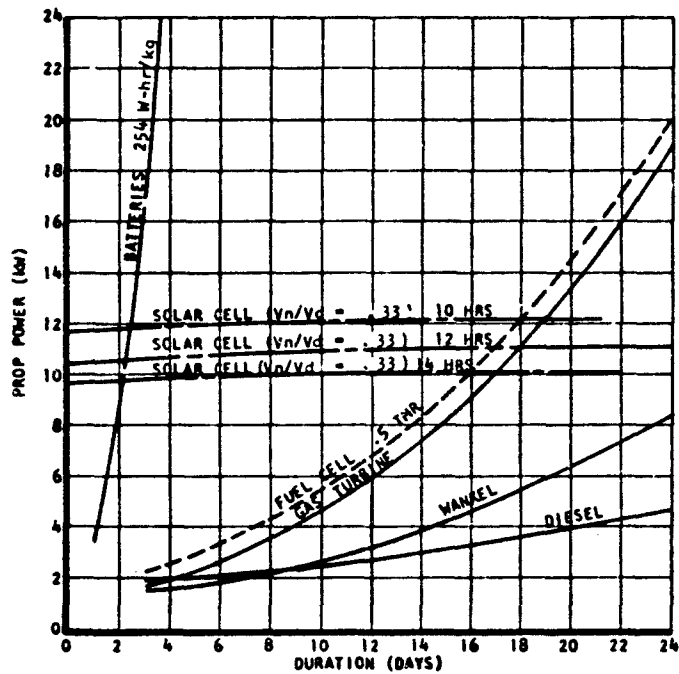
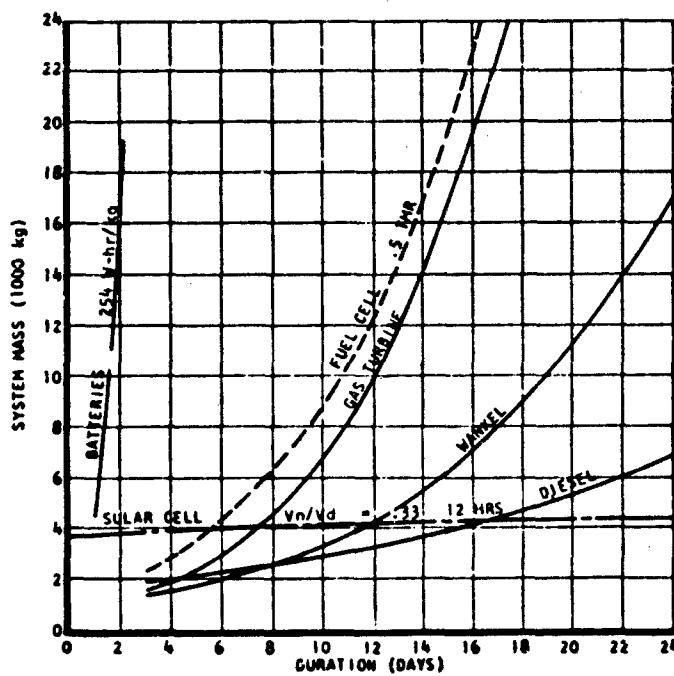


Figure 2



MATERIAL: NYLON ( $\sigma = 8300 \text{ N/cm}^2$ )



ALTITUDE: 21 km  
 FREE LIFT: 20%  
 VELOCITY: 10.3 m/s  
 PAYLOAD: 90 kg  
 CD: .05

Figure 3. Base Data, All Systems Comparison

increase slightly as the number of charge-discharge cycles for the batteries increase. On the power versus duration curve, three solar cell curves are plotted—one each for 10, 12, and 14 hours of sunlight. The 12 hour sunlight case is the one used in the remainder of the graphs. The other two cases are shown to depict the power variation with more or less sunlight. With 2 hours less sunlight the propulsion power required increases approximately 11 percent whereas with 2 additional hours of sunlight the propulsion power decreases approximately 8 percent.

The power required and the system mass are very high, as shown, for the batteries only case. The best available batteries, 251 W-hr/kg, are presented. Beyond a one day mission the battery powered system size becomes excessively large. Future developments in batteries should significantly improve their energy density capabilities and if an energy density greater than 600 W-hr/kg can be attained then the battery system should be considered further.<sup>3</sup>

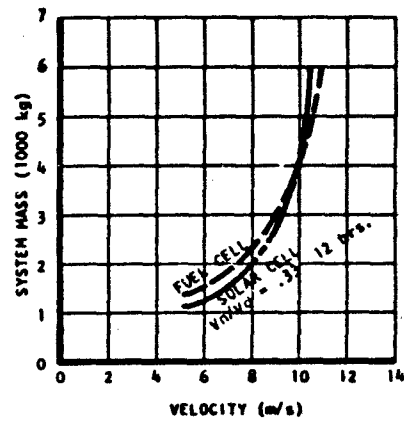
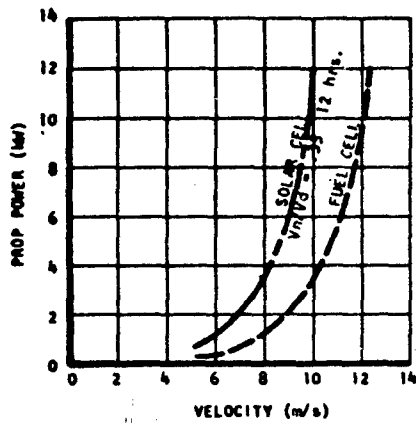
The base data curves, as well as all remaining curves, show a fuel cell system utilizing a TMR = .5 (i.e. the tank mass is .5 times the fuel mass). The relative advantage of using a lightweight tank can be shown by using a TMR = .5 as compared to a system using a TMR = .85. For a 7 day mission, the power required drops by approximately .5 kW and system mass by approximately 20 percent.

The gas turbine, Wankel, and diesel engines are all tentatively superior power sources in terms of propulsion power required and system mass. However, none of these power sources has been developed for this application and, as such, are not available. The variation in system mass and power varies between these three engines as a result of specific fuel consumption rates ranging from .24 to .73 kg/kW-hr.

All three of the combustion power sources would require either a ballonnet or pump and valving scheme to maintain altitude as fuel is consumed. This would require additional power and system mass which has not been included in these curves. These curves consequently would be shifted higher on the graph to compensate for the additional power and mass. Since these power sources are not considered reliable or tested sources, this effort was not pursued.

Wind velocity is one of the most sensitive parameters for any of the given systems. It has been decided that the most favorable winds exist at the 21,000 m altitude level. The first two graphs of Figure 4 show the effect of velocity on propulsion power and system mass. The velocity scale of the graphs is average velocity so that a comparison can be made between the two systems although the solar cell system has been designed to fly at higher velocities during daylight hours. For a constant size vehicle, propulsion power increases as the cube of

### POWER AND MASS VS VELOCITY



MATERIAL: NYLON ( $\sigma = 8300 \text{ N/cm}^2$ )

ALTITUDE: 21 km

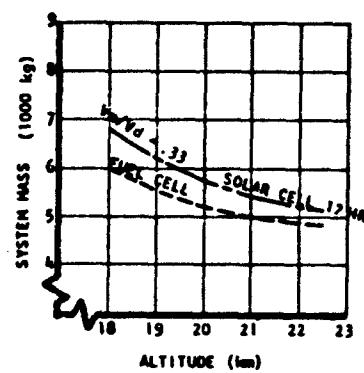
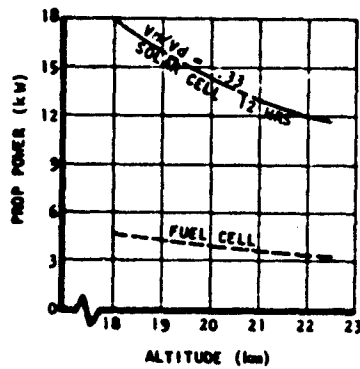
FREE LIFT: 20%

PAYLOAD: 90 kg

CD: .05

DURATION: 7 DAY

### POWER AND MASS VS ALTITUDE



MATERIAL: NYLON ( $\sigma = 8300 \text{ N/cm}^2$ )

FREE LIFT: 20%

VELOCITY: 10.3 m/s

PAYLOAD: 90 kg

CD: .05

DURATION: 7 DAY

Figure 4

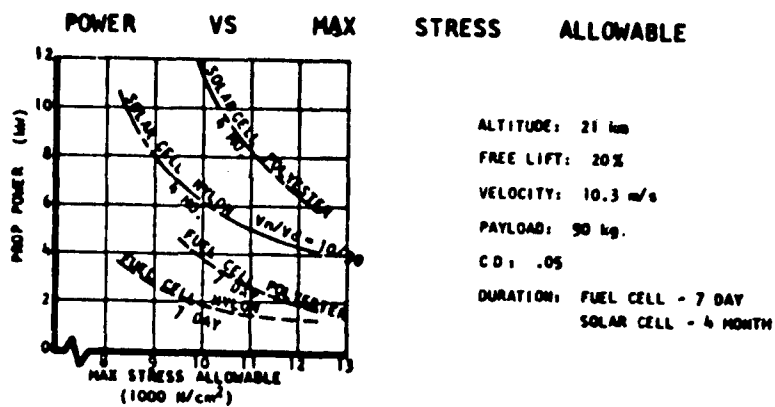
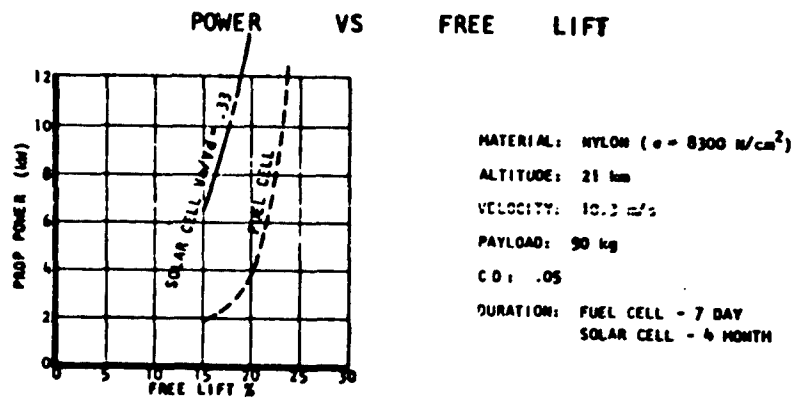
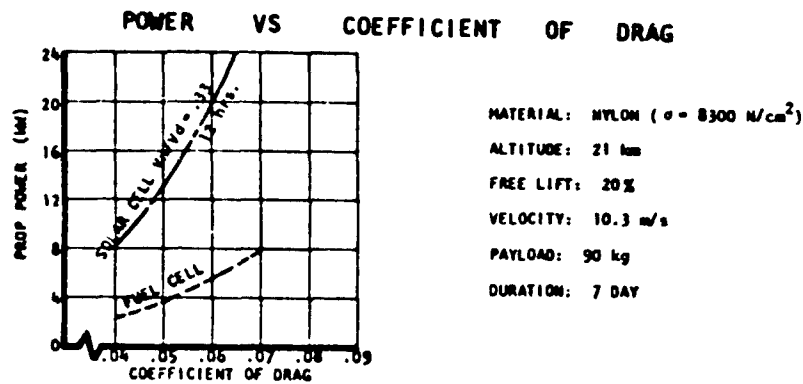


Figure 5

the velocity, however, since the system necessarily grows larger to accommodate the increased propulsion system weight the power increases even more than as by the cube of the velocity. The system mass for the solar cell nearly doubles between 5.1 and 7.7 m/s and triples between 7.7 and 10.3 m/s. Beyond an average velocity of 10.3 m/s the system mass grows even faster.

The last two graphs of Figure 4 show the effect of altitude on propulsion power and mass. As altitude is increased, less power is required due to lower density air. This along with a lower super-pressure, which results because of the decreased absolute pressure, reduces the thickness of the envelope. Thus, even though the volume increases the system mass decreases. By going from 18,000 to 21,000 ft the propulsion power for a solar cell system decreases by approximately 25 percent.

Figure 5 shows how propulsion power varies for the fuel cell or solar cell system for other parameters. A review of these graphs indicates that it is very important to determine accurately what the coefficient of drag will be, what minimum free lift can be used, what the true stress limit on the balloon material is, and what balloon material (polyester film or biaxially oriented nylon 6 film) can be used.

Many other graphs can be derived by using data generated by the computer program, but a more concise presentation of system mass sensitivity is shown in Table 1. This sensitivity analysis was performed by using the HASKV computer program to generate data for a one percent variation of each parameter for a fuel cell powered system.<sup>3</sup> All variations were taken as positive. Except for the parameter that was varied, all other parameters remained unchanged. The table shows results of some of the most sensitive parameters in order of decreasing sensitivity.

Table 1

Parameter Increased by 1 Percent	Absolute Mass Change $\Delta M/M$
Envelope Material Stress Allowable	4.01 percent
Envelope Material Density	3.70
Free Lift Ratio	2.61
Supertemperature Ratio	1.64
Specific Fuel Consumption	0.64
Coefficient of Drag	0.63
Payload Mass	0.59
Subsystem Power	0.57
Tank Mass Ratio of Fuel Mass	0.29

### 3. SYSTEM DESIGN

It was decided that the design of the fuel cell powered airship would be pursued in more detail. The final configuration is shown in Figure 6. Table 2 lists the masses of various system components, and Table 3 shows the power distribution allocations. A brief discussion of the major components follows.<sup>4</sup>

#### 3.1 Hull

The POBAL-S hull is a class C shape with a fineness ratio of 5:1. The inflated length is 113.0 m with a volume of 29,270 m<sup>3</sup>. The basic hull material is biaxially oriented nylon 6 film. This material has the same stressing capability as polyester while having a density of 1.15 g/cm<sup>3</sup> as compared to 1.38 g/cm<sup>3</sup> for polyester.

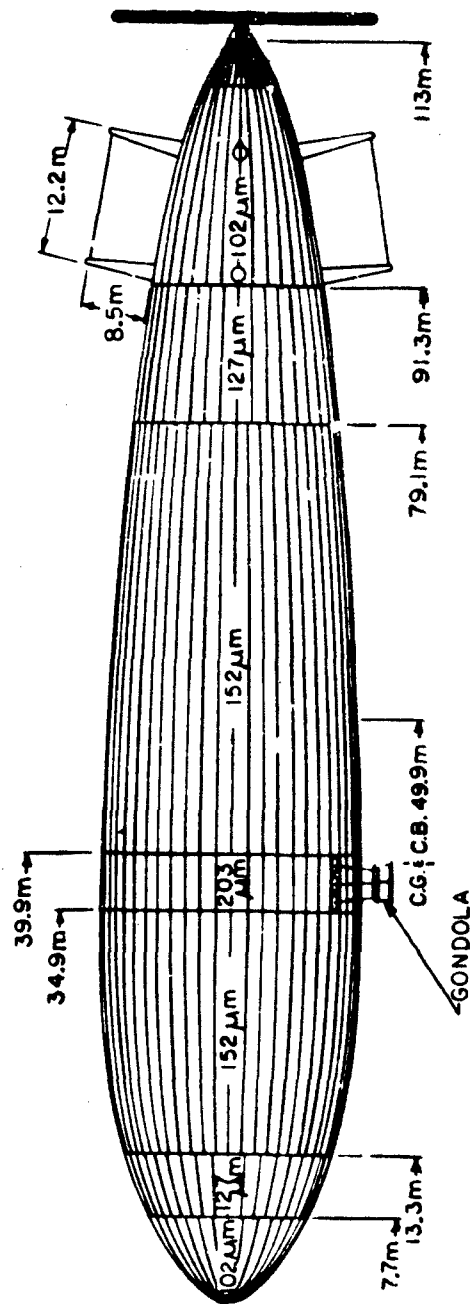
Because the film is highly stressed and the thickness can be tailored for a particular design it can be shown that, for a given volume, as the fineness ratio increases the balloon weight decreases. The limiting factors would be buckling of the airship, available film thicknesses, and drag increase. It should be noted that aerodynamic forces are very low, as compared to such forces on conventional airships; and the pressurization required because of supertemperature effects is more than adequate to overcome buckling due to component weight or aerodynamic forces. Depending upon radiation and atmospheric conditions the superpressure will vary from a minimum of 240 N/m<sup>2</sup> to a maximum of 1100 N/m<sup>2</sup> (ambient pressure is 4400 N/m<sup>2</sup>).

To help minimize system size the hull has been partitioned to vary material thickness depending upon local stressing. Material thicknesses of 102, 127, 152, and 203  $\mu$ m were used. As a result of only 25  $\mu$ m material being available, this corresponds to laminations of 4, 5, 6, and 8 plies. The thinner material is used at the ends and the thicker material is used at the larger diameter sections where the stressing is greater (see Figure 6). This results in a 30 percent reduction in propulsion power and a 40 percent reduction in system mass as compared to using only a 6-ply material reinforced at the center with 2 more plies.

#### 3.2 Fins

Fin sizing and location is based upon reference 5 and the fin construction is based on reference 4. Total surface area for the cross configured fins is 285 m<sup>2</sup>. The mean aerodynamic center is 45.9 m aft of the center of buoyancy. The fins are constructed of biaxially oriented nylon material and consist of a 25  $\mu$ m membrane supported by two air inflated cones. The support cone material is 51  $\mu$ m. The base diameter of the cone is 1.3 m and the tip diameter is .2 m.





FINENESS RATIO - 5:1  
 VOLUME - 29,270 m<sup>3</sup>  
 SHAPE - CLASS C

Figure 6. Pobal-S Fuel Cell Powered Airship

Table 2

<u>Item</u>		<u>Mass (kg)</u>
<b>Balloon Components:</b>		
Fins	17.2	
Hull	1227.3	
Total Balloon	1244.5	1244.5
<b>Stern Components:</b>		
Motor	3.5	
Converter	22.7	
Gimbal motors	0.4	
Speed reducer	7.0	
Structure	19.6	
Propeller	20.0	
Total Stern	73.2	73.2
<b>Gondola Components:</b>		
Fuel Cell	62.1	
Payload	90.7	
Electronics	29.6	
H <sub>2</sub> tank (full)	71.2	
O <sub>2</sub> tank (full)	185.9	
Water storage (empty)	2.3	
Radiator	15.9	
Frame structure	36.5	
Parachute assembly	31.7	
Total Gondola	525.9	525.9
Wire - Gondola to Motor	22.1	22.1
<b>Total System Mass</b>		<b>1865.7</b>

Table 3. Power Distribution

<b>Fuel Cell Power Allocations:</b>			
Payload		500 W	
Autopilot, telemetry, gimbal, etc.		200 W	
Motor		1800 W	
		2520 W	Total
<b>Drive Train Power Allocations:</b>			
Motor:	input	1800 W	
	efficiency	75 percent	
	output	1350 W	
Speed Reducer:	input	1350 W	
	efficiency	96 percent	
	output	1300 W	
Propeller:	input	1300 W	
	efficiency	78 percent	
	output	1010 W	

Each fin is approximately 8.5 m x 12.2 m. The cones are separate gas cells from the balloon envelope and are pressurized with an air pump to 68 percent of the ambient pressure.

### 3.3 Gondola

The gondola includes the fuel cell with associated hardware, fuel tanks, payload, telemetry control unit, autopilot, and parachute. Aluminum honeycomb is fitted to the base for minimizing shock impact upon parachute landing. Pratt & Whitney designed the fuel cell<sup>6</sup> and did much of the work on the gondola. The net power output of the fuel cells is 2,520 W (see Table 3) and can operate continuously for 7 days. The water output of the fuel cell is stored so as not to change the system center of gravity or mass. The entire gondola is supported by a network of patches to allow proper deployment and suspension of the gondola during launch and ascent.

### 3.4 Propulsion System

The airship is controlled by a gimballed propeller mounted at the rear center line of the envelope. Stability is maintained by an auto-pilot which controls the gimbal assembly. The gimbal assembly is mechanically moved by electric motors and ball screws. The stern structure is fabricated from 6061-T6 aluminum tubing with a wall thickness of 1.24 mm and diameters varying from 13 mm to 38 mm.

The propulsion motor is a Lear Reno brushless DC motor having an electronic converter. This motor operates with an efficiency of 75 percent and provides an output power 1.35 kW. The shaft speed is 10,000 rpm.

A three stage belt type speed reducer was used to obtain a reduction ratio of 133:1. The efficiency is 96 percent.

The propeller is fabricated of 6 mm thick x 6 mm Hexcell honeycomb with face sheets of 127  $\mu$ m aluminum. This structure provides a high degree of stiffness considering the weight of the assembly. The propeller has three blades with a disc diameter of 10.4 m. It provides a thrust of 119 N at 75 rpm with an efficiency of 78 percent.

### 3.5 Launch

The launching of this vehicle is relatively complex and not within the scope of this paper. Briefly, it should be mentioned that a tail first launch employing a tow balloon and crane would be used. This technique allows for the large propeller to be safely deployed, the system to be slowly erected to a vertical position, and a controlled ascent rate.

At the conclusion of the mission only the gondola containing the fuel cell will be returned by parachute. The remainder of the system is considered as expendable.

## References

1. Rice, C.B. (1973) Power Sources For Powered Balloons, Emmanuel College. Proceedings, Seventh AFCRL Scientific Balloon Symposium, AFCRL-TR-73-0071, George F. Nolan, ed., Air Force Cambridge Research Laboratories.
2. Beemer, J.D., Parsons, R.R., Rueter, L.L., Seuferer, P.A. (1973) Study of High Altitude Station Keeping Vehicles, Raven Report No. 0373003, Raven Industries, Incorporated. Advanced Research Projects Agency, ARPA Order Number 1973, Final Report.
3. Beemer, J.D., Parsons, R.R., Bueter, L.L., Seuferer, P.A. (1973) POBAL-S, R&D Design Evaluation Report, Part I, System Concept Choice, Raven Report No. 0273001, Raven Industries, Incorporated. Air Force Cambridge Research Laboratories, Contract No. F19628-73-0076.
4. Beemer, J.D., Parsons, R.R., Rueter, L.L., Seuferer, P.A., Swiden, L.R. (1973) POBAL-S, R&D Design Evaluation Report, Part II, Raven Report No. 0673006, Raven Industries, Incorporated. Air Force Cambridge Research Laboratories, Contract No. F19628-73-0076.
5. McLemore, H.C. (1962) Wind-Tunnel Tests of a 1/20-Scale Airship Model with Stern Propellers, NASA TN D-1026, Langley Research Center, National Aeronautics & Space Administration.
6. Handley, L.M. (1973) Study of Fuel Cell System for Powered Balloon, PWA-4792, Pratt & Whitney Aircraft. Air Force Cambridge Research Laboratories, AFCRL-TR-73-0447.

**Session 2**  
**Tethered Balloons**

**Richard S. Cesaro, Chairman**  
**TCOM Corporation**

**Preceding page blank**

#### **Contents**

1. Introduction	59
2. Background	60
3. Programs and Applications	63
4. Future Programs and Applications	67

## **A Summary of Tethered-Lighter-Than-Air Development Conducted by the Range Measurements Laboratory**

**Walter H. Manning, Jr.  
Range Measurements Laboratory  
Patrick AFB, Florida**

### **Abstract**

A presentation that traces the development of the Family II tethered balloon system by the Range Measurements Laboratory and summarizes the scientific and operational considerations addressed by scientists, engineers and technicians from government and industry.

#### **1. INTRODUCTION**

The Family II balloon is the product of an extensive research and development program that has been conducted by the Range Measurements Laboratory, Patrick AFB, Florida beginning in the late 1960s under the sponsorship of the Defense Advanced Research Projects Agency (ARPA). The goal of this program was the development of a stable balloon platform for exploiting balloon-borne sensor applications.

The Family II 200,000 cubic foot balloon system is an aerodynamically shaped balloonet balloon with a cruciform stabilizer designed to operate at altitudes

to 12,000 feet above ground level and carry 750 pounds of useful payload. Aerodynamic shape and structural integrity are maintained by an automatic pressurization system that operates electrically powered blowers and relief valves that control hull and empennage pressure. An on-board 5KW power generation system provides electrical energy for the balloon and payload requirements. The payload system is attached under the hull and is covered by a windscreen which is designed to reduce aerodynamic drag and to protect the payload. The balloon is flown by a single tether cable composed of a high strength to weight ratio polyester material covered with a protective neoprene jacket. The winch used to handle the tether cable during flight, launch and recovery operations is mounted on a self propelled truck and allows ascent/descent at a rate of 200 feet per minute.

The mooring system consists of a tower with a rotating latching mechanism for attaching to the nose of the balloon permitting 360 degree rotation of the balloon with the wind. The handling lines are secured to a gondola system which is ballasted to offset the high positive buoyant lift of the balloon during mooring. An alternate mooring system consisting of a tower and a monorail, which serves the same purpose as the gondola, has been developed for use at permanent or semi-permanent balloon operating sites.

The accomplishment of the RML in tethered-lighter-than-air (TELTA) development has resulted in a quantum advancement of balloon and sensor technologies:

- . Developed equations of motion for tethered balloons.
- . Development and operation of stable balloon sensor platforms.
- . Demonstrated feasibility of electronic and optical sensors and communications relays.
- . Demonstrated feasibility of the operational deployment of tethered balloons.
- . Demonstrated environmental survivability of tethered balloons.
- . Demonstrated the cost effectiveness of tethered balloons.
- . Since first Family II flight, 19 December 1971: Over 200 successful data flights have been flown.

## **2. BACKGROUND**

Balloons have been used as platforms for scientific and military missions since 1783. In June of that year, the Montgolfiere brothers first flew a 35 foot diameter hot air balloon near Paris. The success of this flight led to a great

flurry of scientific activity and balloons have since amassed a distinguished record of scientific service. Meteorology, stratospheric physics, cosmic ray physics and astronomy have been the principle scientific beneficiaries of free ballooning activity.

The history of tethered balloons is less illustrious (and more military) than that of free balloons. They have been used to lift aerial observers for surveillance roles. During World War II, the British developed and made extensive use of aerodynamically shaped balloons as an enemy aircraft deterrent. The techniques applied to previous balloon design and development have been largely a cut and try effort with little analytical investigation of the phenomena associated with tethered balloon flight, but as the need for improved performance increased, more sophisticated approaches were required.

Early balloon work by the RML began with the development and deployment of a remotely controlled drone blimp equipped with acoustical sensors to Southeast Asia. A 5,300 cubic foot balloon called Silent Joe was propelled by two battery powered one HP DC motors. The flight path was remotely controlled from the ground by controlling the speed of one motor and in finite steps. The system carried microphones and a radio transceiver and was designed to detect truck convoys and troop movements.

Because there was no established body of technology on which to draw, it was necessary to proceed by trial and error and from first principles. Tethered operations began at Cape Canaveral, Florida using a 5,300 cubic foot "Baldy" balloon. An extensive program was initiated using elaborate balloon-borne instrumentation and film and video cameras to obtain the beginnings of a data base. Data from these flights provided first order information relating to balloon motion and the effects of the tether on stability.

Using a World War II BJ British barrage balloon of 84,000 cubic feet, the RML embarked on the development of a balloon-borne radar system that would be capable of detecting vehicular ground targets for use in Southeast Asia. During this early work, extensive improvements were made in mooring and ground handling techniques. Not only must a balloon system be capable of lifting a useful payload to altitude, it must also be handled on the ground and moored. A system was devised in which the nose of the balloon was attached to a tower with a rotating latch which would allow the balloon to weathervane with the wind. The high buoyant lift of the helium was offset by attaching the balloon handling lines to a circular monorail through a travelling dolly.

Improvements were made in the hull and empennage configuration through the addition of a pressurization system. Blowers, pressure sensors and relief valves powered by an on-board generator system added a new dimension to the flight characteristics of these early balloon systems.



In order to meet the requirement of attaining altitudes in excess of 10,000 feet with sensor payloads weighing 700 pounds or more, a tandem system utilizing the BJ+3 balloon was devised. The first tandem flight in the United States with large balloons was conducted at Cape Canaveral by the RML on 10 August 1969. The first balloon was launched with a tether approximately 3,000 feet in length. Upon reaching this altitude, the tether was transferred to a cable running through a tunnel in the second balloon to its tether confluence point. In this configuration, the top balloon reached an altitude of over 13,000 feet, supported the payload and 3,000 feet of tether, while the second balloon supported the weight of 10,000 feet of tether. Several tandem flights were conducted subsequently and the system proved to be valid.

Even with vast improvements that had been made in all phases of tethered balloon work, it was obvious that the inherent limitations of the empirically designed BJ balloons were not satisfactory. An advanced program to develop a reliable, stable, all weather balloon system to be known as Family II was begun. Working with NASA Langley and the G. T. Schjeldahl Corp., the RML directed the birth of scientifically based tethered balloon technology in this country. Extensive use of wind tunnel data, tow testing of scale models, as well as the development and use of computerized equations of motion, led to the selection of the hull and empennage configuration for the 200,000 cubic foot Family II series balloons. Additional investigations were conducted into fabric materials. Numerous fabric/sealer/coating combinations were tested and evaluated to meet the requirements for a lighter, stronger, less permeable, aging resistant and easy to seal and join balloon material. Design improvements were made to all balloon hardware including helium valves, instrumentation systems and ground support equipment.

First flight of the Family II balloon was conducted on 19 December 1971 at Cape Canaveral. This flight fulfilled the expectations of the many talented people who had labored long and hard on this program. Continuing flights were conducted to evaluate the system and its operational procedures. As part of this in-depth analysis, the system was deployed to Wingfoot Lake, Ohio in early 1972 in order to subject the balloon to ice, snow and cold weather conditions. Operational evaluation was conducted at Cudjoe Key, Florida with the flight of an advanced radar surveillance system for the Aerospace Defense Command.

In response to a requirement by the United States Army Security Agency, the RML began a follow-on program which would capitalize on the success to date. Specialized mooring and handling equipments were developed that would enable the system to operate as a highly mobile tactical surveillance tool.

A detailed verification of the design criteria used in the development of the Family II tethered balloon began in 1973. Sophisticated instrumentation and data gathering, as well as in-depth test design characterised this segment of the program.

38 flights were flown in which over 2,000 measurements were recorded. From this data has come the knowledge and information that will be recognized as the reference material and basic literature for tethered balloon operations.

### **3. PROGRAMS AND APPLICATIONS**

#### **3.1 Acoustic Surveillance**

This type of mission is probably possible only with balloons. Prior development programs were unable to achieve a satisfactory detection sensitivity because of background noise from the vehicle. Tethered balloons are virtually silent. Achievement of the required low background noise necessitates battery or fuel cell power, both being available. Applications for directionally sensitive acoustic detectors include vehicle and troop movement detectors and enemy artillery mortar and rocket firing-site detection, among others.

#### **3.2 Radar Surveillance**

The RML has demonstrated the operational feasibility of a balloon-borne surface search radar system in the acquisition and tracking of high performance, low altitude aircraft against a high clutter background. Extended testing has been conducted at Cudjoe Key, Florida for the Aerospace Defense Command (ADC). The success of these operations has led to a commitment by the United States Air Force to accept the balloon-borne radar system as part of the Air Defense Network for this country. Other studies by the Air Force have examined the feasibility of expanding coverage to include the entire southern perimeter of the United States.

It is a particularly noteworthy point that a network of balloon-borne radar systems could provide reliable surveillance and detection capability for the Mexican American border and effectively seal off the entrance, via light aircraft and vehicular traffic, of vast quantities of narcotics that are now flowing into this country through this area.

#### **3.3 Optical Surveillance**

Tethered balloons make excellent elevated platforms for optical surveillance because of their excellent short-term stability and intrinsic station-keeping. The stability is derived from the long time-constants which characterize balloon motion; and it is the primary requisite for the platform for high-resolution optical sensors. The application for these systems vary from general battlefield reconnaissance and defense perimeter control to point and area security against

infiltration and encroachment. High-resolution and highly sensitive image-producing systems both in the visible and other spectral regions are the obvious sensors. Optical systems may azimuth scan and/or be directed to areas of interest by ground command. Relatively wide-angle, fixed optics, directed downward could cover any desired area from any altitude used.

Based on the results of field tests with prototype equipment, the RML has designed a high resolution optical surveillance system under the FINE LOOK program which used a vidicon camera system coupled to a Questar telescope in a precision remotely-trainable mount.

### 3.4 Communications

One of the most attractive tethered balloon applications, the communications relay, is both very flexible and very cost effective compared to other alternatives (satellite, tropo-scatter, microwave tower, aircraft, etc.). Whether for point-to-point relaying, or area "broadcasting," the tethered balloon spans very long distances or covers very large surface areas as desired. Military applications include message and data relaying and area-coverage broadcasting for tactical management, propaganda, and entertainment. Moderate altitudes provide large line-of-sight paths and permit relatively complex payloads. It is noteworthy that the advantages of tethered balloon relays are being exploited on a commercial basis. This work is based on the success obtained during feasibility tests with R&D relay systems developed by the RML under the GRANDVIEW and TRIMLINE programs. Studio quality TV video was transmitted 125 miles via a balloon-borne relay to line of sight distances. VHF communications data was received and relayed to a ground communication point.

### 3.5 Navigation and Antenna Elevation

Position location of airborne and ground vehicles at extended ranges was demonstrated by the RML during feasibility tests under the NITE DIAL Program. With on-board equipment, which received and retransmitted LORAN C signals through a balloon-borne relay, U-2 aircraft and a truck were successfully located and tracked to line of sight distances. Military and governmental applications of such a capability are apparent.

#### 3.5.1 ANTENNA ELEVATION

Antennas are of such a wide range of sizes that the application must be described somewhat generally. Two examples may be cited. Simply by elevating a wire, the effective range of small packaged transceivers in SEA has been greatly increased. In this case, a small balloon raised the radiator above the shielding

canopy of tropical vegetation. At the other end of the scale, a tethered balloon has been used to elevate an antenna weighing several tons to a moderate altitude.

### **3.6 Transport**

The RML has conducted a series of tests to evaluate the feasibility of adapting the heavy lift natural shape balloon, which is used commercially by the logging industry for harvesting timber, to offload containerships in areas without prepared dock facilities.

The U.S. Navy does not now have nor does it intend to have a military logistics resupply capability. The Navy intends to rely on the U.S. commercial maritime fleet to support post-amphibious resupply operations. The U.S. commercial fleet will, by the 1980s be about 90 percent containerized. These ships are designed to operate from one prepared port facility to another. However, for a military resupply mission, the ships would be required in most cases to anchor anywhere from 1,000 feet to several miles offshore. The cargo containers weighing up to 20 tons must be extracted from the hold of the ship and transported to shore.

One of the most promising, cost effective techniques for this operation appears to be a balloon logistics facility in which the balloon is attached to a container, the container is lifted out of the hold and then the balloon and container are pulled to shore via a cable/winch system.

The RML is conducting an engineering study which will define such a system and establish its operational criteria for use by the military.

### **3.7 Atmospheric Sciences**

The RML has conducted an extensive Atmospheric Sciences Program designed to extend the Family II balloon system operating duration through the reduction of weather limitations, particularly those resulting from lightning hazards. In consultation with the leading atmospheric scientists in the United States, a flight test program and an evaluation of materials and equipment have resulted in the implementation of safety features for tethered balloons. The features are categorized as: (1) Warning; (2) Personnel and Equipment Protection; and (3) Protective Procedures.

#### **3.7.1 WARNING**

Lightning warning is required at two levels; early warning and immediate hazard detection.

For early warning, long range weather forecasts and weather radar augmented by a recently developed lightning azimuth detector, permit sufficient warning for retrieval of the balloon if such action is necessary.

Immediate warning is defined as a short term warning of an immediate hazard. This warning is obtained through the measurement of the magnitude and frequency of changes in the atmospheric electrical field in the immediate vicinity and presented in the form of lamp indications to the balloon operations personnel.

### 3.7.2 PERSONNEL AND EQUIPMENT PROTECTION

A well bonded, shielded enclosure at the winch operator's position provides adequate protection against a direct stroke. The balloon protection is provided by controlling the point that lightning will strike. This is accomplished by installation of lightning rods on the balloon along with shield wires similar to those used for protection of power lines. The lightning currents so intercepted are then guided to the tether in a manner which will prevent arcing - the principal form of lightning damage. Sensitive electronics are located in areas where direct lightning contact is least probable, and are protected against indirect effects by transient suppressors.

### 3.7.3 PROTECTIVE PROCEDURES

The warning systems, to be maximally effective, are integrated into a well conceived and strictly enforced system of safety procedures. Specific provisions of these procedures define:

- (a) Minimum operating crew
- (b) Crew positions
- (c) Criteria for balloon recovery
- (d) Criteria for site evacuation and safe areas
- (e) Sequence of activity

Inputs to the safety plan include management/command decisions as to the tolerable level of hazard to the system weighed against possible personnel hazards during attempted retrieval under adverse circumstances.

## 3.8 Power and Tether Systems

During the development and test of the Family II balloon system, two related areas of investigation played a prominent role; power systems and tether cables. Each pound of system weight supported by balloon penalizes its payload and altitude capability. Great strides were made in the design, development and test of a lightweight auxiliary power system which would extend the tethered balloon mission altitude and duration through the reduction of specific weight and fuel consumption. Successful experiments were conducted in which gaseous fuel was provided to the on-board power system from the ground via a nylon tube. Prototype tethers were constructed and tested which incorporated the fuel tube inside the balloon tether cable.

The development by the Dupont Corporation of a new lightweight, high strength-to-weight ratio organic fiber known as Kevlar 29 was investigated by the RML for its suitability as a tether material. Preliminary calculations indicated a 40 percent weight reduction in tether weight over the conventional polyester Nolaro cable used (a weight savings of approximately 735 pounds for a 9,000 foot tether cable), while retaining the same breakstrength (26,000 pounds). This weight reduction is reflected directly as an increase in balloon payload capability. Sample lengths were tested for flexibility, elongation, abrasion, resistance, performance on a winch sheave and splicing characteristics.

### 3.9 Heavy Lift Station Keeping

Another promising application for the Family II tethered balloon system is as the lifting device for a munitions high angle impact facility. Successful tests were conducted for the Armament Development and Test Center, Eglin AFB, Florida using a triad cable arrangement and three winch trucks for positioning of simulated ordnance. Three pull down angles were tested: 30°, 45° and 70°.

The test results indicated that use of a tethered balloon, configured for low altitude heavy lift operations, as the lifting device for munitions testing, is both feasible and practical. The encouraging results of these tests and the cost-effectiveness of the balloon system had led Eglin AFB to plan for an installation.

## 4. FUTURE PROGRAMS AND APPLICATIONS

### 4.1 Family II Upgrade

The Family II development program has attained its objectives of payload and altitude capability and operability in high winds. The vehicle design that has evolved has been successful to the point of inspiring commercial application using the same basic envelope. The emergence of a system of great versatility and dramatic cost effectiveness for a wide variety of missions now seems assured. The years of research, development, test and evaluation have pointed the way for those refinements that would even further enhance system capability.

#### 4.1.1 EMPENNAGE IMPROVEMENT

Because of structural and operational limitations of the previous and current design, it is highly desirable to undertake a third design iteration of the empennage. The basic tail aerodynamic design is very good and has little room for improvement. The areas of improvement are centered on structural integrity, reliability and repairability. Maximum use of improved fabrics, adhesives and sealing

techniques will be made while recognizing the importance of operational acceptability; i.e., field repairability and interchangeability.

#### **4.1.2 IMPROVEMENT OF ON-STATION-TIME CAPABILITY**

Based on the feasibility shown during tests in which the on-board power generator was supplied with fuel from the ground and on studies of the practicability of supplying electrical energy directly to the balloon system from the ground, there is ample technical base from which to project greatly extended mission duration limited only to MTBF of on-board systems. Implementation of either system obviates the need to penalize the payload, altitude and/or mission duration by carrying on-board fuel that must be replenished from time to time.

#### **4.1.3 WEIGHT REDUCTION**

As stated before, each pound of system weight supported by the balloon penalizes its payload and altitude capability. In addition to improvements in power systems, two areas that are exploitable for overall weight reduction are balloon materials and the on-board nose mooring structure.

The application of recent developments in materials technology to balloon fabric will allow substantial weight improvement in the hull, ballonet and empenage. The on-board nose mooring structure, which weighs approximately 500 pounds, was originally to serve a two-fold purpose; to help prevent nose dimpling from wind pressure during flight operation and to distribute the loads through the hull structure during moored conditions. Results from design verification flight testing indicate that the hull structural integrity is such that the nose structure is not needed during flight.

#### **4.2 Radar Surveillance**

Flight and training operations are being conducted by the RML for Aerospace Defense Command of a prototype balloon-borne radar surveillance system that has proven feasibility of this concept for air defense and surveillance. The follow-on plans include a system which will provide 24 hour a day operations with 95 percent on station time capability.

#### **4.3 Applications**

##### **4.3.1 MILITARY**

Through the use of the technology developed in producing the Family II, a family of balloon systems to meet individual mission requirement is now possible. These range from the complex radar surveillance programs at high (12,000' MSL) altitudes requiring large balloon systems to simple antenna relay stations operating at or below 1,000 feet altitudes requiring balloons as small as 3,000 cubic feet.

## TETHERED BALLOON APPLICATION SUMMARY

<u>MISSION</u>	<u>PAYLOAD TYPE</u>
Aircraft Defense Intercept	MTI Radar
ELINT and COMMINT	E/M Spectrum Search and D/F
Stand-Off Sensing	High Resolution TV, Radar
Optical Surveillance	Visible and IR
Acoustic Surveillance	Acoustic Search and D/F
Bombardment Reconnaissance	Acoustic and Optical
ASW Sonobuoy and Magnetic	Comm Relay and D/F
Anomaly Detection	
Communications	Comm Relay
Containership Off-Loading	Cargo Containers
Heavy Lift Station Keeping	Test Ordnance
Navigation Aid	LORAN Antenna

### 4.3.2 ATMOSPHERIC AND OCEANOGRAPHIC SENSING

A generalized balloon support system is being defined to permit austere budgeted programs to use balloon systems at altitudes below 10,000 feet for a variety of ecological or scientific applications such as sensing airborne pollutants, measurement of meteorological cross sections, determination of airborne insect counts and a variety of other applications requiring stationary sensors at low altitudes. Systems of this type have been extensively used in oceanographic monitoring work.

### 4.3.3 FORESTRY

The efficient management of forestry resources, which includes as one of its primary responsibilities the preservation of timber and seedlings from the damages of fire and disease, lends itself to tethered balloon technology.

Current forestry and land management techniques which can be enhanced and simplified through the adaptation of this technology include:

#### (a) Forest Management

Assessment of the type, amount and "health" of vegetation is required. Current procedures consist of ground and other observations based on field experience and research results.

#### (b) Fire Detection

- Ground station detection is by visual observation and aircraft IR sensors.
- Fire detection communications utilize overloaded radio and telephone channels.
- Fire detection data handling features maps and hand drawn displays which are distributed to fire bosses.



**(c) Fire Suppression Command and Control**

During fire suppression operations, control of personnel and equipment is mostly person-to-person. Point-to-point communications are hampered by terrain features and channel over-use.

**(d) Meteorology**

Weather forecasting information is supplied by NOAA and local ranger stations. Specialized lightning warning and detection, local meteorological profiles and weather modeling use is limited.

**(e) Disease Detection**

Long term, wide area coverage of forested areas for the detection of timber damage from disease and insects is not available. Present procedures use limited local observations.

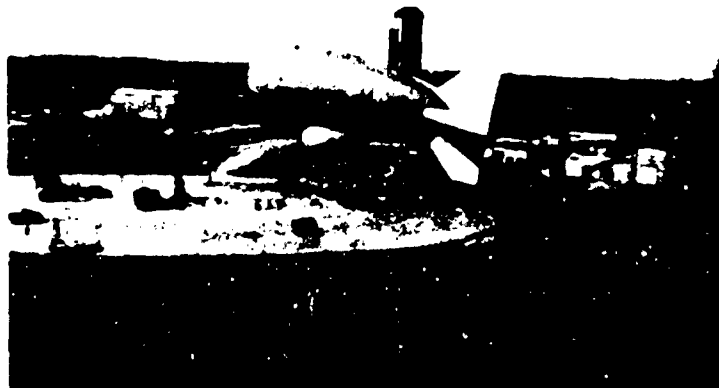


Figure 1. Telta Balloon Test Facility, Cape Canaveral, Florida



Figure 2. Family II, 200,000 cubic foot Aerostat



Figure 3. Family II Aerostat Moored Using Gondola System

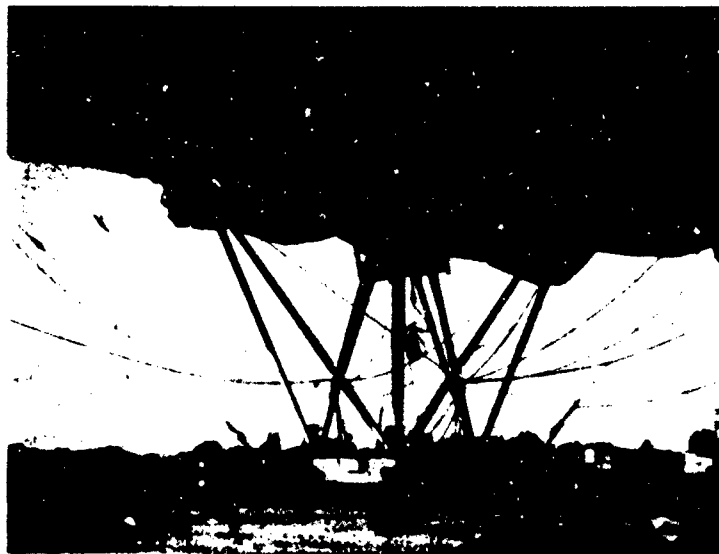


Figure 4. Gondola Mooring System

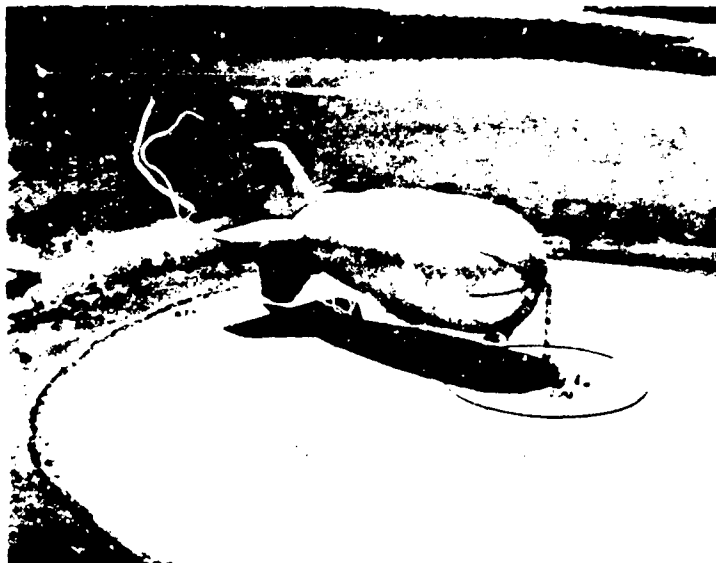


Figure 5. TELTA Balloon Test Facility, Cudjoe Key, Florida  
Featuring Monorail Mooring System



Figure 6. Monorail Mooring System



Figure 7. Cold Weather Environmental Tests at Goodyear Airship Facility, Wingfoot Lake, Ohio



Figure 8. Aerodynamic and Aerostructural Tests. CH47 Helicopter Towing Family II Aerostat



Figure 9. Family II at 68 Knots Windspeed Attained During Helicopter Tow

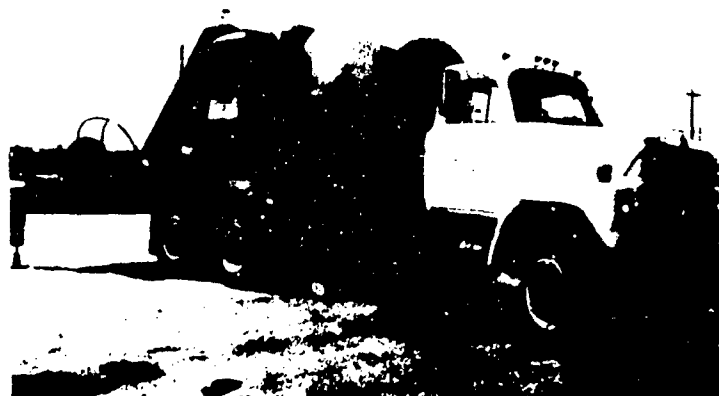


Figure 10. Mobile Winch Vehicle

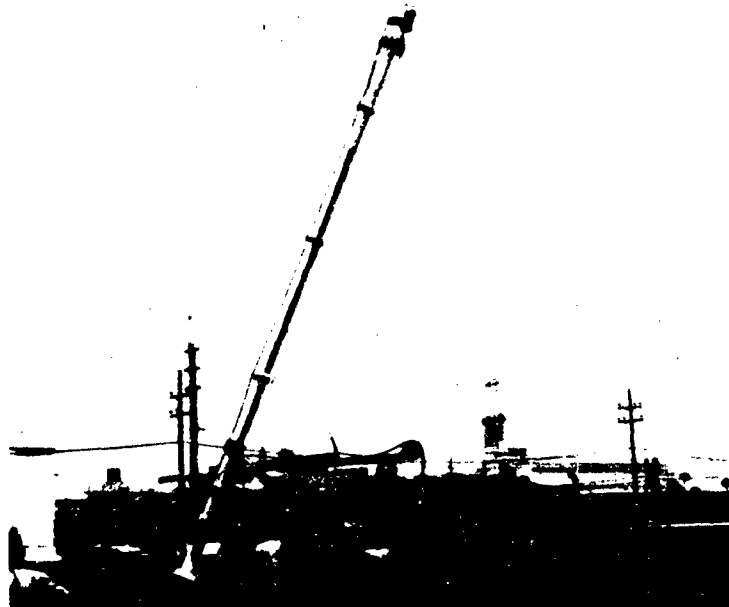


Figure 11. Tower Erector Vehicle

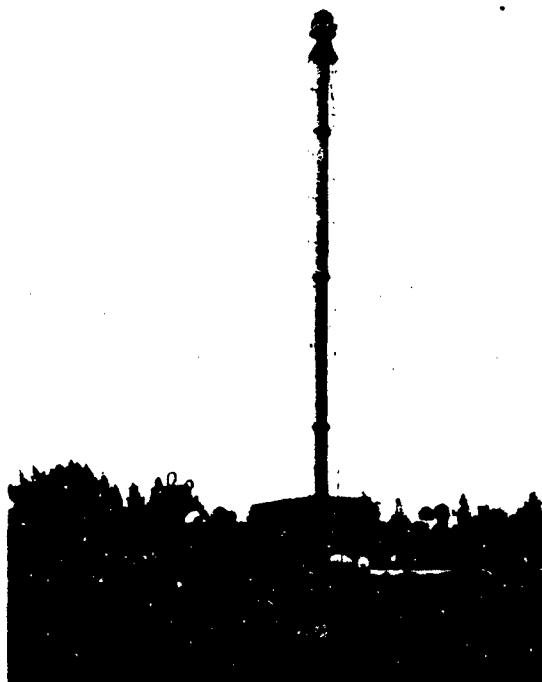


Figure 12. Mooring Tower

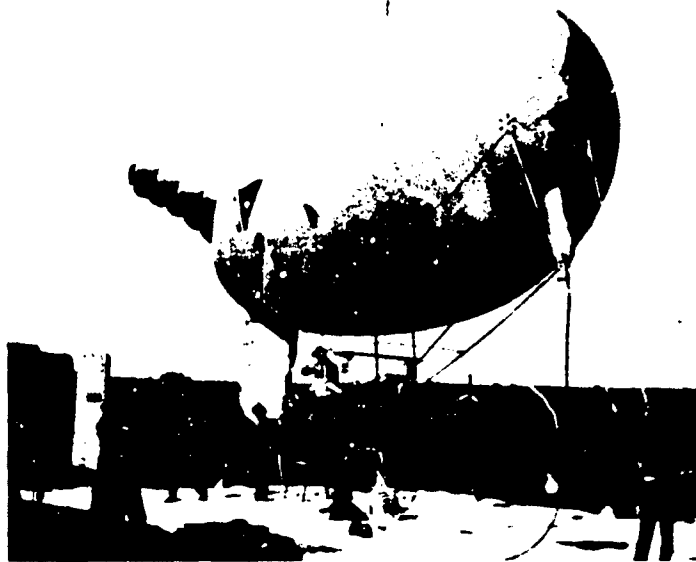


Figure 13. Silent Joe - Drone Blimp

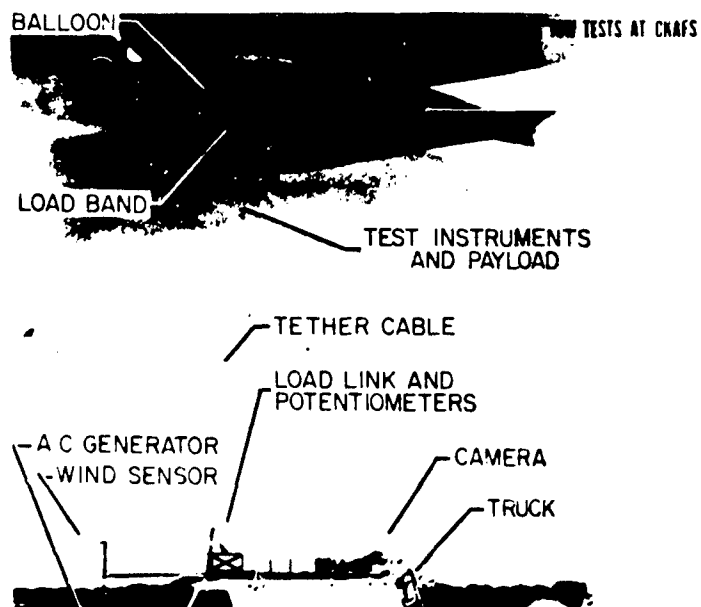


Figure 14. Aerodynamic Test Model Used During Family II Development Program



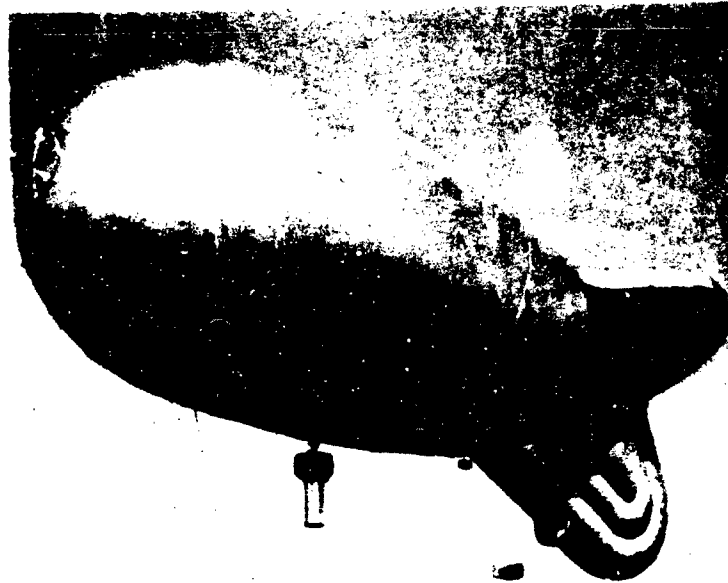


Figure 15. BJ+3 84,000 Cubic Foot Balloon with Communications Payload

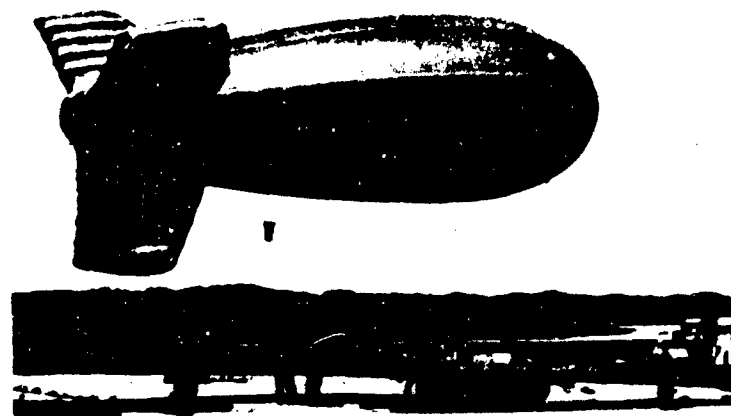


Figure 16. Atmospheric Science Experiments with Baldy, 5300 Cubic Foot Balloon

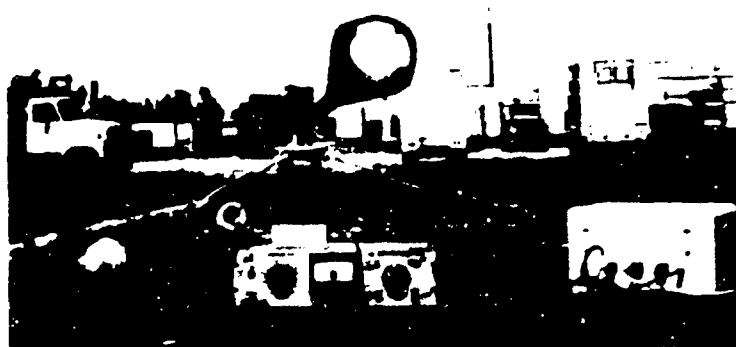


Figure 17. Tether Current Measurements



Figure 18. Instrumented Aircraft Measurements of the Earth's Electrical Field as Perturbed by a Balloon System



Figure 19. Prototype Optics System Tested During Fine Look Program

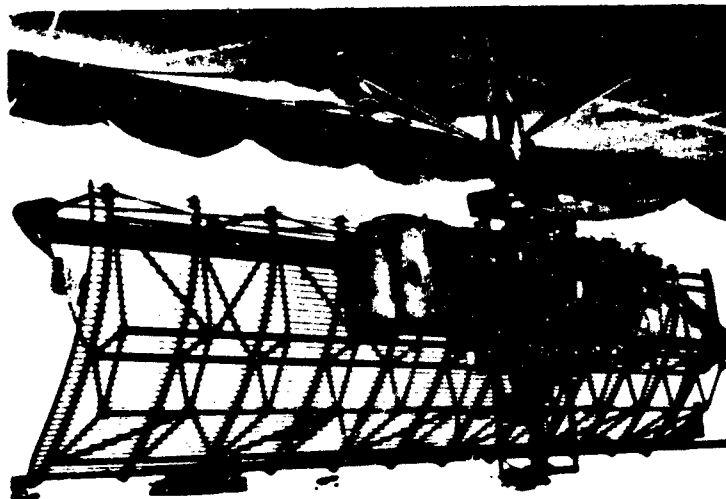


Figure 20. Balloon-Borne Radar Surveillance System



Figure 21. 530,000 Cubic Foot Natural-Shape Balloon



Figure 22. Feasibility  
Experiments with Military  
Cargo Containers



#### Contents

1. Introduction	84
2. The Captive Stratospheric Balloon	84
3. Problems to be Solved	84
4. Development Program	85
5. The 1973 Experiments	86
6. Current Work	89

## Captive Stratospheric Balloons

R. Regipa  
National Center For Space Studies (CNES)  
Systems and Methods Division  
Balloon Systems and Projects Department  
18 Avenue Edouard Belin  
31055 Toulouse Cedex, France

### Abstract

In collaboration with the National Weather Bureau, the National Center for Space Studies performed a series of experiments with captive Stratospheric balloons at the Guyana Space Center in October and November 1973.

After failure of the first flight, due essentially to a winch breakdown, it became possible to place a 10,000 m<sup>3</sup> balloon and a 350-kg gondola in position at an altitude of 17 km for twelve hours with an ambient temperature of less than -80°C.

The gondola had about 60 sensors at the flight altitude for measuring temperatures and temperature changes on the outside and at various inside points, vibrations and inclinations, wind speeds, and the movements of the balloon itself.

For future programs the National Weather Bureau is developing a more efficient winch while the CNES is investigating another type of positioning to eliminate stresses caused by passing through jetstreams.

In addition, an array of gondolas capable of moving along the cable is being evaluated. They would permit continuous probing of the atmosphere while both stationary and moving.

## 1. INTRODUCTION

Operation of Stratospheric balloons in free flight for long-term missions presents serious financial, political and safety difficulties. For this reason, technical and operational studies have been undertaken in France to develop captive Stratospheric balloons and show how they can be usefully applied to many fields such as meteorology, telecommunications, aeronomy, and detection of earth resources.

## 2. THE CAPTIVE STRATOSPHERIC BALLOON

Its main usefulness is that of maintaining experiments for a long time in the Stratosphere with almost complete immobility with respect to earth; we may call it a geostationary sub-satellite.

The following advantages are expected in the operational phase, apart from the purely scientific advantages;

- The telecommunication links are very short, some tens of kilometers, and always within optical range. They can thus be permanent and have a very high capacity.

- A single transmission and receiving station will provide the radio links. The operating costs are thus very low.

The cable moors the balloon to the ground. It also provides a point of support for the gondolas such that the atmosphere can be continuously investigated along a vertical line. The measurements taken have a true physical sense as there are no disturbances by slipstreams as for probes in free flight.

## 3. PROBLEMS TO BE SOLVED

The problems of building an operational system may be grouped under two headings.

### 3.1 Technical

The dynamic effects of the atmosphere make it necessary to rethink the mechanical and thermal designs of the balloons and gondolas.

The cable is a fundamental problem. Without the recent appearance of the new synthetic fibers, captive Stratospheric balloons could not reasonably be contemplated.

### 3.2 Operational

The procedures and facilities necessary to position the balloon and cable, without exceeding their mechanical strength limits, must be defined.

### 3.3 Safety

This involves safety hazards to general air traffic posed by the tether line to the ground. Until the technical and operational problems have been well defined and solved, experiments cannot be performed without a total safety guarantee, to the detriment of the cost, simplicity, and rapidity of developments. Only then can operational conditions be defined.

## 4. DEVELOPMENT PROGRAM

In view of the budget available and the desire of the scientists to obtain results very rapidly, it has been impossible to work out an ideal technical development program.

Two projects are under way with different objectives, technical means, and operational procedures.

### 4.1 Project "ESSOR" (English "Flyaway")

This project is being implemented by the National Weather Bureau and the National Center for Space Studies (CMES). It has a number of objectives:

- A technological mission to measure the conditions to which the system is subjected.
- A meteorological and scientific mission. The gondola, weighing 400 kg, must remain at a constant altitude for several days, after which it must be recovered.

The balloon is tethered at the time of launch and the cable is let out from a winch on board a ship. During the flight, control of the balloon is possible through the interaction of the winch and the ship. These important operational procedures allow for recovery of both the tether line and the gondola.

Moreover, light-weight sensing devices (about 10 kg), capable of movement along the tether line, permit continuous meteorological measurements.

### 4.2 Project "ARAIGNEE"

This project is being carried out by CNES in collatoration with the Aeronomy Service.

It is designed to accommodate long-duration experiments in aeronomy and meteorology (greater than 1 month).

The system consists of several fixed or mobile packages (gondolas), with a maximum single package weight of 100 kg.

The balloon, the tether cable and some packages are launched in free flight. During the ascent the cable is unreeled and, after the balloon is at ceiling height, the lower extremity of the cable is recovered and secured to an anchoring device.

Long duration station-keeping, is carried out without ground control in the interest of keeping project costs low.

Recovery of the tether cable is not guaranteed.

#### 4.3 A Practical Operational System

Upon completion of the two preceding projects a practical operational system will be developed.

### 5. THE 1973 EXPERIMENTS

The first ESSOR and ARAIGNEE experiments took place in October and November at the Guyana Space Center.

#### 5.1 The ESSOR Campaign

There were two launchings: The first was unsuccessful as the polyester cable broke at an altitude of 4000 m, following a mechanical failure in the winch. The second was successful, whereby a 320 kg gondola was maintained at a ceiling of 17,000 m for twelve hours, at an ambient temperature of less than  $-80^{\circ}\text{C}$ . The cable used was made of Dupont de Nemours PRD resin which had twice the strength of the previous polyester cable.

For both flights the other system characteristics were as follows:

- Balloon: of the open type, natural shape, volume  $10,000\text{ m}^3$ , made of a polyethylene, mylar, and polyester-polyethylene mesh complex. The central exhaust duct was 25 meters long, thus avoiding large gas exhaust with aerodynamic wind pressure. The balloon envelope could withstand tension at the hook of nearly two tons.
- Gondola: Ballasted take-off weight: 740 kg  
Weight at ceiling: 320 kg



— Technological Measurements Made With About 60 Sensors:

Measurements of atmospheric conditions: pressure, temperature, wind speed (with several types of sensors, in the interest of aiding future selections and of obtaining operational evaluations).

Numerous temperature measurements in the gondola and on the balloon.

Cable tension, vibration, and inclination measurements.

Measuring the gondola's dynamic behavior.

Measuring operational control of the gondola.

- Winch: Power rating: 80 HP, set-up on a naval ship, maximum unwinding speed 10 m/s; maximum wind-up speed 8 m/s.

— Launching Procedure:

The launching site, situated on Ile Royale, off Guyana, offers a surface, protected from the prevailing winds, of only 35 x 50 meters.

The launching method used was that of the auxiliary balloon plus guidelines, acting as guides and brakes.

— Guidance Procedure During Ascent:

A program was worked out whereby the ship was moved as the winch unwound, to avoid severe stresses on the cable (caused by aerodynamic forces acting on the balloon) until it had been completely filled.

— Field Test Results:

The ESSOR Field Test allowed qualification of both the balloon and the operational procedures. The parameters, recorded for 12 hours only, due to a false remote control order, showed: The existence of an important heat problem as the temperature at the center of the gondola dropped at an average of 3°C per hour.

Absence of substantial harmonic vibrations in the gondola; however, atmospheric conditions were particularly favorable.

Good behavior of the balloon at the ceiling, but the mechanical balloon-cable coupling makes it difficult to design a stabilized gondola.

## 5.2 ARAIGNEE Campaign (English "Spider")

One flight took place: a failure, caused by cable rupture after it had unwound 3 km.

The system characteristics were as follows:

- Main Balloon:

Twin-envelope balloon, the outer envelope with a volume of  $6,800 \text{ m}^3$  and the inside envelope  $2,800 \text{ m}^3$ . The helium is between the two envelopes. The inside envelope is filled with air through a long hose serving as a dynamic pressure sensor. The balloon thus keeps its natural shape between the altitudes of 16 and 19 km despite the relative wind. Aerodynamic forces are minimized and the risk of loss of lifting gas is nil.

- Auxiliary Lifting Balloon:

Volume  $600 \text{ m}^3$ , for vertical guidance of the system during its free-flight ascent.

- Cable:

Polyester, total untensioned length—17 km. The first length of 3 km is 5.5 mm in diameter, and the second of 14 km, 4 mm in diameter.

- Cable Unwinding Procedure:

The cable is wound on its drum and is suspended from the balloon as the assembly rises in free flight. At the chosen altitude, according to the wind profile, a pressure contact releases the reel which descends, unwinding the cable. To brake this descent, the cable, when it leaves the reel, passes around a capstan. The latter is braked as it rotates, by blades turning in the air on the Renard Mill principle.

- Renard Mill:

Designed and built in a very short period, it had an empty weight of nearly 150 kg, achieved by a configuration based on aluminum alloy structural shapes.

- Launching Method:

Analogous to that of the ESSOR Project, but the additional presence of the auxiliary ascent balloon required development of an automatic device to jettison this balloon in the dynamic launching phase.

— Flight Results:

This flight was an "all or nothing" trial of the ARAIGNEE System. The 3 km of cable, 5.5 mm in diameter, unwound according to theoretical calculations up to an altitude of ascent of 9 km. The breakage was at the beginning of the 4 mm diameter section. Dynamic stresses caused by a capstan rotation speed of 2,000 rpm were doubtless incompatible with the local weakness of the polyester cable. By design, the balloon provided its own safeguards; the outer envelope burst at 19 km altitude, and the scientific gondola was recovered in good condition thanks to the inside envelope which remained full of air during the entire descent.

## 6. CURRENT WORK

Experiments planned for 1974 and 1975 have the same objectives as the previous year, and are also motivated, scientifically speaking, by atmospheric physics experiments, requested by COVOS (Committee for Studying the Consequences of Stratospheric Flights).

### 6.1 ESSOR Technical and Operational Program

Three flights are scheduled for late October and early November 1974 at the Guyana Space Center.

The main purpose of the first two is to obtain scientific results without seeking operational and technical innovations which would involve the risk of failure.

The third flight is a technological attempt of recovering the gondola and cable with a parachute. Technically speaking, the following improvements have been made:

- New winch, 600 hp, providing a maximum speed of 20 m/s for unwinding and the possibility of high-tension winding. It is characterized by excellent flexibility in use and automation in piloting, control, and safety.
- The cable, 5 mm in diameter, is of PRD 29 fiber and is able to stretch by about 4 percent instead of 2 percent as with the 1973 cable.
- The gondolas have been redesigned from the heat standpoint: new arrangement of sensitive elements, and testing of a catalytic heating device. However, due to lack of time, methods based on very low temperature technology will not be tried until 1975.

- Operational:

The launching conditions are improved by setting up a wind break protecting the inflation area.

The equilibrium of the balloon-gondola-cable system is more stable. If necessary, extra tension of about 200 kg more than the 1973 conditions will be achieved at the ceiling by remote control ballasting.

Control procedures during the ascent and at ceiling are better designed, safer, and will benefit from a mathematical program of static and dynamic equilibrium, operating on real-time.

During this field trip, the first VAMPIRE prototype light gondolas, capable of moving along the cable, will be tested. They will be operationally developed in 1975.

#### 6.2 ARAIGNEE Operational and Technical Program

The year 1974 is devoted to the operational studies and technical improvements in the devices necessary for correct operation of the ARAIGNEE System.

In July, August and September 1975, the first long-duration test will be attempted at the Guyana Space Center.

- Flight Procedures:

Ascent of a twin envelope balloon in free flight (Volume 35,000 and 15,000 m<sup>3</sup>), a gondola of about 100 kg, a ballast base of 400 kg, an auxiliary ascent balloon, and a cable unwinder.

During the ascent, the cable unwinding function is activated according to the wind profile and to the manner in which the vertical rate of travel of the balloon is controlled.

The balloon will be at its temporary ceiling at an altitude of about 20 km, chosen because winds are light.

The cable unwinder is picked up at sea. It is towed by a small boat to the anchoring point and cable unwinding continues until the balloon reaches the rated altitude of 22 km. The cable is attached to its mooring point.

The balloon will be in position for a long time. Equilibrium conditions are achieved by deballasting.

Depending on the wind profile, ascent of the first mobile 70 kg gondola up to 20 km and a second identical gondola up to 18 km will occur. These two gondolas will be maintained on station for a long time.

Depending on the scientific program and the weather conditions, repeated explorations in the atmosphere between 0 and 18 km will be conducted with 40 kg slow-moving gondolas.

After recovery of all the mobile gondolas, the flight is brought to an end by breaking the cable. The outer balloon envelope bursts and the inside envelope constantly fills with air thus braking the free descent of the gondola attached at the topmost point.

#### Contents

1. Introduction	93
2. Effects of the Balloon System on the Electrical Environment	94
3. Experimentation	95
4. Geometric Models	96
5. Summary of Test Results	96
6. Vulnerability of Tether Materials	97
7. Relative Probabilities of Lightning Strike	99
8. Safety Considerations	99

## The Interaction of Tethered Aerostats with Atmospheric Electricity

Texey A. Hall  
Project Engineer  
Pan American World Airways  
Aerospace Services Division

### Abstract

This program was conducted to determine the effect of interactions between tethered balloon systems and the atmospheric electrical environment and to identify practical and effective approaches to lightning protection for such systems. A series of experimental flights were designed by the University of Miami, School of Atmospheric Science and conducted by the Range Measurements Laboratory with the assistance of University of Miami professor, Dr. Don J. Latham. Assessment of hazards, based on these experiments, was performed by Dr. E. T. Pierce and Mr. Gary Price, Stanford Research Institute. Extensive materials' testing was performed by J. R. Stahman, Lightning and Transients Research Institute. A commercially available lightning hazard level indicator was evaluated by the RML. This paper summarizes the program approach and results.

### 1. INTRODUCTION

The Range Measurements Laboratory (RML) has long regarded lightning hazards and attendant limitations as the last obstacle to a truly operational tethered balloon system. Toward the end of surmounting this obstacle, RML has

conducted an extensive research program in the interaction of tethered balloon systems with atmospheric electricity. Under a contract with the University of Miami, Dr. Don J. Latham designed a series of experimental test flights to determine the effect of the balloon and tether on the natural electrical field. The total program approach was reviewed by three other highly respected atmospheric electricians: Dr. Edward T. Pierce, Stanford Research Institute, Prof. Charles B. Moore, New Mexico Tech, and Dr. Martin A. Uman, University of Florida. The results of this testing were analyzed by Dr. Latham and also by Dr. Pierce and Mr. Gary Price of Stanford Research Institute, who performed statistical prediction of the probability of lightning strike to tethered balloons.

Testing of balloon materials with simulated lightning for the purpose of quantizing the vulnerability of these materials and identifying optimum materials and protective techniques was conducted by Mr. J.R. Stahman of the Lightning and Transients Research Institute.

## **2. EFFECTS OF THE BALLOON SYSTEM ON THE ELECTRICAL ENVIRONMENT**

A long vertical grounded conductor will distort the natural electrical field as shown in Figure 1. The electric flux lines intercepted by the tether result in interception of a small amount of air-earth current which flows down the tether to ground. Compression of equipotential surfaces above the balloon results in an enormous field intensification in that region.

The effective shorting of the field by the tether results in suppression of the field near the tether, at ground level.

The field intensification at the top of the balloon results in streamers - the significance of which is indicated in Figure 2.

### **2.1 Development of the Stepped Leader**

At the inception of a lightning stroke, an ionized column of air moves from the cloud toward a charge opposite to its own. This column advances about 50 meters in a microsecond, pauses infinitesimally, then advances again frequently branching, always in the general direction of opposite charge. This precursor of a lightning stroke is called a stepped leader.

The approaching leader induces an opposite charge on the ground and the resulting high field causes breakdown of the air at points of localized field intensification and ionized columns 50 or so meters in length extend upward from these points - which could be fence posts, pine needles or perhaps tethered balloons. Eventually the stepped leader connects with one of the streamers - probably the highest one and at that instant the developing lightning stroke has found a home and its path is certain.

Note, before we go to the next view, the downward branching of stepped leaders for this type of stroke.

## 2.2 Triggered Lightning

Now if the ambient field is quite high - say over 10,000 volts per meter, and there exists at the top of the balloon a local discontinuity well in excess of one megavolt, then the streamer emitted from the top of the balloon may become self propagating and create a stepped leader extending upward to some charge center before that charge center has had an opportunity to develop its own leader. The resulting stroke is said to have been triggered, since it would not have occurred if the balloon had not been there. Triggered lightning strokes can generally be identified by their upward branching, as shown in Figure 3. Careful observation of lightning to tall structures has indicated that structures less than 70 M high seldom trigger lightning, whereas the Empire State Building, about 400 meters high, triggers over 80 percent of the lightning that strikes it.

So far we have assumed that the balloon is at ground potential, which is not obviously the case, since the tether materials presently used are highly dielectric when clean and dry. The assumption of ground potential by a balloon tethered by a poorly conductive rope can only occur by gradual charge transfer. The parameters indicative of this process are field enhancement above the balloon, field suppression at the tether point and current flowing down the tether. These indicators can be measured in fair weather.

## 3. EXPERIMENTATION

### 3.1 Airborne Measurements

Potential gradient above the balloon was measured by NASA 6. This instrumented aircraft, operated by the NASA - Kennedy Space Center, is equipped to measure field along three axes. The measurements were made with the aircraft flying overhead passes on upwind and crosswind headings at various altitudes from 100 to 1,000 feet above the balloon. One such overflight is shown in Figure 4.

### 3.2 Ground Measurements

Five deployable measuring systems as shown in Figures 5 and 6 were located near the winch and 100, 200, and 500 feet away. Potential gradient was measured by a device known as a field mill. Air-earth current was collected by a one square meter plate and measured by a sensitive ammeter. These measurements were strip recorded along with tether current and wind velocity.



Three different balloon systems were used for these tests - the 205,000 cubic foot Family II system, the 84,000 cubic foot BJ+3 and the 5,300 cubic foot Schjeldahl balloon (Figure 7) which we generally refer to as "Baldy".

A special winch system was built for Baldy to facilitate the comparison of well conducting and poorly conducting tethers. Two winches, one loaded with 1/8" steel cable and the other with 1/4" nylon rope were mounted on porcelain insulators permitting the winch to be grounded or isolated from ground as desired. (Figure 8).

The flying sheave was similarly isolated. As shown in Figure 9, tether current was measured by grounding the system through a pico ammeter. If all grounds were removed and the system allowed to float, the potential of the tether could be measured by a field mill located below a plate attached to the winch. For comparison with test data, several geometric models of the balloon system were considered.

#### 4. GEOMETRIC MODELS

With a well conducting tether and a poorly conducting balloon, we assume that the dominant geometry would be that of the tether. The mathematics in this case are greatly simplified by modeling the tether as a long thin vertical grounded semi-ellipsoid - here of course the minor diameter is greatly exaggerated to emphasize the geometry. (Figure 10).

If we assume that more field lines terminate on the balloon than on the tether, then the balloon, modeled as a horizontal prolate ellipsoid above a conducting plane, would be the most representative geometry. For a well conducting tether the ellipsoid is assumed to be grounded. For a poorly conducting tether, it is assumed to be charged to some potential. (Figure 11).

#### 5. SUMMARY OF TEST RESULTS

The results of test data analysis can be summarized as follows: the data from balloons with poorly conducting tethers agreed reasonably well with the charged horizontal ellipsoid model. Cumulative charging with time was noted, and charging rate was consistent with measured tether current.

The BJ+3 balloon flying at 1,000 meters with .625 Nolaro tether was fully charged in about one hour. The Family II balloon, flying at 1500 meters with .775 Nolaro tether was only charged about 3 percent after 3 hours aloft. This balloon was operating above the mixing layer where the air was more conductive than the tether material.

The data collected during balloon flights with steel tether fits none of the above models.

We learned that the dominant effect in the case of a well conducting tether, as predicted by C. B. Moore, is a plume of corona-produced space charge flowing downwind from the tether. From the field graph, Figure 12, it can be seen that potential gradient increased gradually as the aircraft approached the balloon from downwind then decreased abruptly after the aircraft passed over the balloon. This effect is indicative of a corona space charge plume flowing downwind from the tether near the balloon. These measurements are consistent with the theoretical charge density for a stream of space charge diffusing downwind in a conical pattern with a  $10^\circ$  cone angle.

Additional evidence of corona production is given by the measured values of tether current, which greatly exceeds any possible current due to air to earth current - but agrees more closely with theoretical values of corona current.

## 6. VULNERABILITY OF TETHER MATERIALS

A prime concern for tethered balloon users is that a lightning stroke will part the tether and allow the balloon to escape. Although this did occur a number of times during the second world war, none of the five strikes to balloons, that we are aware of, in recent years has resulted in loss of a balloon, though all resulted in some damage. Our experience at Cudjoe Key in August 1972 is an interesting case. (See Figure 13).

The balloon, flying at about 4,000 feet, was struck by a flash from a cloud which we believe was about five miles away. The initial point of attachment appears to have been about 264 feet below the confluence where a section was de-jacketed. Damage also occurred at four other zones along the tether. The length of these damaged areas varied from five to 80 feet and about 4 percent of the total length of the tether was effected. Breaking strength was reduced from 26,000 lb to 8,000 lb - dangerously close to pulls which might be encountered under the same conditions where lighting is probable. The significant factors here are that a balloon with a poorly conducting tether was struck from a flash from a relatively distant cloud but nobody was killed and the system survived intact.

### 6.1 Synthetic Fiber Tethers

We have extensively tested Nolaro tether samples by exposure to electrical pulses up to 200 kilo amps and have been able to produce damage resembling that of actual lightning. General conclusions which we reached are:

(1) The probability of the tether being damaged on a per stroke or per length basis is relatively unpredictable.

(2) It is very difficult to damage short samples of Nolaro with simulated lightning unless the interior of the cable is wet. However, we were not able to simulate the very destructive long duration - low current phase of a lightning flash.

(3) Anything which encourages entry of the lightning streamer through the jacket resulted in damage or total destruction of the test sample - for example - introduction of wires inside the tether.

(4) Superficial wetness or dirt did not diminish the survivability of the tether. In fact it appeared that any measure which increased external conductivity relative to internal conductivity appeared to enhance survivability. Limited testing indicates that aluminum paint on the tether reduced the likelihood of damage.

#### 6.2 Steel Wire Ropes

The materials testing program also included testing of steel cable samples. The two most promising materials appear to be stainless steel and extra improved plow steel. Plow steel is much cheaper and as Figure 14 indicates, it has a better strength to weight ratio at normal temperature. Stainless steel has better corrosion resistance and retains more strength at elevated temperatures than does plow steel. As indicated in Figure 14, stainless steel exposed to a 120-coulomb lightning flash would be slightly stronger than extra improved plow steel of the same cross section. Also near this crossover point, the plow steel has reached a temperature of 600°F, beyond which it will not regain full strength even after cooling. Stainless steel (type 304) regains full strength after cooling down from temperatures up to 1,000°F. Some actual test results for one quarter inch cable are shown in Figure 15.

#### 6.3 Comparative Performance of Steel and Synthetic Fiber

The performance of steel cable is more predictable than that of Nolaro, since the steel cable is forced to conduct the entire lightning current - the statistics of which are reasonably well known. Based on a mixture of theory and experiment we cautiously offer a rule of thumb that a steel tether less than 3/8 inch diameter should be stainless steel. A tether of 1/2 inch diameter or greater can be made of extra improved plow steel with reasonable safety. In between, we must trade off cost and weight against system survivability.

A lightning stroke traveling down a jacketed Nolaro tether is guided rather than conducted by the tether. The energy for the most part appears to flash along the surface, possibly hopping from one speck of surface contaminant to the next,

however, it occasionally penetrates the sheath with destructive results. More development and testing is needed to fully evaluate the effectiveness of protective coatings as well as the feasibility of producing tether with such coatings.

## **7. RELATIVE PROBABILITIES OF LIGHTNING STRIKE**

We believe that a balloon tethered by a well conducting material such as steel is more likely to be struck by lightning than a balloon tethered by a poor conductor such as dry clean Nolaro - however, we don't think the difference is great for several reasons: First, we have shown that the poorly conductive tether does transfer charge and will eventually look like a grounded system to the environment. Second, it is operationally difficult to maintain a poorly conducting tether as such, especially in a coastal environment. In either case the probability of a stroke is sufficiently high for durability to be a prime concern.

## **8. SAFETY CONSIDERATIONS**

### **8.1 Warning Systems**

Another region of concern has been warning and safety. Lightning warning is needed to two time phases - early and immediate. Notice that thunderstorms are an hour or more away must be based primarily on meteorology. Weather radar is needed for this and iso-echo contouring is valuable but not essential. Any radar such as a surplus airborne radar with weather mode is better than none at all. The value of a radar can be considerably enhanced by the addition of a lightning direction finder. A simple UHF lightning direction finder has been developed by Krider (University of Arizona) and Uman (University of Florida). This system puts a strobe on a radar scope indicating the direction of the ground contact of the stroke. Unlike HF sferics systems, it is effective at ranges less than 50 KM.

Much of the lightning menacing Florida balloon operations is from air mass storms which grow in the immediate area rather than advecting from afar. For these storms and for general short term warning a system embodying the features of a field meter and a flash counter is needed. We have obtained and are evaluating one such instrument. This system provides readily interpretable indications of the probability of a lightning flash to ground within a nominal 8 mile radius. The data collected indicates that this approach is promising.

### **8.2 Crew Protection**

In the event that a lightning flash does come down the tether, the most endangered person would normally be the winch operator. Proper grounding of the winch reduces hazard to other personnel on the pad, but does relatively little for the winch operator. The safety of the winch operator can be enhanced by enclosing his operating position in a Faraday cage, with all conductors from the outside world entering through conduits well bonded to the outside of the cage.

### **8.3 Requirements for Personnel Safety**

The key principles of lightning safety for balloon operating personnel are:

- (1) An early warning system giving sufficient warning to permit appropriate action without undue haste.
- (2) Short term warning to indicate the need of clearing the pad of all non-essential people.
- (3) Protective enclosures for anyone who must remain near the tether point.
- (4) And last, but equally important - a well conceived and firmly implemented safety plan.

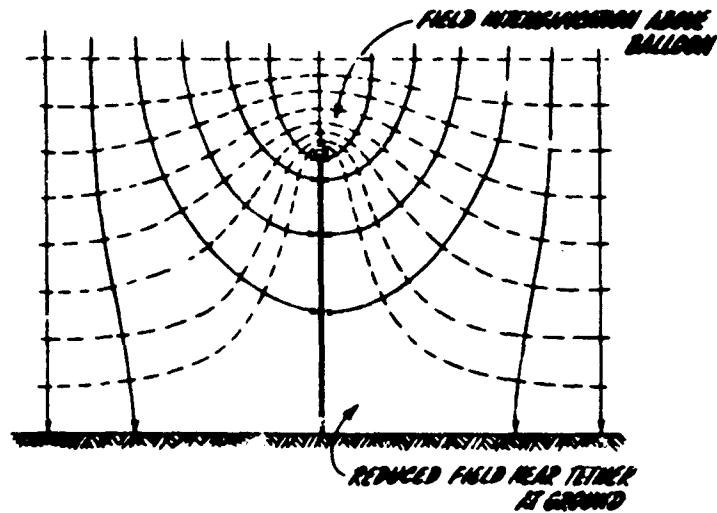


Figure 1. Electric Field Pattern Perturbed by Presence of Balloon

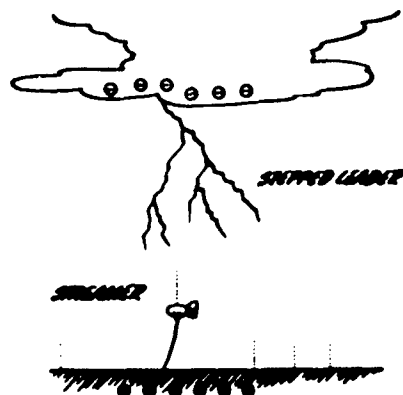


Figure 2. Formation of Downward Stepped Leader

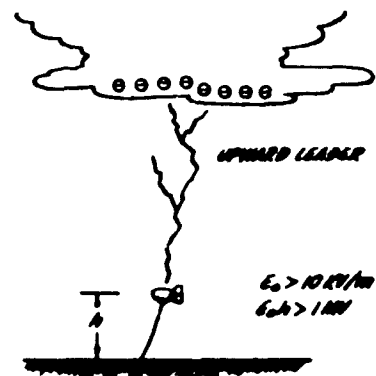


Figure 3. Triggered Lightning



Figure 4. Overflight of the "Baldy" Balloon by NASA-6, an Aircraft Instrumented for Measurements of Potential Gradient



Figure 5. The Deployable Measuring System for Ground Level Measurements of Potential Gradient and Air-earth Current

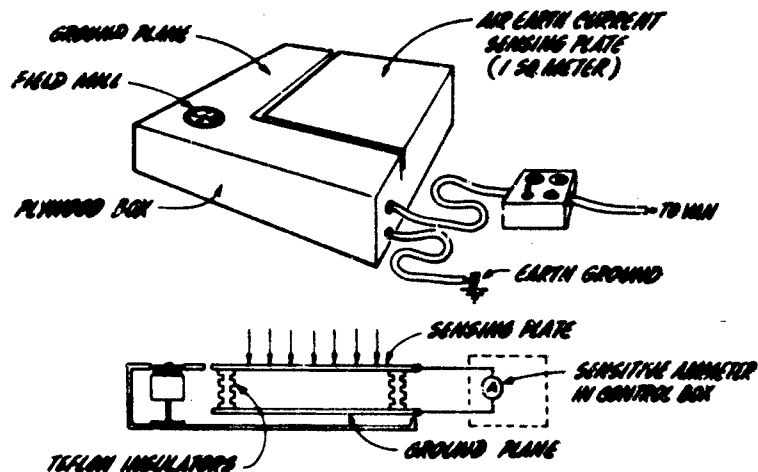


Figure 6. Deployable Measuring System

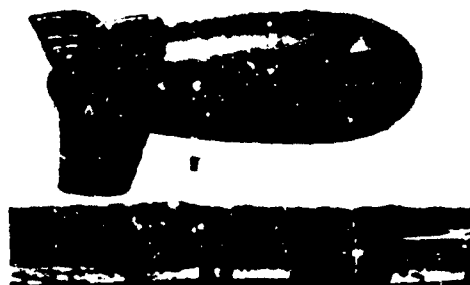


Figure 7. "Baldy", the 5300 cu ft Schjeldahl Balloon Prepared for Ascent



Figure 8. Winches for Steel and Nylon Tether Cables Mounted on Porcelain Insulators

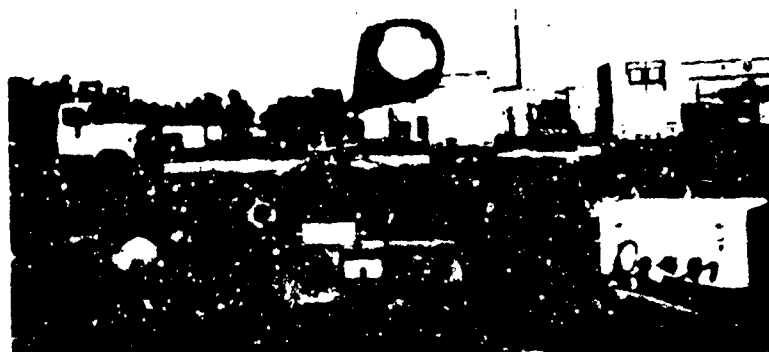


Figure 9. Tether Current Measuring System Consisting of Isolated Flying Sheave Grounded Through a Sensitive Ammeter With Recorder Interface



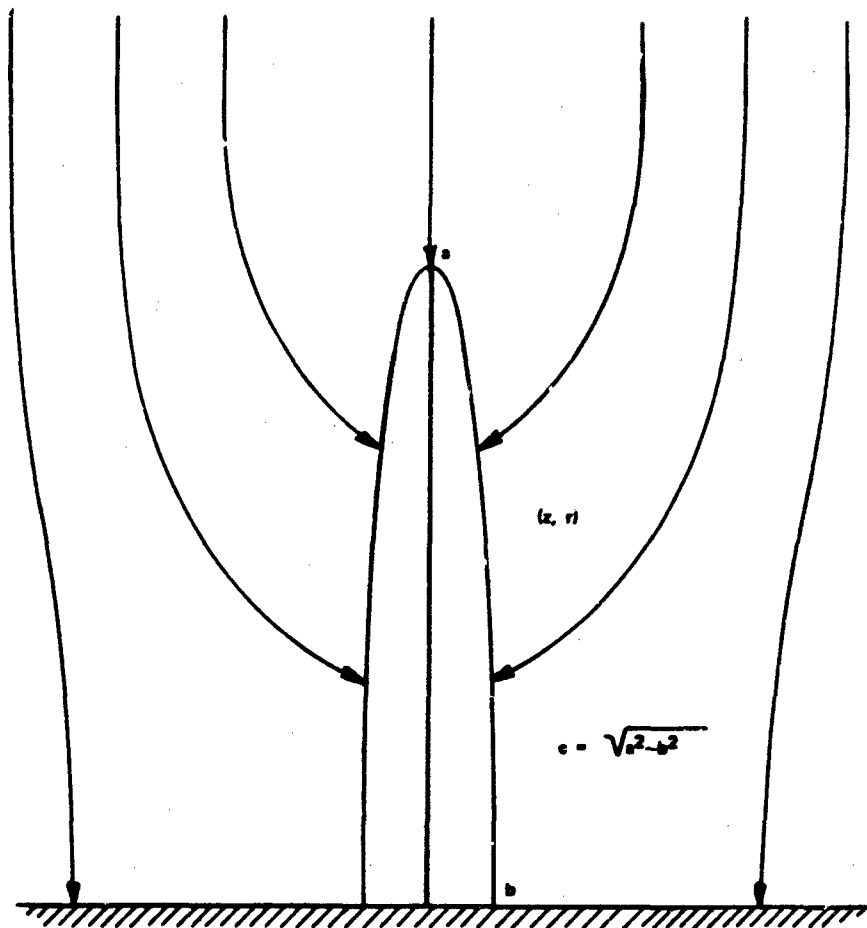


Figure 10. Tether Modeled as a Vertical Prolate Ellipsoid

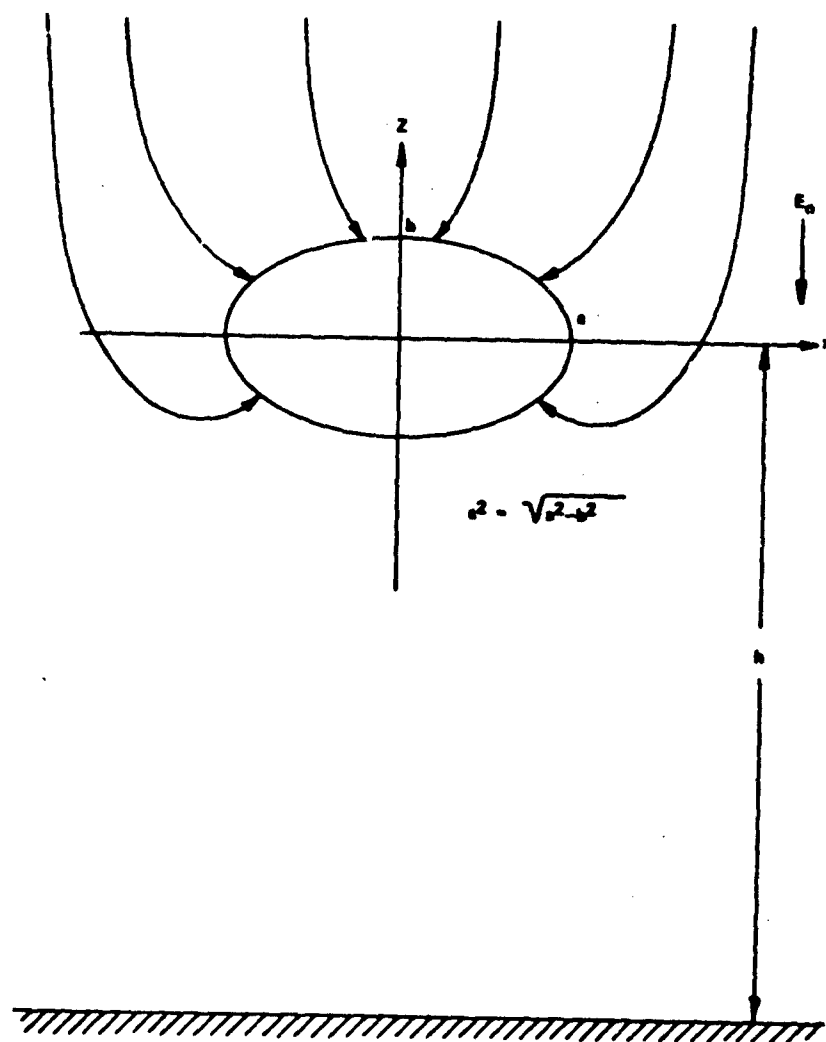


Figure 11. Balloon Modeled as a Horizontal Prolate Ellipsoid

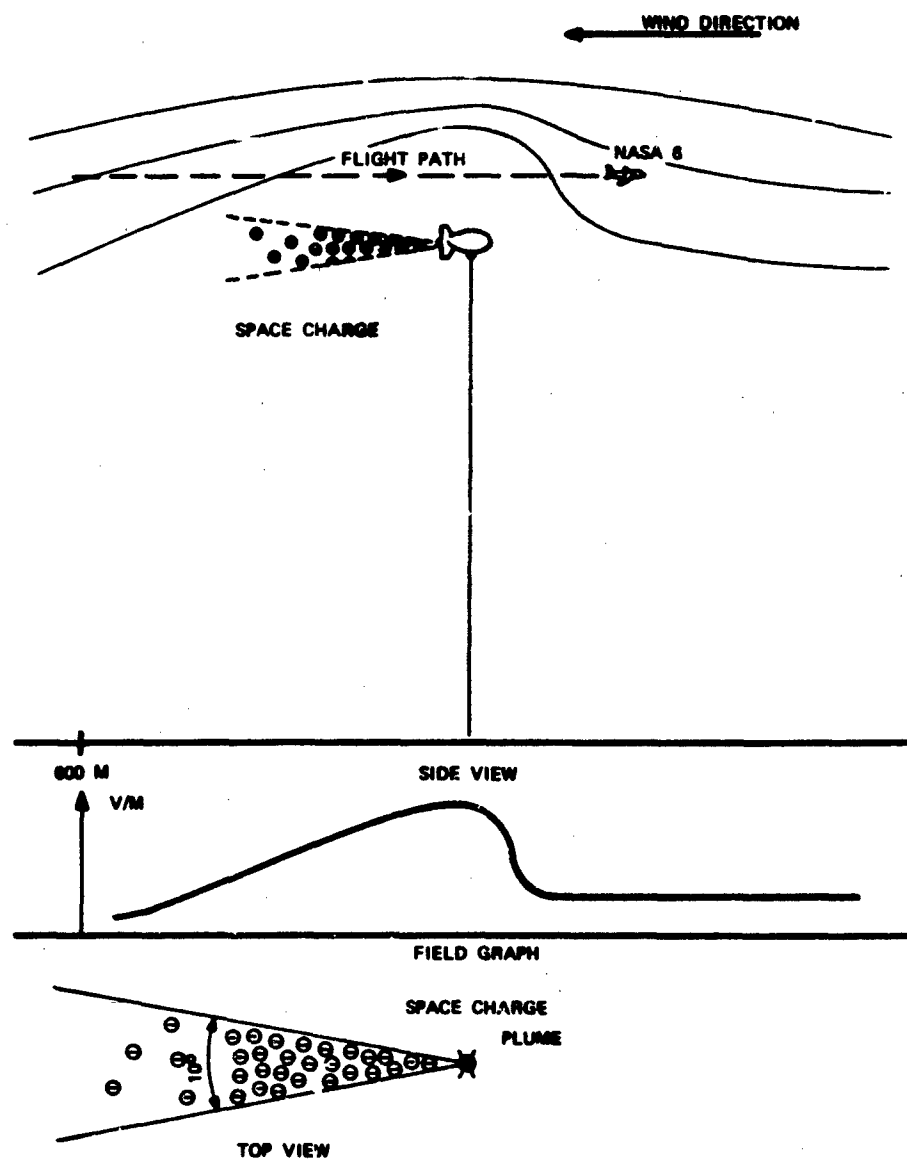


Figure 12. Effect of Negative Charge Plume Blowing Downwind From Balloon

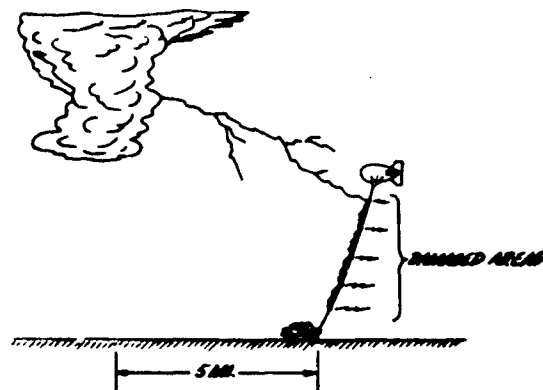


Figure 13. Lightning Incident at Cudjoe Key - 18 August 1972

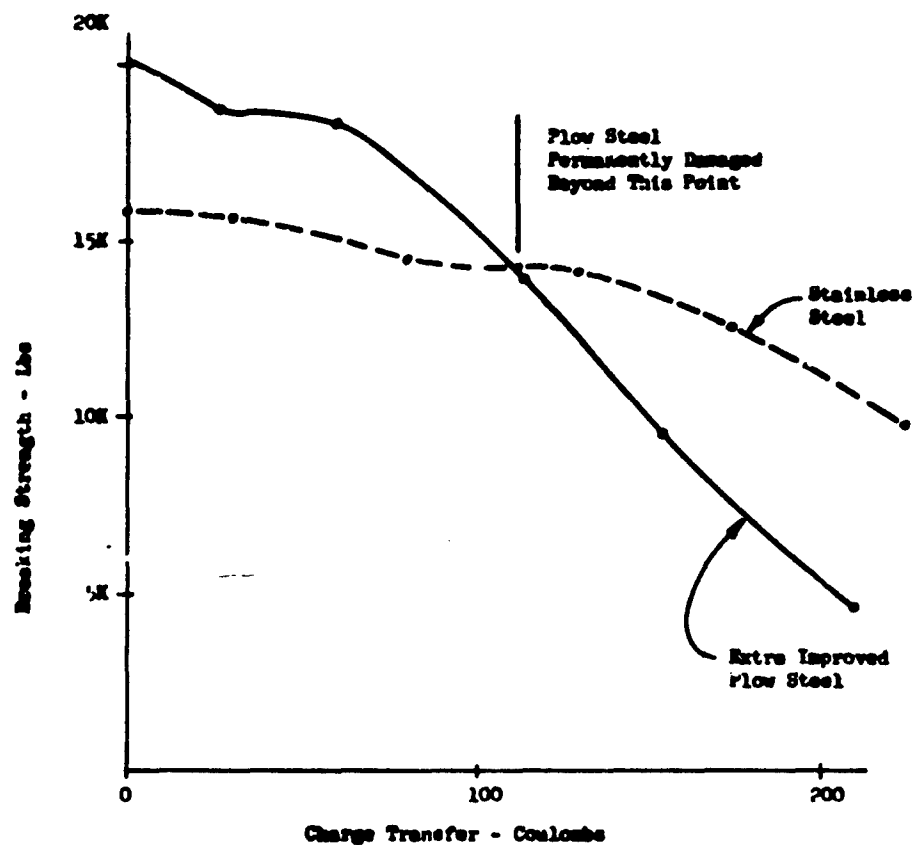


Figure 14. Theoretical Effect of High Charge Transfer On Breaking Strength of Steel Cables

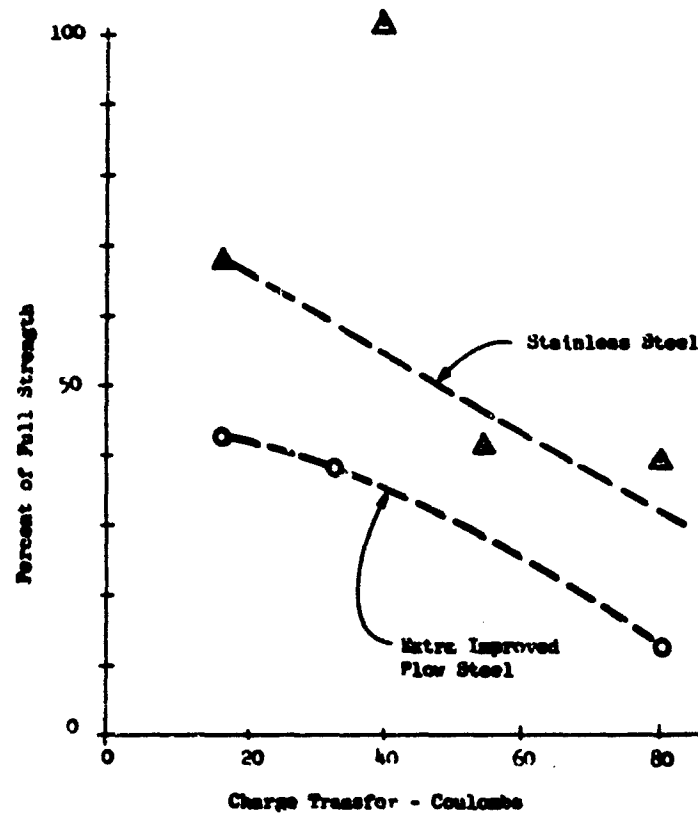


Figure 15. Observed Effect of Charge Transfer On Breaking Strength of Steel Cables

#### Contents

1. Introduction	109
2. Aerodynamics Considerations	111
3. Improved Materials	111
4. Improvements in the Pressurization System	112
5. Power Supply Developments	115
6. The Nose-Structure Problem	116
7. Summation of Improvements	117
8. Conclusions	119
Acknowledgment	119

## Design Trends of Future Aerostat Systems

E.L. Crosby, Jr. and T.H. Yen, Jr.  
R.C.A. Tello Project\*

### Abstract

A rationale is developed for an improved design large tethered balloon to replace the IID-7 model currently in use by the Range Measurements Laboratory. Substantial gains in flight performance and mission duration are seen to be possible.

### 1. INTRODUCTION

For the last 3 1/2 years the RML has been flying balloons of the IID-7 design. This balloon is a 200,000 cu. ft. aeroform balloon designed to carry a 750 lb. payload to 10,000 feet and supply it with 2.7 KW power. Its weather design limit is 90 kts. wind velocity and it has flown successfully at more than 65 kts. All of the more than 200 flights have been heavily instrumented; and, with minor and very infrequent exceptions, we have been fortunate in getting good data. These

---

\* (RCA International Service Corp. is a Contractor to the Range Measurements Laboratory (RML) of the Air Force Eastern Test Range, Patrick Air Force Base, Florida).

data have been analyzed together with wind-tunnel results and theoretical inputs, and have provided a reasonably complete and acceptably accurate understanding of the IID-7's performance. TELTA Report TR 74-058, "Design Verification of the IID-7 Balloon" contains the details. Also, practical daily contact with this active vehicle has given an unusually good opportunity to observe the many technological aspects of the system design—such things as durability of materials, power plant operation, lifting gas management and so forth.

Based upon this experience, and upon contemporary progress in contributing technologies, there has emerged a well-founded concept of an improved-design vehicle for this general mission. This paper will describe the details of these improvements, their basis, and the results expected. In this discussion, our basis will be the "standard IID-7" which is an hypothetical "centerline" version of the balloon.

As all balloon designers know, since the balloon is a buoyant vehicle used to elevate and suspend a mass, its weight is of paramount importance. In fact, other considerations such as stability being equal, the figure of merit by which comparisons are made is the payload weight/balloon-size ratio. It is not surprising then, that the advantageous design improvement usually affect gross weight either directly or indirectly. This is the case with the discussion which follows. To get an idea of the interactions which affect weight, consider the diagram of Figure 1. Here are shown a number of improvement topics in the

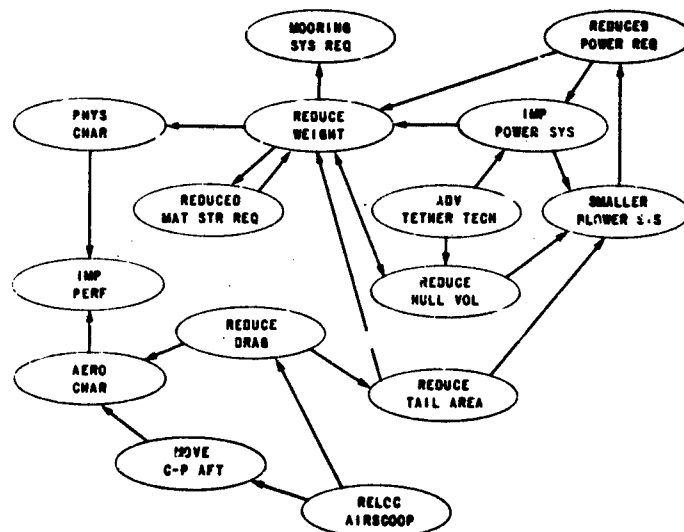


Figure 1. Relation of Balloon System Design Parameters to Vehicle Gross Weight

context of the IID-7 and how they relate to vehicle weight. We shall now go into detail on the contemplated design innovations, beginning with those which are rather directly connected with aerodynamic performance.

## 2. AERODYNAMICS CONSIDERATIONS

Analysis of flight records indicates that the chin airscoop accounts for 10 percent to 14 percent of the total balloon drag and it is desirable to relocate it. Estimates based on drag calculations for some of the other appendages which could be improved such as trailing lines, give a value of possible drag reduction of about 1 percent from these sources. Taking the median value of scoop drag, a value of 13 percent is obtained. By subtracting this drag and solving for the resulting trim angle at 65 kts on the standard IID-7, a value of  $2.68^{\circ}$  is obtained, as compared with  $2.95^{\circ}$  without drag reduction. We would like to restore the trim angle, primarily to maintain aerodynamic efficiency. Using lift and drag coefficients established for the hull only compared to the fin only as obtained in wind-tunnel tests, and applying the direct proportionality of forces and areas, we find that a 5 percent reduction in horizontal (tail) surface area brings the pitch trim angle back to  $2.74^{\circ}$ . However, it is accompanied by a net reduction in total lift. Therefore since the balloon's optimum performance is so dependent on lift, an engineering tradeoff is called for. The elimination of the chin scoop, in any case, is desirable because of the reduction in drag. Another advantage lies in the improvement in lateral stability because of the resulting movement aft of the net effective center of pressure.

Relocation of the chin airscoop to a location at which its drag is appreciably less is limited to integrating it with the forward end of the windscreen. This has been carefully considered and is advantageous because the profile drag of the windscreen is already accounted for and addition of the scoop would probably not increase it significantly. The disadvantage is primarily the structural complication.

Further consideration of the chin scoop drag problem led to the simple but elegant solution of merely eliminating it, and deriving hull ram air from the tail scoop. This proposal will be carried further in a later paragraph, since it involves operation of the hull and tail at the same pressure.

## 3. IMPROVED MATERIALS

Turning to improvements of other types, we again look to flight test results. Data indicate that at 65 kts the highest fabric stress was 53 lb/in. at the point



of maximum hoop-stress. This point also was loaded by the suspension system. This value is less than 1/3 of the ultimate grab-tensile strength of the material, indicating that a considerably lighter fabric of the same type would suffice. However, a fiber of higher specific strength, Kevlar, also has a considerably greater elastic modulus. We could therefore postulate an idealized fabric of greatly reduced weight, somewhat lower ultimate strength but which would still have less deformation due to stretching under load. In this connection it would be most desirable to fully evaluate triaxially woven cloth since its shear stability and high tear-strength would make it unnecessary to use multiple-ply fabric. This feature, among its other advantages, greatly improves fabric performance where ply adhesion is a problem, such as at seams and load patches. The coating plays a particularly important role in fabric of this type; and it is very desirable to use the same or a similar compound on both sides of the cloth. For this application, the polyurethanes are currently favored because of their optimum combination of properties. A triaxial Kevlar/urethane hull material of 6 oz/yd<sup>2</sup> appears to be a conservative choice for 200K ft<sup>3</sup> volume.

While on the subject of materials, the tether should be discussed since it is the heaviest single component. The IID-7 has been flown on a polyester Nolaro tether rated at 25K lb break strength and weighing 202 lb/K ft. Flight experience indicates that this design is too conservative, since the highest tension we have measured was about 8,000 lb. In a future design we recommend a break strength of about 17K lb giving a safety-factor of two over our worst case. Making this cable of Kevlar results in a tether weight of about 75 lb/K ft. For a deployed tether length of 15,000 ft, the weight saving is about 1900 pounds! The tether tension due to drag will be considerably reduced because of the decreased diameter, the exact value of which depends on construction. For the NOLARO construction, the diameter would be about 0.6 of that of our present cable, and the drag reduction would appreciably reduce blowdown.

#### 4. IMPROVEMENTS IN THE PRESSURIZATION SYSTEM

Figure 2 is a photograph of the hull air-scoop and fan arrangement of the IID-7 balloon. Note the fabric "flapper-valve" in the throat of the scoop and note also the location of the fan assembly, well above the scoop. These structures are shown schematically in Figure 3. Note the large flapper valve in the air-scoop throat and the anti-return sleeves on the fan discharge ends. The two air retention structures are redundant, and the fans do not efficiently use the ram boost pressure. Both of these drawbacks can be remedied as shown in Figure 4. Here the flapper valve is eliminated, the fan sleeves providing this function. The



Figure 2. Nose and Chin Area IID-7 Balloon

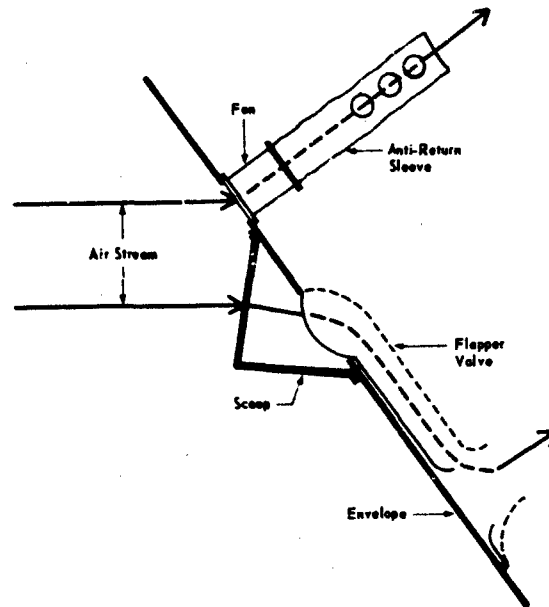


Figure 3. Schematic Cross-Section of Typical Present Airscoop and Fan Area

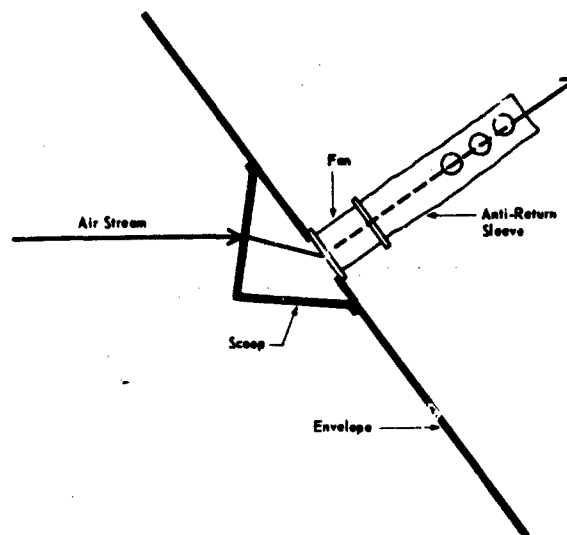


Figure 4. Schematic Cross-Section of Improved Typical Airscoop and Fan Arrangement

fans are relocated to receive maximum developed boost pressure. The net result is a saving of considerable power not only because of higher inlet pressure but the flapper valve does not provide an effective seal, as we found throughout the test program.

We previously discussed chin airscoop elimination and operation of the hull and empennage at the same pressure. While this is considered feasible, it requires relatively close control of pressure since the empennage low-limit and the hull high-limit must always straddle the effective d-p. A pressure regime of  $Q+n$  which has been our goal, can better be realized with the relocated fans and should be instrumented with a well chosen static port and a "Q" transducer.

On the subject of pressure control it would be desirable to redesign the gas valve. The ID-7 uses four valves, two each for helium and air. On flight programs of long duration it is a great convenience in management of helium to be able to compute gas loss due to both the checkout exercise of the He valves and to their valving off gas at altitude, which occasionally occurs. Our present valves take about 25 seconds to open or close; although we have had only one valve malfunction instance (and it was brief) we would like a redesigned valve which would "fail-safe closed". Preliminary design work indicates that such a feature could be incorporated in a valve having a 3 second half-cycle time and weighing about 7 lbs. This represents a weight saving of about 35 lbs for the four valves.

Another test program spin-off was the realization of the superiority of a-c operated fans. The brush wear of the d-c powered fans has an MTO of 1000 hours. A-C fans' MTO is at least 10 times longer. Besides being lighter, the a-c units save more than 100 lbs because of their lighter, high-voltage cabling. Use of a-c fans of course eliminates the safety feature of standby storage-battery fan operation if the power-supply engine stops; however, limited experience has shown that the air-scoop will maintain envelope shape sufficiently for balloon recovery. Elimination of the storage battery saves another 90 lbs.

It was found that a well-sealed payload windscreen could become over pressurized, which resulted in hull distortion and risk of windscreen rupture. This was prevented by installation of poppet-type relief valves. A better solution, which is recommended, is to port the windscreen into the ballonnet, with a manual shutoff to be used when the windscreen is opened.

## 5. POWER SUPPLY DEVELOPMENTS

A discussion of technological improvements would not be complete without citation of the fuel supply tether. Mr. Duggins will report this interesting development but it has a ramification which is significant here. The weight saved by

elimination of on-board fuel storage is considerable. A 24 hr supply for the 5kW IID-7 power plant, including the tank weights about 200 lbs.

The fuel supply tether lengthens the mission time to the point that engine maintenance is the limiting factor. Our logged flying time does not yet permit a sufficient basis for an accurate figure, but for our equipment, 200 hours is beginning to be a good interval for engine adjustment. A comparatively recent development of the thermoelectric converter appears as an attractive alternative. Burning clean gaseous fuel, such a power plant would have an MTO of in the range of 5000 to 10,000 hours. This type of power plant would be slightly heavier than the present one, but its reliability is much higher. This is not a firm recommendation for new balloons but is a very attractive solution to lengthening mission time which is a prime candidate for trial if mission duration is important.

#### 6. THE NOSE-STRUCTURE PROBLEM

The IID-7 balloon carries a 500 lb metallic nose-structure in flight. A view of it is seen on Figure 2. Its massive proportions are evident in Figure 5. It was originally incorporated to prevent dimpling under pressure from high wind

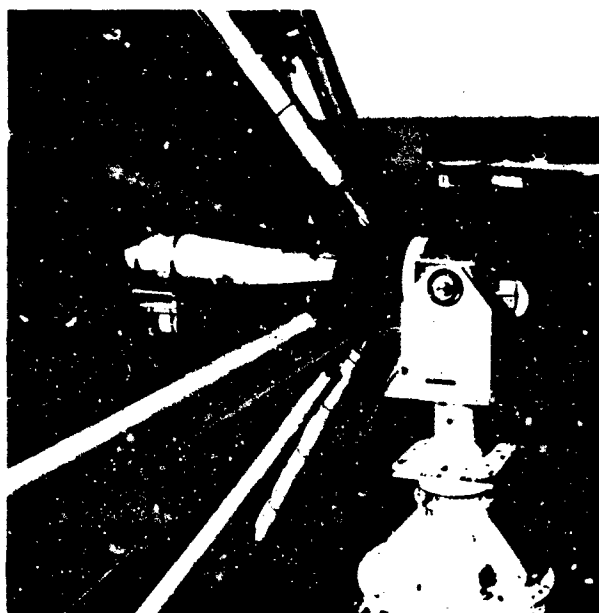


Figure 5. IID-7 Nose Structure

velocities. Our high speed flights showed no dimpling and subsequent analysis has shown that no such danger exists at wind speeds below at least 90 kts. The present purpose of the nose structure is to distribute into the hull the loads imposed by the tower while the balloon is moored. It is obviously most undesirable to penalize the balloon with parasitic weight which is of no use in flight. Therefore a prime target in any new balloon system design would be the elimination of the nose structure. There are several approaches which appear feasible and little doubt that with reasonable development effort it can be done.

## 7. SUMMATION OF IMPROVEMENTS

Let us consider what the foregoing have accomplished. Figure 6 shows a somewhat simplified comparative weight table for the standard IID-7 and a similar balloon to which the improvements we have discussed have been made. The performance of the improved balloon is shown in Figure 7. As can be seen, we have arrived at a balloon which, at 200,000 cu. ft. volume, is much too large for the job, unless a large excess lift margin at some intermediate altitude, say 15,000 feet, is desired. As you who have prepared balloon sizing estimates know, the procedure requires several iterations because when one has excess lift and reduces volume, he again has an excess lift remainder because of reduced weight, and so on.

	<u>STD IID-7</u>	<u>IMP.</u>
Hull Wt.	1950 lbs.	1170 lbs.
Tail Wt.	1065	800
Fan Sys. Wt.	190	90
Battery Wt.	117	27
Valve Wt.	69	34
 TOTAL WT.	 6291 lbs.	 5021 lbs.
TETHER WT.	202 lbs./Kft.	75 lbs./Kft.
MAX. ALTITUDE	12,000 ft.	21,000 ft.

Figure 6. Comparison of STD IID-7 With Improved Balloon of Similar Size

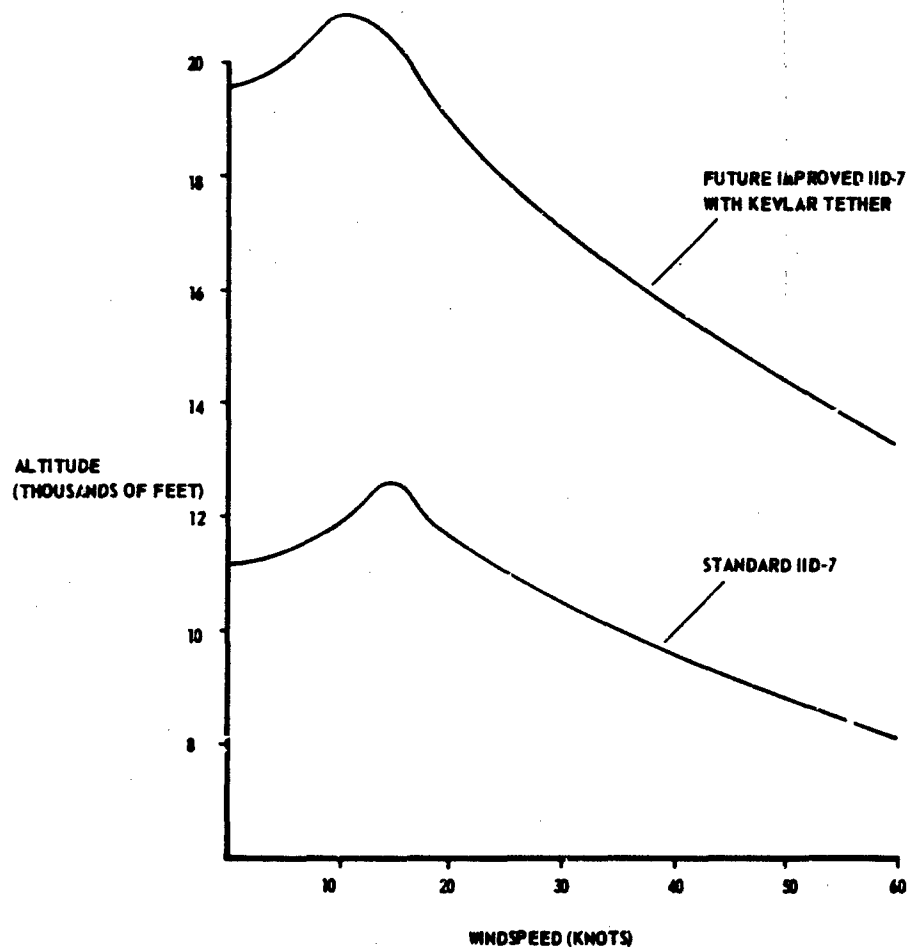


Figure 7. Altitude Vs. Windspeed Performance Comparison of Standard IID-7 Balloon and Improved Version (See Text)

Retaining the original boundary conditions and preparing only the first iteration for a reduced-size IID-7 (more correctly, a IID-8), we obtain a set of numbers using conventional volume-area-weight relationships which are tabulated in Figure 8. The new volume is only 125,000 cu. ft. and the original mission is unchanged.

The resulting superiority in cost and operational convenience is very worthwhile. It should be pointed out, the size reduction would require downward re-estimation of fabric and tether requirements, and, as a result, the new balloon would be somewhat smaller, still.

Payload	750 lbs.
Altitude	10,000 ft.
Volume	125,000 ft. <sup>3</sup>
Length O/A	115 ft.
Hull Dia. Max.	38 ft.
Tail Span	55 ft.
Tether Wt.	60 lbs./Kft.

Figure 8. Predicted Approximate Features of Resized Balloon (Similar to IID-7)

## 8. CONCLUSIONS

The IID-7 has proven to be a very good aerodynamic design. Long practical experience has revealed a number of areas where design revision would result in improved performance. Art-state progress permits other improvements. The next design generation should be smaller and considerably cheaper.

## Acknowledgment

The authors gratefully acknowledge the support and encouragement of Walter H. Manning, Jr., Director of the Range Measurements Laboratory, of Lt. Col. J.H. Watts, Chief, Sensor Platforms Branch, and of Robert P. Murksche, RCA, Manager of the TELTA Project, under the direction of all of whom the TELTA balloon technology has been developed.



**Session 3**  
**Free-Balloon Technology**

**James F. Dwyer, Chairman**  
**Air Force Cambridge Research Laboratories**

## Contents

1. Introduction	123
2. Capability In-The-Large for Zero-Pressure Balloon Systems	132
3. Historical Capability Trend	135
4. Capability Trend Significance	138
5. Capability Trend Extrapolation	139
6. Capability Growth Control	142
7. Relevant Payload and Gross Load Accomplishments	150
8. Conclusions and Recommendations	154
Acknowledgments	155
Bibliography	155
Appendix A	157
Appendix B	161

## Free Balloon Capabilities: A Critical Perspective

James F. Dwyer  
Air Force Cambridge Research Laboratories  
Bedford, Massachusetts

### Abstract

Free balloon systems, classified as zero-pressure, superpressure and air-ballast systems, are reviewed with respect to both achievable flight profiles (in terms of possible flight stages) and the payload subsystems necessitated thereby. Air-ballast systems, with noted exceptions, are treated as having merely theoretical capabilities, sufficiently documented elsewhere. The capabilities and potential of the superpressure balloon are briefly considered and recommended as warranting a thorough independent analysis. For zero-pressure balloons, a capability in-the-large is numerically defined and this macrovariable is proposed as suitable for assessing and planning capability growth. Implications are stated with respect to the historical trend of this variable and, based thereon, suggestions are offered concerning future research and development of zero-pressure balloons. Historical data are appended and references are given.

### 1. INTRODUCTION

An overview of free balloons with respect to capability provides a unique opportunity to examine critically the classes of free balloons, the essential similarities and differences in their flight profiles, and the distinct payload subsystem

functions required for their performance. Moreover, it affords a proper philosophical environment in which to speculate on, and hopefully to establish the existence of a macroscopic capability measure and possible subordinate capabilities. It is my intention to take this approach and where appropriate to introduce supporting historical data. Detail will be limited to ensure an orderly and precise development of the topic and subordinate elements will be introduced and expanded only when needed to clarify, supplement or reinforce the development.

A free balloon system, consisting of the balloon proper and the necessary payload subsystems\*, will be treated as the "carrier", and the user's or project payload\*\* as the "cargo". With noted exceptions, capabilities will be interpreted as relating to providing a time-varying atmospheric environment free of "balloon" induced disturbances, subject, of course, to the limitations of physical laws (ascent and descent necessarily subject the project payload to certain forces). Stated as a definition, capability is a measure of the ability to move a project payload through a specified profile with no "significant" sense of the presence of the balloon system. Two important facts concerning capabilities should be kept in mind. First, they exist in response or relationship to needs either real or hypothesized (independent of whether the capabilities are merely discovered or intentionally developed). Second, they are inherently susceptible to improvement.

The propositions to be developed herein are not the only objectives. Rather, they are intended to serve as stimulants to the imaginations of both the designers and manufacturers of balloon systems. Further, the methods used or referenced are recommended for use in future exercises in planning or analyzing the growth of free balloon capabilities, including both superpressure and air-ballast systems which are treated only peripherally herein. Finally, it is impossible to over-emphasize the importance of a complementary heuristic analysis of requirements (as opposed to capabilities) from the peculiar vantage of the scientific and military user; the historical evidence in this field being predominantly supportive of the viewpoint that technological progress is generally in response to externally imposed requirements, not self-generated goals (i. e. teleological).

Before examining free balloon system capabilities or even rigorously defining capability in the large sense, it is in order that we look at the various types of free balloon systems in terms of how they are constituted and how they perform. The

---

\* The term "payload subsystems" refers to those subsystems described in Figure 2.

\*\* The term "Project Payload" refers to that part of the payload dedicated to mission objectives as opposed to the "payload subsystems." Taken collectively, they comprise the payload (total suspended), symbolically represented as  $W_p$ .

details furnished will be consistent with the established philosophy for the development of the topic and explicit comment will frequently be omitted in favor of a reference to the literature.

#### 1.1 Classes of Free Balloon Systems

Free balloon systems can be divided reasonably and satisfactorily into three classes:

Zero-pressure systems\*

Superpressure systems

Air-ballast systems

The first two classes are (in name) distinguishable by the amount by which the balloon internal pressure at the base exceeds the ambient atmospheric pressure for the fully inflated balloon floating at its design ceiling altitude: zero in the former case and greater than zero in the latter case. Air-ballast systems are named somewhat arbitrarily for one system of their class, one which used the weight of contained pressurized air to ballast the system.

The most widely used class, and the one we shall most fully explore, is the zero-pressure system. There are numerous references to every aspect of this class, but perhaps the most complete catalog was compiled by Rice (1974).

Air-ballast flight systems, from the point of view of the objectives of this presentation, surface a rather unique problem. Except for the new and scientifically exciting work of Blamont (1974), using the air-ballast system principle to fly an isentropic profile, we are confronted with an almost totally theoretical capability. Although considerable effort was expended by Vitro Laboratories under contract to Air Force Cambridge Research Laboratories (AFCRL) and reported by Davidson (1967a, b) and (1968), a successful system was not flown. The only known flight of such a system, within this country, was a partially successful, but none the less significant, experimental system flown by National Center for Atmospheric Research (NCAR) in 1963 and reported in their September 1963 issue of Scientific Ballooning. The works of Blamont and Davidson should stand as descriptive of capabilities in this emerging class of free balloons.

Superpressure balloon systems have been most notably discussed by Grass (1962) and Lally (1967). An effective treatment of their capabilities, actual and potential, is only possible in a separate overview, the scope of which would be adequate to their complexity and uniqueness. This is consistent with the approach and also avoids slighting the importance of the Eole and Ghost programs by a too

---

\*Insofar as is practical, terms and symbols used herein are consistent with those published in the "GLOSSARY OF SCIENTIFIC BALLOONING" available through the Scientific Ballooning Association, National Scientific Balloon Facility, Palestine, Texas 75801.

superficial treatment based on the expedient of time and the limited availability of factual data. It should be sufficient to note the approximately one million dollar National Scientific Balloon Facility (NSBF) effort as proof of the future role of the superpressure balloon system in military and scientific applications.

I do feel compelled to make one observation in passing. With the advances in high strength fibers, with improved polyethylene films, with our increased understanding of the mechanical responses of these materials and finally with our ability to analyze large deformations, a true technological breakthrough may be possible through development of the e-balloon. This design was conceived by and reported on by Smalley (1970) at the Sixth AFCRL Scientific Balloon Symposium.

## 1.2 Flight Profiles

Time-altitude profiles typical of these free balloon systems are shown in Figure 1. The constant altitude a-profile, long considered to be the ultimate profile, provided impetus for the development of super-pressure systems and represents typical superpressure balloon performance. Although theoretically attainable with a zero-pressure system, it is not practical for reasons implied in Section 6.4.

The c-profile depicts the classical zero-pressure flight profile described in detail by Braun and Kelly (1957). Its significant feature is the diurnal ballast demand imposed by sunset cooling. This profile can also be effected by use of an air-ballast system.

The b-profile, a combination of a step profile and the c-profile, presents a common requirement for zero-pressure systems, but is also attainable using an air ballast system.

The number of possible free flight profiles is truly infinite, but each can be reduced to certain elementary stages as shown in Table 1. Note that some stages are unattainable with pure superpressure systems and may not be attainable, either totally or for practical reasons, with certain air-ballast systems. Only the zero-pressure systems are capable of all stages. This latter fact contributes tremendously to their versatility and undoubtedly accounts for their wide ranging applications.

Some flight stages are passive (natural), while others require active initiation, sustaining action or a combination thereof. The need for such actions imposes requirements for specific payload subsystem control functions. Table 2 clarifies the relationship between these flight stages and the subsystem functions. (I have refrained from using the terms valving and ballasting in Table 2 because they are too specific and represent contemporary methods, thereby suggesting a closed book in so far as technique is concerned. Closed book presentations have frequently foreclosed progressive thinking in many an overview/planning exercise.)

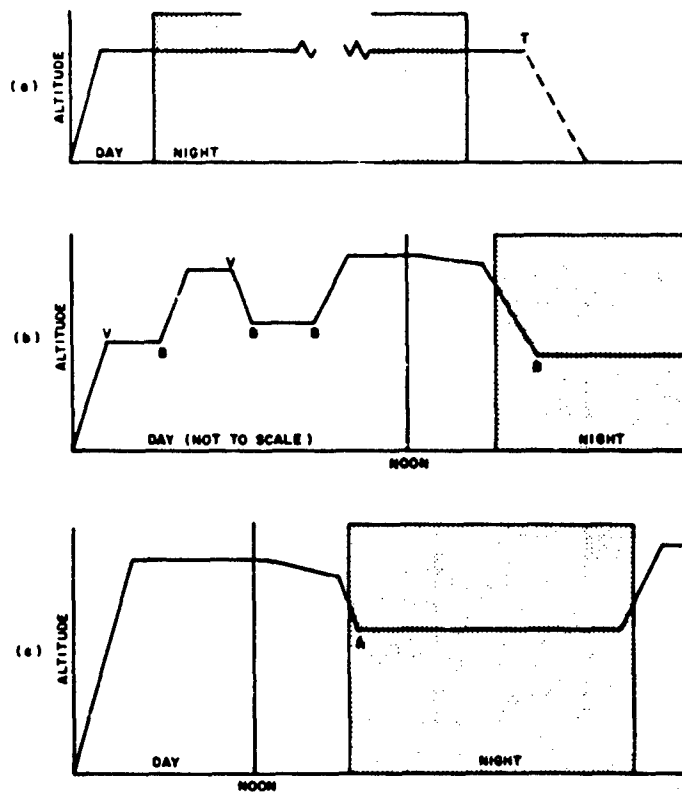


Figure 1. Typical Free Balloon Time-Altitude Profiles. Letter V denotes requirement to valve gas and letter B denotes requirement to drop ballast. Letter A denotes ballast drop for zero pressure balloon system or air-ballast function for air-ballast system. Letter T denotes termination and dashed line represents terminal descent, common to all profiles

Table 1. Flight Stages for the Three Classes of Free Balloon Systems

Class	Flight Stage					
	Ascent	Float* (Slack)	Float (Full)	Controlled Descent	Terminal Descent	Landing
Zero-Pressure	Yes	Yes	Yes	Yes	Yes	Yes
Superpressure	(1)	N/A	Yes	N/A	Yes	Yes
Air-Ballast	Yes	(2)	Yes	(2)	Yes	Yes

\*Slack deployment is the normal condition at night except with the superpressure systems and some air-ballast systems.

1 Unlike the others, this class experiences only initial ascent.

2 These are possible depending on the type of air-ballast system.

Table 2. Flight Stages in Relation to Needs for Control Functions

Flight Stage	Passive (Natural)	Active	
		Initiate	Sustain
Ascent	Yes(1)	Add lift or reduce weight	(3)
Float (slack)		If ascending reduce lift or add weight. If descending add lift or reduce weight	Alter lift or weight as appropriate
Float (full)	Yes		Add lift or reduce weight
Descent (Controlled)	Yes(2)	Reduce lift or add weight	
Terminal Descent		Separate payload	
Landing	Yes		

1. For ascents other than initial or those induced by sunrises, action is required.
2. Although, strictly speaking, descent resulting from natural phenomena (not leaking) is not controlled, it is included here because it is controllable at the will of the user, subject to capability limitations.
3. Thermodynamic effects may require further additional lift or reduced weight.

Thus far, we have viewed the profile only in the narrow vertical sense of a time-altitude relationship. Limited as it may be, it has a horizontal dimension, a dimension that has long been recognized as crucial to certain capabilities. Two particular types of flights have made use of this, boomerang flights and those with flight target requirements such as PEPP and Voyager, classified as precision balloon flights. Such horizontal control is based on two factors, one passive and one active. The passive factor is knowledge of the actual and probable local climatology and the active is control of the time-altitude profile thereby enabling use of the existing wind field variations to effect the desired space-time profile. The ability to achieve a total profile is thus contingent upon our ability to alter the weight and lift of the system.

### 1.3 Payload Subsystems

For the free balloon system viewed as a carrier, Figure 2 shows those payload subsystems that are necessary and sufficient for the required flight functions. The interactions of the various subsystems are shown schematically by the arrows defining the directions of information flow.

Two of the subsystem's functions may not be totally understandable from their names, COMPENSATION and VERTICAL CONTROL.

The latter subsystem, VERTICAL CONTROL, is comprised of those components which are positively or conditionally actuated to effect a change, a rate of change or the stabilization of balloon system altitude. This is the subsystem used for the active flight stages. Most of us are reasonably familiar with the usual control processes; solid ballast in the form of a steel dust (or fine lead or glass beads), dispensed by a magnetic or mechanical metering device, and lifting gas valving, using an electrically operated valve mounted in the balloon apex fitting. However, many users may not be aware of such devices as the canopy and the shroud, investigated by the University of Minnesota (1955), which are conditionally effective (based on atmospheric conditions) in reducing the requirement for ballast. Step flight functions have been achieved using the "boomerang duct", while controlled irreversible descent is possible using either a trap door valve\* or a quick descent duct\*\*.

The concept of a COMPENSATION subsystem is new, not in function, but in distinction. This subsystem is in part active and in part passive, but wholly intended to isolate the payload from or compensate for disturbances caused by the presence of the balloon system. Some familiar examples include:

---

\*A device used in the early Ash Can Program.

\*\*A promising technique under development to bring the system quickly down to an altitude more favorable for in-line parachute deployment.



reel down (active) to isolate the payload from the balloon's thermal environment; shielding (passive) to eliminate electromagnetic interference with the project payload or rotation (passive or active) to compensate for balloon system rotation. COMPENSATION, then, is the subsystem that ensures the project payload will not significantly sense the presence of the balloon system.

Two additional points should be noted with respect to their relevance to the COMPENSATION subsystem. First, interest in the measurement of gradients below balloon systems is being reflected in present plans to develop a reversible reel. Second, due to the direct relationship between project payload experiments and pointing accuracy requirements, responsibility for advanced pointing controls has been inherited by the project payload engineers.

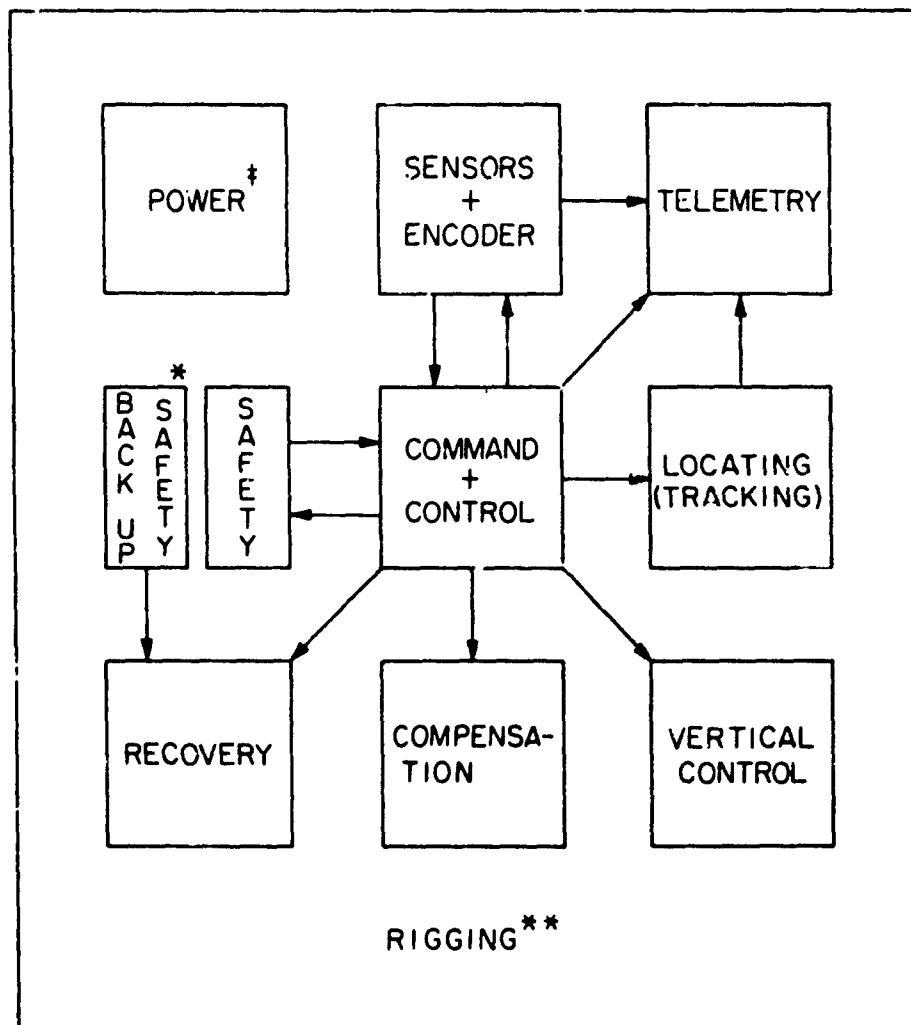
Having moved from flight profiles through flight stages to payload subsystems, comment on their contribution to capability is now mandatory. From Figure 2 and from the foregoing discussion, the COMPENSATION and VERTICAL CONTROL subsystems are clearly related to capability, the latter being of a somewhat higher order in that there are numerous possible project payloads for which a COMPENSATION subsystem is totally unnecessary.

The RECOVERY subsystem, consisting (basically) of the payload release mechanism, an aerodynamic decelerator/stabilizer and a landing shock absorbing system, has traditionally utilized parachute technology developed for either men or cargo. The relatively uncomplicated needs and the demand for low cost have long been met by the standard capability range of flat circular canopy parachutes which, for recovery loads up to 1500 pounds, appear to be eminently efficient. Beyond this range the ring sail parachutes, developed for the manned space programs, offer improved efficiency, but at a substantial increase in cost and with a weight savings in the order of only 3 per cent of the suspended payload. The RSR parachute, reported on at the last AFCRL balloon symposium, Corbalis (1973), appears to have an intermediate efficiency. However, unresolved problems still confront us in this area. More urgent perhaps than the heavy payload recovery requirement is development of the ability to reliably deploy parachute systems at stratopause altitudes. Up camera movies of parachute deployment at 170,000 feet dramatically underscore this need.

The power subsystem supplies the needed power to all but the backup safety system and with modern electronics it is not a significant factor in limiting flight duration or control.

The safety subsystem requirement, except in so far as it relates to protection of the project payload, is extrinsically imposed and thus indirectly related to capability.

The rigging is generally considered to be an engineering problem. Except for thermal considerations, rigging is probably the least restricted aspect of system



- \* Includes independent power source
- \*\* Includes thermal packaging
- ‡ Power source services all subsystems except back-up safety

Figure 2. Diagram of Essential Free Balloon Subsystems Showing Interactions

design as evidenced by the wide variety of configurations flown to date. A considerable amount of study has been undertaken on the thermal packaging of balloon payload subsystems and project payloads. Probably the best known works are Piacentini (1965), Kreith (1970) and Carlson (1973a, b).

The remaining subsystems (sensors and encoder, locating or tracking, command and control, and telemetry) constitute the intelligence processing portion of the payload. These subsystems control the flow of preprogrammed instructions within themselves and the other subsystems. Further they provide the sensing-feedback loop and enable command instruction processing essential to maneuvering the system through a prescribed profile.

Current tracking capabilities are covered by Laping (1974) in his paper on the VOR system. The complex relationships between control and the intelligence processing payload subsystems warrant an independent, detailed presentation, ideally in conjunction with the results of the present AFCRL study of ballast-duration relationships and detailed analyses of ascent and descent rate control. Particularly with respect to the sensors and their accuracies, the establishment of requirement trends is vital.

It is recognized that in the real world there is often no clear separation between the balloon system as the "carrier" and the project payload as the "cargo". However, breaking down the total suspended payload into the project payload and a fixed number of subsystems does (at least in theory) offer advantages. Aside from clarifying the necessary subsystem interactions, it also suggests possible limits with respect to the required number of sensors, command and telemetry channels, programmable functions and controls in general. Obviously the need for power and programmable functions, at a minimum, will be a function of flight duration. An analysis along these suggested lines could provide a useful tool for those involved in the planning of very high altitude and/or long duration flight programs. Further, the potential with respect to both flexibility and improvement of reliability (due to minimized interaction between the system and the project payload) deserves some consideration.

## 2. CAPABILITY IN-THE-LARGE FOR ZERO-PRESSURE BALLOON SYSTEMS

Capability has been defined in a moderately restrictive way with respect to the balloon system as a project payload carrier, and free balloon flight profiles have been analyzed into a finite number of exclusive stages. Finally, the payload has been analyzed into those subsystems needed to ensure the ability to accomplish these stages. What remains (in part) is to rigorously define capability in-the-large and to show that it is representable by a quantifiable, historically significant macrovariable.

Viewed as a carrier, the free balloon system must be able to provide for the user's payload an adequate flight time at a prescribed altitude (or altitudes) including required altitude steps to alter the horizontal trajectory. These are the requirements that must be specified to permit the balloon system itself to be specified. Consequently they relate to what are here termed primary capability components (DURATION, ALTITUDE, MANEUVERABILITY and PAYLOAD\*\*). Equally important in many cases is the COMPENSATION capability which is here designated as the secondary capability component, but only because it is at times unnecessary. One can easily conceive of a project payload, the intended function of which is totally insensitive to normal balloon system induced disturbances (as they are known and understood).

The capability definition viewed in this light reveals payload and altitude\*\*\* as the only directly quantifiable components. The preceding treatment of flight profiles clearly indicates that both duration and maneuverability (profile change) are dependent upon the ability to alter system weight and lift. Reductions in lift (except when the instantaneous system free lift is excessive) require compensating reductions in system gross weight for restabilization. The result of each maneuver (including counteraction of sunset) can thus be numerically stated as a change in system gross weight as follows:

$$(W_g)_n = (1-d_n)(W_g)_{n-1} \quad (1)$$

where  $W_g$  is the system gross weight

$d$  is system gross weight reduction expressed as a fraction of the prior gross weight

if the flight profile requires  $N$  distinct actions to be effected by reductions in the system gross weight, the gross weight after the  $N^{\text{th}}$  action will be:

$$(W_g)_N = (W_g)_0 \prod_{i=1}^N (1-d_i) \quad (2)$$

Since the final gross weight is equal to the sum of the balloon weight,  $W_b$ , and irreducible payload weight, then:

$$(W_g)_N = W_p^* + W_b \quad (3)$$

---

\*\* The irreducible payload,  $W_p^*$ .

\*\*\* Altitude is specified in terms of the corresponding specific lift of the inflant, assumed throughout to be helium.

and it follows that:

$$(W_g)_0 = (W_p^* + W_b) \prod_{i=1}^N (1-d_i)^{-1} \quad (4)$$

Subtracting the balloon weight from each side, the total suspended payload,  $W_p$ , is found to be:

$$W_p = -W_b + (W_p^* + W_b) \prod_{i=1}^N (1-d_i)^{-1} \quad (5)$$

If we now define the variable,  $\lambda$ , such that:

$$\lambda^3 = W_p/b \quad (6)$$

where the parameter,  $b$ , is the specific lift of the inflatant at float altitude for the full balloon with the initial gross load, and if we now divide both sides of Eq. (5) by the parameter,  $b$ , we obtain:

$$\lambda^3 = \frac{-W_b}{b} + \frac{W_p^* + W_b}{b \prod_{i=1}^N (1-d_i)} \quad (7)$$

Now by collecting the terms containing the parameter,  $W_b$ , we have:

$$\lambda^3 = \frac{W_p^* + W_b \left[ 1 - \prod_{i=1}^N (1-d_i) \right]}{b \prod_{i=1}^N (1-d_i)} \quad (8)$$

Thus it is clear that the ability to carry a payload,  $W_p$ , to an altitude implied by a specific lift,  $b$ , is directly related to the comprehensive primary capability of a zero-pressure free balloon system considered as a carrier for a project payload. In addition to numerically describing capability in terms of the expression,  $\lambda^3$ , Eq. (8) shows that this measure is, as could have been expected, sensitive to technological improvements as reflected in the actual balloon weight.

The variable,  $\lambda^3$ , increases with both increasing payload and increasing altitude. It was first recognized as a reasonable indicator of capability in an

earlier effort in technology forecasting\*, Dwyer (1972). This variable, or rather its cube root,  $\lambda$ , is now recommended as a macrovariable well suited for the analysis of capability in-the-large for zero-pressure free balloon systems. Selection of the letter,  $\lambda$ , follows prior use by Smalley (1963) to describe the function  $(W_p/b)^{1/3}$ .

### 3. HISTORICAL CAPABILITY TREND

The intuitively obvious capability, the ability to fly at higher altitudes with heavier payloads, has been meaningfully and quantitatively expressed by the variable,  $\lambda$ . The variable,  $\lambda$ , has been shown to be truly macroscopic in that it encompasses measures of capability as related to the balloon "carrier" concept, and in that it reflects aspects of the entire technology base, as reflected in the size and weight of the balloon itself.

This macrovariable must now be shown to possess the attribute, IMPROVABILITY, based on its ability to grow as the technology base expands. In other words it must show significant historical growth.

The tendency for growth to occur exponentially, and the ease of computing  $\lambda^3$ , rather than  $\lambda$ , resulted in Figure 3, a semi-logarithmic plot of  $\lambda^3$  for polyethylene balloons for the time period since 1950. The maximum value of  $\lambda^3$  is plotted for each year in which there was an improvement over the prior year. Where there was no new maximum, but where there was a value reasonably representative of the trend of the maximums, such value is plotted. From the plot we see that some years failed either criterion and some years satisfied both. Considering just the envelope, two inescapable conclusions can be drawn: first, there is a definite historical tendency toward improved capability and second, the capability growth rate is diminishing.

Figure 4, a similar plot for balloons made from polyester film reinforced with a grid of dacron fibers\*\*, is much less convincing, but not contrary to the  $\lambda$ -thesis. Not evident from this curve alone is the fact that its present capability growth rate is exceeded by that of polyethylene balloons. Actually, only one point has coordinates placing it significantly outside of the Figure 3 envelope.

---

\*Since  $\lambda^3$  does not distinguish between light payload-high altitude and heavy payload-lower altitude capabilities, the existence of two nearly parallel trends was postulated. Although this distinction may have been subconsciously created by the then popular capability distinction, it is not yet rejected and warrants investigation as part of a broad general analysis of the capability trend.

\*\* Film thicknesses and grid reinforcements are not necessarily similar in this plot.

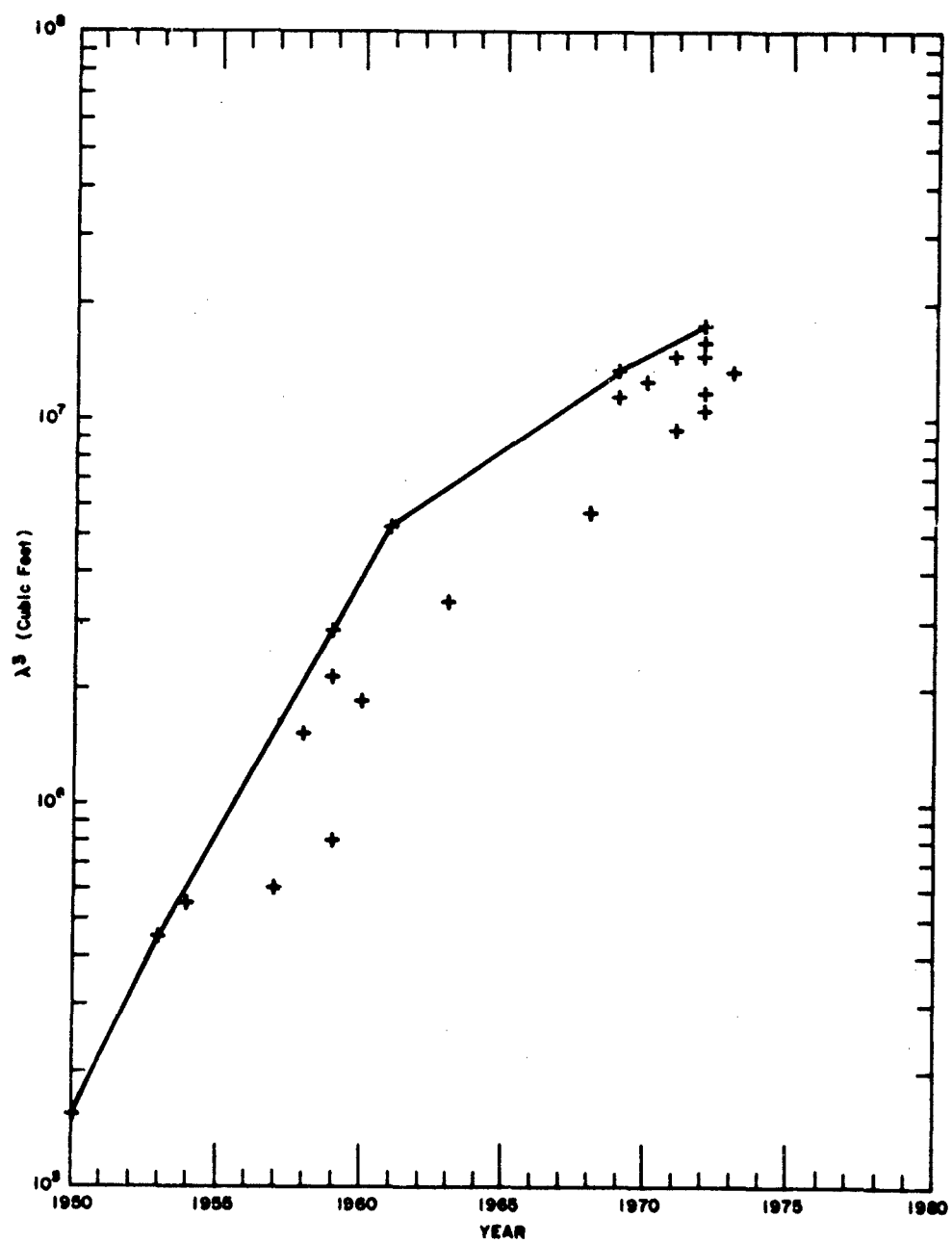


Figure 3. Zero Pressure Polyethylene Balloon Capability Growth

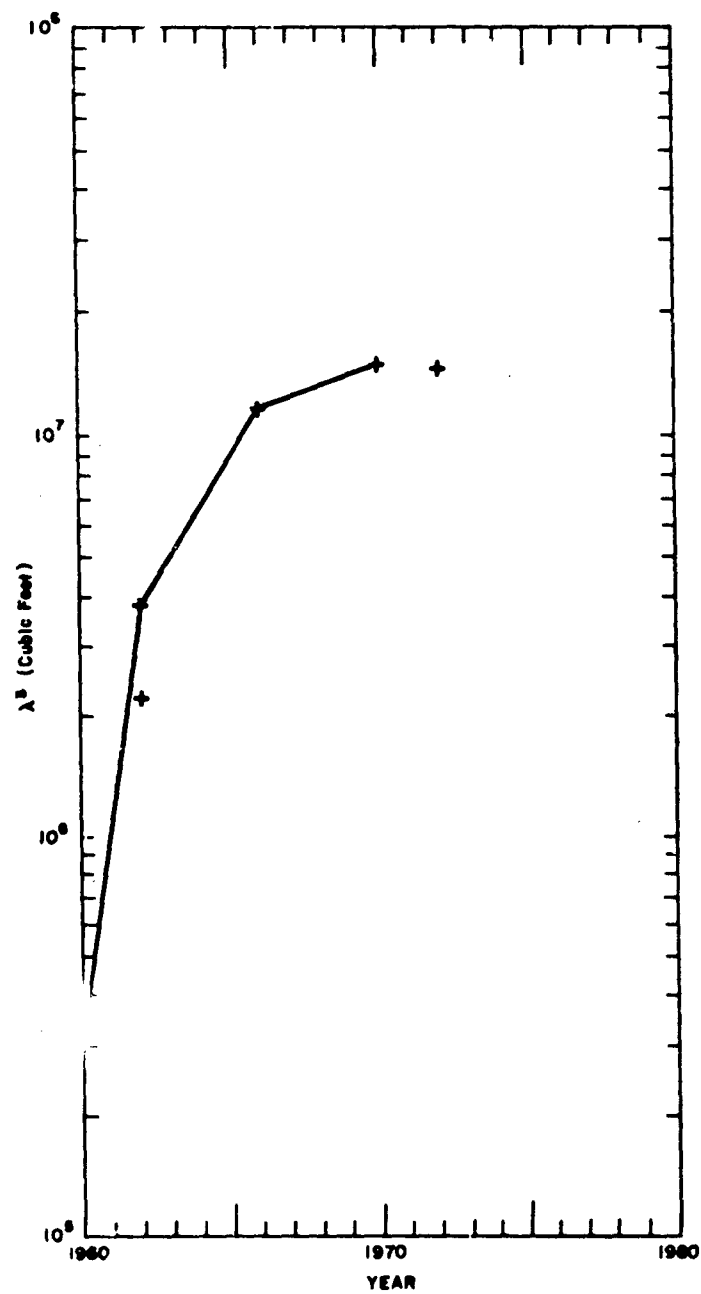


Figure 4. Capability Growth Trend For Reinforced Polyester Film Balloons



The source of the data used to compute the plotted values of  $\lambda^3$  (Figure 3 and Figure 4) was the AFCRL balloon branches' library, containing information from nearly every organization active in the technology. \* The data points are representative of all types of flights, research, development and operations. The macrovariable is thus reasonably established as a quantifiable historically significant measure of capability in-the-large.

#### 4. CAPABILITY TREND SIGNIFICANCE

It is unfortunate, but trends are not self explanatory. They do, however, offer significantly more information than a random collection of facts. Although they cannot precisely indicate tomorrow's capability, they do provide the planner with the knowledge of the probable range of capabilities in the absence of dramatic changes in the technology.

By measuring capability in-the-large, we maximize our confidence in the accuracy of the trend, for it is an underlying assumption that macrovariables ( $\lambda$  in our case) change relatively smoothly, continuously and slowly, without violent fluctuations. According to Ayers (1969), this is due in part to the contribution of a significantly great quantity of independent parameters; stability thus being related to the operation of the "law of large numbers".

In the sense that the action of observing influences the observed action, it is eminently probable that trend recognition will be perceptibly reflected in the subsequent trend. I believe this to be particularly true in the later phases of technological development. This hypothesis will be seen to be particularly relevant to zero-pressure balloon technology.

Before examining the zero-pressure balloon capability trend in detail, a comparison of two very common capability trends is appropriate. Figure 5 is a graphic comparison of exponential growth and limited growth. The mathematical representation of the S-shaped or sigmoid curve implies an asymptotic limit, which may or may not be absolute. For example, if performance (capability) were measured in terms of efficiency, then there would be a limit of one hundred percent, an absolute. In general, and particularly so in the present context, this limit should be regarded in the street sense of "where you'll (probably) end up if you don't mend your ways".

Exponential growth is assumed to be familiar territory to those involved in ballooning. Further, the data presented in Figures 3 and 4 definitely do not follow an exponential trend, although the semi-logarithmic plot leaves the actual trend in doubt.

---

\*See Appendix A.

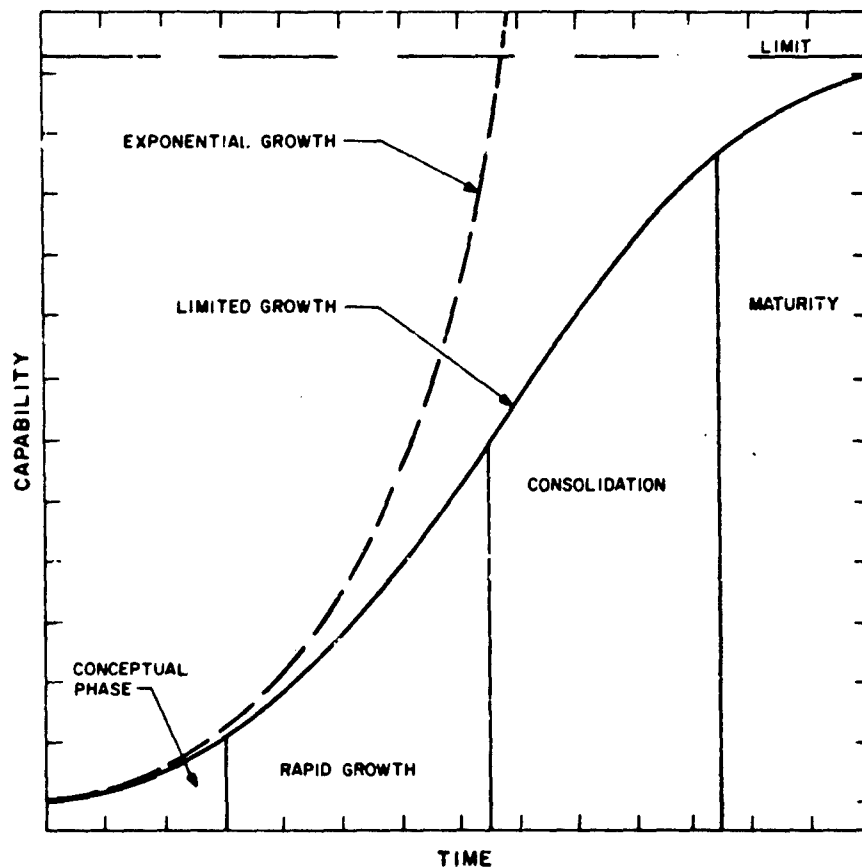


Figure 5. Generalized Comparison of Exponential and Limited Growth as Applied to Capability as a Function of Time. The figure, including the metaphorical phases, was suggested by Starr and Rudman (1973)

### 5. CAPABILITY TREND EXTRAPOLATION

The envelope points from Figure 3 were selected as adequately defining a relatively smooth timewise variation of  $\lambda^3$ . Both for dimensional simplicity and due to prior use by Smalley,  $\lambda$  was selected as the macrovariable for the capability trend extrapolation. Because of the eyeball trend of the data, and because of the common occurrence of sigmoid patterns in the measurement of technological growth\*, a regression analysis was used to fit the data to the following equation. (Time,  $t$ , is the independent variable).

\*For examples see Schon (1967) or Martino (1967).

$$\lambda = \frac{\text{LIMIT}}{1 + Ae^{-Bt}} \quad (9)$$

Estimating values of the variable, LIMIT, solutions for A and B were sought so as to maximize the correlation coefficient. \* For a correlation coefficient of 0.998, the obtained values\*\* were:

LIMIT = 291.78

A = 4.403

B = 0.16027

The resulting curve is shown as Figure 6.

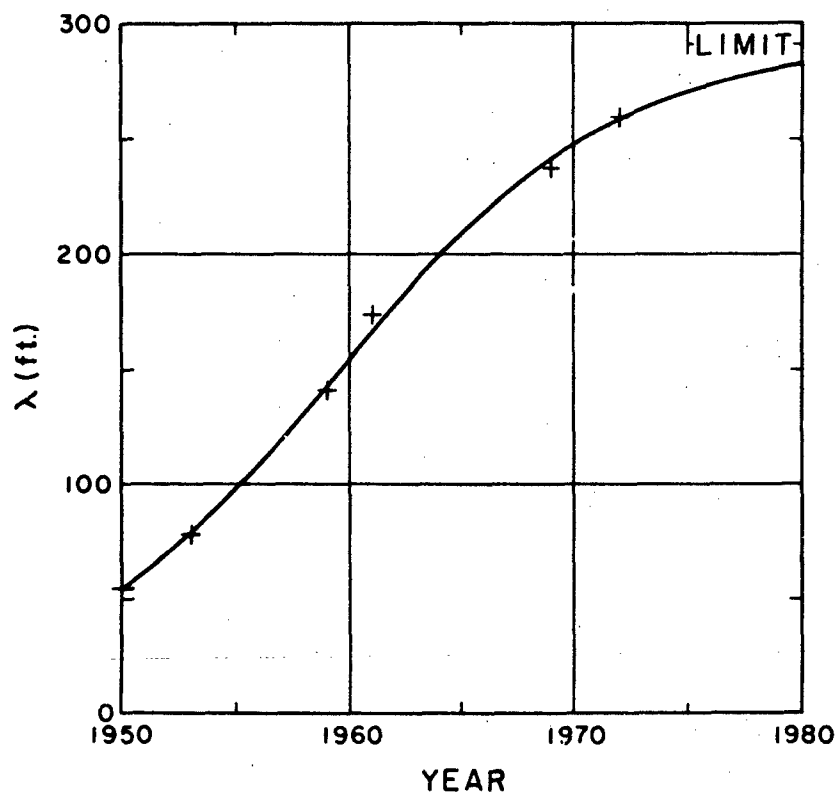


Figure 6. Polyethylene Balloon Capability Trend Data With Best Fit Logistic Curve

\* Since estimation of an initial value for LIMIT was most simple, and because of both the intended use and high correlation coefficient, further approaches were obviated.

\*\* The fact that B differs from  $1/(2\pi)$  by less than one percent is intriguing, but beyond the scope of this analysis.

Since a model such as Eq. (9) is developed solely to provide a mathematically sound basis for extrapolation and not to clarify the dynamics of the contributing parameters, no effort was made to extrapolate the trend shown in Figure 4, which is based on data both limited and short term. It is interesting to note, however, that the trend of the combined data (Figure 3 and Figure 4) tends to a lower limit.

Only limited inferences should be drawn from Eq. (9) since it is no more than a mathematical or phenomenological model. Most importantly, the prior admonition about regarding the limit as "where you'll (probably) end up if you don't mend your ways" must be kept in mind.

Whether or not one agrees with the previously suggested analysis of trends into the four phases of growth (see Figure 5), it seems clear that the 1950 data, upon which the Gopher program was based, represents both historically and graphically the end of the conceptual phase and the beginning of the rapid growth phase. Further, if  $\lambda$  is an historically significant measure of capability in-the-large as proposed, then polyethylene zero-pressure balloon capability may reasonably be considered as being (not per se, but based on contemporary design and utilization standards) well into the maturity phase. The same may be said of the reinforced polyester film balloons, but in either case there is no indication that the limits are absolute and every reason to believe that our existing design and utilization standards are predominating capability constraints.

Concern over the results of the extrapolation should not obscure the fact that what is learned about the trend (particularly positive or negative response thereto) should have a great tendency to be ultimately reflected in the trend itself.

Table 3 shows  $\lambda$  extrapolated to 1975 and analyzed into payload and altitude components over the payload range 625 pounds to 20,000 pounds. Analysis over the same range is shown for the limiting case where time approaches infinity. Using an algorithm (now considered to be oversimplified, but reasonable within limits) certain system features were calculated for the 1975 capability. Some results deserve comment. First the capability for the 625-pound payload requires a balloon gorelength in excess of the length of present manufacturing facilities. Second, the capability for the 10,000 pound payload closely resembles that of the large reefed polyethylene balloon (32 million cubic feet) scheduled for modification and launch by AFCRL in the Fall of 1975. Finally, material thickness might be reduced below present standards for heavy payload range and increased efficiency should be achievable by using sub-loaded balloon shapes for the lower payload range.

With respect to the mid-range (2500 to 5000 pounds), experience suggests that progress might be the least constrained, but there appears to be no present interest. Based on the fact that mid-range grows as maximum payload capability increases, the data base was examined, but showed no indication that the  $\lambda$  trend

**Table 3. Capability Variable Resolved Into Payload and Altitude Components for Years 1975 and Infinity**

Payload	Altitude in Feet	
	1975	Infinity
625	179,100	185,500
1,250	160,500	166,500
2,500	143,400	148,900
5,000	127,500	132,700
10,000	112,600	117,500
20,000	98,000	102,900

**Table 4. Annual Percentage Increase in Payload Capability Based on Trend with 1975 as Base Year**

Year	Payload Increase (Percent)
1975	----
1976	3.37
1977	2.98
1978	2.65
1979	2.31
1980	2.03

was mid-range controlled. This impression again suggests the merit of further analysis along the lines of the original dual capability trend concept (high altitude and heavy load).

Finally with regard to the extrapolation, Table 4 shows that for any given altitude-payload capability, existing in 1975 and satisfying the extrapolated capability, if the trend continues and is not intentionally altered, the payload capability at the respective altitude will increase from year to year by the percent indicated. In the limiting case, the payload will have increased by only about 26 percent over the 1975 payload.

## 6. CAPABILITY GROWTH CONTROL

There are two factors that will dominate any effort to influence capability growth: identification of technological barriers\* and recognition of the most promising avenues for innovation. Low (1961) has addressed the former both practically and philosophically, offering many valuable insights, and Ayers (1969) has pointed out a cataloging method\*\* which is applicable to the recognition of opportunities for innovation. Both of these factors will be treated, but only the latter in detail.

\* The importance of trend extrapolation with respect to barrier identification was demonstrated with respect to present balloon gore length limitations.

\*\* A technique labeled the "morphological method" by its progenitor, Fritz Zwicky.

### 6.1 Barriers to Capability Growth

Aside from technological constraints that may be inherent in the balloon structure itself, there are other obvious engineering barriers that arise in the direct support areas. While the latter may not dominate capability growth, they nevertheless impede either capability itself or the free exercise thereof. Most important in this class of barriers are launch techniques. Even the very promising "reefed balloon launch" will have limits and will impose a balloon weight penalty in the order of 100 pounds for the lengthy (gorelength) high altitude balloons. This, for any number of users, will be a totally unacceptable weight penalty.

The barriers to zero-pressure balloon capability growth warrant a thorough classification and tabulation, and a philosophical approach may prove to be essential. Distinction is required between those barriers that can be solved by money only (production plant enlargement to provide increased gorelength) and those that require significant effort with only a probability of complete success (predicting ballast requirements for duration flights under statistically varying conditions). In addition, a reasonably complete study of barriers must consider such other facets as: expected time of encounter, cost to eliminate, time to eliminate, and numerous others.

### 6.2 Opportunities for Innovation

Before we consider Zwicky's technique and how it can apply to our problem of capability growth control, let us examine at least one possible representation of the capability trend in terms of historical balloon structural designs, for it is structural design characterization that we will use to demonstrate this technique. Figure 7 is a hypothetical capability trend depicting the envelope of hypothetical capabilities for various actual balloon structural designs. It shows how we might expect to see  $\lambda^3$  increase not only with time, but also with improved and more efficient balloon design. The design approaches represented by their several trends are in historical order and there is no disputing the fact that each did provide both theoretical and actual capability growth. This is only one of the many possible parametric analyses of the capability trend. It is important to remember that although this example is both hypothetical and idealized, the method can yield great insights.

What Zwicky's technique offers is more than a cataloging procedure that enables us to characterize actual and potential systems parametrically. It is a method for evaluating mathematically the opportunities (and to some extent the probabilities) for breakthroughs in the respective technology. The steps in implementing this technique require: 1) precise statement of the problem to be solved, 2) a characterization of the system by enumeration of pertinent

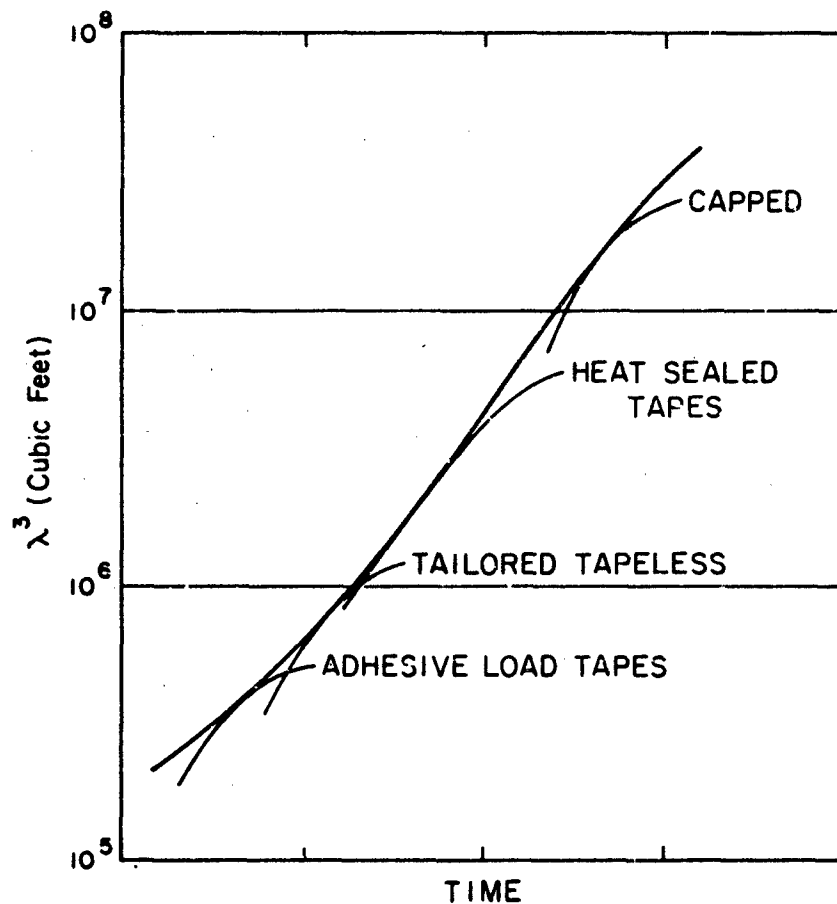


Figure 7. Hypothetical Capability Trend and Analysis of Macrovariable,  $\lambda^3$ , Based on Actual Balloon Load Bearing Structural Components

parameters, 3) analysis of parameters into their distinguishable states, and finally 4) definition of an evaluation procedure compatible with the objective of the analysis. Exhaustion of the possible parameters or states is never a certainty and procedure definition (step 4) is no simple challenge. The method will be partially exemplified in section 6.3.

An obvious inference to be drawn from this method is: if the growth rate of capability is proportional to the remaining opportunities for innovation, and if the known parameters and their known distinctive states are completely enumerated, then the capability trend will be a sigmoid type curve tending to a limit. In this regard, the immediate consequence of the discovery of new parameters and new

states (either or both) is the creation of new capability limits and a potential upswing in the capability trend. These hypotheses have important implications for zero-pressure balloon technology. The general impact on a capability trend is schematically depicted in Figure 8.

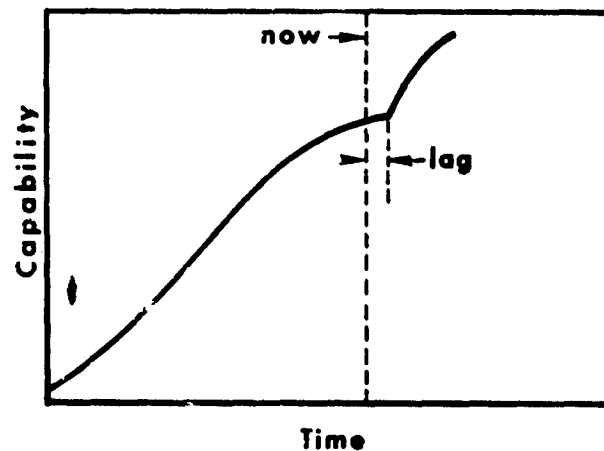


Figure 8. Hypothesized Impact of New Opportunities for Innovation Upon Generalized Sigmoid Capability Trend

For zero-pressure balloon systems, we have seen that the extrapolated capability trend indicates a consolidated and maturing technology. We have also seen that the absolute validity of such a judgment is predicated upon having completely enumerated opportunities (for innovation) within the technology. Further it has been proposed that the relationship between opportunity and capability growth suggests that a positive change in the trend will result from an increase in the parametric states reasonably suited for productive exploitation. It is further indicated by the trend and by the knowledge of the general historical use of the known parametric states that the zero-pressure balloon technology has been progressing as if the opportunities for innovation were completely defined, when, in fact, they are not. Positive action to alter the capability trend is thus seen to be a productive venture.

### 6.3 Parametric Characterization Exemplified

Table 5 is the author's limited attempt to parametrically characterize potential and actual zero-pressure balloon design configurations in relation to



Table 5. Parametric Characterization of Zero Pressure Balloon Configurations (Actual and Potential) with Regard to Payload Capability Component

Type (Single Cell, Tandem)
Film (Poly <sup>1</sup> , Mylar <sup>R</sup> , Polyester, Nylon, B 100, <u>Others</u> )
Gore Pattern (Rectangular, Semi-tailored, Tapered-tangents, Fully Tailored <sup>2</sup> , <u>Others</u> )
Shape (Sphere, Tetroon, Sphere-cone, Natural, <u>Others</u> )
Shell Reinforcement (Cap, <u>Others</u> )
Principal Load Bearing Element (Gore <sup>3</sup> , Load Tape, Scrim, "SVT", <u>Others</u> )
Tape Attachment (Adhesive, Heat Sealed, <u>Others</u> )
Tape Location (Seams, Gore Center Line, Both)
Tape Fiber (Glass, Nylon, Fortisan-36, Fortisan, Polyester, Kevlar, <u>Others</u> )
MD Scrim Fiber (Dacron, Polyester, Kevlar, Nylon, <u>Others</u> )
TD Scrim Fiber (Dacron, Polyester, Kevlar, Nylon, <u>Others</u> )
Scrim Pattern (Rectangular, Triangular, Tailored, Lateral, Meridional, Random, <u>Others</u> )
Apex Deployment Control (Vista Dome, Vista Cone, <u>Others</u> )
Excess Material Control (Sleeve, Clutch, <u>Others</u> )
Pressure Relief Appendix (Open Base, Attached Duct, Horsetail Duct, <u>Others</u> )
Base Fitting (Spool, Wedge Collar, <u>Others</u> )
Apex Fitting (Banded, Plate-Hoop-Ring, <u>Others</u> )
Launch Method (Dynamic method 1, 2, ----n, Static method 1, 2, ----m)

<sup>1</sup>Subdivided into X-124, Stratofilm<sup>R</sup>, DFD5500, Others.

<sup>2</sup>Base needs excess width for assembly.

<sup>3</sup>Cylinder and tailored tapeless balloons have no reinforcement.

parameters affecting load carrying ability. If the list of the distinguishable states\* of each parameter is exhaustive and the enumeration of parameters is also complete, a tabulation of every possible design can be made. Each design will consist of a combination of every parameter, each in one of its states. Thus if we have M parameters each with N distinguishable states there will be  $N^M$  possible designs. In reality, the selection of a particular state of one parameter may preclude some state of another parameter. For example, a sphere-cone shape precludes using rectangular gores.

The hundreds of thousands of possible designs indicated by Table 5 forewarn us of the impracticability of an analysis of each and every one, even after eliminating incompatible states as previously mentioned. Among other possibilities what Table 5 does provide (due to the large number of parameters) is an a-la-carte menu from which the experienced designer may select with gourmet-like discretion\*\*. If deemed appropriate, a formal evaluation of the number of tried and potential designs as well as an evaluation of the probability of satisfactorily achieving any selected design can be undertaken.

This parametric characterization is likewise applicable to other factors and systems related to the capability trend. For these, also, evaluation procedures must be established to enable capability (or performance) predictions and assessments of relative value.

#### 6.4 Possible and Actual Efforts to Improve Capability

We have seen generally and by example a method with the potential to produce improved capabilities. Specific approaches to improve capability must now be considered. Without analyzing  $\lambda$  into more than the suspended payload (total) and altitude components, it is clear that improved balloon efficiency will automatically improve capability in-the-large. Clearly what is needed is a modern analogy to the natural shape balloon. Such an analogy must be constrained to maximize balloon efficiency by establishing designs based upon: (1) consideration of pertinent mechanical properties of the load bearing structural materials, (2) critical use environment parameters, (3) critical deployment stages and (4) operational considerations (ascent rate, launch winds, etc). This ideal solution will pose further problems with respect to both parametric design characterization and establishment of evaluation procedures related thereto (sec 6.2).

\*For continuous parameters, the states must be meaningful ranges. An example for ballooning might be payload or better yet, film thickness, since important properties vary significantly with thickness (particularly for polyethylene).

\*\*Appendix B lists some patented inventions which could easily have issued from just such an analysis as this.

In so far as parameters are concerned, material deformation, the effects of thermal contraction, recognition that balloon gores are fabricated from flat sheets, the existence of circumferential stress as well as other states and parameters must be acknowledged and considered. Alexander (1973) in analyzing balloon stresses has made positive recommendations extremely pertinent to aspects of this problem, and related studies, done at AFCRL, have yet to appear in the literature.

In connection with the problem of evaluation procedures, the admonition that a candidate balloon film be "generally suited to balloon use" may hold a key. Considering the evaluation procedure both from this point of view, and from that of a film problem superimposed on a design problem, the following is instructive.

The relationship between launch temperature and stress and tropopause temperature and film strength, investigated for polyethylene film by Dwyer (1965) and Kerr and Alexander (1967), and the existence and relevance of a temperature-critical strain rate relationship, shown by Weissmann (1972), are factors reasonable to assume as pertinent to any new film. These factors taken in context with balloon length, balloon material deployment, ascent rate and atmospheric wind shears will be reflected in the ability (of any chosen film) to survive the consequent dynamic loading as it is superimposed on the ascent static stress field which can now be reasonably approximated, Alexander (1973, 1974). These factors partially define the requirement, "generally suited to balloon use" and comprise a set of critical parameters which constitute the basis of a unified theory of balloon ascent burst. However important this ascent stage might be, it will never be encountered by a film incapable of accommodating a launch method which is compatible with the intended payload or gross load. Likewise, if the film is unsuited for prolonged static loading (particularly at the warmer high altitude temperatures), its ability to survive launch and ascent may be meaningless. In brief, "generally suited to balloon use" must be understood to include all stages of flight.

This approach to maximization of zero-pressure balloon efficiency is only one possible step toward the improvement of capability. There are other long range and shorter range steps, among which are: 1) comprehensive analyses of capability with respect to trends other than time (e.g. materials, load structures, launch methods, etc); 2) study of launch techniques with respect to their advantages and disadvantages (shorter range and related to barriers rather than to innovation); 3) study of launch stresses and strains in balloon film and tapes for a large variety of balloons, used over a period of years (use a method such as Alexander's and relate findings to flight performance); and 4) analysis and test flight of subloaded natural shape balloons particularly in the heavy payload range (an attempt to understand the effects of sub load induced circumferential stress

in the presence of heavy loads and to ascertain whether present polyethylene balloon designs are payloadwise underrated).

Fortunately there are existing or planned research and development efforts in a number of the areas suggested. We are fortunate in this regard since immediate effort is required to minimize the time lag always present between planning and accomplishment.

In the materials field we have had a prolonged and fruitful cooperative effort toward establishing a specification for polyethylene balloon film: soon to be a reality. The by-products of this lengthy investigation, and I feel certain those involved will agree, have overshadowed and will continue to overshadow the specification itself. The resultant increased understanding of the basic film and the implications with respect to design and in-flight behavior will bear heavily on the new materials and design studies presently scheduled.

Design studies along the line of the suggested "natural shape analogy" are planned and will encompass both reinforced and unreinforced films. The design problem has hopefully been posed broadly enough to permit even a finding that traditional reinforcement concepts are counter-productive, and yet specifically enough to find the best designs (within limits) for such new composites as poly-plus. (It should be noted that the AFCRL approach to poly-plus utilization has been coordinated with others actively pursuing this promising new material). It is hoped that the findings of this materials and design effort will assist in dramatically focusing future searches for candidate balloon films.

A specific effort with respect to evaluating tandem balloon designs based on the interactions of material, environment and ascent deployment is underway at AFCRL, and it is understood that the problem of suitable adhesives for related scrim-film laminates is being studied by Princeton University under contract to NASA.

Should this study of tandem balloons reveal structural problems inherent in the tandem concept (as is suspected), a parallel effort in launching heavy loads using a reefed balloon will hopefully fill the gap. The early work by Winzen Research Incorporated (sponsored by the Office of Naval Research) is being pursued (now under AFCRL sponsorship). AFCRL will fly three reefed balloons in the next year, with the final flight carrying a 10,000 pound payload at 110,000 feet.

There is one other serious effort to increase zero-pressure balloon capability in-the-large as we have defined it. It consists of both a theoretical analysis of ballast demand and a statistical evaluation of ballast consumption. Figure 9 shows preliminary indication of how maximum and minimum ballast

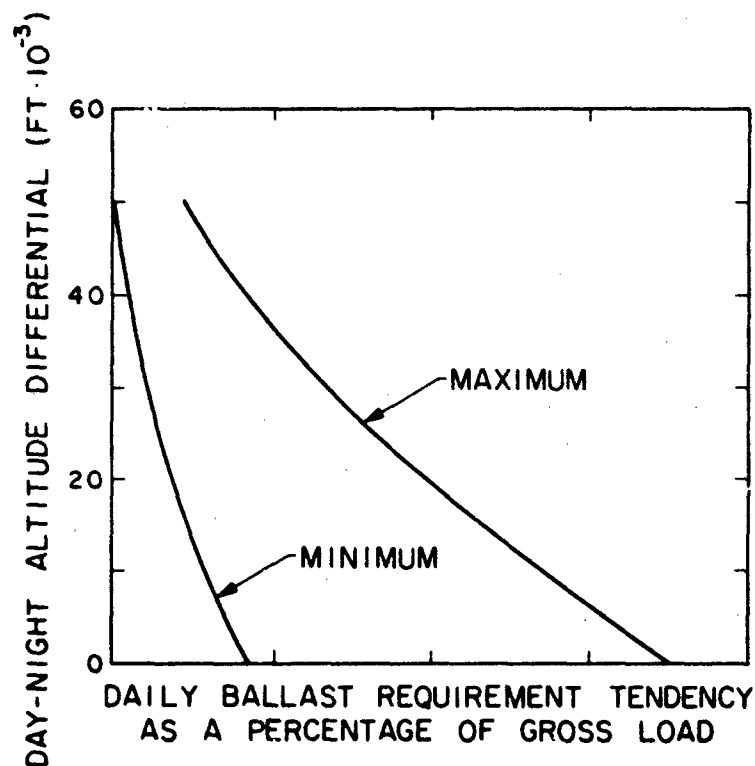


Figure 9. Ballast Requirement Vs. Permitted Altitude Differential

expenditures tend to vary as a function of day-night altitude differential.\* This study is the long range approach to the problem and will hopefully find great application in future flight systems. Progress in the shorter term can be encouraged by the scientific balloon users by their insisting on larger ballast safety margins thereby forcing increases in balloon payload capacity. Admittedly pushing the state of the art increases the possibility of failure, but this is so whenever one operates beyond the realm of experience. However, as earlier stated, the demands by the users generally set the pace for capability growth.

#### 7. RELEVANT PAYLOAD AND GROSS LOAD ACCOMPLISHMENTS

Although a payload or a gross load increase frequently presents a challenge, and successful meeting of such a challenge is often a notable accomplishment,

\*Numerical values have been intentionally omitted from the abscissa scale pending publication of the study in a subsequent report by Mr. G. Nolan.

neither in itself should be considered as an increased capability, at least in the sense of satisfying a definable flight profile requirement. There is no doubt, however, that such increases are important and represent either reduction or elimination of "barriers" to capability growth. In addition, gross load relates to balloon apex pressure, Dwyer (1973), and is therefore a major design and flight control (valving) consideration. Payload, in addition to affecting the static load bearing structure, frequently imposes the need for special design considerations relating to dynamic launch forces.

Figure 10 shows both payload and gross load accomplishments for polyethylene zero-pressure balloons. Although payload tripled in the ten year period (1954-1963), it only doubled in the following nine year period. While balloon weights for the years 1954, 1959 and 1963 were about 30 percent of the payload weights, the balloon weights for the years 1971 and 1972 are in excess of 50 percent of the payload weights. The indicated decrease in balloon efficiency with increasing payload is contrary to what should be expected, but this reversal is consistent with the down trend of capability growth rate: a relationship predictable from Eq. (8) which indicates the sensitivity of  $\lambda$  to balloon weight,  $W_b$ .

Figure 11 shows the payload and gross load accomplishments for reinforced polyester film balloons. What little information there is to be gained from the

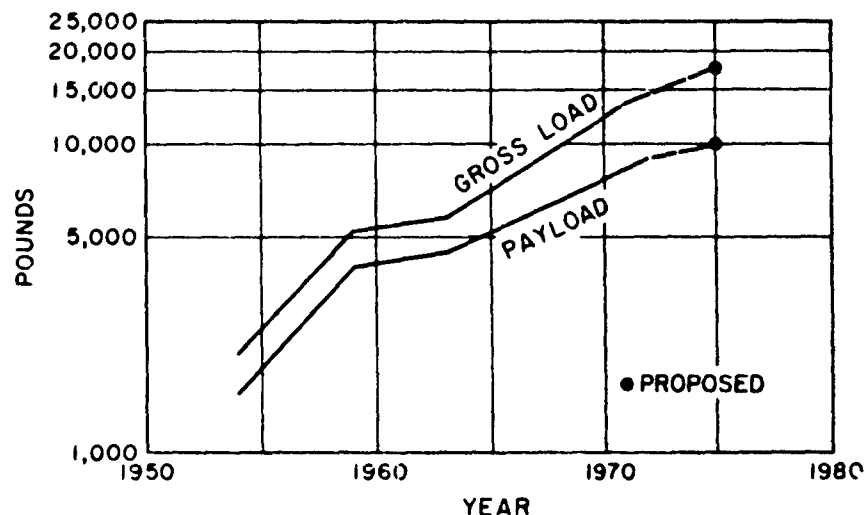


Figure 10. Polyethylene Balloon Payload and Gross Load Trends

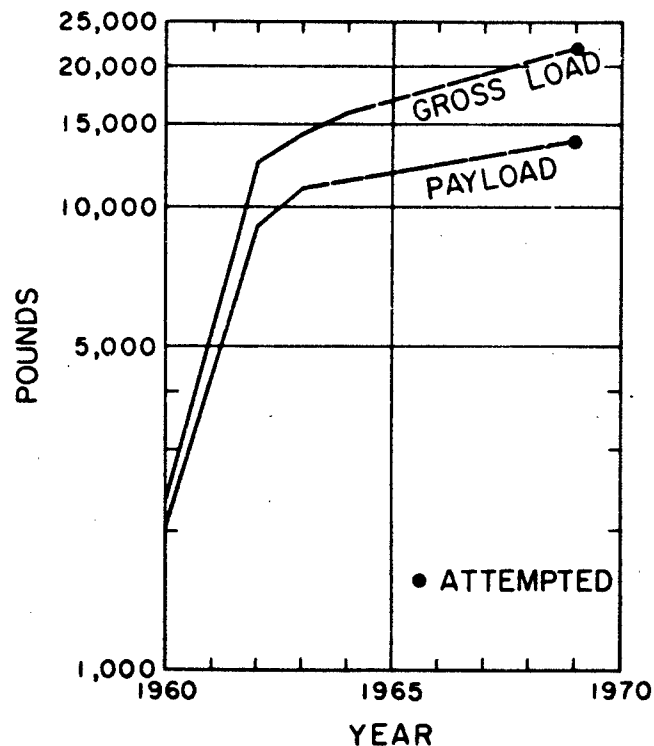


Figure 11. Scrim Balloon Payload and Gross Load Trends

limited data is significant; namely, the same tendency toward decreasing balloon efficiency with increasing payload is evident (from just over 30 percent in 1962-1963, to just under 60 percent for the 1969 CRISP balloon attempt). Only the absolute magnitudes of the accomplishments are somewhat greater.\*

Figure 12, the final graphical representation of payload and gross load accomplishments, compares actual and planned maximum loads for polyethylene balloons with actual and attempted maximum loads for the reinforced polyester film balloons. Ignoring the cost - reliability argument for the use of the latter (and this is debatable), the advantages and potentials are no longer so distinctive, particularly should the proposed flight of the reefed polyethylene balloon succeed with the 10,000 pound payload.

It can reasonably be argued that the reinforced material is being used below its limits and that polyethylene films are being used at or near their ultimates.

\*See Appendix A for data used in Figures 10 and 11.

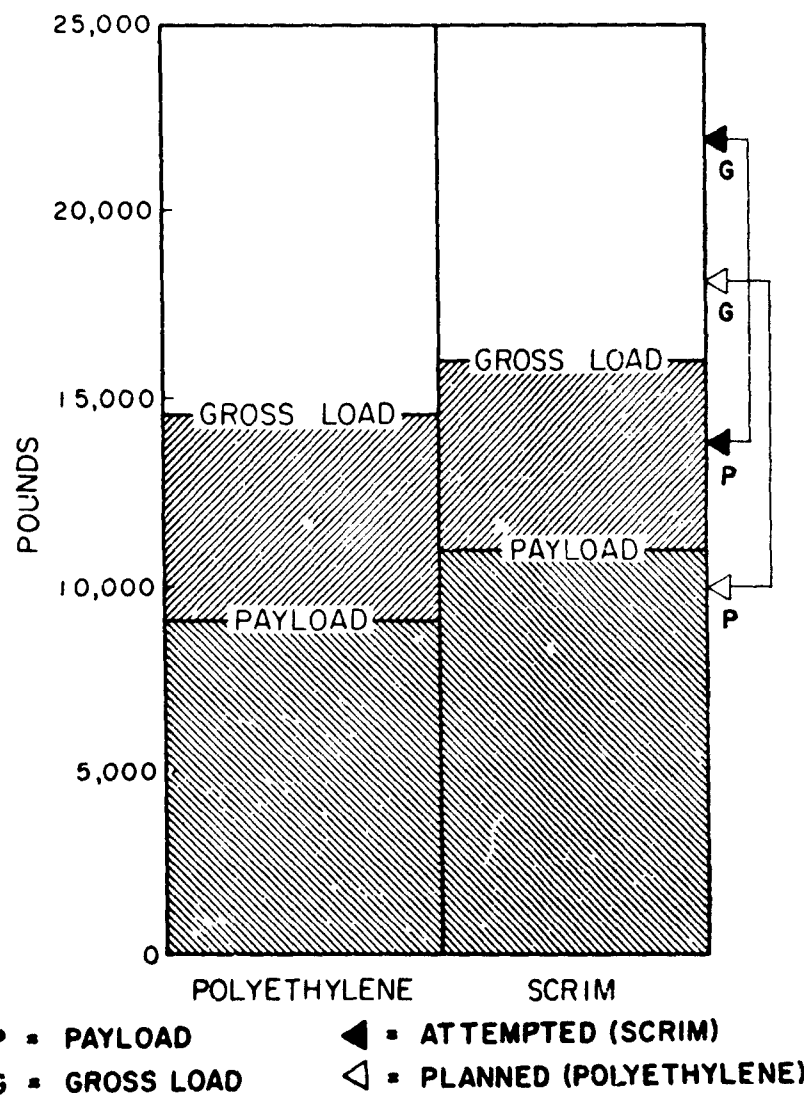


Figure 12. Comparison of Maximum Payload and Gross Load Experience for Polyethylene and Scrim Balloons

However, there is strong evidence that polyethylene film balloons are underrated (a balloon, 2,940,000 cubic feet in volume, designed for a payload of 1250 pounds has successfully carried a 3000 pound payload). Supporting the contention that the reinforced films may be being used below their limits, is the belief that the observed maximum performances may be influenced by the balloon type (tandem) rather than the film alone.



## 8. CONCLUSIONS AND RECOMMENDATIONS

We have seen capability in-the-large defined in the sense of the free balloon system as a carrier and the project payload as the cargo. We have touched on the importance of two classes of free balloons, super-pressure and air-ballast and indicated that both are significant, though the latter is still emerging from its conceptual phase. For the third class of free balloons, zero-pressure, we have seen capability treated thoroughly with respect to system components and flight profiles and critically with respect to its trend. Where appropriate, specific problems and recommendations were noted regarding present and future payload subsystems.

A macroscopic variable,  $\lambda$ , was mathematically defined and defended with respect to its historical significance as a measure of zero-pressure balloon capability in-the-large. Finally, the capability trend, as expressed by  $\lambda$ , was extrapolated and interpreted and, based thereon, recommendations to accelerate the capability growth were made and related to present and planned research and development.

The effectiveness of this type of overview will be measured by the response of the R and D and manufacturing members of the scientific ballooning community and, possibly moreso, by the experimenters, project officers and operations managers who see daily the requirement trends. Their support in clarifying the trends will be the key factor in the establishment of capability goals and in determining the relative emphasis with respect to high, low or mid-range load-altitude capabilities. It is they who must cooperate by documenting their requirements in formats meaningful and compatible with this and other realistic measures of capability.

It is recognized that the preceding recommendations for documenting requirements and planning capability growth imply a rigor somewhat different than this technology has heretofore practiced. However the trend away from the Montgolfier state of the technology (as properly described by astronomer Martin Schwarzschild at the 1963 AFCRL balloon symposium) must not proceed using planning methods less sophisticated than the technology they propose to advance. It is today's short cut that lays the foundation for tomorrow's crises.

## Acknowledgments

The successful overview of a technology as broad as free balloons must surmount many obstacles. A new perspective, attempted in the format of a management science such as Technology Forecasting, is prone to both overstated inferences and vaguely formulated solutions. The degree to which these have been avoided is due in great part to the critical comments of my colleagues, particularly Mrs. Catherine B. Rice and Mr. Ralph J. Cowie.

## Bibliography

- Alexander, H. (1973) The Effect of Material Deformation on the Shape and Stress State of a High Altitude Balloon, Proceedings, Seventh AFCRL Scientific Balloon Symposium, AFCRL-TR-73-0071.
- Alexander, H. and Agrawal, P. (1974) Gore Panel Stress Analysis of High Altitude Balloons, Proceedings, Eighth AFCRL Scientific Balloon Symposium, AFCRL-TR-74-0393.
- Ayers, R. U. (1969) Technology Forecasting and Long-Range Planning, McGraw-Hill Book Company.
- Blamont, Jacques et al. (1974) New Method to Study the Dynamics of the Stratosphere; Principle and First Results, Sciences Physiques. Vol. 278, No. 7.
- Braun, R. H., Kelly, T. W. et al. (1957) Handbook of Geophysics for Air Force Designers, First Edition, Chap. 20, p. 43.
- Carlson, L. et al. (1973) High Altitude Balloon Package Thermal Analysis: Model and Computer Program, Texas A&M University, TAMRF-921-7307.
- Carlson, L. et al. (1973) Thermal Sensitivity of High Altitude Balloon Packages, Texas A&M University, TAMRF-921-7308.
- Corbais, F. W. Jr., Giannetti, A., et al. (1973) The Opening Performance of 100-ft and 140-ft Diameter RSR Parachutes Near 100,000 Feet with Balloon Borne Payloads, Seventh AFCRL Scientific Balloon Symposium, AFCRL-TR-73-0071, pp 239-25P.
- Davidson, A. R. Jr. (1967) Flight Control System and Launching Techniques for Air Ballast Systems, AFCRL-67-0679, Scientific Report No. 2, Contract F19628-67-C-0192.
- Davidson, A. R. Jr. (1968) Development and Testing of Air Ballast Systems, AFCRL-68-0556, Final Report, Contract F19628-67-C-0192.
- Davidson, A. R. Jr., Jackson, J. P. and Bassett, R. E. (1967) A Survey of Methods for Controlling the Altitude of Free Balloons with Air Ballast Systems, AFCRL-67-0372, Scientific Report No. 1, Contract F19628-67-C-0192.
- Dwyer, J. F. (1965) Some Polyethylene Balloon Statistics, Proceedings AFCRL Scientific Balloon Workshop, AFCRL-66-309.
- Dwyer, J. F. (1972) Polyethylene Balloons for High Altitude Operations and Research, Air Force Systems Command Technology Forecasts.

- Dwyer, J. F. (1973) Balloon Apex Pressure Differential, AFCRL-73-0632.
- Grass, L. A. (1962) Superpressure Balloon for Constant Level Flight, AFCRL-62-824.
- Kerr, A. D. and Alexander, H. (1967) On a Cause of Failure of High Altitude Plastic Balloons, Scientific Report No. 2, Contract F19628-67-C-0241, AFCRL-67-0611.
- Kreith, F. et al. (1970) Thermal Analysis of Balloon-Borne Instrument Packages, NCAR-TN-45.
- Lally, V. E. (1967) Superpressure Balloons for Horizontal Soundings of the Atmosphere, NCAR-TN-28.
- Laping, H. and Griffin, A. R. (1974) An Advanced Balloon Locating System, Proceedings, Eighth AFCRL Scientific Balloon Symposium, AFCRL-TR-74-0393.
- Low, W. C. (1961) Identifying and Evaluating the Barrier Problems in Technology, Technological Planning (on the corporate level), Proceedings of a Conference Sponsored by the Associates of the Harvard Business School, Edited by J. R. Bright.
- Martino, J. P. (1967) Long Range Forecasting Methodology, Office of Aerospace Research, USAF.
- Piacentini, A. et al. (1965) Heat Transfer Considerations in the Temperature Control of Instrumentation Packages at High Altitudes, AFCRL-65-380.
- Rice, C. B. (1974) Annotated Bibliography for Scientific Ballooning, AFCRL-TR-74-0040.
- Schon, D. A. (1967) Technology and Change, Delacorte Press, N.Y.
- Smalley, J. H. (1963) Determination of the Shape of a Free Balloon (Balloons with zero superpressure and zero circumferential stress), AFCRL-64-734, Scientific Report No. 2, Contract AF19(628)-2783.
- Smalley, J. H. (1970) Development of the e-Balloon, Proceedings, Sixth AFCRL Scientific Balloon Symposium, AFCRL-70-0543.
- Starr, C. and Rudman, R. (1973) Parameters of Technological Growth, Astronautics and Aeronautics 11 (No. 6):20-27.
- University of Minnesota (1955) Progress Report on High Altitude Balloons, Volume XIII, Contract NONR-710(01).
- Weissmann, D. (1972) The Influence of Changes of Material Structure On the Failure of Polyethylene Balloon Films, Proceedings, Sixth AFCRL Scientific Balloon Symposium, AFCRL-70-0543.

## **Appendix A**

**Date for Capability Trends and Payload and  
Gross Load Accomplishment Trends**

Table A1. Polyethylene Balloon Data for Figure 3

Year	Payload (lbs)	Altitude (feet)	$\lambda^3$ ( $10^6 \times \text{ft}^3$ )	Balloon Volume ( $10^6 \times \text{ft}^3$ )
1950*	431	77,000	0.157	-----
1953*	980	82,000	0.453	-----
1954	1530	76,800	0.552	0.804
1957	444	104,700	0.600	3.10
1958	1250	102,500	1.52	3.50
1959*	1500	111,500	2.81	5.27
	3201	89,500	2.12	3.20
	4001	65,000	0.811	1.06
1960	500	126,000	1.83	4.85
1961*	2000	118,700	5.26	11.85
1963	4500	92,000	3.35	5.02
1968	400	157,900	5.73	28.69
1969*	3800	125,000	13.34	27.30
	4148	119,500	11.32	20.8
1970	5135	117,000	12.49	20.8
1971	3940	126,500	14.81	26.6
	1270	141,800	9.40	30.5
1972*	1834	147,800	17.47	46.1
	3615	130,000	15.90	33.1
	1525	148,000	14.62	36.36
	6155	112,100	11.86	19.76
	510	167,200	10.39	47.8
1973	5152	118,000	13.11	20.8

\* Envelope points.

Table A2. Reinforced Polyester Film Balloon Data For Figure 4

Year	Payload	Altitude	$\lambda^3$ ( $10^6 \times \text{ft}^3$ )	Balloon Volume ( $10^6 \times \text{ft}^3$ )	Reference
1960	2034	59,600	0.319	0.364	1
1962	9100	80,000*	3.82	5.25	2
	4800	82,000	2.22	3.2	3
1966	3627	123,200	11.74	26.0	4
1970	8500	110,000	14.82	27.7	5
1972	5242	120,000	14.64	34.6	6

\* Approximate altitude.

<sup>1</sup>Slater, R. J. (1961) Development of A Heavy Load Carrying Balloon Using High Strength And Tear Stopping Films, Progress Report, Office of Naval Research Contract NONR 2899(00).

<sup>2</sup>Scientific Ballooning, No. 8, March 1963, NCAR, Boulder, Colorado.

<sup>3</sup>AFCRL Post Flight Report No. SG-5.

<sup>4</sup>AFCRL Flight Record H66-68.

<sup>5</sup>AFCRL Flight Record H70-75.

<sup>6</sup>AFCRL Flight Record H72-43.

Table A3. Polyethylene Balloon Data for Figure 10

Year	Payload (lbs)	Gross Load (lbs)	Balloon Volume ( $10^6 \times \text{ft}^3$ )
1954	1530	2084	0.804
1959	4001	5217	1.06
1963	4500	5810	5.02
1971	8379	13672	6.87
1972	9040	14545	6.87

Table A4. Reinforced Polyester Film Balloon Data For Figure 11

Year	Payload (lbs)	Gross Load (lbs)	Balloon Volume ( $10^6 \times \text{ft}^3$ )	Reference
1960	2034	2334	0.364	1
1962	9100	12400*	5.25	2
1963	11000	14300*	5.25	3
1964	----	16000	5.25	4
1969	13808	21959	33.8	5

\* Based on nominal balloon weight.

<sup>1</sup>Slater, R. J. (1961) Development of A Heavy Load Carrying Balloon Using High Strength and Tear Stopping Films, Progress Report, Office of Naval Research Contract NONR 2899(00).

<sup>2</sup>Scientific Ballooning, No. 8, March 1963, NCAR, Boulder, Colorado.

<sup>3</sup>Scientific Ballooning, No. 13, March 1964, NCAR, Boulder, Colorado.

<sup>4</sup>Balloon Notes from Schjeldahl, Vol. 1, No. 2, June 1964.

<sup>5</sup>AFCRL Flight Record H69-70.

## Appendix B

The following patents are examples of the predictable results of a parametric characterization of balloon structural design.

(1) Balloon shape: Variable volume balloon and method of its manufacture, No. 2,612,328, W. F. Huch (13 July 1950 - 30 Sept. 1952).

(2) Heat sealed load tapes: Balloon having reinforced seal, No. 2,858,090, O. C. Winzen et al (21 Feb. 1955 - 28 Oct. 1958).

(3) Tandem balloon: Balloon structure and method of launching the same, No. 2,919,083, V. E. Soumi et al (12 March 1956 - 29 Dec. 1959).

(4) Reinforcement pattern: Balloon envelope structure, No. 3,369,774, A. D. Struble, Jr. (2 Aug. 1961 - 20 Feb. 1968).



#### Contents

1. Introduction	163
2. Package and Thermal Analysis Model	164
3. Application and Comparison With Flight Results	165
4. Thermal Behavior of an Around the World Package	168
5. Conclusions	172
Acknowledgment	173
References	173

## Thermal Analysis of Long Duration Flight Packages

L.A. Carlson\* and P.M. Brondeberry\*\*  
Texas A&M University  
College Station, Texas

### Abstract

A model suitable for predicting the transient thermal behavior of balloon packages is discussed and comparisons with flight measurements are presented. Predictions for a typical around-the-world package are presented and the configuration and environmental factors that affect the package thermal behavior are discussed.

### 1. INTRODUCTION

The success of a high altitude balloon package experiment frequently depends upon maintaining the scientific instruments in the payload within certain specified temperature limits. Since the package may be subjected to both daylight and

\*Associate Professor, Aerospace Engineering Department.

\*\*Graduate Research Assistant, Aerospace Engineering Department.

darkness, it must be designed to survive significant changes in its thermal environment; and, thus, thermal analysis and accurate prediction of payload component temperatures is an important part of preflight planning. This is particularly true with the development of super-pressure balloon technology and the advent of long duration flights since restrictions on package size, weight, etc. will require the package thermal protection systems on such flights to be passive.

The purpose of this paper is threefold. First, it is to discuss a mathematical model suitable for predicting the transient thermal behavior of long duration packages. Secondly, it is to present comparisons between predictions and flight measurements with particular emphasis on the problems associated with night flights. Finally, it is to present thermal predictions for a typical around-the-world package and to discuss the thermal sensitivity of that package to environmental and configuration factors.

## 2. PACKAGE AND THERMAL ANALYSIS MODEL

In order to efficiently provide the package designer with reliable and accurate information, staff members of NSBF in conjunction with researchers at Texas A&M University have developed a mathematical model and computer program for thermally analyzing balloon packages.<sup>1</sup> In

this generally applicable model, the actual package is represented by an equivalent external surface area sphere as shown on Figure 1. Normally, this idealized package is assumed to be covered on the outside by a surface coating, typically paint or tape, followed by a layer of insulation. Non-insulated packages, however, can be handled. Inside, the components are divided into two groups. Those located near the outside wall, such as supporting structure, and those of low heat capacity are grouped together under the heading of internal components. The remaining elements are considered to be part of the reservoir, and it is the latter which normally contains the scientific instruments. (The elements

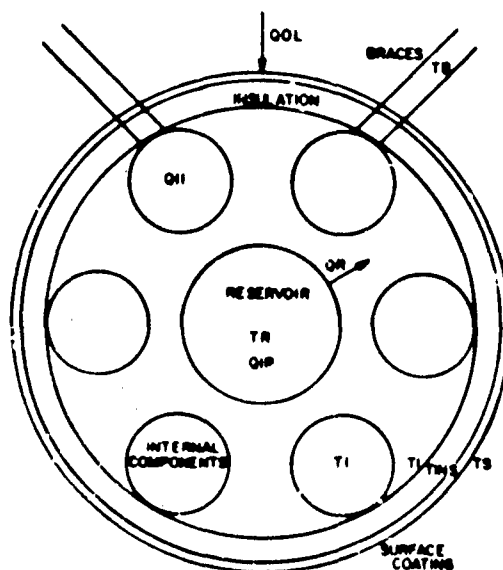


Figure 1. The Equivalent Area Sphere Model of a Balloon Package

near the center are called the reservoir because they respond slowly to changes and serve as a heat "reservoir" for the rest of the package.)

At any instant, all the components in a group are assumed to have the same temperature, and no circumferential variation is considered. All temperatures are, however, considered to be functions of time. Also, the model permits the dissipation of power, such as would be generated by electronics and on-board heaters, in both the internal and reservoir components. Internally, the model accounts for convection between the components and the inside air, radiation between components, and conduction through the insulation and braces, if present. Externally, the heating consists of forced and natural convection with the atmosphere and of radiative transfer. During daylight, the radiative heating to the package is typically 50 percent solar, 25 percent earth albedo, 20 percent atmospheric, and 5 percent earth and balloon infrared. Of course, the solar flux and earth albedo are absent at night.

The model also includes changes due to atmospheric variations with altitude, changes in internal or reservoir power levels, sunrise and sunset, etc. For a typical package, complete results can be obtained in less than two minutes on an IBM 360/65 (Watfiv compiler) computer. A complete discussion of the mathematical model and computer program is given in Reference 1.

### 3. APPLICATION AND COMPARISON WITH FLIGHT RESULTS

During the past two years, the model has been regularly used to analyze flight packages, and comparisons with flight measurements indicate that the model can accurately predict daytime temperature variations on both large<sup>1</sup> and small packages.<sup>2</sup> In addition it has been used to study the thermal sensitivity of balloon packages to various configuration and environmental parameters. The results of this study have been reported in References 3 through 5 and can be summarized as follows:

(1) During daylight, a high altitude balloon package is thermally very sensitive to such configuration factors as type of external coating and amount of internal power supply heat dissipation, moderately sensitive to the type and thickness of insulation, presence of external braces, and interior pressurization, and insensitive to the inside wall coating or size of the balloon.

(2) The daytime thermal behavior is very dependent upon such environmental conditions as time of the year, temperature of the package at launch, and whether or not the package is exposed to sunlight prior to launch.

Many packages, however, fly at night or for twenty-four hours or longer. Package N was typical of such packages, being a cylinder 1.52 meters in diameter

and 3.04 meters in length. This package was pressurized, dissipated internally 463 watts, and contained about 20 components which were designed to operate at temperatures above freezing. Originally, the package had no external insulation and was painted white. For a daytime flight, this configuration would probably have been excellent since the 463 watts internal power might have created an overheating problem and white paint usually yields cool skin and wall temperatures.

Almost all paints, however, have infrared emissivities of about 0.9;<sup>2</sup> and thus, at night any external painted surface will radiate away large amounts of heat and may cause excessive cooling. To check this possibility, a thermal analysis of Package N was performed. For a sunset launch, the results indicated that the inside wall would go below freezing twenty minutes after launch and that the reservoir would pass freezing three hours after launch. In fact, ten hours after ascent, the inside component temperatures were predicted to range from  $-22^{\circ}\text{C}$  to  $-36^{\circ}\text{C}$ . Obviously, some type of change was indicated.

Since the problem was an excessive radiative heat loss from the external skin, the solution was to coat the package with a material having a low infrared emissivity. At present, only three materials have this property—Al-Mylar tape with mylar out ( $\alpha = .12$ ,  $\epsilon = 0.34$ ), Al-Mylar tape with aluminum out ( $\alpha = .12$ ,  $\epsilon = 0.04$ ), and aluminum foil ( $\alpha = .15$ ,  $\epsilon = .04$ ). An analysis for the package covered with aluminum foil predicted reservoir temperatures  $14$ - $23^{\circ}\text{C}$  and inside wall temperatures of  $-3^{\circ}$  to  $23^{\circ}\text{C}$ , well within flight requirements.

For the actual flight the investigators decided to zebra strip the package with aluminum foil and white paint, preheat it to  $18^{\circ}\text{C}$ , and place it on the pad 1.5 hours prior to launch. Figure 2 compares predicted results for this configuration with the average temperatures measured in flight. Obviously, even with only about 50 percent of the surface coated with white paint ( $\alpha = .263$ ,  $\epsilon = .895$ ) the cooling effect is substantial. Also, the agreement with flight data is excellent and indicates that the present model can be successfully used for night flight predictions.

On twenty-four hour flights, the problem of large solar radiative input during daylight is combined with possibly large radiative losses at night; and usually, large temperature variations in package components must be expected. However, these variations can be controlled through proper choice of insulation and surface coating. This control is demonstrated on Figure 3 where the effect due to doubling the insulation and changing the coating can be observed. For this package, some of the important instruments were modeled as internal components and some were modeled as the reservoir; and, thus, both areas were of interest. Notice the large temperature changes associated with sunset and sunrise and the power change at sunrise. Notice also that for the thicker insulation aluminum-mylar tape case (mylar out) that the night time temperatures are significantly warmer and the

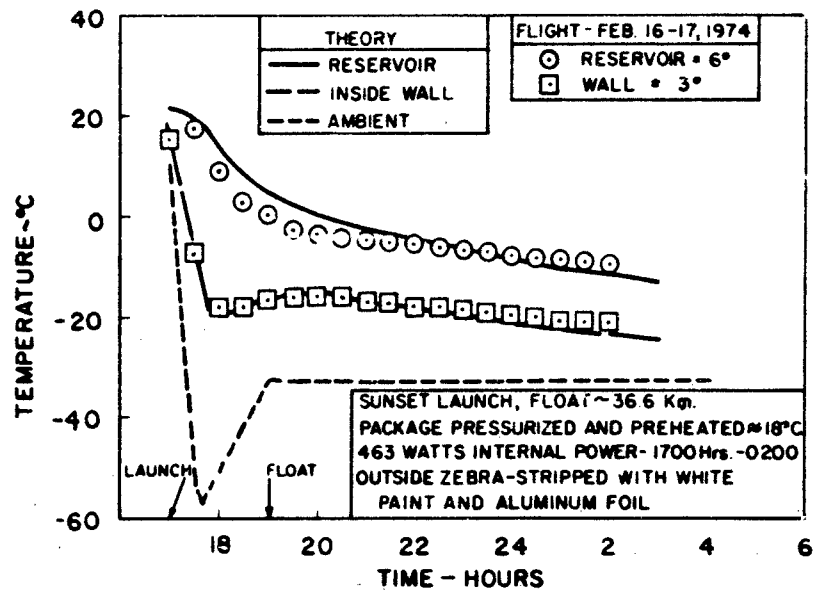


Figure 2. Comparison of Flight Measurements and Predicted Temperatures for a Night Flight

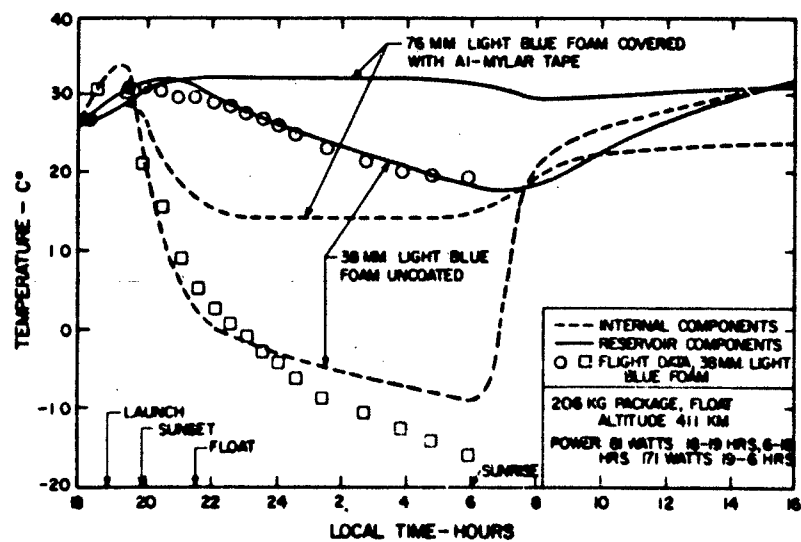


Figure 3. The Effect of Insulation Thickness and Surface Coating on Component Temperature

daytime values are slightly cooler than the thin insulation case. Obviously, the thicker insulation reduces the temperature gradients, and the aluminum-mylar tape prevents excessive cooling during the night.

Some night measurements for the thin insulation case are also shown on Figure 3. It is felt that the predictions agree quite well with the data considering the details of the actual flight. At 2330 hours the balloon experienced an unplanned descent from 41.1 km to about 37 km, where the ambient temperature is about  $5^{\circ}\text{C}$  colder. At about 0400 hours the package heaters failed, and the flight was terminated at sunrise. Even so, as can be seen, the predictions were quite good.

Many other 24-hour packages ranging in size from 1 kg transducers to 1000 kg gondolas have been analyzed with the present model. These packages have ranged in complexity from spheres to a configuration that involved ten separate boxes mounted on a large plate. (In the latter case, each box was analyzed separately.) In general, flight and vacuum chamber results have verified that the present model is adequate for determining the thermal protection system of such packages.

#### 4. THERMAL BEHAVIOR OF AN AROUND THE WORLD PACKAGE

With the development of super-pressure mylar balloons, long duration flights which enable a package to circumnavigate the earth are now or soon will be possible. To give the flight scientist and package designer an idea of the temperature variations that will be encountered, a "typical" around the world package was analyzed for a variety of conditions. The initial package weighed 181.5 kg, was a 0.92 m cube, had 35 watts of internal power, and a float altitude of 39.6 km. Internally, it was assumed that the components and structure near the outside weighed 90 kg and were 80 percent aluminum and 20 percent electronics. The reservoir was assumed to be 80 percent electronics and 20 percent aluminum structure. Externally, the package had two inches of dark blue foam insulation coated with aluminum-mylar tape.

For the first calculation, it was assumed that the package was pressurized and that launch occurred from Australia in December. Also, even though they would vary during the flight, the earth albedo and temperature were assumed constant at 0.22 and  $20^{\circ}\text{C}$  respectively. These values are typical of those encountered over the Indian and Pacific Oceans.

Figure 4 shows the first day of the flight. Since December is during the Australian summer, the initial temperature is quite high,  $26^{\circ}\text{C}$ , and this results in fairly warm temperatures during the first day. Notice that during the first day the reservoir is between  $15^{\circ}\text{C}$  and  $26^{\circ}\text{C}$  and is warmer than the skin temperature. This indicates that during the first day the heat flow is from the inside to the outside. Also notice that the temperatures are relatively constant after arrival at float.

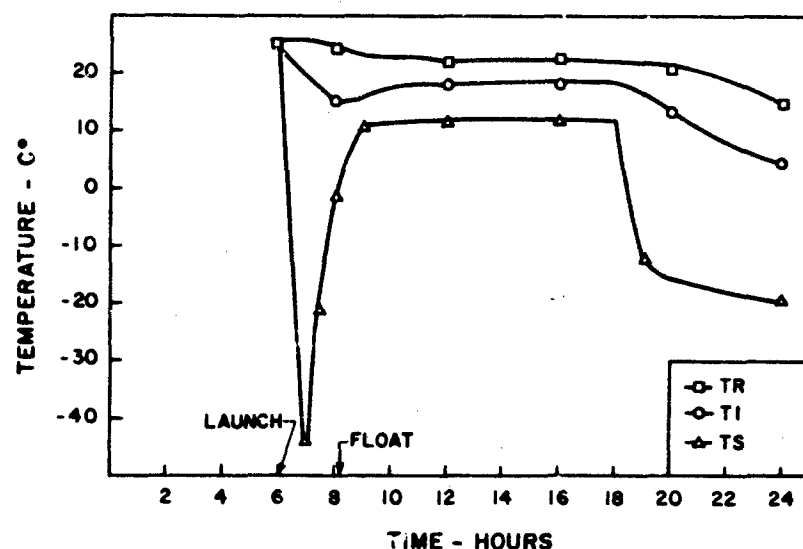


Figure 4. The First Day of an Around the World Package

Beginning with the first night and lasting for about four days, the package begins a general cooling off with the maximum temperature achieved each day being less than that reached the day before. Apparently, it takes several days for the effect of the high initial temperature to disappear. It had previously been noted<sup>3</sup> that on short flights the initial temperature was very important, but it was surprising to see the initial effect last for several days.

After seven days, the thermal behavior takes on a pattern that is identically repeated every 24 hours; and this pattern is shown on Figure 5. In this cycle, the reservoir temperature ranges from about  $-2^{\circ}\text{C}$  to  $9^{\circ}\text{C}$ , and at night the heat flux is from the inside to the outside. During the day, however, the skin temperature is above the inside and the heat flow is from the outside inward. The latter is opposite of the heating pattern experienced by the package during the first day of the flight. Also notice that the internal and reservoir temperatures are  $10^{\circ}$ - $20^{\circ}\text{C}$  colder than those predicted for the first day.

As indicated, the earth albedo will vary as the package travels around the earth; and, consequently, a subsequent calculation including variable albedo was conducted. While this variation did create some small oscillations in the temperature profiles, the results were never more than  $2^{\circ}\text{C}$  different from those obtained assuming constant albedo. It should be noted, however, that this study only included the variation encountered in passage over land and ocean and not that due to a cloud cover.

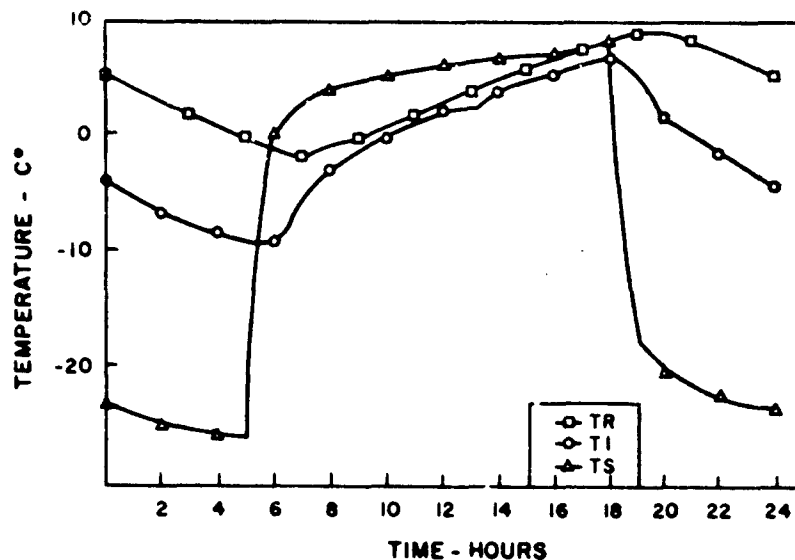


Figure 5. The Equilibrium Pattern Obtained by an Around the World Package

Figure 6 shows the daily temperature range experienced by the package for the situation where the albedo varies. For this case, after about four days, the albedo factor remains fairly constant around 0.25. Thus, the equilibrium temperatures are slightly higher than those shown on Figure 5. Nevertheless, the basic pattern of a four day cooling period followed by equilibrium cycles is the same.

As can be seen on Figure 6, the equilibrium temperatures inside the package range from about  $-8^{\circ}\text{C}$  to  $10^{\circ}\text{C}$ ; and for some experiments these values may be too cold. Figure 7 shows the effect of doubling the thickness of insulation on the package while retaining the same external coating. Basically, this extra insulation slows the night-time conduction of heat to the outside and increases the cooling period to about 5.5 days. In addition, the final inside temperatures are warmer, being  $0.5^{\circ}$  to  $14.5^{\circ}\text{C}$ , and the maximum-minimum difference is smaller. Thus, it appears that extra insulation can increase the component temperatures  $4$  to  $8^{\circ}\text{C}$ .

Another surface coating that may be attractive for long duration flights is aluminum foil or aluminum-mylar tape with aluminum out. These have a very low infrared emissivity,  $\epsilon = 0.04$ , which should prevent any significant night-time radiative cooling. Their solar absorptivity,  $\alpha$ , however, is believed to be between



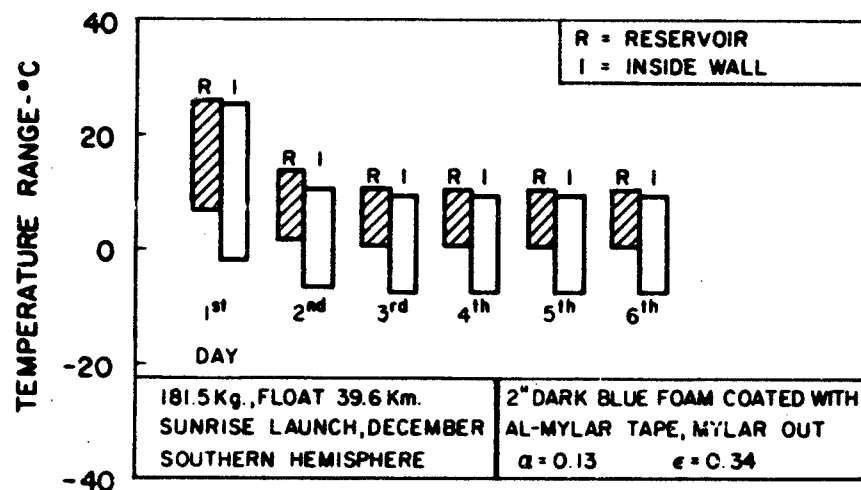


Figure 6. Daily Temperature Variation of an "Around The World" Balloon Package

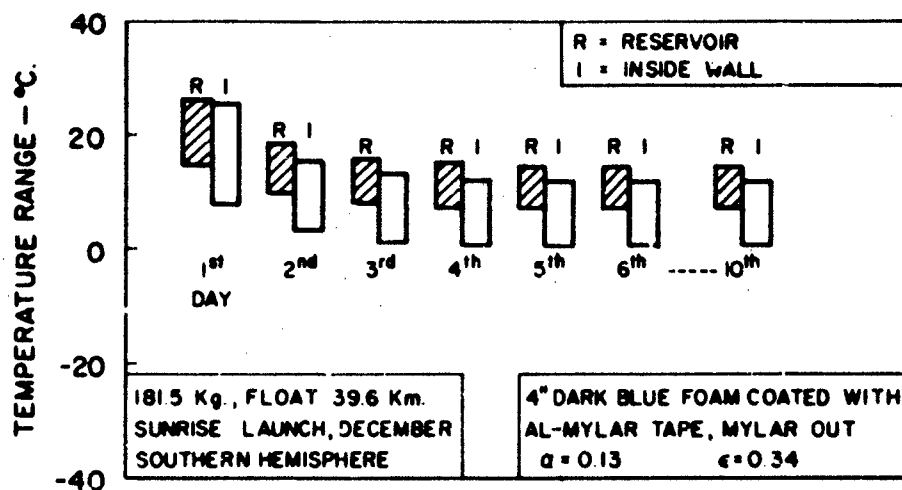


Figure 7. Daily Temperature Variation of an "Around The World" Package, Thick Insulation Case

0.10 and 0.14, which yields an  $\alpha/\epsilon$  ratio of about three. As a consequence, during daylight a surface coated with such a material should absorb more heat than it radiates and should warm up.

Figure 8 shows results for the "typical" around the world package coated with aluminum foil. Notice that the package continually warms up over a period of about six days and achieves temperatures which might be considered too hot for some instruments. While these particular results may not be exactly accurate due to uncertainties in the value of the solar absorptivity of aluminized surfaces, they do indicate that the thermal behavior of long duration packages is very sensitive to the type of coating used on the external surfaces of the package. Thus, further investigation of the properties of practical coatings would be desirable.

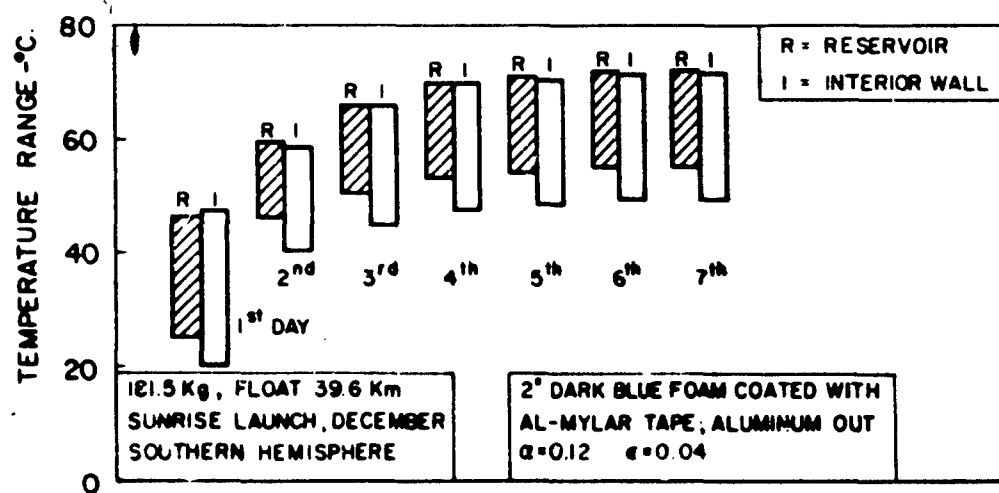


Figure 8. Daily Temperature Variation of an "Around The World" Package Coated with Aluminum-Mylar Tape (Aluminum Side Out)

## 5. CONCLUSIONS

Based upon these results, it is believed that the following conclusions can be stated:

- (1) The present model can be used to accurately predict the thermal behavior of long duration high altitude balloon packages and to design their thermal protection systems.

(2) For both short and long flights, packages are thermally most sensitive to the radiative properties of the external coating and to the package prelaunch temperature. The latter can affect the package temperature for several days.

(3) For night flights, surface coatings having low infrared emissivities are desirable.

(4) For long duration flights, cyclical temperature variations of 15°C or more must be expected in the package components. However, reasonable control can be maintained by proper choice of insulation and surface coating.

## Acknowledgment

The information upon which this report was based was obtained while performing research for the University Corporation for Atmospheric Research which is sponsored by the National Science Foundation. UCAR's technical representatives for the work herein are Mr. Alfred Shipley, Manager, National Scientific Balloon Facility, and his delegated representative, Mr. Mike Pavey, Head of Engineering Department.

## References

1. Carlson, L.A., Morgan, P.S., Stefan, K., Wilson, W.C., and Cormak, R.H. (1973) High Altitude Balloon Package Thermal Analysis: Model and Computer Program, Texas Engr. Expt. Station Rept. TAMRF-921-7307.
2. Morgan, P.S., and Carlson, L.A. (1973) Thermal Analysis of the Multi-Therm Balloon Packages, Texas Engr. Expt. Station Rept. TAMRF-921-7306.
3. Carlson, L.A., and Morgan, P.S. (1973) Thermal Sensitivity of High Altitude Balloon Packages, Texas Engr. Expt. Station Rept. TAMRF-921-7308.
4. Carlson, L.A. (1974) Thermal Analysis-Survival, Atmospheric Technology, March 1974 pp. 40-30
5. Morgan, P.S. (1974) A Study of the Thermal Sensitivity of High Altitude Balloon Packages, M.Sc. Thesis, Texas A&M Univ., also Texas Engr. Expt. Station Rept. TAMRF-921-7401.

#### Contents

1. Introduction	176
2. The Superpressure Principle	177
3. Stress Distributions	180
4. Shear Lag Effects	183
5. Conclusions	188
Acknowledgments	189
References	189

## Balloon Design

James L. Rand\*  
Texas A&M University  
College Station, Texas

## Abstract

The status of superpressure balloon technology for design purposes is reviewed and the effects of various simplifying assumptions are evaluated. A comparative analysis is made between two large superpressure balloons, one that was flown successfully and another that failed catastrophically. Under design float conditions, the maximum stresses are shown to be in the vicinity of the load introduction point where shear stresses tend to dominate the state of stress. It is concluded that the stresses due to superpressure are sufficiently large to neglect the effects of balloon and payload weight during preliminary design. It is also demonstrated that "shear lag" effects in the vicinity of load introduction may be calculated which will provide the designer with needed information on stress concentrations. A system of limit load factors should be defined for the benefit of the designer so that he may protect the film from undesirable stress concentrations. In addition, material characterization of balloon films in the "as used" condition is necessary if there is ever to be a correlation between design stresses and actual flight conditions.

---

\*Associate Professor, Aerospace Engineering Department.

## 1. INTRODUCTION

The design of high altitude scientific balloons has evolved over the years strongly influenced by material quality and manufacturing techniques. However, the possibility of long duration flights has created a demand by the scientific community for balloon vehicles utilizing superpressure technology in an environment where no prior experience exists. In the period from the late 1950's to early 1960's, an Air Force Cambridge project was conducted involving the design and flight testing of superpressure balloons. This program resulted in a few successful, although relatively short lived, flights of 300 pound payloads on 120-foot diameter superpressure spherical balloons. Much of the current design and fabrication technology used for this type of balloon was originated in this program. Additionally, a wealth of information has been gleaned from the Southern Hemisphere GHOST (Global Horizontal Sounding Technique) flight program where 85 flights were made in 1966 and 1967. The superpressure balloon technology developed in this program for relatively small balloons has been reported by Lally.<sup>1</sup> The results of these two programs essentially constitute the state of the art. In the past 7 years, this technology has been used to design approximately 60 superpressure balloons with diameters from 30 to 71 feet. These systems have successfully lifted 230 pounds, reached an altitude of 108,000 feet, and remained at altitude for as long as 261 days.

In early 1972, a program was initiated at the National Scientific Balloon Facility to fly superpressure balloons from Australia, allow them to circumnavigate the earth and successfully recover the scientific payload after one or more "orbits", thereby demonstrating the feasibility of long duration ballooning. As a part of this program but prior to the Australian expedition, a 110 foot diameter superpressure balloon successfully lifted 153 pounds to 99,000 feet on a test flight from Palestine. In early 1973, a 64-foot diameter sphere carried 150-pounds to 80,000 feet for 36 days and two "orbits" of the earth. The scientific experiment was cut-down by radio command and was successfully recovered only nine miles from the launch site. Encouraged by many scientists as a result of this successful flight, the National Scientific Balloon Facility requested funds to develop a capability of launching, monitoring, and commanding a superpressure balloon system capable of circumnavigating the earth carrying a 500-pound payload at an altitude of 130,000 feet. This program has been recently approved and represents the current design goal.

Two subsequent test flights attempted to lift 325 pounds to an altitude of 120,000 feet with a nominal 200-foot diameter balloon but were not completely successful. In one case, the system could not be adequately pressurized at sunset due to radiant cooling causing it to lose altitude after reaching the design altitude.

The second balloon ruptured while being pressurized at altitude. Therefore, since attainment of an intermediate design objective has not yet been successful it would appear that a more detailed analysis of these superpressure systems is not only advantageous, but essential if the design objective is to be met in the next two years.

## 2. THE SUPERPRESSURE PRINCIPLE

Current superpressure balloon technology has been thoroughly documented by Lally<sup>1</sup>, but a very brief review of the governing principles is justified for those not familiar with these systems. A superpressure balloon is a fixed volume system which is sealed to prevent loss of the lifting gas. The balloon is filled with a controlled amount of gas which creates sufficient free lift to reach the desired altitude. As the balloon rises, the gas expands to a point where the bag is fully deployed to its design shape. At this point, since the gas can no longer expand, any remaining free lift causes the gas to increase in pressure at a fixed volume. Since the mass of gas and volume of air displaced are fixed, the system will float at a constant density altitude. In addition, any fluctuation in temperature or ambient pressure will cause the balloon pressure and pressure differential across the gas barrier to fluctuate, but the system will remain at the same density altitude.

A superpressure balloon is a pressure vessel which must maintain sufficient tensile stress in the film to maintain a relatively constant volume while undergoing these periodic changes in differential pressure. It can be shown that this pressure differential is related to the free lift at launch and supertemperature through the following expression:

$$\frac{\Delta p}{p_{amb}} = f + (1 + f) \frac{\Delta T}{T}$$

where  $f$  is the free lift ratio at launch based on total system mass (including the mass of lifting gas), and  $\Delta T/T$  is the ratio of supertemperature to ambient temperature. For design purposes it is assumed that the temperature ratio may vary from -0.12 to +0.10. Based on this lower limit it is obviously necessary to have a free lift ratio of at least 0.137 to maintain a positive pressure differential. The upper limit will be dictated by the strength of the film material used to construct the gas barrier.

The selection of an appropriate balloon material is governed by not only the unique requirements of the overall system but also by the imagination of the

designer and flexibility of the manufacturing technique. In general, it would be desirable to have a system that is impermeable to the lifting gas, transparent to the entire spectrum of radiation, experience no volume change during pressurization and survive rough ground handling. Unfortunately, no existing material can be used with conventional manufacturing techniques to achieve this goal; but, reasonable success has been attained in the past using laminated polyester films and modern design and manufacturing techniques. In these designs, the film itself must provide the stiffness for the system since there is no circumferential load carrying capability except through the film. The polyester films have a modulus of elasticity in excess of 500,000 psi at float conditions and thereby produce a change in volume (and corresponding change in altitude) that is acceptable. The material is reasonably transparent to radiation and the lamination process results in a film which is adequately impermeable to helium. The launch technique is somewhat more delicate than normal and a tow balloon and excess ballast is necessary to help the system rise through the troposphere.

Experience to date indicates only that the polyester films have worked in the past. There is no evidence to indicate that it is the optimum material to use. It is well known that this material is significantly weakened by creasing, folding and other types of ground handling and aerodynamic buffeting. It is understandable that the manufacturers are interested in new designs and materials that will meet the superpressure mission requirements with improved reliability and reduced cost. Other materials such as nylon, polyethylene and other fiber reinforced polymer matrix materials are being carefully studied. The use of these materials will ultimately require a more general characterization of the material such as that reported by Alley<sup>2</sup> and Faison. Design techniques will then have to be refined to the point of utilizing the non-linear characteristics of these materials to exploit their full capability.

Since a superpressure balloon vehicle is a pressure vessel, designers have focused their attentions on the general class of oblate spheroids and in particular on the sphere. If it is assumed that the balloon is manufactured from a homogeneous and isotropic material without seams, and if both the payload and balloon vehicle are weightless, then the stress will be the same in both meridional and circumferential directions and is given by the expression:

$$\sigma = \frac{\Delta p R}{2t} = \frac{p_{amb} R}{2t} \left[ 1 + (1+f) \frac{\Delta T}{T} \right]$$

In the past, superpressure balloons have been manufactured in a manner similar to zero pressure, natural shape balloons. They are constructed of a number of flat gores or half-gores and then joined together with seams or seal

tapes running in the meridional direction. The resulting balloon is then stiffer from top to bottom than in the circumferential direction. Recognizing this, it is normally assumed that the stress in the meridional direction is only two thirds of the circumferential stress.

A number of small superpressure balloons made of bi-laminated polyester film have failed apparently due to overpressurizing the system. Based on the measurement of pressure at failure and the preceding equation with all its inherent assumptions, it has been determined that 13,000 psi represents the ultimate stress of this material after fabrication into a spherical shape. In accordance with aerospace engineering practice, a factor of safety of 1.25 is considered adequate for an unmanned flight vehicle. Therefore, the designer has been required to produce a design where the stress predicted by the preceding equation does not exceed 10,000 psi under design conditions. The previously flight proven design procedure has been carefully followed by the manufacturers; however, a nominal 200-foot diameter superpressure balloon has not yet been successfully flown.

It is obvious that the design procedure used must be improved if we are to achieve the current design goals or assess the altitude or load limitations of superpressure balloon systems. This problem should be attacked in at least two directions. First, it is known from laboratory testing of polyester films that the yield strength of the virgin material is greater than 13,000 psi. However, the material is not used in this optimum condition and the resulting strength figures are misleading. Therefore, it would be advantageous to the designer if some type of laboratory testing technique could be developed which would yield strength values of a more practical nature.

The second avenue should be a detailed analysis of the state of stress in the balloon itself. It will be shown that the stress predicted by the preceding equation is anything but conservative. It is common practice to apply the factor of safety to the worst possible conditions to be anticipated in flight. This means that the worst combination of stress distributions and stress concentrations should be identified and evaluated before the factor of safety is applied. Evaluation of these locally high stress concentrations could be accomplished by a detailed stress analysis or the establishment of a set of limit load factors which is a standard procedure in the aircraft industry. It is only after the actual stress and the actual strength of the material are known that the adequacy of a design may be ascertained without extensive flight testing.



### 3. STRESS DISTRIBUTIONS

In an effort to evaluate the effects of various assumptions on the state of stress in superpressure balloons that have been designed in the past, several particular systems have been analyzed in more detail than has been previously reported. The effect of system weight which is assumed to be negligible in the preliminary design phase may be evaluated after the shape is known. All of the equations necessary to evaluate these effects have been developed by Smalley<sup>3</sup> and are readily available to the designer.

In developing these equations, it is assumed that the film is an elastic, homogeneous, isotropic material which has no bending rigidity and obeys the membrane equation. The balloon is again assumed to be formed without seams or seal tapes and the stresses are assumed to be uniformly distributed through the thickness and circumferentially about the balloon. Shear stresses are assumed to be non-existent and the resulting meridional and circumferential stresses are principal stresses. The payload is assumed to be introduced as a uniformly distributed load applied tangentially along a circumferential ring. Assuming the shape to be spherical, the resulting differential equation may be integrated to yield the following:

$$\frac{\sigma_m}{bR^2} = \frac{\Delta p}{2bR} + \frac{P}{3bV} K_m + \frac{\sin \phi}{3}$$

$$\frac{\sigma_c}{bR^2} = \frac{\sigma_m}{bR^2} - \frac{P}{3bV} (2K_m - \sin \phi)$$

where

$$K_m = \begin{cases} \frac{1}{\sin \phi + 1} & \text{if } \phi > \phi_0 \\ \frac{1}{\sin \phi - 1} & \text{if } \phi < \phi_0 \end{cases}$$

In this formulation  $\phi$  is the angular position on the sphere measured from the equator;  $P$  is the payload;  $b$  is the specific lift of the gas and  $\phi_0$  is the angular position of payload attachment.  $R$  and  $V$  are the radius and volume of the balloon respectively and  $\Delta p$  is the pressure differential at the center of the balloon and is assumed to be that given by the preceding equations.

These equations have been evaluated for a number of superpressure balloons that have already been designed and flown. For comparison purposes, results are presented here for two superpressure balloons which were designed to fulfill two completely different mission requirements. The first is the 110-foot diameter balloon that flew successfully in 1972 and the second is the 196-foot diameter balloon that failed catastrophically while being pressurized. The mission requirements and balloon characteristics were substantially different and are presented in Table 1.

Table 1. Balloon Characteristics

Radius (ft)	55	98.45
Payload (lbs)	158	367
Altitude (K ft)	100	120
Altitude (mb)	11	4.4
Free Lift, F(percent)	20*	20*
Supertemperature (percent)	10	10
Volume ( $\text{ft}^3 \times 10^6$ )	.697	3.987
Gross (lbs)	630	1407
$\phi_o$ (degrees)	-60	-60
P/bV	.25	.26
Half-Gore Width (in)	57.6	55.4
Half-Gores (nr)	72	134
Load Lines (nr)	72	67
Film Thickness (mil)	1.5	1.0

\*Standard Free Lift

The results of this analysis are presented in Figure 1 and graphically demonstrate the influence of vehicle weight and payload on the stress distribution when it is assumed that there is no circumferential variation in stress. The horizontal line in each figure represents the  $\Delta pR/2t$  term on which each design is based. In the first case, this stress is 9,985 psi and in the second case the stress is 10,724 psi. Although this second figure exceeds the 10,000 psi design objective, the balloon was flown with only 16.5 percent free lift so that under flight conditions it was well within the specified maximum stress levels.

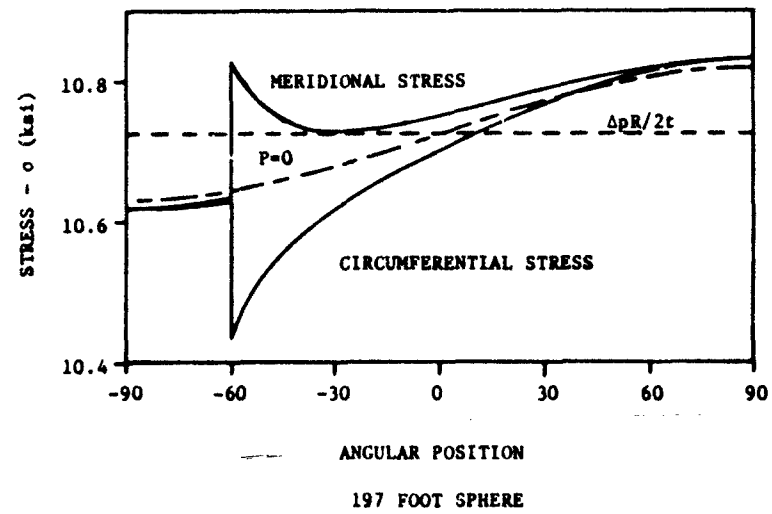
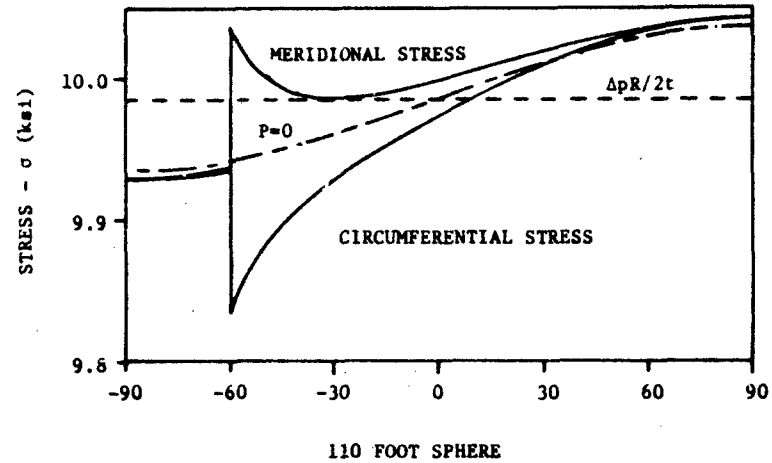


Figure 1. Effects of Balloon and Payload Weight

The curves labeled  $P = 0$  represent the stress distribution due to vehicle weight and the change in  $\Delta p$  due to head height. In each case, the meridional stress is equal to the circumferential stress and the payload is assumed to have a negligible effect on the stress distribution. The difference between this curve and the remaining two curves represents the influence of load introduction into the film. Since equilibrium must be maintained normal to the film, for an increase in the meridional stress there must be a corresponding decrease in the circumferential stress. In both cases, the maximum stress occurs at the apex of the balloon but an equal stress in the meridional direction very nearly occurs at the point of load introduction. The shear stress which is assumed to be zero in the coordinate system chosen, will be a maximum along a  $45^\circ$  line bisecting the meridional and circumferential axes. Since the difference in principal stresses is a measure of the maximum shear stress, the maximum will occur at the point of load introduction. However, the maximum difference in principal stresses is 200 psi in the first case and 390 psi in the second case; neither of which would appear to be significant.

It appears that the design stress is sufficiently large that the variations in stress due to vehicle weight and payload will not be a cause of failure so long as the stress is uniformly distributed around the circumference of the balloon. Therefore, the initial assumption of a weightless system would appear to be justified if the assumptions made in this analysis are reasonably accurate. Although polyester bilaminates are probably neither homogeneous nor isotropic, this appears to be a reasonably accurate approximation for design purposes. If St. Venant's principle is invoked, the assumption of a uniform stress distribution is justifiable except at points in the proximity of the load introduction point. Therefore, it appears justifiable to challenge this approximation in the region of  $\phi = \phi_0$  and consider in detail the mechanism by which the load is introduced into the film.

#### 1. SHEAR LAG EFFECTS

The term "shear lag" was introduced by Kuhn<sup>4</sup> while attempting to analyze the state of stress due to load introduction into thin sheets of aircraft materials. The term is equally appropriate to characterize the introduction of loads into superpressure balloon films. Unlike zero pressure balloons, the superpressure balloon is relatively stiff and can support shear once pressurization has occurred. The force required to support the payload is transferred through the load lines to the seam or seal tapes where it is introduced tangentially into the balloon film. By examining the small area immediately adjacent to the seam, as shown in Figure 2, it is obvious that the only mechanism operative in reducing the force in

the seam is a shear stress acting on the edge of the film. This shear stress must then obey the governing equilibrium equations in the film to transfer this load across the width of the gore.

Several analysts have attacked the problem of the effects of material deformation on the state of stress. The approach of Alexander<sup>5</sup> and Agrawal has successfully ascertained the effects of lobing on the state of stress in a "natural" shape balloon by assuming the change in tape force is uniformly distributed about the circumference. Lagerquist<sup>6</sup> utilized a large displacement finite element analysis of the TCOM system to determine the deformations and stresses. It is expected that the approach taken here will result in a more general design procedure rather than the analysis of a particular system.

In establishing a model of the problem in the area of load attachment, it is assumed that the effects of curvature are unimportant and the region can be assumed to be a rectangle subjected to in-plane forces only. Again, the material is assumed to be homogeneous and isotropic. The loads are assumed to be introduced symmetrically along each load line as shown in figure 2. Due to the symmetry of the deformations, the panel dimensions were chosen to be half the distance between load lines by twice this dimension. This latter dimension was chosen on the basis of St. Venant's principle as a position where the load should be reasonably uniformly distributed.

The governing differential equations when formulated in terms of displacements may be written as:

$$\frac{\partial}{\partial x} \left\{ K^* \left( \frac{\partial u}{\partial x} + \nu \frac{\partial v}{\partial y} \right) \right\} + \frac{(1-\nu)}{2} \frac{\partial}{\partial y} \left\{ K^* \left( \frac{\partial v}{\partial x} + \frac{\partial u}{\partial y} \right) \right\} = 0$$

$$\frac{\partial}{\partial y} \left\{ K^* \left( \frac{\partial v}{\partial y} + \nu \frac{\partial u}{\partial x} \right) \right\} + \frac{(1-\nu)}{2} \frac{\partial}{\partial x} \left\{ K^* \left( \frac{\partial v}{\partial x} + \frac{\partial u}{\partial y} \right) \right\} = 0$$

where  $K^* = Et/(1-\nu^2)$ , the in-plane stiffness. By observing the symmetry of the deformations, it is obvious that the shear stress must be zero along a meridional line between two load lines. Because of this condition, the simplification of assuming constant shear strain across the panel, introduced by Kuhn<sup>4</sup>, cannot be made in this case. Along the meridional line containing the load line, the change in force per unit length is related to the shear stress in the film as shown in Figure 2.

Solutions were obtained for the above set of equations by rewriting the derivatives in finite difference form and solving the resulting set of simultaneous equations for the displacements in both meridional and circumferential directions.

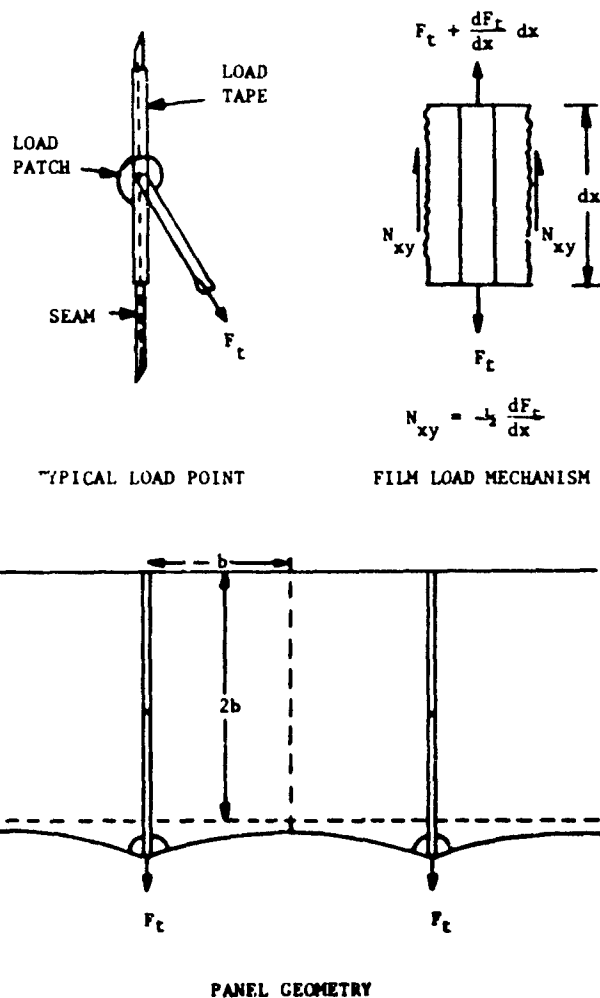


Figure 2. Load Introduction Model

Stresses and strains were then calculated as well as principal stresses and direction of the principal stress. The results of this calculation are shown in Figure 3 for the two balloons previously described. It should be remembered that these stresses must be superimposed on the  $P = 0$  curves of Figure 1 since these stresses are the result of load introduction only, and do not reflect the effects of balloon weight or superpressure.

There are several important parameters which influence the distribution of the load into the film other than material properties. The most significant

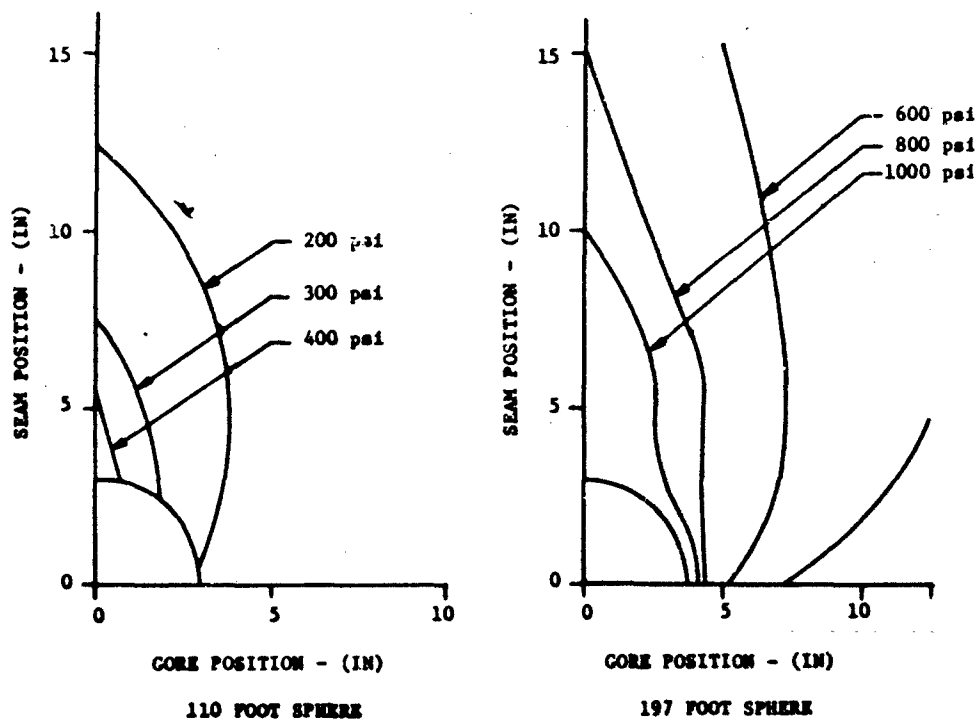


Figure 3. Principal Stress Distribution

parameter appears to be the number of load lines since this dictates not only the magnitude of the load per line, but also the distance between the load lines. In the case of the small balloon the load per line was 4.39 pounds and the distance between lines was 28.8 inches at the point of load attachment. The second balloon introduced 10.95 pounds per line with 55.4 inches between each line at the point of load attachment. From the formulation of the problem it is known that all results are linearly related to the magnitude of the load per line if everything else is held constant. However, the influence of the distance between load lines appears to be a highly nonlinear effect.

The role of film thickness is again a linear effect in the computation of stresses. However, the seam which introduces the load into the film is a boundary where the stiffness is proportional to the tape thickness. The stiffer this seam becomes, the lower will be the shear stress in the film along the edge of the seam. Therefore, in the small balloon the film thickness of 1.5 mils provides a stiffer seam than the 1.0 mil film in the larger balloon.

In reality, the film is stiffened by means of a small (6 inch diameter) patch of reinforcing film at the point of load attachment. The effect of this patch is assumed

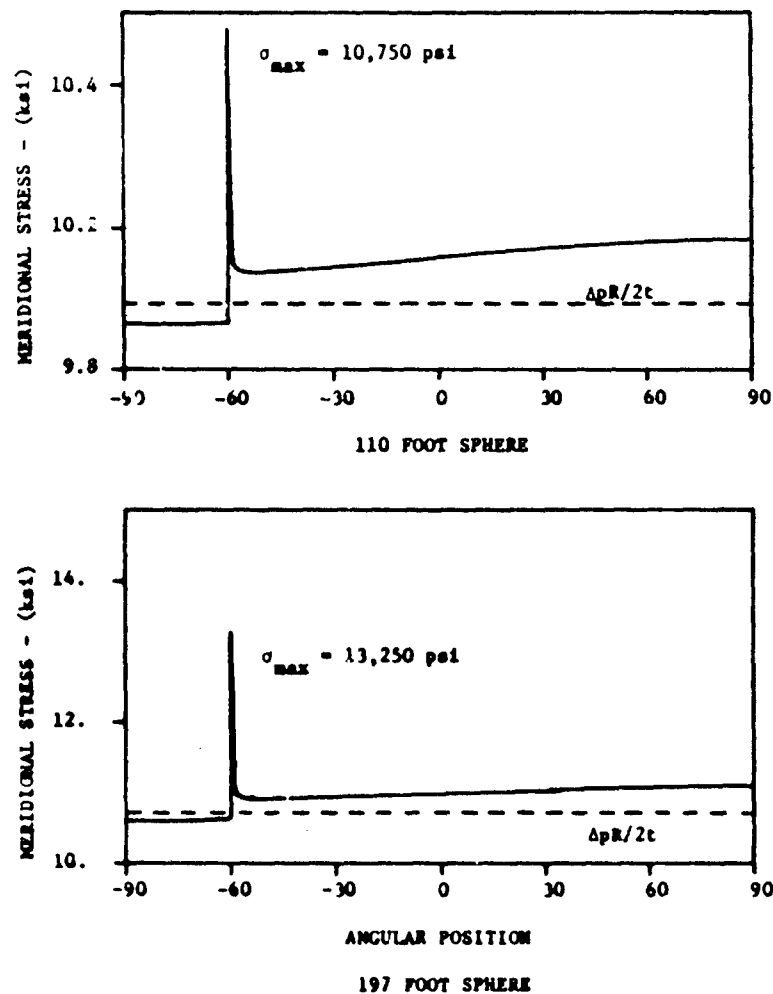


Figure 4. Effects of Superpressure and Load Introduction



to reduce the stresses at that point but will not significantly alter the results presented here a small distance away from the patch. The maximum meridional stress due to load introduction will occur along the seam and has been superimposed in Figure 4 on those results previously obtained to account for the effects of superpressure and weight. The maximum stress very clearly occurs at the point of load introduction and is accompanied by a shear stress that is normally assumed to be negligible. In the smaller balloon, the maximum shear stress is 246 psi while in the larger system this stress increases to 975 psi.

It should be noted at this point that these results are not intended to suggest that the cause of failure of the 196 foot balloon was due to an improper design. The stress levels predicted here should be well within the capabilities of an undamaged polyester film. It would be more reasonable to assume that the violent ascent of this vehicle caused damage which led to the subsequent failure of the system.

## 5. CONCLUSIONS

A technique has been developed to predict the distribution of stresses in a superpressure balloon system manufactured from a homogeneous, isotropic, elastic film which includes the effects of change in pressure due to head height, system weight and payload introduction. It has been shown that the most highly stressed area is in the vicinity of the load introduction point where shear stresses may be significant. It can be concluded that the stresses due to superpressure are sufficiently high to neglect all other effects for design purposes except in the vicinity of the load introduction point. As superpressure balloon systems become larger, careful attention will have to be given to load lines, spacing and seam stiffness.

In the future, the results presented here will be used to formulate a set of limit load factors which the designer may use to improve the reliability of the system. It has also been recommended that an effort be made to develop a testing technique which may be used to characterize materials in their "as used" condition. In addition, other areas of possible stress concentrations, such as pinholing, should be identified and evaluated. The use of new materials, new shapes and manufacturing techniques should continue to be explored so that the most reliable system at the lowest cost will be produced.

## Acknowledgments

The information upon which this report was based was obtained while performing research for the University Corporation for Atmospheric Research which is sponsored by the National Science Foundation. UCAR's technical representatives for the work herein are Mr. Alfred Shipley, manager, National Scientific Balloon Facility, and his delegated representative, Mr. Mike Pavey, Head of Engineering Department.

## References

1. Lally, Vincent E. (1967) Superpressure Balloons for Horizontal Soundings of the Atmosphere, NCAR-TN-28.
2. Alley, V. L. Jr., and Falson, R. W. (1972) Decelerator Fabric Constants Required by the Generalized Form of Hooke's Law, *Journal of Aircraft*, Vol. 9, No. 3.
3. Smalley, Justin H., Balloon Design Considerations, Handbook of Scientific Ballooning, Section V, NCAR-TN (to be published).
4. Kuhn, P. (1948) Shear Lag in Axially Loaded Panels, NACA TN, No. 1728.
5. Alexander, H. and Agrawal, Purushattam (1973) The Effect of Material Deformation on the Shape and Stress State of a High Altitude Balloon, Proceedings of the 7th AFCRL Scientific Balloon Symposium.
6. Lagerquist, D. R. (1973) A Computer Program to Predict Stresses and Deformations of Inflatable Structures, Proceedings, 7th AFCRL Scientific Balloon Symposium.

#### Contents

1. Introduction	192
2. The Materials Problem	192
3. Viscoelastic Fracture	194
4. Testing for Cold Brittleness	195
5. Mechanical Characterization	197
6. Experimental Results	205
7. Conclusions	208
Acknowledgments	208
References	208

## Balloon System Strength and Failure Analysis

L. Dale Webb\*  
Texas A&M University  
College Station, Texas

### Abstract

Balloon loading conditions are discussed wherein it is proposed that serious alterations in mechanical behavior can result from the loadings imposed prior to the system achieving float altitude. Handling, sealing, folding, deployment, etc. are known to reduce the service life. Testing methods and machines are discussed which measure the influence of various stress histories upon service life. Viscoelastic fracture mechanics formulations are proposed which are applicable to the balloon problem. Tests for cold brittleness are reviewed. It is shown that the race track diaphragm tester can be used for determination of cold brittle points. Various other testing devices are described including an articulated diaphragm and a pinhole generating mutilation tester. Typical results of race track cold brittle determinations are presented along with results of pre-load enhancement of brittle behavior useful in discriminating between films. Various relations between parameters important in the interpretation of results of race track and diaphragm tests are shown in graphic form.

---

\*Research Engineer, Texas Engineering Experiment Station; Assistant Professor, Civil Engineering Department.

## 1. INTRODUCTION

To the materials engineer, the most amazing thing about scientific ballooning is that almost 90 percent of the balloons actually reach float altitude. This is surprising because balloons are designed for float conditions at ceiling altitude—conditions that do not reflect the load history represented by manufacturing, packaging, crating, shipping, subsequent storage, uncrating, inflation, launching, wind shear, buffeting, sailing and high rate, high stress unfurling of the film. The film must survive these severe mechanical and environmental loading conditions before it can reach design float altitude and conditions. The loading history of most systems is as yet unrecorded. This means that very little is known about the actual stress relationships and structural changes the materials may undergo during the handling and ascent portions of a flight.

## 2. THE MATERIALS PROBLEM

Without knowing the exact nature of these stress relationships it is difficult to determine which materials will perform adequately. Fortunately, balloon designers ignored the uncertainties and, with considerable finesse and/or brute force, created systems that have performed with a high degree of success under nearly all conditions encountered in a balloon flight. But we also know that over the past 10-15 years there have been "qualified" balloon materials which did not perform as expected. It had been assumed that by thoroughly examining every characteristic of each of these films a definite pattern could be established among various mechanical and physical properties to discriminate between good films and bad. Characterizing every thus far defined aspect of every film to achieve discrimination has proven, however, to be a time-consuming, expensive, and largely unsuccessful, process.

Logically, the solution would be first to determine the actual stresses in a balloon so that test techniques could be developed. Actual information on stress, strain, and skin temperature obtained during inflation, launch, and ascent would enable simulation tests to be performed in the laboratory. However, this kind of information is very elusive. The NSBF conducted a number of test flights to this end but found that nearly the entire surface of a balloon would have to be covered with strain gages and thermistors to determine the actual stress and strain distribution. Although temperature distributions were recorded, the lack of corresponding stress and strain data obscured the definition of useful laboratory test requirements. The development of discriminatory testing techniques is, therefore, both an exercise in duplicating the extremely severe environmental

conditions that a balloon undergoes in flight and a search for a means of detecting possible structural changes that could have occurred in the materials before the flight. For example, how much abuse is the film subjected to when the balloon is being fabricated? What changes in the molecular structure of the film occur during heat sealing? The material can also be significantly affected by the abrasion, folding, and creasing that occur during packing and shipment of the balloon to the launch site and during pre-launch handling. Despite the importance of these considerations they are assumed to be relatively minor compared to the problems encountered during launch and ascent.

At launch the balloon is only partially inflated. The helium in the balloon "bubble" at ground level is highly compressed by atmospheric pressure and occupies only a small percentage of the balloon's fully expanded volume. Stress on the film, however, is greatest just at launch of the balloon system. Near the top of the balloon the film is subjected to a biaxial stress state. Below the bubble the film may be constrained under the launch spool during inflation, creating a region of probable abrasion and heavy creasing or folding of the film while it is stressed. Upon release from the spool the previously constrained balloon suddenly "leaps" skyward, creating a large mushroom effect with rapid unfolding of the material. This severe loading, with its high rates of deformation and high stresses, sometimes results in a system failure.

Most balloon failures have occurred during ascent through or close to the tropopause (coldest region) where the temperatures are commonly in the range of  $-70$  to  $-85^{\circ}\text{C}$ . At this level, shear winds can be encountered and the loosely hanging film may suddenly catch the wind, forming a "sail." The "sailing" and cold temperatures in combination are probably the most severe conditions the balloon film will encounter. Unfortunately, it is also during this period in the life of the balloon that we know least about the actual shapes and stresses involved.

The designer endeavors to maximize the lift-to-weight ratio of the balloon. This requires stressing the films near their elastic limit. Since many of the films are thermoplastics, their viscoelastic nature dictates that their elastic limit depends upon the temperature and duration of the applied stress. Many flaws are inherent in the films and more are created by handling and fabrication. Small flaws, such as microscopic pin holes or disorders on the molecular level, grow at a rate depending upon both magnitude and direction of the applied load. The seriousness of any existing flaw depends on stress magnitudes and directions as well as temperature.

### 3. VISCOELASTIC FRACTURE

In a paper published in 1965,<sup>1</sup> M. L. Williams suggested an energy balance approach which resulted in expressions for the criticality of a flaw in a viscoelastic material. Boundaries could be prescribed in terms of either applied stresses or applied displacements. However, because of the time-dependent nature of the material properties, it was necessary to prescribe the boundary conditions, either the stress or displacement, as a function of time. The problem remains analytically tractable for all practical loading histories, thus it provides an approach to evaluating the influences of the viscoelastic nature of the material properties on the service life when such materials are subjected to sequences of loadings.

The simplified geometry that Williams considered was a spherical flaw centered in a spherical body of material. The boundary conditions were required to be point symmetric and the material incompressible so the stresses or displacements are defined everywhere when the stress or displacement is prescribed. Further, if the relaxation modulus,  $E_{rel}(t)$  (or the creep compliance,  $D_{crp}(t)$ ), is known, the time dependent stored strain energy and viscous dissipation can be calculated.

The criticality expressions derived using the approach were of the form (for the stress prescribed boundary)

$$\sigma_{cr} = k \sqrt{\frac{\gamma}{a f[D_{crp}(t_0)]}}$$

where

$\sigma_{cr}$  = the critical boundary stress

$k$  = a coefficient depending on the geometry

$a$  = flaw radius

$\gamma$  = characteristic strain energy release rate

$f[D_{crp}(t_0)]$  = a function of the creep compliance,  $D_{crp}(t)$ , which depends upon the prescribed loading.

The coefficient  $k$  is identical to that which would be calculated using an elastic fracture mechanics approach.

As time progresses, the values of both sides of the balance equations can be calculated (as a function of time). At that instant,  $t_0$ , when they first become equal, fracture is incipient.

An extremely simple illustration of this equation is obtained if one assumes a linearly increasing stress boundary,  $\sigma = ct$ , where  $c$  is a constant, is imposed.

$$\sigma_{cr} = ct_0 = \frac{4}{3} \left(1 - \frac{a^3}{b^3}\right) \sqrt{a \left[ \frac{2}{3} t_0 \dot{D}_{crp}(0) + 2 \int_0^1 \xi D_{crp}(\xi) d\xi \right]}$$

where  $\dot{D}_{crp}(0)$  is the derivative of the compliance evaluated at true zero and the integral is the first moment of the area under the creep compliance curve.

### 3.1 Applicability to Membranes

A similar approach to that described above for a spherical flaw is being pursued for a circular flaw in a thin (plane stress) membrane. Except for the differences in the geometric term the resulting expressions are identical.

Theoretically, at least, these expressions will permit one to go to the laboratory, evaluate the creep compliance and the characteristic strain energy release rate for a membrane material and predict the time, or number of cycles, to failure (flaw growth) under a prescribed service load history. However, because of the complexities introduced by large strains, nonlinear behavior, non-circular flaws, non-uniform thicknesses, reinforcements, and the like, such meaningful failure predictions are considered unlikely.

Suppose one had a balloon design which had demonstrated a capability to fly to a given altitude with a given payload but which usually survived only one day. And suppose he wished to modify the design, using the same material, so that the balloon would survive 30 day/night cycles. One could, by using the equation given above, evaluate the parameters implied with the first load history. Then, with these parameters, one could calculate whether or not the new design could survive the 30-day cyclic loading.

Clearly such analytical expressions, if they can be shown by laboratory tests to reflect the real material behavior, will be extremely useful to the engineer attempting to design a balloon to survive a specified service life.

## 4. TESTING FOR COLD BRITTLENESS

$D_{crp}$  and  $\gamma$  are strongly temperature- and stress history-dependent. The creep compliance  $D_{crp}$  decreases as temperature decreases and the energy required to enlarge the flaw,  $\gamma$ , becomes smaller as the film gets cold, reaching a minimum value at the "brittle" transition temperature for the film. The

longer a balloon system is exposed to loads which enhance flaws in the film, the more likely system failure becomes as the balloon reaches the low temperature extremes of the upper atmosphere.

Since flaws are inherent in all balloon systems, their seriousness must be defined in terms of size and growth rate for any given stress and temperature. Quality control tests must, therefore, be developed that will measure the significance of inherent flaws in terms of their importance to balloon flight.

Flaws intensify applied stress in their immediate vicinity. A film that is unable to deform plastically in regions of high stress must necessarily fracture. For this reason, it is very important that prospective balloon films be "ductile" in their behavior at all temperatures encountered in the upper atmosphere. Because the significance of microscopic flaws is minimized in ductile films, valid measurement of a film's cold-brittle temperature and subsequent strength loss is essential.

A number of testing techniques and procedures have been used to check balloon film for cold-brittleness properties. Studies of environmental and testing parameters have revealed several that could influence both the cold-brittle point and the film strength; these factors are summarized in Table 1. Until the mid-1960's the cold-brittle point for all polyethylene used in balloons was required to be at least  $-68^{\circ}\text{C}$ . At that time, the accepted way to make cold-brittle determinations was to drop or roll a steel ball through a diaphragm of film and then to inspect the geometry of the resulting tear to determine whether the failure was ductile or brittle.

From 1962 through late 1964 the balloon failure rate became excessively high. Since balloon design and fabrication had not been altered, one of the major suspected causes of this high failure rate was an undetected change in the properties of the polyethylene. The normal cold-brittleness and strength tests showed no differences between the films of that period and the earlier, more successful films of the late 1950's through 1961. In lieu of any discriminatory test, a

Table 1. Factors Influencing Cold Brittleness and Strength at Failure

Factors	Cold-Brittle Point Temperature	Failure Strength
Increase pre-load	Warmer	Decrease
Increase pre-load temperature	Warmer	Decrease
Increase pre-load time	Warmer	Decrease
Increase strain rate	Warmer	Increase
Increase pre-load rate	Warmer	Decrease



proposed solution to the problem was simply to develop films capable of passing the standard cold-brittleness test at temperatures considerably colder than  $-68^{\circ}\text{C}$ . In 1964, StratoFilm<sup>®</sup> became the first film especially developed to meet the new criterion. Both StratoFilm<sup>®</sup> and the subsequently developed X-124 had cold-brittle points at or below  $-80^{\circ}\text{C}$ . The use of these films immediately brought about a significant increase in the number of successful balloon flights, a trend that has continued to the present time.

Because former test techniques are still used to determine cold brittleness, changes in the film can still occur without detection by testing. In fact, some films which now pass all current resin and finished film property tests (such as having a properly low brittle transition temperature, adequate uniaxial tensile strength, and strong heat seals) make apparently unreliable balloon systems.

Records of many actual flights have helped in the search for discriminatory tests for prospective films. Studies showed that temperatures and handling of the balloons at ground level had a significant effect on the altitude at which brittleness and, hence, fracturing occurred! Air Force-sponsored research<sup>2</sup> revealed that subjecting film to the static loading characteristic of pre-launch balloon restraint could cause a significant increase in the temperature at which the film became brittle (i. e., the film became brittle at a much warmer temperature than before it was stretched). The cold-brittle transition temperatures of films that had exhibited problems in flight were found to have been significantly altered by the preloading; successful films were much less influenced. The preloading had, in a sense, improved the test's capacity for discriminating between good and bad films.

Still this technique has a number of drawbacks, including, in particular, the necessity to obtain specifically fabricated heat-sealed cylinders for the test. Moreover, actual samples from production balloons could not be directly evaluated, the tests were expensive and time-consuming, and the parent film could not be evaluated without the ever-present seals influencing the results. The development of the race track technique discussed below has alleviated these problems.

## 5. MECHANICAL CHARACTERIZATION

In mid-1972 the NSBF, with Texas A&M University, initiated a program to explore means of developing practical test methods and relevant acceptance criteria for balloon material systems. One effort has been the development of methods of mechanical characterization that subjects the film to multiaxial stresses presumably similar to those induced during the service life of the balloon system.

### 5.1 Diaphragm Testers

Each of the three types of diaphragm testers to be discussed has in common the following features:

- (1) An environmental chamber in which the low temperatures that are characteristic of the upper atmosphere can be maintained.
- (2) A "diaphragm" sample holder in which a sheet of film with or without seals can be clamped along its edges in an airtight fashion so that it can be inflated to failure.
- (3) A pressurization and pressure measuring system, with the capacity for producing constant volume flow rate, constant film stress rate, constant strain rate, constant film stress or constant pressure.
- (4) A film-height monitor and a variety of strip charts to record all events and levels important to balloon materials testing.

#### 5.1.1 RACE TRACK

The race track device (Figure 1) is a diaphragm tester capable of applying a  $\sigma_y = 2\sigma_x$  stress field to the specimen where  $\sigma_y$  is across the narrow dimension of the sample holder. The race track geometry simulates a section of an inflated cylinder and allows the selective characterization of anisotropic films without the problem of edge effects. The hoop stress in the film is computed from knowledge of the inflation pressure, radius of curvature of the film, and film thickness ( $\sigma = PR/t$ ).

The film and its holder are inserted in the chamber (Figure 2) and liquid nitrogen is injected to produce a desired low temperature. The assembly is allowed to reach equilibrium and the film is then pressurized to failure. Just above its cold-brittle point the film fails by smoothly tearing along a fairly straight line normal to the hoop stress (Figure 3, top). Below its cold-brittle point the film shatters into a jagged tear pattern, exposing "new" surface area orders of magnitude greater than before (Figure 3, bottom).

To achieve control of the loading or strain rate it is necessary to relate the geometry of the tester to the pressure and film height. The race track constrains the specimen to inflate into a segment of a 9-inch long cylinder capped by segments of a sphere. The central region of the sample is subjected to a state of plane strain. The height of the sample is measured with a linear variable differential transformer mounted at the center of the sample. For a constant strain rate test, the inflation gas flow rate must be varied to produce a height/time trace that equates to a constant strain/time trace. The geometric relations between the diaphragm, film strain, diaphragm height and displaced volume are shown in Figure 4.



Figure 1. Race Track Sample Holder Along With Tested Films Showing Ductile (top) and Brittle (bottom) Fractures

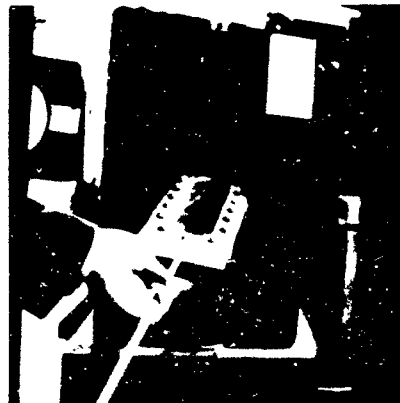
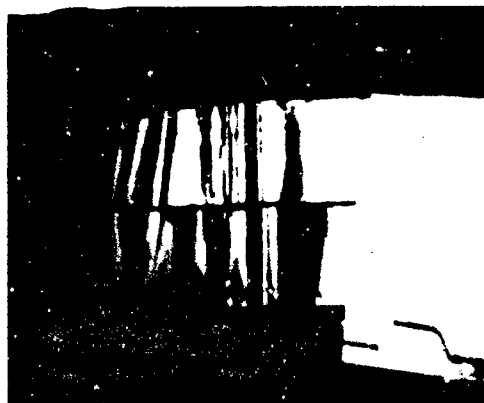
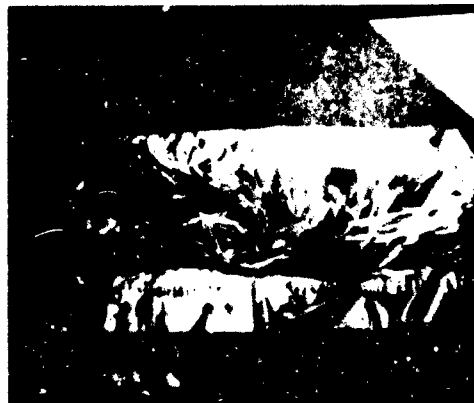


Figure 2. Race Track Environmental Chamber. This unit contains all the necessary elements to indicate the induced stress and strain for each test temperature



(A)

A typical ductile failure consists of a straight line tear with minimum exposed new surface area



(B)

When the sample cools below its cold brittle temperature for a given strain rate its failure appears as a shattering exposing large amounts of new surface area

Figure 3. Typical Race Track Modes of Failure

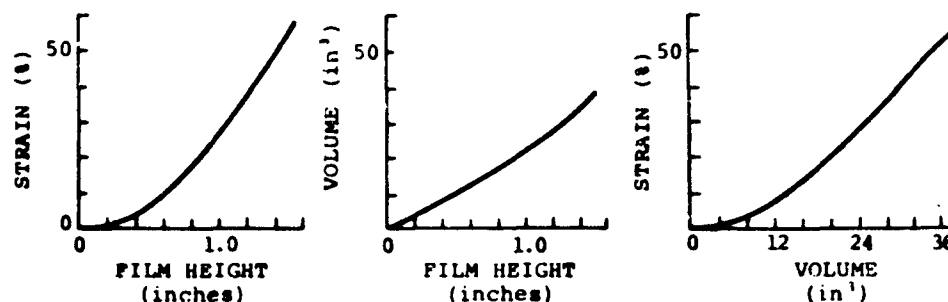


Figure 4. Relationship Among Strain, Volume, and Height for a 3" x 12" Race Track Tester

Of particular interest is how to conduct a long term creep test with the film stress held constant with a diaphragm tester. The problem is controlling the parameters in the stress equation  $\sigma = PR/2t$  where  $P$  = inflation pressure,  $R$  = radius of curvature which must be related to the height of the diaphragm from its flat starting position ( $R = \infty$ ), and  $t$  is the film thickness. As the film is pressurized both its height (radius) and thickness are changed. The balloon films have a Poisson's ratio of 0.5; that is, they are essentially constant volume materials. Under this assumption the actual film thickness can be computed for any radius of curvature. The method of holding the film stress constant as required for a creep measurement is to compute the relation between pressure and resulting film height, taking into account the change in thickness as necessary to hold the value of  $PR/2t$  constant. A typical plot for such a calculation is shown in Figure 5. There it is seen that initially the radius effect predominates; then the thickness change becomes most significant.

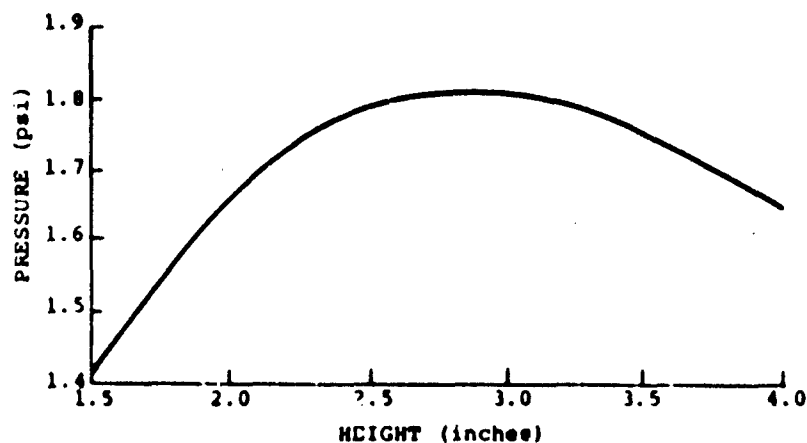


Figure 5. Pressure Versus Height for Constant Skin Stress = 7,000 psi

### 5.1.2 CIRCULAR DIAPHRAGM TESTERS.

A small 10-inch diaphragm tester (Figure 6) is used for routine testing of isotropic films. A long stroke linear variable differential transformer (LVDT) is used to measure the height of the film. This device is especially valuable for measuring creep at various temperatures and loading conditions. The LVDT is mounted on a long travel precision micrometer useful both for in situ calibration and for bringing the LVDT back to null following initial pressurization. This enables highly accurate observations of small creep levels. An arbitrary function programmer is used to slave the pressure to film height in order to obtain desired loading histories.

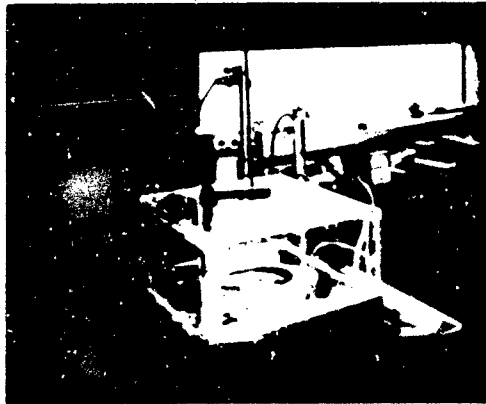
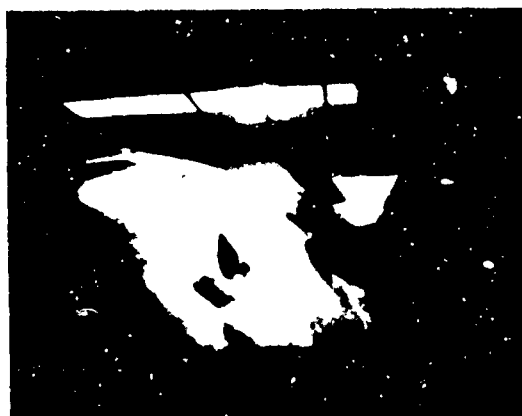


Figure 6. 10-inch Diaphragm Test Facility. The diaphragm base is seen through the walls of an acrylic cold chamber. The surrounding instrumentation records such parameters as pressure, temperature, and film height

A large 42-inch diameter diaphragm tester (Figure 7) is used to investigate the macroscopic influence of flaws, heat seals, inflation fittings and various methods of attachment of load straps on the structural integrity of the film. A mirror and polaroid filter are hinged on the base plate such that large field examination of the stress pattern induced in the film can be made. A cylindrical environmental chamber attaches to the tester's articulated support. The complete system can be tilted and/or rotated  $360^\circ$  for control of applied load. The cold chamber can be rotated with respect to the diaphragm tester to locate a view port and/or load lines for observation and/or loading at any position.

For each test performed on the race track or other diaphragm testers, four items (shown in Figure 8) comprise the data. The top sheet is the pressure-time trace. The second sheet is the record of film height versus time. The third item is the test sample and the last page in the master data record containing film identification, thickness profiles, etc.



(A)



(B)

(C)

(D)

Figure 7. Large Diaphragm Tester. (A) The base plate has a polarized light source which enables the operator to view large field stress patterns. (B)-(D) The sample holder as well as its environmental chamber is articulated and can be tilted or rotated through  $360^\circ$ .



Figure 8. Data Records. Four items are collected from each test: the pressure-time trace, the height-time trace, the film sample, and a master data sheet

### 5.1.3 MUTILATION TESTER

The mutilation tester (Figure 9) provides the means for determining a figure of merit for comparing the ability of a polyester type film to withstand repeated cross folding. This facility is designed to subject 10-inch diameter by 36-inch long tubes of balloon film to repeated cycles of extended inflation and collapsed deflation with a full twist to achieve cross folding about the major axis of the cylinder being superimposed upon the collapsed film. A pair of cylinders is mounted within the test frame which is then inserted within a tubular cold chamber. A leak detector is used to signal the initiation of pin holes or tears and a counter records the number of cycles to failure.

Figure 9. Mutilation Tester. The tester is shown standing beside its environmental chamber where one of two film cylinders is visible during one half cycle. The device twists and crushes one of the cylinders while untwisting and inflating the other. The completion of the cycle reverses the roles of the two cylinders.





Figure 10. Polariscope. Each sample cut for testing is examined for flaws within the field of the polariscope. Also visible in the figure are one of two large field magnifying glasses useful in examining the film surface



Figure 11. Micrometer and Microscope. The movable stage eases the job of profiling films. A Starrett precision micrometer is used to measure the thickness and the microscope is used to examine any film discontinuity

#### 5.1.4 POLARISCOPE

Twin large field (21-in. dia.) polaroid plates mounted on a rail plus a pair of 10-inch diameter magnifying lenses comprise this examination system (Figure 10). Each balloon sample is optically scanned while in the polariscope. Any irregularity, color bands, and light or dark spots are causes of rejection. A slight stress is often necessary to cause microscopic irregularities to show.

#### 5.1.5 THICKNESS MEASUREMENT

A Starrett micrometer capable of resolving a thickness of 0.05 mils ( $\pm 1.5$  mils full scale) has been mounted on the barrel of a microscope (Figure 11) such that a film can be translated under the probe by means of the stage micrometers. Various magnifications enable the film surface to be scanned for flaws not evidenced by the thickness profile.

Observations made with the scanning beam electron microscope have provided one of the major reasons for the interest in diaphragm testers for material characterization. Uniaxial samples cut with a shear produce edges typical of those shown in Figure 12 (magnification 100x). View at 20,000x, even of the





Figure 12. Shear Cut Edge of Polyethylene. A look at 100x magnification shows the severe edge damage which causes ultimate properties to scatter badly

finest blade cut specimens, show large fissures and cracks. The obvious irregularities cause the ultimate properties to scatter badly.

## 6. EXPERIMENTAL RESULTS

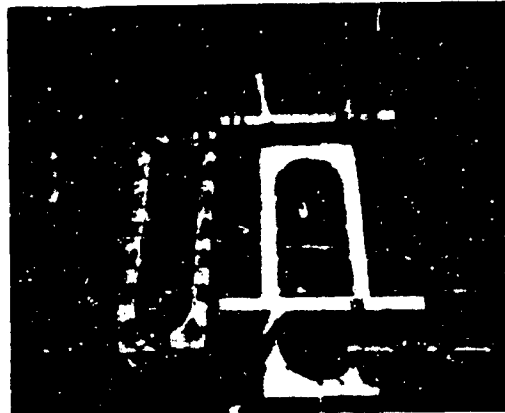
Following the lead of Kerr<sup>3</sup> and Alexander<sup>4</sup> where creep was shown to cause a deterioration in the mechanical properties, various loading techniques were explored to simulate these earlier tests. With the race track device, it was found that long term creep load influences could be simulated by short term extensions.

Pre-stretching the balloon films to extension ratios,  $\lambda$  (final length/initial length), up to 2.0 emphasizes the differences among otherwise similar films. In this technique the films are cut to a rectangular shape 15 x 38 cm; one end is clamped to a load frame, and the other is stretched to the extent necessary to achieve any given extension ratio. The films are held stretched at the same extension ratio by the sample holder which is bolted together, sandwiching the already stretched film between its plates. (See Figure 13.)

Tests were made from sections cut from films of actual balloons that had failed; these results were then compared with those from tests on new material known to have come from film lots that had performed satisfactorily. Figures 14 and 15 show results from these early tests. In both instances, fairly well defined cold-brittle temperatures were determined. A cold-brittle temperature was also found for material specimens containing heat seals. These two sets of data represent the first time that inflation of a diaphragm of film had been used to determine a cold-brittle point. They also are the first sets of data to indicate a shift in the cold-brittle point when a heat seal is introduced into the film.

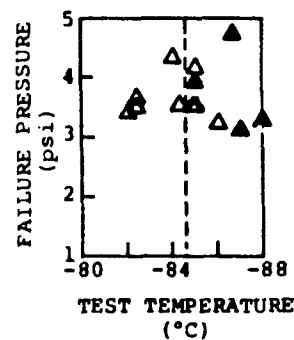
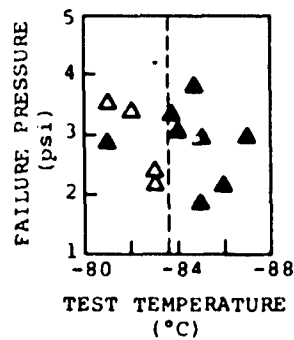


(A)



(B)

Figure 13. Two Methods of Preloading the Test Samples Have Been Utilized. In the first, (A) the sample was clamped under a constant load inducing creep for a period of time. Then, while still under load, it was bolted into a race track holder and immediately inserted into the cold chamber. The second, and simpler, method (B) is where the sample is stretched and held at a fixed extension while being bolted into the sample holder. As before, the sample is immediately inserted into the cold chamber



--- Cold Brittle Point

▲ Brittle Failure

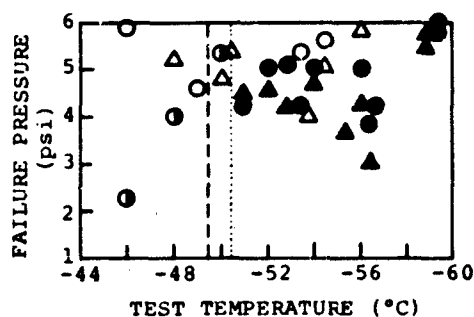
Figure 14. Race Track Cold Brittleness Determination of 0.70 mm StratoFilm<sup>R</sup> with no Preload

Figure 15. Race Track Cold Brittleness Determination for 0.75 mm X-124 With No Preload

The next phase of testing was to determine the cold-brittle points on "old" and "new" DFD 5500 balloon films. These are the films which only the pre-loaded cylinder tests had previously been able to discriminate as being "good" and "bad," respectively. As expected, when tested in the diaphragm tester in an unstretched condition, both films indicated almost identical cold-brittle points. This result corresponds with those from unloaded cylinder tests which also revealed no difference between the two films.

Techniques were then established for stretching the film to the specified elongation percentages. The "race track" holder was clamped on the stretched specimens. These samples were then cooled in the chamber and inflated to rupture. Figures 16 and 17 give the results of tests performed in this way on the old and new DFD 5500 film. These results indicate a marked difference in the cold-brittle point for any  $\lambda$  greater than 1.0 for the two films.

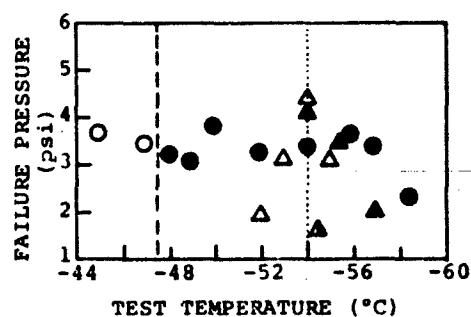
This research indicates that a valuable method of generating acceptance criteria for films and heat seals is to measure both the biaxial film strength and the influence of extension ratios on the brittle transition temperature. An "envelope" curve can thus be generated for each good and bad film which can serve both as a check on each new batch of good film and as a standard for comparison with any candidate film. Such tests will serve adequately during the period necessary for discovering the true nature of the film microstructure (molecular type, crystallinity, cross-link density, entanglements, etc.) and how it is influenced by extrusion, heat sealing, and launch and flight loadings.



△ Old DFD 5500 film  
○ New DFD 5500 film

(solid figures denote brittle failure)

Figure 16. Race Track Cold Brittleness Determination for Old and New DFD 5500 With No Preload



Cold Brittle Point

..... Old DFD 5500 film

----- New DFD 5500 film

Figure 17. Race Track Cold Brittleness Determined for Old and New DFD 5500 With Preload That Induced an Extension Ratio of 1.5

## 7. CONCLUSIONS

The development of instrumentation with which to generate a realistic film stress history on a diaphragm tester, devoid of specimen edge effects, is expected to significantly improve the relevancy of materials characterization.

The viscoelastic fracture mechanics approach is expected to yield a cumulative damage "law" which will account for the stress history prior to, during, and after launch including the day/night stress cycling. The large diaphragm tester has provided valuable stress distribution data through the use of the photoelastic effect and is expected to produce even more spectacular information when the photoelastic measurements are conducted at low temperatures where the flaw criticality is enhanced.

The race track is valuable for the determination of cold brittle temperatures, especially as enhanced by creep or preloading, as well as valuable for stress-strain characterization with temperature and strain rate as parameters.

## Acknowledgments

The information upon which this report was based was obtained during the conduct of research sponsored by the National Science Foundation through the University Corporation for Atmospheric Research. UCAR's technical representatives for the work herein are Alfred Shipley, Manager, National Scientific Balloon Facility, and his delegated representative, Mike Pavey, Head of the Engineering Department. Many of the parametric studies were accomplished by Steve Smith while an Engineering student at Texas A&M University and as part of his duties at the National Scientific Balloon Facility. The viscoelastic fracture application to balloon systems reviewed in this paper was developed by Dr. Jim Noel who is a new and already invaluable member of the Balloon Team.

## References

1. Williams, M. L. (1965) "Initiation of Growth of Viscoelastic Fracture," International Journal of Fracture Mechanics, Vol. 1, No. 4.
2. Alexander, H., and Weissman, D. (1972) A Compendium of the Mechanical Properties of Polyethylene Balloon Films, Stevens Institute of Technology (January), various pagings.

3. Kerr, A. et al. (1968) On a Cause of Failure of High Altitude Plastic Balloons, New York University Contract F19628-67-C-0241, Scientific Report 5, AFCRL-68-0486.
4. Alexander, H., and Weissmann, D. (1972) A Compendium of the Mechanical Properties of Polyethylene Balloon Films, Stevens Inst. of Tech., Contract F19628-69-C-0069, Scientific Report 2.

#### Contents

1. Introduction	212
2. Material Selection Strategy	214
3. Balloon Performance Requirements	215
4. Balloon Material Requirements	217
5. Material Candidates	223
6. Evaluation and Screening Methods	233
References	236
Appendix A	237

## Material Selection for High-Altitude, Free Flight Balloons

James B. Munson  
Sheldahl, Inc.  
Northfield, Minnesota

### Abstract

Modern scientific ballooning dates from the introduction of synthetic, polymer films. The contribution of balloons to scientific research is largely due to the refinement of these and more recently available materials. Geometric growth in the number of new materials has been accompanied by development of necessary techniques for more effective material selection and application. Simultaneous design of materials and the products which incorporate them has become commonplace. However, many designers and users of balloons and other flexible structures continue to regard material application in traditional ways.

To illustrate more effective methods, a strategy is discussed along with definition of material requirements and generation, characterization, evaluation and screening of material candidates for a powered balloon (HASPA), a long-duration balloon application and heavy load, natural shape balloons. Elastic and viscoelastic stiffness, strength, creep, permeability, puncture and fold resistance, transparency, and UV stability requirements are outlined. For a representative assortment of films and film-fiber composites, preliminary evaluation is made of the biaxial, shear and tear strength, creep effects, permeability, transparency, and UV stability. Screening methods are considered and an example of material-requirement trades is given.

Preceding page blank

## 1. INTRODUCTION

In the past, material selection for a given application was a casual process. Engineers relied heavily on previous experience to fit to the requirements the few materials with which they were familiar. Under these circumstances, material changes took place gradually and each change provided only a small improvement.

More recently, increases in the variety of materials, the rise of new and more severe service requirements, and the demand for lower costs have made such haphazard approaches obsolete. Necessarily, effective material selection has become a complex process, operating throughout the entire span of product evolution and involving a number of technical disciplines:

- Analytic procedures have been developed to deal with the complex interactions between performance requirements and material properties.
- The growing use of composite materials has created a manifold increase in the options available to the designer.
- Materials selection is pursued as a full-time technical specialty, operating as an adjunct to more traditional design and manufacturing disciplines.

The materials selection process in product development is distinctly different from material improvement in existing end items. In the former, it tends to be specific, directed and hardware oriented. In the latter, it has a less formal, unassigned character.

At the concept-formulation state of product development, Table 1, characteristics and limitations of existing materials may suggest concept modifications. If the limitations are lack of sufficient performance or design data, a development program may be warranted to fill the information gap. Or a modification program may be initiated to obtain a material that meets concept requirements. Analysis of principal material requirements is an important part of feasibility study.

As the concept is reduced to a practical engineering design, a major share of the materials evaluation is performed. Performance, cost, producibility and reliability of candidate materials are analyzed in detail.

As preparations are made for fabrication of prototype and follow-on units, design modifications which are made to use existing facilities or to achieve production economies may require significant material changes. As fabrication begins, material problems in joining or finishing may arise requiring further changes.

The actual material selection for a specific product is rarely as smooth and compartmented as suggested. Material changes in later development phases frequently require iteration through previous phases, for example. However, the principle of beginning with a wide field of candidates and progressively narrowing

Table 1. Material Selection Activities During Product Evolution

Development Phase	Selection Activities
Concept Formulation	<ul style="list-style-type: none"> <li>• Trade concepts between material characteristics</li> <li>• Generate field of material candidates</li> <li>• Fill information gap on material properties, producibility</li> </ul>
Engineering Design	<ul style="list-style-type: none"> <li>• Detail analysis of performance, cost, producibility of candidate materials</li> <li>• Choose prototype material(s)</li> </ul>
Prototype Evaluation	<ul style="list-style-type: none"> <li>• Change materials to fit existing facilities or to achieve other production economies</li> <li>• Correct material deficiencies revealed by tests</li> </ul>
Production	<ul style="list-style-type: none"> <li>• Change materials to correct joinery, finishing and other fabrication problems</li> </ul>

It by test and interaction with the evolving design has repeatedly demonstrated its effectiveness in improved products.

There are many reasons for considering material changes in existing products despite the technical, economic and political "inertia" attached to incumbent materials:

- Improvement of functional performance, reliability or service life of a product by taking advantage of a new material or processing development;
- Use of a lower cost basic material or a lower cost form or part of that material; or
- Reduction of production costs by substitution of a lower cost process or by elimination of a production problem.

Material changes in existing products are the result of generalized study programs carried out to find solutions to broad material problem areas affecting current and future end items.

The emphasis in material selection has shifted from what nature provides to what man requires. The tools have become available for designing the material, along with the product.



The number of inquiries received by Sheldahl concerning materials designed for previous applications indicates that a large number of designers continue to select materials in the traditional way. Of course, there are sound reasons for considering existing materials. "Demonstrated suitability" is rarely one of these. A material choice without consideration of the specific requirements of the end item and without regard for the variety of alternative materials is poor management of money and time. Use of material science in design won't guarantee a relative "optimum" material. It will, however, greatly increase the likelihood of saving money and obtaining superior performance.

To illustrate how this may be applied in balloon design, preliminary requirements and material candidates for three specific balloon missions are discussed in parallel and the alternatives for one potential use are evaluated.

## 2. MATERIAL SELECTION STRATEGY

Material selection is fundamentally similar to any other decision-making process because success tends to depend on:

- Adequate definition of the requirements,
- Adequate knowledge of available options, and
- A rational method for selecting the relative "best" alternative.

Material requirements for balloon applications are often unclear, especially at the outset, because of the remote service environment. Data on low temperature mechanical properties, UV stability and similar material properties important to balloon use are particularly lacking even for commonly available materials. If the essential requirement and property data are not identified early in the selection process, and missing information obtained, considerable waste may occur in later phases when heavy commitments have been made.

On the surface, material requirements implied by a design, Table 2, may appear either as absolute, quantitative attributes like strength and weight, or as relative, qualitative ones like "producibility" and "handling resistance" which are to be made "large" or "small", consistent with other requirements. The distinction blurs when we consider that weight and strength are random variables with values scattered around a mean and that, given a sufficient reason, we can numerically characterize properties like material response to handling.

A breakdown of material requirements into categories, Table 2, helps in assembling the field of material candidates by focusing the designer on a small number of attributes at one time. Selecting a material to meet each of the requirements, starting with the most critical, is a useful technique. Past experience and current practice will suggest additional candidates.

Table 2. Examples of Material Requirements Classed by Category

Requirement Category	Example
Functional	Mechanical, physical, thermal requirements
Environmental	Radiation and chemical requirements
Reliability	Standard materials are usually more reliable than new materials
Producibility	Handling resistance, seam efficiency, stock dimensions and weights
Cost	<ul style="list-style-type: none"> <li>• End item cost target</li> <li>• Cost of product failure</li> <li>• Cost per unit material property (\$ lb, \$/psi, etc.)</li> <li>• Cost to obtain design data</li> <li>• Cost to define any new process required for use of material</li> </ul>
Service Life	Time response of material to static and cyclic loads, radiation, ozone, etc.

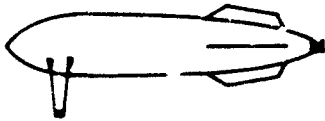
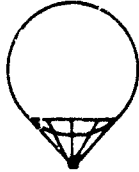
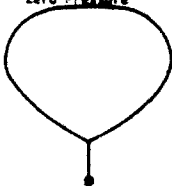
Materials with serious shortcomings can often be made acceptable by combining them with another material in a composite. The list of candidates can be held to manageable size by rejecting the least desirable ones, based on a cursory survey.

A test program is usually required to obtain material data not available from published sources.

Evaluation and screening of the alternatives should begin with the most critical requirement. Requirements can be ranked by means of failure analysis or similar analytic technique.

### 3. BALLOON PERFORMANCE REQUIREMENTS

Performance requirements for three balloon applications are summarized in the sketch at the top of the following page.

	HASPA	LDP	Free Flight Zero Pressure
MISSION:			
Load	1,700 lb	500 lb	> 4,000 lb
Altitude	65 - 70,000 ft	130,000 ft	80 - 130,000 ft
Duration	30 days	90 days	1 - 3 days

BALLOON MISSION REQUIREMENTS

### 3.1 High Altitude, Superpressure, Powered Aerostat (HASPA)

This will be used as a communications relay platform with limited station-keeping ability (Petrone, 1974). The volume is to be limited to less than one million cubic feet. One design concept consists of a class "C" shaped hull, 370 feet long by 75 feet in diameter. Preliminary analysis indicated the minimum allowable internal pressure to resist buckling would be about one inch of water (column) and the maximum superpressure will be about four inches of water. The balloon will be launched in the flaccid state like a conventional free-flight balloon.

### 3.2 Long-Duration Platforms (LDP)

About three dozen scientific groups working in the atmospheric sciences and in infrared, X-ray, gamma ray and cosmic ray astronomy require a scientific platform which can be developed in one to two years to support 500 pounds at a 3-millibar pressure altitude for several months. The National Scientific Balloon Facility under sponsorship of NSF has initiated a development program for the necessary balloons and electronics.

Since the superpressure stress in the envelope is about ten times larger than the load suspension stress, it has been assumed here that a sphere is the most efficient shape. Based on materials previously used for large superpressure spheres, a balloon diameter of 200 to 300 feet is indicated.

### 3.3 Heavy Load, Free-Flight, Zero Pressure Balloons

When introduced in the 1950's, polyester films proved generally unsuitable for balloons because of poor tear resistance. In 1960, ONR sponsored a development program to reinforce polyester film with a woven scrim of DACRON. Heavy load balloons of polyester film-yarn composites have established a high reliability record since that time.

In the interim, polyethylene balloons with polyester tapes arranged along seams have been highly refined for heavy load applications. Under unfavorable wind or temperature conditions, however, a considerable number of material failures have occurred in balloons with envelopes larger than  $20 \times 10^6$  cubic feet and loads in excess of 3000 pounds. To extend the balloon capabilities of polyethylene film, NSBF and ONR have sponsored a program to develop yarn-reinforced polyethylene. A suitable adhesive system was demonstrated for bonding DACRON yarn to polyethylene film, material samples were produced, and various seam configurations evaluated (Morfitt, 1972), and additional seam development was conducted (Fouchard, 1973; Munson, 1974). A 40-foot diameter test balloon was constructed for hanger inflation to evaluate material and seam performance in a large structure.

## 4. BALLOON MATERIAL REQUIREMENTS

Some requirements are set by the structural configuration; others, by the service environment and by the particular ways in which balloons are fabricated, transported and launched. The list below is not exhaustive, but will serve to illustrate preliminary definition of the application-material interface.

### 4.1 Mechanical Properties

#### 4.1.1 STIFFNESS REQUIREMENTS

Altitude stability is usually an important performance requirement for super-pressure balloons. Changes in altitude caused by diurnal temperature fluctuations and material creep depend on the inherent tensile stiffness of the material.

Figure 1 shows how the minimum required stiffness (modulus times thickness) varies with allowable altitude changes. The diurnal (short-term) material stiffness was assumed to be the elastic (Young's) modulus. Diurnal changes are assumed to be elastic and recoverable. The long-term (apparent) stiffness was taken as the ratio of average diurnal material stress to total creep deformation over the

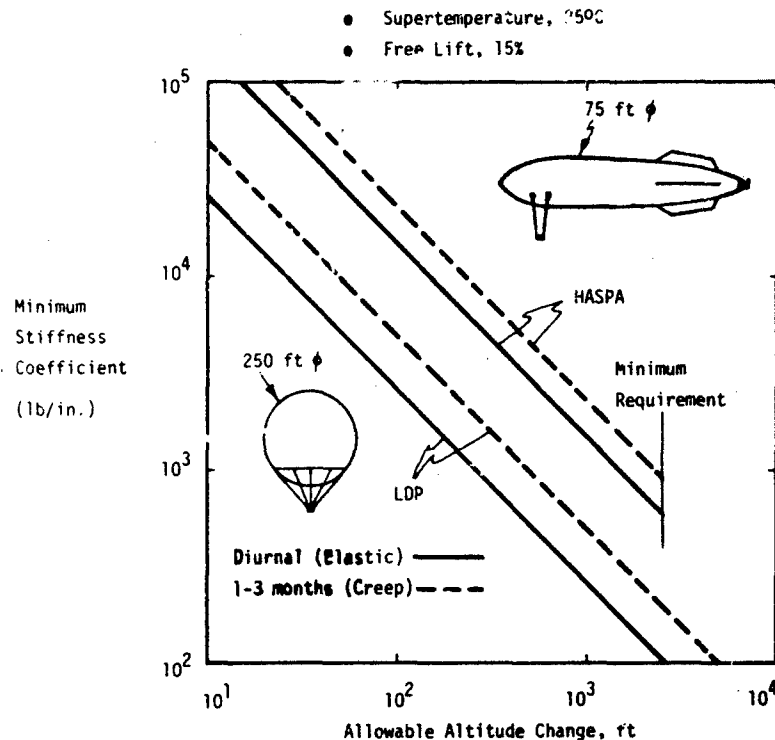


Figure 1. Material Stiffness Required to Maintain Balloons Within Various Altitude Ranges

service life. The latter can be determined by extrapolation from constant load creep tests at appropriate temperatures and stress conditions. Creep causes a superpressure balloon to grow in size and to float higher. Both effects raise the material stress. Material rupture will occur if the creep modulus is low enough (Lally, 1967).

Tensile stiffness in zero pressure balloons is much less important than material strength.

#### 4.1.2 STRENGTH REQUIREMENTS

The maximum, internal, pressure stress in a superpressure balloon is usually many times larger than local stresses applied by the load suspension system. So simple membrane theory will serve for preliminary characterization. Taking the radius  $R$  at the maximum diameter and the ratio of maximum superpressure to ambient pressure:  $\Delta P/P_a = F + (1 + F) \Delta T/T_g$  for the conservative values of free lift,  $F = 0.15$  and supertemperature  $\Delta T = 25^\circ\text{C}$ , the required operating material strength is obtained, Table 3.

Table 3. Strength Requirements - Operation

Balloon	Stress		
	Direction	Function	Maximum Value
HASPA	Hoop	$\Delta P \times R$	96 lb/in.
	Axial	$\Delta P \times R/2$	48 lb/in.
LDP	(A11)	$\Delta P \times R/2$	10 lb/in.

Material requirements implied by localized load suspension stresses require detailed analysis and testing at the engineering design phase.

Since all three applications considered will be launched in the flaccid state, material deployment stresses must be considered. The arrangement of material in a typical, partially deployed balloon, Figure 2, is generally nonuniform and the stresses cannot be predicted analytically except within broad limits. The enormous surface area of a typical balloon and the lack of suitable instrumentation have hindered stress distribution measurements.

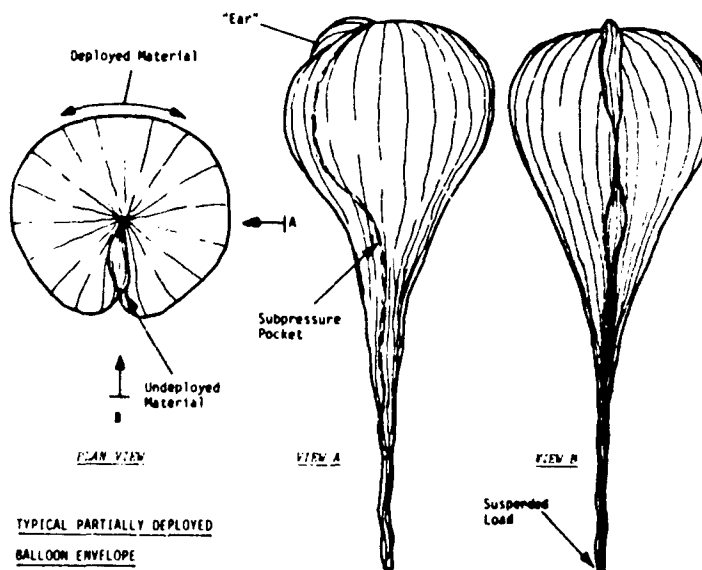


Figure 2. Typical Partially Deployed Balloon Envelope

- △ Nonwoven, triaxial reinforcement, 0.5-inch yarn spacing
- Leno weave scrim reinforcement, 0.2-inch yarn spacing
- Envelope failure in flight (2)

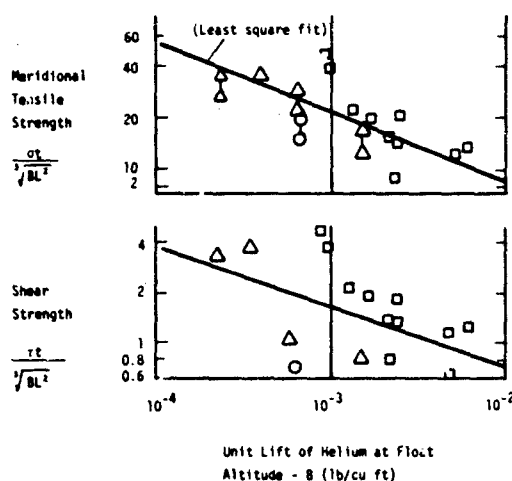


Figure 3. Ultimate Material Strength at  $-70^{\circ}\text{C}$  for 67 Free Flight, Natural Shape Balloons Made of DACRON-Reinforced MYIAR Film. (L = Weight of suspended load)

Ultimate tensile and shear capabilities of the envelope material in a group of polyester film-yarn balloons flown from 1962 to 1972 are shown in Figure 3. Strength data are presented in terms of gas density at float altitude and the suspended load which affect envelope size and material stress intensity. Although other factors like ambient temperature and wind shear during ascent may be more important in determining success or failure, the information available at the design stage is typically limited to payload and altitude.

The data serve to indicate, approximately, the levels of material strength which have withstood actual deployment stresses. Strictly speaking, they apply only to natural shape balloons made of yarn-reinforced polyester film. For the applications considered here see Table 4.

Table 4. Strength Requirements - Deployment

Balloon	HASPA	LDP	Natural Shape, Zero Pressure
Suspended Load (L)	1,700 lb	500 lb	8,000 lb
Altitude	67,000 ft	130,000 ft	100,000 ft
Unit Helium Lift (B)	$4.5 \times 10^{-3}$ lb/cu ft	$2.3 \times 10^{-4}$ lb/cu ft	$9.2 \times 10^{-4}$ lb/cu ft
Tensile Strength (Meridional)	24 lb/in.	12 lb/in.	72 lb/in.
Shear Strength	2 lb/in.	1 lb/in.	6 lb/in.

#### 4.2 Requirements for Gas Barrier Integrity

Experience indicates that gas leakage through small holes is the most common failure mode for superpressure balloons. Figure 4 indicates that one hole (or equivalent aggregation) on the order of 0.1 to 1 inch diameter will reduce superpressure in the HASPA and LDP balloons to the minimum acceptable value within the required operating life. The balloons must be fabricated to this standard and resist gas barrier damage during packaging, inflation, launch and

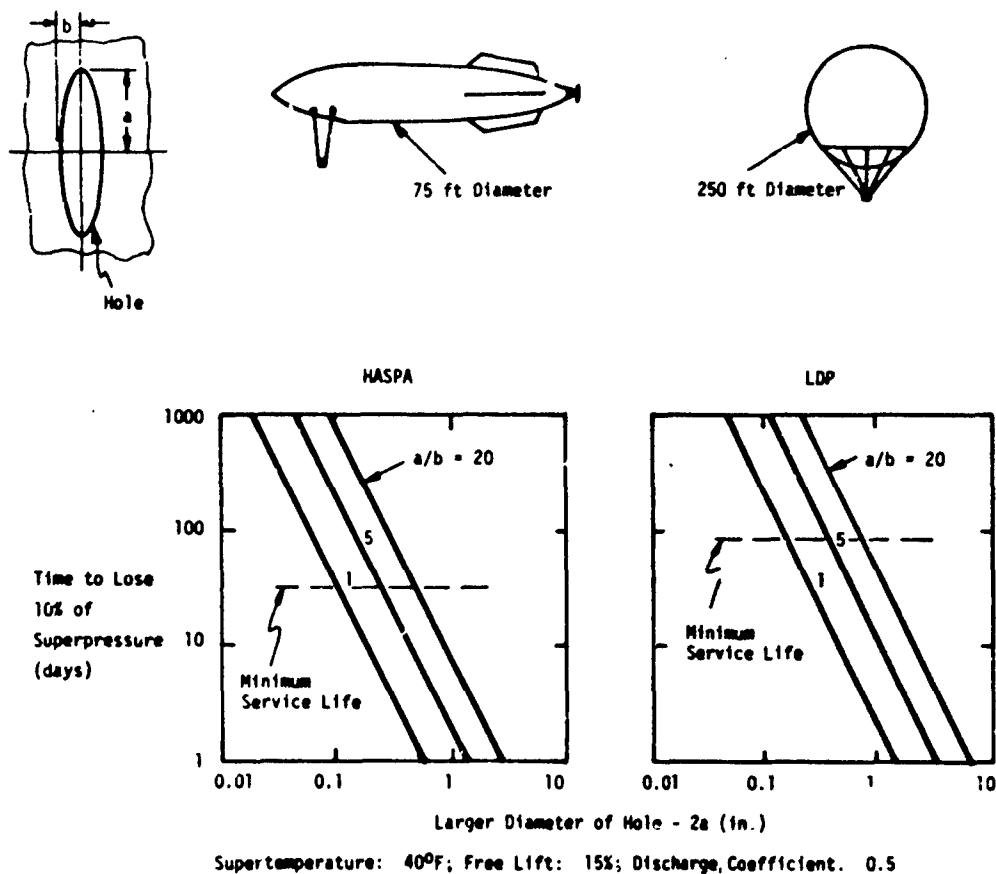


Figure 4. Effect of Elliptical Hole in Balloon Wall on Service Life



ascent. Since HASPA has a surface area of about 70,000 cubic feet and LDP about three times that value, the material chosen must be highly damage-resistant and extraordinary handling measures must be applied to safeguard barrier integrity.

Material candidates can be ranked according to damage resistance by applying a controlled folding or creasing action using a twist-flex apparatus, Bally flexometer or similar technique (Keen, 1974). It is probably not feasible to completely characterize the forces applied to the material during fabrication and operation.

The balloon area and volume also determine the minimum material thickness required to control pressure loss by permeation. Lally (1967) suggests that plastic films for extended duration superpressure balloons should have a minimum permeability of  $4 \times 10^{-11}$  std cc-cm per sec per sq cm per cm Hg pressure.

Zero pressure balloons flown for a few days are far more tolerant of localized gas barrier damage because of the lower pressure and expendable ballast usually carried.

#### 4.3 Transparency Requirements

Ideally, materials for any balloon flown more than 24 hours should be transparent to the entire spectrum of solar and earth radiation. Practically, the radiation properties of a balloon material largely determine the diurnal temperature extremes of the confined gas. These, in turn, determine the pressure sustained by a superpressure balloon or the ballast expenditure for a zero pressure balloon.

Analytical methods have been developed for determining balloon thermal response based on material radiation properties. More experimental verification of these techniques would be desirable (Kreith, 1971).

#### 4.4 Ultraviolet Stability Requirements

Available evidence on superpressure balloons made of polyester film indicates that the practical operating life is determined by material photo-degradation. Average life varies inversely with altitude and balloons which drift into the Antarctic night have lives extended in proportion to the time sunlight is absent.

With few exceptions, organic polymers exposed to sunlight are chemically changed, causing deterioration of properties. Ultraviolet radiation energy, even at the Earth's surface, is sufficient to rupture most chemical bonds in polymers. Typical exposure effects are:

- Changes in material radiation properties,
- Cracking and crazing of surfaces, and
- A reduction in strength and ductility.

Unfortunately, it is extremely difficult to simulate the UV radiation environment for a balloon material. Materials and stability treatments can be ranked by testing samples exposed on the ground, but reliable deterioration rates can only be obtained from samples exposed at the balloon operating altitude (Tobin, 1973-74).

## 5. MATERIAL CANDIDATES

### 5.1 Individual Films and Yarns

Figure 5 shows polymer films and fibers suggested by previous balloon use.

There are many variants of these candidate materials which differ slightly in mechanical and physical properties. Other commercially available films and fibers might be considered, such as FEP fluorocarbon film which has superior transparency and UV stability. The list on the preceding page will serve to illustrate the selection process.

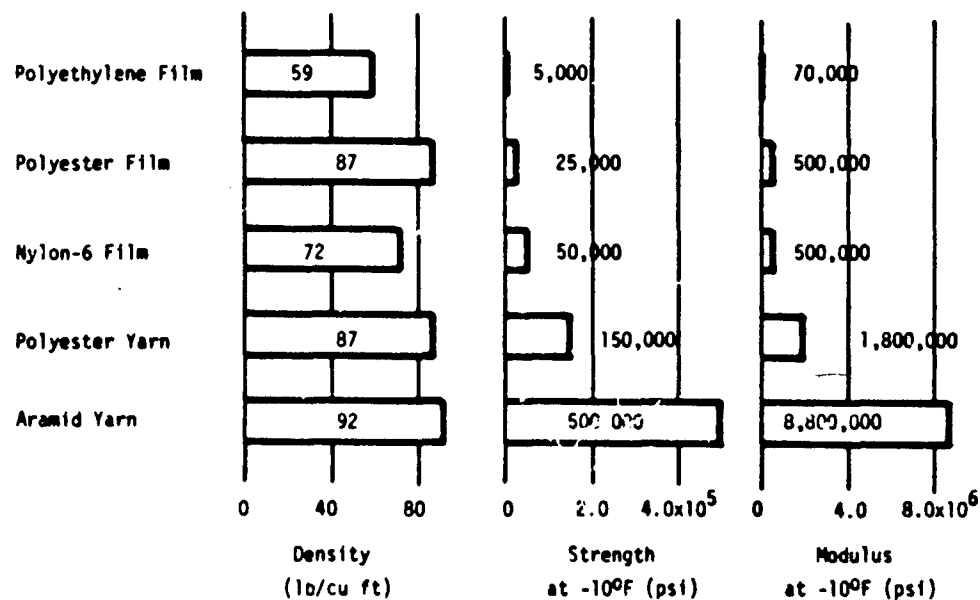


Figure 5. Candidate Materials

## 5.2 Combinations of Films, Coating and Yarns

Most current balloons use several materials in combination to enhance strength, gas barrier efficiency, or other properties. Polyester film, super-pressure balloons are generally made of two film layers bonded together to seal small holes in the stock film. Most heavy load, natural shape balloon envelopes consist of polyethylene film reinforced with high-strength fibers bonded along the seams.

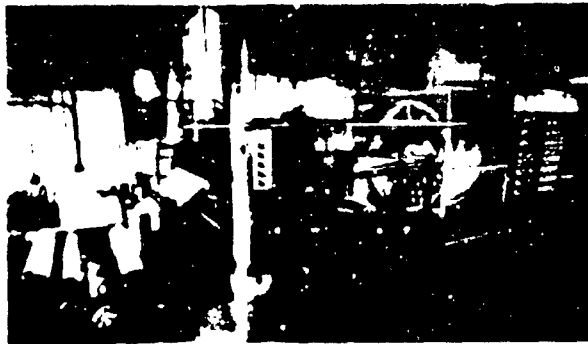
Different films can be laminated or coatings applied to improve permeability and increase resistance to flex damage and puncture. Ultraviolet stabilizer systems are available as additives for the film resin or as surface coatings.

When combinations of films and yarns are considered, film selection can be based primarily on transparency, damage resistance and similar attributes since strength and stiffness can be provided by the yarns. Although films and yarns come in relatively few stock thicknesses, strength can be closely matched to applied loads by varying yarn spacing. Open weave fabrics or nonwoven, multi-axial yarn arrays can be applied to films with equipment similar to that used for reinforcing paper and films for building construction (Figure 6). The rotating drum winds yarn around cables at both edges of the web to obtain two, diagonal yarn arrays. A third array is aligned with web travel direction. The cables carry the diagonal yarns through rollers which bond the yarns to the film. Yarns are cut at the web edge so the cables can recirculate. By varying the number of supply spools and the speeds of drum and web, the angle and spacing of yarns can be continuously varied.

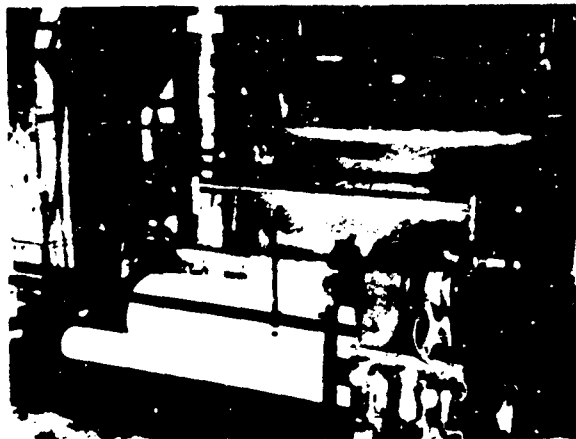
Figure 7 shows how composite production methods have been adapted to various end uses. Pressurized spheres require a symmetric construction, Figure 7a. Unequal principal stresses in an aerodynamic-shaped balloon permit weight reductions by adjusting the amount of yarn to the load in each direction, Figure 7b. With automatic controls, weight can be saved by varying the number of yarns per unit width over a balloon's surface to match a varying stress field, Figure 7c.

## 5.3 Strength/Weight Properties

For a given polymeric material, pressure vessels made of film or sheet will weigh less than those made of the same polymer in fabric form. Although the fiber usually has a higher strength-to-weight ratio than the film, two sets of fibers are required to resist the biaxial stresses and additional material is needed to seal the spaces between yarns.



(a) Production Line



(b) Take-up Station



(c) Yarn Positioning Apparatus

Figure 6. Equipment for Production of Film-Yarn Composites

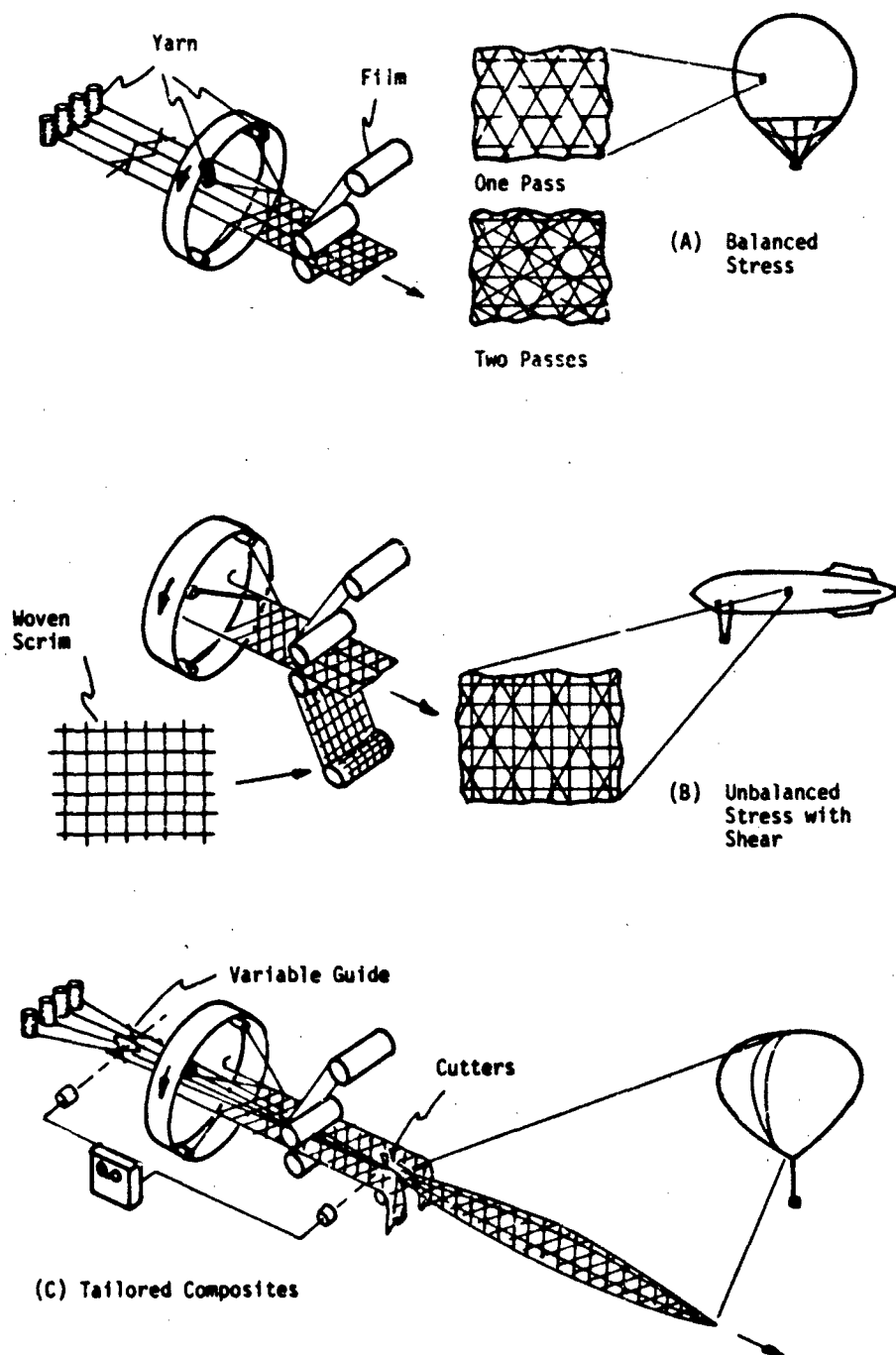


Figure 7. Production Methods for Film-Yarn Composites

Fabric or fiber composite materials can provide weight savings through use of material like KEVLAR aramid fiber which has a superior strength-to-weight ratio, but is not available in sheet form.

Like three-dimensional composites, strength and stiffness of films reinforced with parallel arrays of yarns tend to follow the rule of mixtures: composite strength is determined by the relative strengths and volume proportions of film and yarn, and composite stiffness follows a similar relation. More strengthening occurs when the film is more ductile than the yarn so it can deform without fracturing to redistribute yarn forces at seams, load patches and other discontinuities.

### 5.1 Tear Resistance

Pressure vessels made of homogeneous isotropic sheets are unstable unless large safety factors are used because of the influence of combined stress. Brittleness and ductility are material states, not intrinsic properties. The degree of brittleness depends on the volumetric or combined stress as well as the applied temperature, strain rate, and strain history. Balloon material in the brittle state is unstable because:

- It cannot deform to distribute stress around thickness variations, scratches and tears;
- It cannot deform to relieve stress concentrations from seams, load patches and assembly tolerances; and
- It has increased sensitivity to impact loading and vibration.

Fabrics have a higher tear resistance than films since the basic material is always stressed uniaxially and does not become brittle as rapidly. At stress concentrations in a biaxial stress field, fabric yarns deform uniaxially to relieve the overload while a film may become brittle under the stress and fracture.

The stress concentration at the root of the film crack causes it to spread rapidly, while in the fabric, should a tear start, the concentration may be relieved by uniaxial ductility of individual yarns (Topping, 1957).

Although uniaxial ductility of structural fibers is not great, tear propagation in a fabric or fiber composite requires a stress field many times greater than for a homogeneous film of the same weight, Figure 8.

Figure 9 shows the effect of polyester reinforcing yarns on the strength of cylindrical specimens of polyethylene and polyester film subjected to biaxial stress with shear, which is a severe condition of volumetric stress. All specimens were formed with adhesive taped, butt seams, except the Stratofilm and X-124 (polyethylene) specimens which had thermally welded seams. Film fracture was considered as specimen failure. None of the specimens showed local yielding along the fracture line:

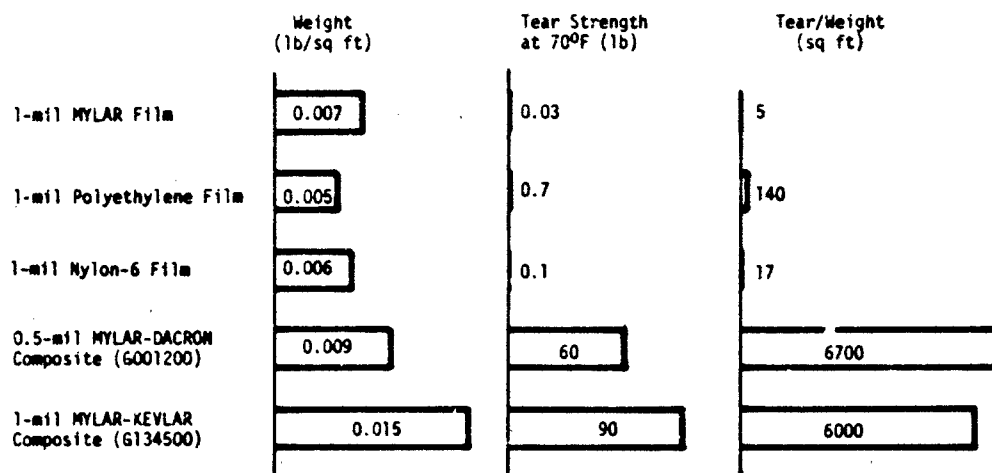


Figure 8. Tear Propagation Strength (FTM 5136)

- All unreinforced MYLAR cylinders failed by tearing across the specimen at a high rate.
- Unreinforced polyethylene (Stratofilm, X-124) cylinders tended to fail at the seams.
- Most DACRON-MYLAR specimens failed by localized film fracture between or along the yarns.
- Most of the DACRON-polyethylene cylinders failed by tearing of both film and yarn. In some cases, tearing was stopped by yarns after proceeding for several inches.

A quadratic failure theory was assumed and the ellipses were fitted to the data by standard, least squares methods. Shear capability of the polyethylene was increased in proportion to the weight of yarn and adhesive added. Although MYLAR film weight was doubled by yarn reinforcement, shear strength was only slightly improved. This may be attributed to the higher ductility of the polyethylene compared to DACRON which improves relief of overstress caused by variations in yarn tension, spacing, and bond strength.

### 5.5 Creep Effects

Generally, evaluation of creep effects requires measurements for each variant of film, fiber or composite. For most polymers, creep data obtained at several constant temperatures and stresses can be used to estimate creep strain or mean time to creep rupture for a different temperature-stress history.

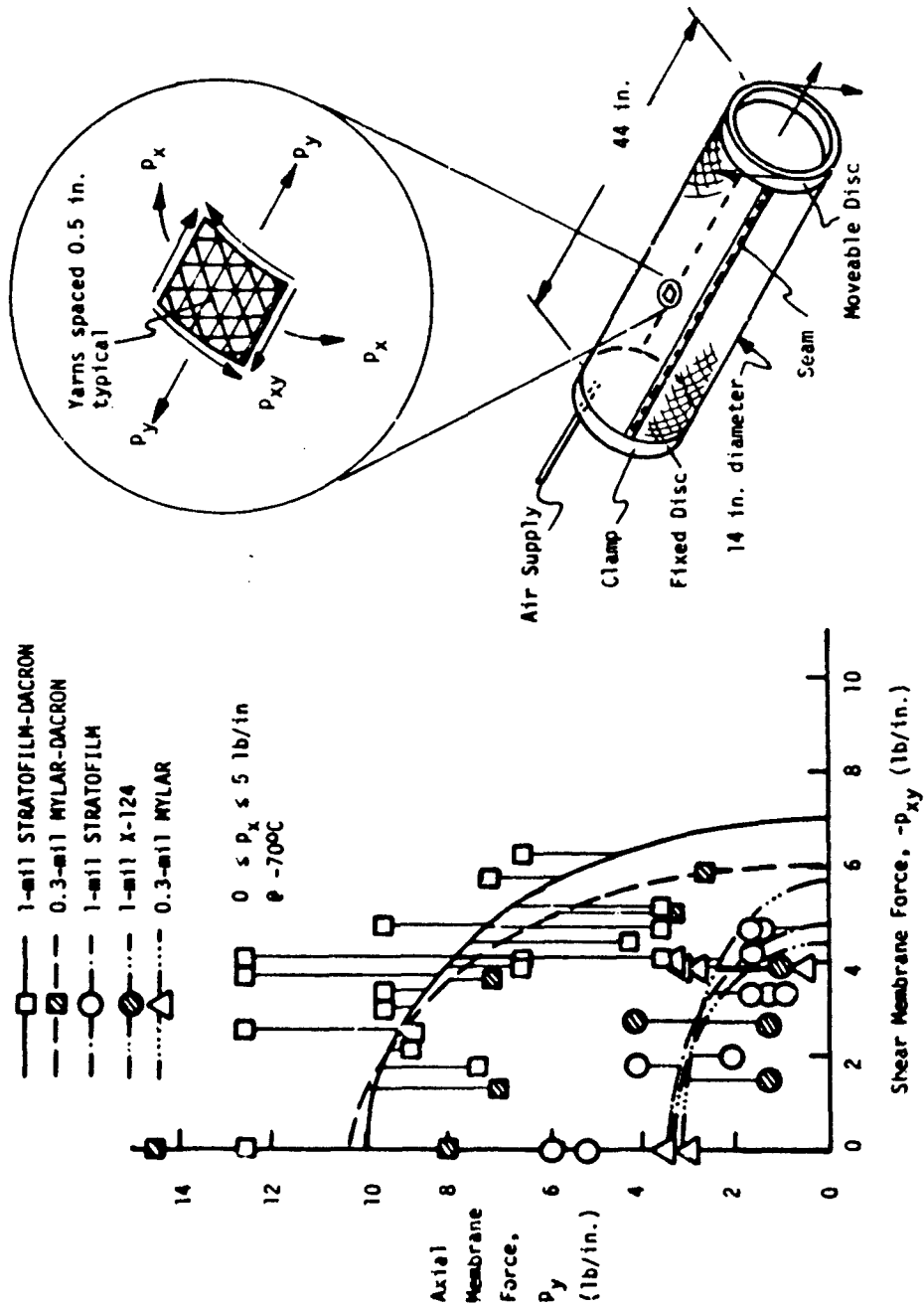
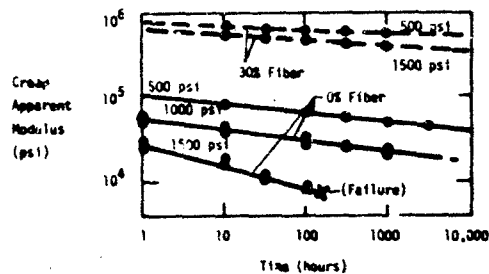
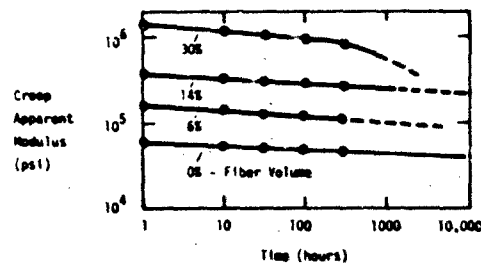


Figure 9. Low-Temperature Strength for Cylinders of Reinforced and Unreinforced Film Subjected to Combined Loading





(a) Effect of Initial Stress and Glass Fiber Reinforcement on Creep of HD Polyethylene



(b) Effect of Glass Fiber Volume Fraction on Creep of Nylon 6 at Constant 2000 psi Stress and 50 Percent R.H.

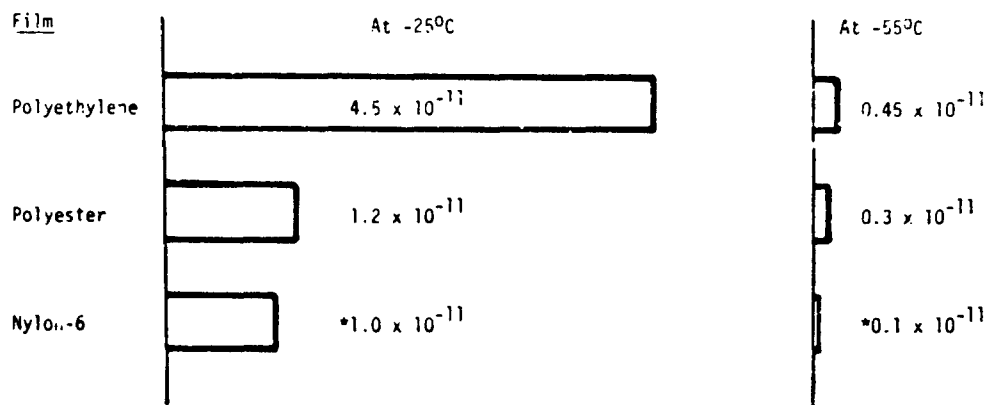
Figure 10. Typical Creep Effects at 130°F

Figure 10 shows typical creep effects of polyethylene and nylon 6 for various loads and volume fractions of fiber reinforcement (O'Toole, 1967). Addition of 20 to 30 percent glass fiber by volume changes the creep strain for both materials by an order of magnitude. The strain indicated for nylon at 50-percent relative humidity is four to five times the creep at zero water content.

Creep of some polyethylene films during balloon inflation has been shown to reduce film strength by 50 percent or more under combined loading (Kerr, 1967). Fiber reinforcement could control such deformation and preserve the original molecular orientation of the film.

#### 5.6 Gas Barrier Properties

Permeation of helium through plastic films depends on the partial pressure, film thickness and a temperature dependent parameter characteristic of the film and gas, Figure 11 (Brubaker, 1953).



\*Extrapolated from data above +20°C.

Figure 11. Helium Permeability Parameter  
(cc - cm/sq cm - sec - cm Hg)

Resistance to punctures and to similar damage during folding and handling is a primary requisite for a superpressure balloon film. Polyethylene and nylon are superior at temperatures above 0°C. Nylon is particularly tough and ductile after absorbing water. It may be desirable or necessary to water-condition nylon balloon film prior to fabrication and launch to enhance damage resistance.

Flex resistance of a gas barrier can be improved by combining layers of the same or dissimilar films in various ways. A continuous ductile coating on a high modulus film, Figure 12a, may better resist development of holes from folding than the current practice of joining two high modulus sheets.

Bonding sheets at regular intervals with a pattern of adhesive dots or stripes (Figure 12b, c) would reduce surface stress at creases, compared to a single sheet with the same total thickness. This is analogous to stranded cable or yarn, which is a more reliable tensile element than a solid rod or monofilament because it receives less damage from sharp bends and because superficial nicks or scratches in one wire or filament cannot propagate through the entire cable. Another advantage of several film layers is that leakage can be reduced, even for coincident holes, because the flow would be throttled several times as in a labyrinth seal.

The "spot bonded" barrier would probably be limited to two sheets so two independent gas barriers would be formed by adhesive tapes applied to each side at balloon seams. A quilt-bonded barrier could have three or more layers with staggered bond lines since all the cells would be sealed except along seams.

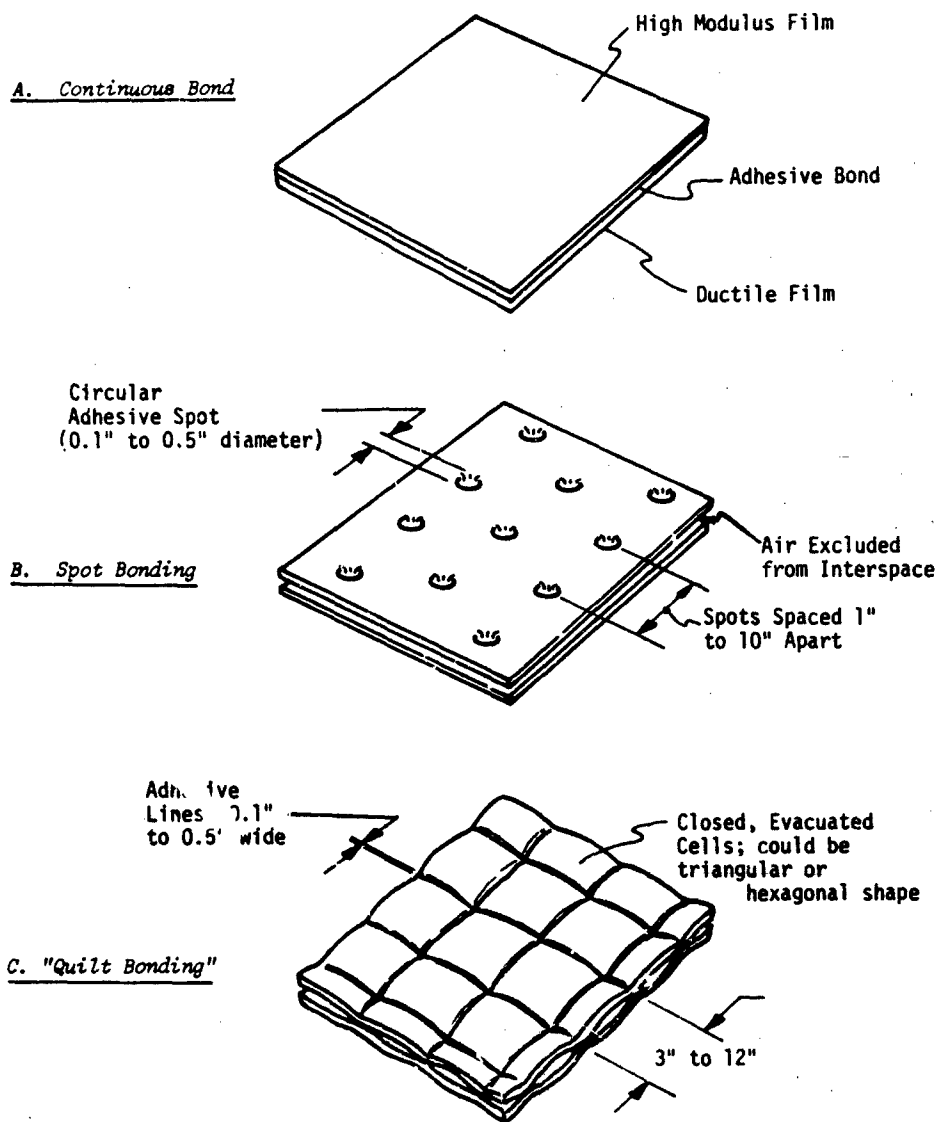


Figure 12. Concepts for Increasing Resistance of Gas Barrier to Damage from Folding and Handling

Layered, interval bonded, gas barriers could be compared with single sheets using one of the flexibility tests referenced in Section 4.2 to determine whether or not the added complexity is justified.

#### 5.7 Thermal Radiation Properties

Solar and infrared absorptivities of balloon materials have been obtained by measuring spectral transmissivity and reflectivity and integrating these over the solar and infrared energy spectra.

Solar absorptivity of polyethylene film is slightly less and the infrared absorptivity many times less than for polyester film of equal thickness.

Since polymer fibers are nearly opaque to solar radiation, for film-yarn composites, it is desirable to use larger diameter yarns and wider yarn spacing, consistent with other requirements, to minimize balloon heating.

#### 5.8 Ultraviolet Stability

Little photostability data useful for balloon design are available. Polyesters have generally superior resistance to sunlight, compared to polyamides (nylon, KEVLAR) and polyethylenes. Based on accelerated weathering tests with artificial light in which rates of loss of mechanical properties were compared, polyethylene and nylon 6 are rated "fair to good" and polyester is rated "excellent".

KEVLAR yarn (770 denier) was found to lose about 40 percent of its tensile strength after 100 hours, and 50 percent after 200 hours exposure to sunshine carbon arc (Weatherometer) and xenon lamp (Fadeometer) sources. These supply two to three times as much ultraviolet energy to test specimens as natural sunlight at sea level.

### 6. EVALUATION AND SCREENING METHODS

If material selection is to interact effectively with the design process, evaluation and screening activities should begin early in the development effort to provide feedback on material constraints and to permit refinement of the screening method as additional requirements and material data become available.

If there are a large number of requirements and material candidates, the following general method has proved useful:

- A. Assign a weighting index to each requirement in proportion to its importance to the design objective, as determined by analysis of failure modes, cost, etc.

B. For each property, assign a weight index to each material in proportion to its rank among all other candidates for that property. Multiply each material index for a given requirement by the requirement index.

C. Sum the product of material and requirement indices over each material.

The resulting number for each material reflects the relative importance of all requirements and the relative number of times the given material exceeded properties of other materials. This procedure is not a substitute for second judgment by the designer. It does provide a systematic way of comparing a large group of requirements and options.

To determine the best combination of material dimensions, the best constituent mix in a composite or other design variable trades, various constrained optimization methods can be used. These involve definition of an objective variable, and the failure and geometric constraints in terms of the design variables. The point in design variable space where the maximum number of constraints intersect is usually "best" because the design is taxed to the utmost through all failure modes.

A reduced problem will illustrate. For the LDP mission, the combination of polyethylene film thickness  $t_f$  and DACRON yarn weight/area  $w_y$  is sought for which the balloon cost will be a minimum. Assuming a spherical structure, and cost proportional to surface area, a minimum diameter (D) sphere will have the lowest cost. Failure constraints are defined in terms of the design variables (D,  $t_f$ ,  $w_y$ ), Appendix A.

- Material stress must be less than 60 percent of the short-term ultimate strength, which yields:

$$D < [1.9 \times 10^5 w_y + 1.8 \times 10^6 t_f]$$

- To prevent altitude changes greater than 100 feet caused by day-night temperature variations:

$$D < [1.2 \times 10^5 w_y + 2.3 \times 10^6 t_f]$$

Similarly, if the balloon is to support itself and a 500-pound load at 130,000 feet:

$$[1.2 \times 10^{-4} D^3 - (4.8 w_y + 206 t_f) D^2] \geq 500$$

The constraints are shown in Figure 13 for 0.5-mil and 1.0-mil film thicknesses. The minimum feasible balloon diameter is determined by the deflection requirement for the thinner film and by strength for the thicker one. For cost proportional to surface area, the 1-mil balloon will cost about a third more than

the 0.5-mil structure. The graph at the top of Figure 13 indicates how the yarn spacing varies with weight for available sizes of DACRON yarn applied in three parallel arrays, forming equal angles.

Mathematic procedures are more convenient than graphical ones for this kind of problem and mandatory for large numbers of design variables.

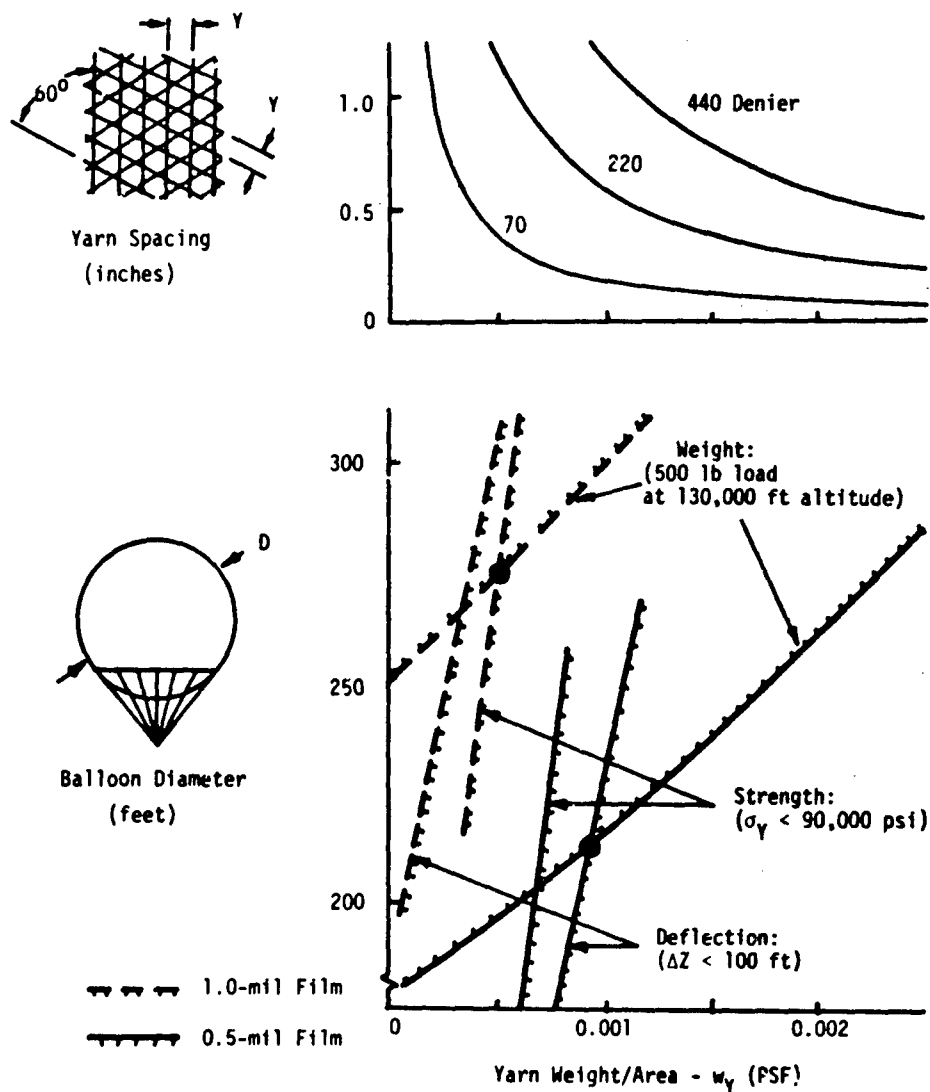


Figure 13. Weight and Failure Constraints Applied to LDP Mission: Polyester Yarn, Polyethylene Film

## References

- Brubaker, David W. and Kamarmeyer, K. (1953) Flow of gases through plastic membranes, in Industrial Engineering Chemistry, 45(No. 5):1148.
- Fouchard, P. (1973) Poly Plus Seal Study, Report No. 1 (prepared for NSBF), Centre National D-Etudes Spatiales: Systems and Balloons Projects Division, Toulouse, France, Note No. 109/CNES/CT/BA/VE/MA.
- Keen, L. (1974) Technology update on tethered aerostat materials development. \*
- Kerr, A.D. and Alexander, H. (1967) On a Cause of Failure of High Altitude Plastic Balloons, AFCRL-67-0611, Scientific Report No. 2.
- Kreith, F. (1971) Performance of High Altitude Balloons, NCAR-TN/STR-65.
- Krenchel, H. (1964) Theoretical and Practical Investigation of the Elasticity and Strength of Fibre-Reinforced Materials, Akademisk Forlag, Copenhagen.
- Lally, V. E. (1967) Superpressure Balloons for Horizontal Soundings of the Atmosphere, NCAR-TN-28.
- Morfitt, G. L. and Niccum, R. J. (1972) Poly Plus Balloon Material Development Program, Phase I and II, Final Report, National Scientific Balloon Facility Contract 27123-71.
- Munson, J. B. (1974) Poly Plus Seam Study: Cylinder Testing, Interim Report, Office of Naval Research Contract No. N00014-72-C-0494.
- O'Toole, J. L. (1968-69) Creep properties of plastics, in Modern Plastics Encyclopedia, McGraw-Hill, New York, p. 48.
- Petrone, F. (1974) High altitude superpressured powered aerostat (HASPA). \*\*
- Tobin, W. W. (1973-74) Ultraviolet stabilizers, in Modern Plastics Encyclopedia, 50(No. 10A), McGraw-Hill, New York, p. 268.
- Topping, A. D. (1957) Behavior of materials under combined stresses in pressurized structures, Aeronautical Engineering Review, 16(No. 2):55-69.

\*Proceedings, Eighth AFCRL Scientific Balloon Symposium AFCRL-TR-74-0393

\*\*Proceedings, Eighth AFCRL Scientific Balloon Symposium, Supplemental Volume, AFCRL-TR-74-0596, p. 9.

## **Appendix A**

### **Superpressure Balloon Constraints Imposed by Material Mechanical Properties**

#### **1. REQUIREMENTS**

- A. A minimum cost, spherical superpressure balloon is desired to operate at 130,000 feet in the U.S. Standard Atmosphere for 90 days with a 500-pound suspended load. Free lift is assumed to be 0.15, and the super-temperature, 25°C. The balloon is to be constructed of plastic film or a film-fiber composite.
- B. Maximum material stress must be less than 0.6 x (short-term ultimate strength) to prevent creep rupture.
- C. Diurnal changes in balloon deformation must not change equilibrium altitude more than 100 feet.

#### **2. OBJECTIVES**

The lowest-cost balloon is assumed to be one with minimum diameter. The design variables are balloon diameter, film thickness and yarn weight per unit area of film.

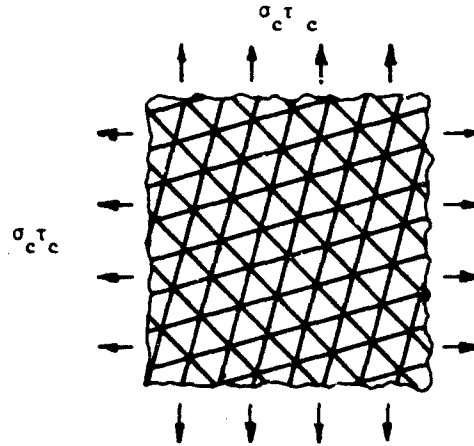


### 3. FAILURE CONSTRAINTS

#### 3.1 Material Stress

Assume three, parallel fiber arrays forming equal angles, bonded to a plane, film matrix and subject to equal biaxial loads. If the constituents are uniform in strength and dimensions and they deform equally and elastically, the composite stress is given by (Krenchel, 1964):

$$\begin{aligned}\sigma_c &= \left[ E_y V_y / 2 + E_f (1 - V_y) / (1 - \nu) \right] \epsilon_c \\ &= E_c \epsilon_c\end{aligned}$$



Assuming the yarn adhesive to have the same mechanical properties as the film and a weight/area of  $(0.4 w_y)$ , the apparent composite thickness is:

$$t_c = w_y (1/\rho + 0.4/\rho_a) + t_f \quad (A-3)$$

In terms of membrane forces:

$$\sigma_c t_c = \sigma_y \left[ \frac{w_y}{2\rho_y} + \left( t_f + \frac{0.4 w_y}{\rho_a} \right) \left( \frac{1}{1-\nu} \right) \frac{E_f}{E_y} \right] \quad (A-3)$$

Neglecting stress variations due to load suspension, and setting  $\sigma_c t_c = \Delta P D/4$  and the yarn stress  $\sigma_y = 0.6 \times$  (ultimate value of  $\sigma_y$ ):

$$D < 1.45 \sigma_c t_c$$

(A-4)

### 3.2 Material Deformation

For a superpressure balloon with diurnal supertemperature variation  $\Delta T$ , the corresponding altitude change  $\Delta Z$  is approximately (Lally, 1967):

$$\Delta Z \approx \frac{75 D \Delta T P (1+F)}{t_c E_c} \quad (A-5)$$

For the conditions above:

$$D < 7.39 \times 10^{-3} t_c E_c \quad (A-6)$$

### 4. DISPLACEMENT CONSTRAINT

Allowing 10 percent for weight of seams and load suspension, at equilibrium altitude, for the given conditions:

$$\left[ 1.2 \times 10^{-4} D^3 - (4.8 w_y + 3.5 \rho_f t_f) D^2 - 500 \right] > 0 \quad (A-7)$$

### 5. DEFINITIONS

<u>Symbol</u>	<u>Description</u>	<u>Unit</u>
D	Balloon Diameter	ft
E	Young's Modulus	lb/sq ft
F	Free Lift	Dimensionless
P, $\Delta P$	Absolute and Differential Pressure, respectively	lb/sq ft
$\Delta T$	Supertemperature	$^{\circ}K$
V	Volume Fraction	Dimensionless
$\Delta Z$	Balloon Altitude Deviation	ft
t	Thickness	ft
w	Weight/Area	lb/sq ft
$\epsilon$	Deformation	(in./in.)
$\nu$	Poisson's Ratio for Films	Dimensionless
$\rho$	Density	lb/cu ft
$\sigma$	Stress	lb/sq ft

<u>Subscripts</u>	<u>Description</u>
a	Adhesive
c	Composite
f	Film
y	Yarn

#### Contents

1. Introduction	242
2. Range of Balloons Used	243
3. Onboard Equipment	244
4. Ground Equipment	250
5. Conclusion	257

## Twelve Years After the First Launching: Operational Activities of CNES in Stratospheric Balloons

M. Rougeron  
Centre de lancement de ballons stratosphériques  
(National Center for Space Studies -  
Stratospheric Balloon Launching Center)  
B.P. 44 - 40800 AIRE-sur-ADOUR France

### Abstract

Side by side with revolutionary developments in the field of stratospheric tethered balloons, the "Balloon Systems and Projects" Division of CNES is pursuing unremitting efforts in the better-known field of free Stratospheric balloons.

Two years ago, before this same audience, the CNES had announced the startup of a production facility for natural-shape balloons, extremely original in many respects. Managed by the Zodiac-Espace Company, this production unit today enables the CNES to launch some fifty balloons of this type every year ( $350,000 \text{ m}^3$  -  $100,000 \text{ m}^3$ ) as well as a roughly equal number of tetrahedral balloons ( $85,000 \text{ m}^3$ ) for scientific packages weighing less than 150 kg.

However, the CNES has not been doing work solely on the vehicles. Important related developments, accomplished during the same time period, enable a variety of on-board and ground-based equipments to be placed in service today:

#### - On-Board Equipment

- Telemetry transmitter and receiver, remote-control (command) decoder
- Electronic servo-equipment
- Various mechanical systems

- Ground Equipment
  - . Complete telemetry station
  - . Real-time processing system
  - . Launching equipment

In addition, very strict procedures have been worked out with the responsible agencies to ensure that balloon flights are compatible with civil and military air traffic.

## 1. INTRODUCTION

The "Balloon Systems and Project" Division of the National Center for Space Studies is charged with designing, developing, and operating "balloon systems" made available to experimenters under:

- (1) The French Space Program (conventional flights).
- (2) Various research activities from laboratories of all nationalities (funded flights).

Each balloon system is comprised of:

- (1) The balloon itself.
- (2) The standard on-board equipment.
- (3) Ground equipment needed for launching, in-flight monitoring and recovery operations.

The first French stratospheric balloon flight took place twelve years ago. Since then, a number of "balloon systems" have been studied by the CNES. Some of them were tested with various degrees of success. Only some reached the operational stage, such as the pressurized balloons launched under the EOLE Project in the second half of 1971.

Today we have a new "balloon system": the tethered stratospheric balloon which opens up many new fields of application to pure and applied research. The difficulties still to be overcome to make such a revolutionary vehicle operational, however, are still numerous. (Ref. R. Regipa, CNES "Stratospheric Captive Balloons".)

At the same time, however, efforts have been continuing in the field of free stratospheric balloons. About 100 balloons of this type are launched every year by the CNES from its AIRE-sur-ADOUR and GAP-TALLARD Centers, or on the occasion of field campaigns.

These are the figures for 1973:

- |                                       |                        |
|---------------------------------------|------------------------|
| (1) Total number of flights.          | 108                    |
| (2) Percentage failures.              | 18 percent             |
| (3) Mean volume of launched balloons. | 107,000 m <sup>3</sup> |

- |                               |        |
|-------------------------------|--------|
| (4) Average launched payload. | 210 kg |
| (5) Average ceiling time.     | 6 hrs  |

## 2. RANGE OF BALLOONS USED

### 2.1 Tetrahedral Balloons

This is the first type of stratospheric balloon developed in France. The characteristic shape makes production costs very low. They are made by continuous sealing of a strip of polyethylene film 25 microns thick, and of constant width, spiralling along the surface of the tetrahedron.

However, the tetrahedral shape is unsuitable from the mechanical standpoint. Moreover, it is impossible to reinforce the skin.

These reasons have led us to limit:

- (1) The volume of tetrahedral balloons to  $85,000 \text{ m}^3$ .
- (2) The payload to 200 kg.

These extreme values, established through experience, cannot be exceeded without considerably increasing the risk of failure.

### 2.2 Natural-Shape Stratospheric Balloons

In view of the limitations on tetrahedral balloons and the constant and inevitable increase in scientific experiments, in 1970 the CNES set up the techniques and industrial facilities necessary for manufacturing natural shaped balloons. At the 7th AFCRL Balloon Symposium, Mr. R. Regipa described to you in detail the manufacturing system of the Zodiac Espace Company. Despite its original nature it rapidly produced some fifty balloons per year divided more or less equally between volumes of  $100,000 \text{ m}^3$  and  $350,000 \text{ m}^3$ .

What are the limitations of this type of balloon today?

(1) The thickness of the polyethylene film used is 20 microns, which is a minimum for European industry. 15-micron film has been produced in small quantities but cannot yet be used for manufacturing.

(2) The payload is limited to 500 kg. This is not a technical but an operational limitation, as the risk of parachuting very heavy loads into as densely populated a country as France is unacceptably hazardous.

(3) The balloon volume is limited to  $350,000 \text{ m}^3$ . Here again this is not a question of technology, but the return on investment from very large balloon flights must be established in advance.

### 3. ONBOARD EQUIPMENT

As far back as 1961, CNES became aware of the need to develop standard onboard equipment parallel to the balloon. The policy followed:

- (1) Infinite variety of scientific experiments.
- (2) Absolute standardization of equipment (especially telemetering and remote control) enables duplication of effort from one experimental group to another to be avoided and the ground equipment to be rationalized.

Moreover, the very special environmental conditions encountered with balloon flights made it necessary to impose very strict design standards on these sub-assemblies to achieve excellent reliability.

While at first they were relatively simple and cheap, today on-board equipment components have reached a degree of sophistication which has pushed up costs. However, the near-certainty of recovering them in good condition after each flight makes the utilization cost quite reasonable.

#### 3.1 Standard Telemetering and Remote Control Equipment

The SITTEL system, now widely used, has the special feature of having three integrated functions: (1) telemetering, (2) remote control (command), and (3) ranging (distance measuring).

##### 3.1.1 TELEMETERING.

The telemetering function may be carried out in two ways.

##### 3.1.1.1 FM/PM Telemetry

FM/PM telemetry, to IRIG standards, can make use of the following very efficient units: (1) a very stable transmitter, and (2) very high quality modulators. In addition, phase modulation permits coherent demodulation with lower signal-to-noise ratios than with frequency modulation. A standard 30-channel selector switch is currently included in this telemetering system.

Principal characteristics of the FM/PM telemetry are as follows:

##### TRANSMITTER:

- (1) Frequencies: 400.650, 400.905, 4-1.160, 401.490 MHz
- (2) Transmitting power: 500 mW on 50 ohms
- (3) Modulation: Peak phase excursion of 2.6 radians
- (4) Passband: 30 Hz, 150 kHz
- (5) Frequency stability:  $\pm 5 \times 10^{-6}$

#### IM MULTIPLEX:

Channels: 4 to 14 of the standard IRIG system - (0.96 KHz - 2.0 KHz, channel 10 being reserved for the ranging signal)

Frequency excursions:  $\pm 7.5$  percent or  $\pm 15$  percent

Input signals: 0.2 V

Linearity: better than  $\pm 0.5$  percent

Maximum central frequency variation: 1 percent

Maximum slope variation: 1 percent

Note: These specifications are valid for a temperature range of  $-20^{\circ}\text{C}$  to  $+50^{\circ}\text{C}$ .

#### 3.1.1.2 PCM Telemetry

PCM telemetry, benefitting from the most advanced technology, is a powerful and very efficient tool: (1) increased accuracy; the quality of the link is no longer a source of errors, and (2) number of transmitted parameters is over 100.

Principal characteristics of PCM Telemetry are as follows:

TRANSMITTER: Identical to FM/PM transmitter.

#### SWITCH-CODER:

- (1) Format: the format has 16 cycles; one cycle, 32 words; one word, 8 bits. The normal rate may be (a) multiplied by 2 (131,072 bits/sec) or (b) divided by 2, 4, or 8 (8,192 bits/sec., 16,384 bits/sec, 32,768 bits/sec).
- (2) For the normal bit rate, in view of overswitchings and underswitchings, one obtains for the various channel types:
  - (a) High-speed analog channels; from 2 channels with 1,024 points/sec to eight channels with 256 points/sec.
  - (b) Low-speed category 1 analog channels; from 2 channels with 512 points/sec to 64 channels with 16 points/sec.
  - (c) Low-speed category 2 analog channels; 8 channels with 16 points/sec.
  - (d) High-speed digital channels; from 4 channels with 1,024 points/sec to 4 channels with 512 points/sec plus 8 channels with 256 points/sec.
  - (e) Low-speed digital channels; from 4 channels with 32 points/sec to 8 channels with 16 points/sec.
  - (f) Double-precision digital channels (16 bits); from 2 channels with 32 points/sec to 4 channels with 16 points/sec.
- (3) Precision:
  - (a)  $\pm 0.4$  percent for single-precision channels.
  - (b)  $\pm 3 \times 10^{-5}$  for double-precision channels.



(4) Inputs:

- (a) Analog: asymmetric input on two separate terminals; measuring range, 0.2 V.
  - (b) Digital: level 0 between -12 V and +0.5 V, and level 1 between +2.5 V and +12 V. For high speed digital channels synchronization logic can be built in; the experiment then gives a "start to read" signal which is a "O"; telemetry gives an "end read" signal which is a "O".
- (5) Signal rates: all rates available for the experiment.

3.1.2 REMOTE CONTROL

The remote control (telecommand) link is of the PCM/PSK type. The number of individual commands is 10. An addressing system (10 addresses) enables the full remote control capacity to be used in the case of simultaneous flights. Combination order coding enables the number to be multiplied. At present, however, the corresponding interfaces must be made by the experimenter himself.

Principal characteristics of remote control (command) system are as follows:

RECEIVER:

Frequency: 444 MHz  
Frequency modulation  
Sensitivity: 93 dBm  
Noise factor: less than 6 dB  
Passband:  $\pm 15$  KHz

DECODER

Message:	the 10-bit address, twice, then the 10-bit command twice
Bit rate:	1000 bits/sec
Message rate:	5/sec
Number of addresses:	10
Number of commands:	10 x 2 (10 flipflop relays)
Detection rate:	0.99 for a signal/noise ratio of 20 dB
Error rate	$1/10^6$ messages with signal/noise ratio of 0 dB
Output elements:	flipflop relays; cutoff capacity 2 A with 12 V.

3.1.3 RANGING

Ranging (distance measurement) is performed by measurement of the phase displacement a 150 Hz sine wave in travelling from the ground antenna to the balloon and return.

The telemetry transmitter and remote control receiver (on the balloon) are connected to a single antenna through a duplexer. The 150 Hz signal transmitted from the ground on 444 MHz carrier wave is received by the remote control

receiver and then retransmitted from the balloon by the telemetry transmitter (channel 10). The absolute ranging accuracy is about 1 NM.

#### 3.1.4 BAROMETERS

Two barometers, range (0 - 1,000 mb) and (0 - 70 mb) perform operational pressure measurements (accuracy 0.5 percent). Switching between the two capsules is remote controlled.

### 3.2 Electronic or Electromechanical Servo-Equipment

#### 3.2.1 SEPARATION ASSEMBLY

Fully self-contained and independent of the rest of the flight system, this assembly is placed at the top of the parachute or at the center of the triangle formed by the tops of the three parachutes with group parachuting. There is no problem with opening upon separation as long as the load suspended under the parachute or parachutes is at least 10 times the mass of this separating assembly (about 10 kilograms).

The elements of which this assembly is comprised are exposed to launching shocks. They must be particularly rugged and enclosed in a thick container which also prevents them from being cooled when passing through the tropopause.

##### 3.2.1.1 Remote Control Separation

Of the PCM/PSK type, it operates on a frequency of 148 MHz. The on-board receiver-decoder accepts only one command, chosen from the 6 commands which the remote control transmitter may generate. Its specifications are otherwise similar to those of SITTEL remote control. However, particular attention is given to the mechanical soundness of the assembly.

##### 3.2.1.2 Time Switches

The remote control system includes two redundant time switches which cause separation after a given time interval if remote control fails. Although these time switches are in common use they are specially prepared for the flight: complete degreasing followed by painting with a synthetic oil which remains fluid at very low temperatures ( $-60^{\circ}\text{C}$ ).

#### 3.2.2 BEACON

This is a transmitter operating on one of four frequencies: 152.730, 152.750, 150.770, 152.790 MHz. It allows the capsule to be located on the ground after it has landed. It has a self-sustained operating time of about 60 hours and allows postponement of the recovery operation (in bad weather, for example).

The beacon is attached to the center of a sphere, diameter about 2 meters, made of two fibreglass hemispheres. These protect it upon take-off and landing. Floats keep it on the surface of the water if it lands in the sea, a lake, or a river.

The beacon is mounted such that it can swivel and always keep its antenna pointed upward.

### 3.2.3 RADAR RESPONDER

Originally, metallized radar reflectors were introduced in the stratospheric balloon flight systems in order to permit constant tracking by aerial navigation radar and ensure flight safety during ascents and descents.

For about two years air traffic control has been bothered more and more by secondary echoes, which induced the C. N. E. S. to add to the passive reflectors a radar responder, transmitting on a code specific to the balloons, A 44.

Adapting this equipment to balloon flights poses two main problems:

(1) The "high-voltage" part of the responder cannot withstand the rarified atmosphere of the stratosphere. The equipment must thus be sealed into a container.

(2) Since they were designed to operate on board an aircraft, responders available on the market use a great deal of power and are supplied with a high-capacity battery bank which is heavy and costly.

Finally, like the separating assembly, this equipment is exposed to launching shocks. Thus, packaging is particularly important.

For the time being, the radar responder serves only to locate the balloon in azimuth (mode A). Altitude measurement is obtained through telemetering (operational barometer) and transmitted by the C. N. E. S. to the Air Traffic Control Centers. In the near future this procedure is to be modified and a radio altimeter connected with the radar responder will enable air traffic controllers to treat the balloon like an aircraft.

### 3.2.4 DEBALLASTING DEVICE

This device is used to ensure normal ascent for large balloons (over 100,000 m<sup>3</sup> volume). It also enables compensation for the small-amplitude heat effects, which may alter the floating altitude once the ceiling is reached.

The assembly is composed of:

(1) A remote control system, 148 MHz, 1 command, of the same type as the separation remote control system.

(2) A light-alloy ballast tank containing up to 120 kg of iron pellets. The base of this tank is shaped like a funnel, and is closed by a solenoid valve.

A permanent magnet prevents the ballast from flowing out unless there is a remote control signal. The remote control command causes current to be

supplied to an electrical winding which creates an opposite magnetic field to that of the magnet. The ballast then flows out at a constant rate (about 10 kg in two minutes). The reverse order stops the deballasting. This device has very high reliability but has the disadvantage of using iron pellets, the presence of which disturbs any magnetic measurements being made by the experimenter. For this reason, it has become necessary, in many cases, to place the scientific package some distance away.

### 3.3 Mechanical Systems

#### 3.3.1 BALLOON HOOK

This element was developed at the same time as the first French gored stratospheric balloons. Mechanically speaking, the plastic skin is attached to the balloon base in the same manner as with the American balloons (between the core and biconical collar). However, rapid descent of a large metal piece to the ground, after separation, must be avoided as far as possible for safety reasons (remember that the French gored balloons do not have a metal polar piece at the apex). Also it is desirable for the skin to be destroyed after separation by tearing into several pieces.

The above is possible by ejecting the hook at the time of separation. The reinforcing strips between gores are then no longer interlinked, either at the hook or at the pole, and so tears can easily propagate over the balloon skin.

Technologically, the outer shell of the hook is replaced by two half-shells interconnected by two explosive shackles with independent current supplies controlled by the separation assembly. Separation can be affected by explosion of just one of these shackles. After the hook opens the half-shells are kept in place by steel cables.

#### 3.3.2 RELAXER\*

Several accidents happened in the first French gored balloon flights. When the balloon burst during the ascent the skin sometimes fell on the parachute or parachutes, preventing them from opening correctly.

It seemed to the C. N. E. S. that an automatic separation system upon a balloon burst was the only way to prevent this accident as any human reaction (remote-controlled separation) was likely to be too late. We will note that in the case of the French balloon, the burst is often very sudden (perhaps due to the absence of the massive polar piece).

---

\* The "relaxer" senses a sudden release in tension in the load line between the balloon and payload. It performs the same function as its American counterpart, the "burst switch". (Ed. Note)

This function is accomplished by the electromechanical "relaxer" acting directly on the "ejectable hook" in parallel with the normal separation assembly. When the payload is lifted by the balloon after take-off, the system is "armed" (a latching relay closes). If the tension in the load line goes below a certain point (if the balloon bursts) a second relay closes. When these two relays (placed in series) close, separation occurs.

The mechanical part of the relaxer is based on the compression of calibrated springs. It is perfectly reliable in operation provided it is not too sensitive to the "whiplash" which can occur at take-off, causing it to operate at the wrong time (arming delayed by a damping system).

### 3.3.3 AUXILIARY BALLOON SEPARATOR

The launching method employed by the C. N. E. S. uses one or more auxiliary balloons for "soft" take-off of one or more payload packages. Once the load line is extended in its vertical position, these auxiliary balloons are no longer needed and have to be separated.

Several methods have been used: (1) remote control; unusable at nighttime, (2) time switches, and (3) manometric capsule.

Methods two and three are not without danger when shear winds have delayed lifting of the capsule by the main balloon. For this reason, a mechanical auxiliary balloon separator was developed some three years ago. Based on the load line geometry, it allows the auxiliary to escape when the balloon-separator to payload package angle becomes  $180^\circ - \epsilon$  ( $\epsilon$ , very small, can be adjusted as desired).

## 4. GROUND EQUIPMENT

C. N. E. S. has a permanent launching center at Aire-sur-Adour. Fixed installations enable flights to be made with maximum efficiency for the major part of the year.

In summertime (when the stratospheric wind changes direction) the Gap-Tallard base is used for launchings, but its equipment is less sophisticated and the balloon is quickly taken over by the remote metering and control stations at Aire-sur-Adour.

A number of field trips have also been organized abroad (at least one per year). Light and robust equipment is taken into the field by ship or plane and a "light" launching center can be set up in a few days at any point on the globe (Kerguelen Islands, Siberia, Brazil, South Africa, etc.).

### 1.1 Laboratories

The Aire-sur-Adour Center has several laboratories with a total floor area of 350 m<sup>2</sup> for preparing payload packages prior to flights.

A large laboratory with all-glass walls handles experiments equipped with a solar pointer.

A non-magnetic building separate from all the others is available for adjustments and tests on payloads oriented to the earth's magnetic field.

### 1.2 Telemetry Station

#### 4.2.1 TELEMETRY RECEPTION; REMOTE CONTROL TRANSMISSION

The success of the flight depends on correct operation of this assembly. The raw transmitted data are recorded on the magnetic tape and accurately dated. These tapes are the basic element for processing.

##### 4.2.1.1 Antenna (400 - 444 MHz)

The SITTEL antenna (developed at the same time as the associated equipment) is of original aerodynamic design and has great tracking accuracy. It includes:

(1) A telemetry antenna, capable of rotation in elevation and azimuth; equipped with four horns, and possessing directivity, with automatic tracking, of  $\pm 0.4^\circ$ .

(2) A remote control (command) antenna, rotating only in azimuth with fixed elevation of  $15^\circ$ , and connected to the automatic-tracking telemetry antenna. When the balloon is at a high angle (near the station) a second omnidirectional antenna takes over the transmission of remote control signals.

Principal characteristics of the telemetry antenna are as follows:

Gain: over 18 dB with respect to the isotrope of the same polarization

Polarization: linear, normal to the elevation axis

VSWR: less than 1.5.

For the field trips, light helicoidal antennas with 12 dB gain are used. A duplexer enables them to be used simultaneously for telemetry reception and remote control (command) transmission. A built-in pre-amplifier improves the reception conditions.

##### 4.2.1.2 Telemetry Receivers

Their great sensitivity (4 V or 120 dB) enables them to receive the signal correctly whatever the distance of the balloon provided it is in line of sight. In practice, the limit is 800 km.

#### 4.2.1.3 Magnetic Recorders

Three 7-track tape recorders continuously record the raw signal supplied by the telemetry. Two of them operate continuously so that there is no break. The third is kept on standby, should one of the first two fail.

At the maximum recording speed (60 inches/sec), a 300 KHz signal can be played back.

#### 4.2.1.4 Dating

The information recorded on the tape must be dated, sometimes very precisely.

A rubidium clock, periodically recalibrated by reference to standards (compared to TV signals) shows the universal time at all moments with accuracy better than 20.

In general, the time, coded in advance, is recorded on one of the tape tracks.

Sometimes, for greater accuracy, a given event (transmitted by telemetry) causes the time to be read, coded, and recorded on the same track as the telemetered signal.

#### 4.2.1.5 Scientific Remote Control (command) Transmission

The remote control transmitter (10 commands) operates on 444 MHz in PCM/PSK. Its normal transmitting power is 15W. This can be raised to 150 W if need be (but the normal 15 W power is in fact always adequate).

The remote control console is available to the experimenter, who transmits his commands directly (processing room). Operation may be either on "one-time (mono)" or on "recurrent" (order sent repeatedly). The reliability of this equipment is excellent as demonstrated, for example, by the fact that numerous laboratories are now planning to direct their scientific packages by remote control only.

In parallel, the remote control transmitter is used continuously to transmit the 150 Hz wave for ranging purposes to the balloon.

#### 4.2.1.6 Operational Remote Control Transmission

The remote control transmitter (6 commands) operates on 148 MHz in PCM/PSK. Its normal transmitting power is 15 W and can be raised to 150 W if need be.

The console can be activated only by C.N.E.S. operators (telemetry room).

We remind the reader that operational remote control is used for (1) deballasting and (2) separation.

The corresponding remote control antenna is a simple wideband (8-10 dB) Yagi antenna which delivers fully adequate signal transmission power.

#### 4.2.2 REAL-TIME PROCESSING AND DISPLAY

This function, less critical than that above, enables the experimenter to follow the flight and also supplies operational information (pressure, location, etc.) to C.N.E.S. personnel.

##### 4.2.2.1 Decoding the Telemetry

###### (1) FM/PM Telemetry

The multiplexed data signals go to discriminators corresponding to the IRIG channels used. The analog signals relating to the various measured parameters are extracted. A decommutator is added downstream when a channel has been switched.

###### (2) PCM Telemetry

The raw signal is decommutated via (a) a primary synchronizer, and (b) a secondary synchronizer.

##### 4.2.2.2 Display

###### (1) FM/PM Telemetry

16 analog parameters can be recorded simultaneously on two 8-track graphic recorders. Two wide-track graphic recorders are available when greater precision is necessary. A high speed printer (with analog-digital converter) is used for digital printout of the sampled parameters.

###### (2) PCM Telemetry

Four control and display units enable 16 selectable parameters to be read out digitally at the same time. At the output of these units (which include a digital-analog converter) graphic recorders and printers may be used.

#### 4.2.3 COMPUTER

A computer (type CII, Mitra 15) at present enables all operational data to be processed in real time, particularly ranging and pressure measurement.

All useful parameters are transmitted in hard copy to the control room, which is following the flight.

Use of the computer will be extended in the future to the following fields:

(1) management of real time processing, and (2) management of remote control (command) for various operations (deballasting, tracking, payload packages, etc.)

#### 4.3 Weather Station

The launching center employs a weather engineer full-time to forecast ground weather and the weather into which the balloon will run after launching.



A fairly complete weather station provides all necessary data for these forecasts:

- (1) Two radio receivers with teletypes giving the results of measurements taken throughout Europe by the weather system.
- (2) Two facsimiles (one in the field) to receive the weather Cards published by official bureaus.
- (3) One satellite photo receiver.
- (4) On-site measurement apparatus (anemometers, barometers, thermometers, hydrometers, etc.)

#### 4.4 Control Room

This receives the principal information (range, pressure, etc.) from the telemetry station.

Direct telephone links have been set up with air traffic control centers, both civil and military. Despite all precautions taken to see that the balloon shows up clearly on radar scopes (passive reflectors, responder) it is the C. N. E. S. which, in the last resort, is responsible for tracking. The control room must thus be able to give all necessary information to the air traffic control centers.

At the end of the flight, the control room directs the vehicles sent out for recovery to the probable landing spots by radio link.

#### 4.5 Launching

##### 4.5.1 OPERATIONAL TIME TABLE

Launching of H hour is established according to the parameters of the experiment and those of the operations, and a typical time table has been set up for each type of balloon.

- . H - 1 h 45 m for a 100,000 m<sup>3</sup> balloon
- 2 h 15 m for a 350,000 m<sup>3</sup> balloon

Weather meeting - explanation of general situation on the ground and higher up, and predicted trajectory.

- . H - 1 h 40 m for a 100,000 m<sup>3</sup> balloon
- 2 h 00 m for a 350,000 m<sup>3</sup> balloon

Beginning of operations in launching area (launching crew). Operations on scientific payload if required (experimenter).

- . H - 0 h 40 m for a 100,000 m<sup>3</sup> balloon
- 1 h 00 m for a 350,000 m<sup>3</sup> balloon

Scientific payload arrives at launching area (experimenter).

Scientific payload attached to load line (launching crew).

Telemetry and remote control hooked up.

Functional check out of all equipment (telemetry crew and experimenter).

- . H - 0 h 30 m for a 100,000 m<sup>3</sup> balloon
- 0 h 45 m for a 350,000 m<sup>3</sup> balloon

General agreement on how the experiment will run. Scientific payload taken in charge by launching crew.

Beginning of irreversible operations (balloon unfolded and inflated).

- . H - launching.

#### 4.5.2 LAUNCHING METHOD

The launching method adopted in France has several chief advantages:

- (1) The balloon can be launched with a non-negligible ground wind:

- . 5 m/sec average wind gusting to 8 m/sec for a 100,000 m<sup>3</sup>
- . 3 m/sec average wind gusting to 5 m/sec for a 350,000 m<sup>3</sup>

- (2) It is possible to launch from a small unprepared strip of land with no visibility.

- (3) There is an insensitivity to sudden wind direction changes.

- (4) The payload experiences no take-off shock and can, in no case, drag across the ground.

- (5) The shape and dimensions of the payload and the length of the line connecting it to the balloon are of no importance.

The balloon "bubble" is anchored to the ground by a "releaser" attached to the platform of a balance. The lift force during inflation is measured very accurately. However, the ground wind and special heat conditions limit the quality of measurement and sometimes cause non-negligible errors which lead to variations in the rate of ascent ( $\pm 1$  m/sec around the average value of 5 m/sec). However, experience has shown that this did not affect the success of the flight.

Placement of the balloon and payload on their flight path is facilitated by the second balloon, known as an "auxiliary" which is the principal originality of the French method. Small in volume, the auxiliary balloon is attached directly above the payload and its lifting force is slightly greater than the weight of the payload.

In the case where several packages are to be carried by the same balloon, they are spaced 25 or 50 meters apart and attached to several auxiliary balloons.

There are two take-off stages: main balloon; auxiliary balloons and payload packages. The load line is not tensioned and the take-offs are totally independent. All the balloons drift with the wind but the main balloon, with the weights taken off it by the auxiliary balloons, rises faster and progressively takes up the slack

in the load line. When the whole assembly is vertical, the auxiliary balloons are separated (see para 3.3.3).

#### 4.5.3 LAUNCHING EQUIPMENT

##### 4.5.3.1 Gas

Hydrogen is used for inflating the main balloons. The Launching Center has four trailer tanks each with a capacity of  $3,300 \text{ m}^3$ . The gas is stored in cylinders under a pressure of 250 bars.

Helium is used to inflate the auxiliary balloons, since there is a possibility of friction between these balloons and the tether, with associated hydrogen inflammation risks. The Launching Center has three trailer tanks with a capacity of about  $2,000 \text{ m}^3$  (250 bars).

To inflate the balloons the gas is depressurized directly in a pipe connected to the inflation hose. The flow rate is about  $50 \text{ m}^3/\text{min}$  per pipe.

It will be noted that tests were run recently to investigate the hydrogen hazard at launching operations. A volume of  $500 \text{ m}^3$  was ignited and the heat wave propagating from the blast was shown to be very short. The protective clothing used by the personnel (fire-retardant suit, helmet, face cover, and gauntlets) are adequate to protect against all burns, even in the immediate vicinity of the balloon.

##### 4.5.3.2 Releasing System

The first releasing systems used by the C.N.E.S. locked the balloon in, in a purely mechanical manner, by articulated arms.

Pneumatic locking is used to release large or heavily loaded balloons (2-3 tons gross lift force). The skin is jammed into the releasing system by an inflatable bladder (pressurized at about 1 bar) ejected at take-off.

This system has been operating satisfactorily for three years. Tests have shown that the film never slides in the system so that it never tears.

##### 4.5.3.3 Stranglers

This is a "gadget" but very useful when the bubble is inflated. Four or five stranglers spaced about 2 meters apart compress the balloon (below the inflating hose inlet). Upon inflation, the available volume for the gas is limited so that when the wind is blowing it does not act like a sail, which would be catastrophic. The stranglers are lifted out one by one by means of lines hanging to the ground and connected to "pins" (parachute system).

##### 4.5.3.4 Anchoring Auxiliary Balloons

The auxiliary balloon or balloons are generally inflated at the beginning of operations. The lifting force is measured simply by means of a dynamometer anchored to a fixed point.

The auxiliary is then tethered to a small winch mounted on a vehicle (jeep, for example). An explosive cable-cutter is inserted at the tethering point, and controlled from the ground by a wire.

Before launching, the payload package is hooked to the auxiliary. The winch then unwinds to raise the package a few yards off the ground, the balloon being held directly by its hook. At the moment of launching, the operator causes the vehicle and the auxiliary balloon to separate. The auxiliary then takes off, pulling the payload behind it.

#### 4.6 Recovery Methods

The Launching Center has (1) a Do 28 twin-engined aircraft, (2) two light recovery vehicles with trailers (Land Rovers) and (3) a truck to pick up heavy or cumbersome payload packages.

All these vehicles have their own navigation facilities, and in addition (1) a homing device to track the beacon with which each flight system is equipped and (2) VHF and HF (SSB) telecommunication equipment.

The aircraft takes off before the end of the flight, and arrives at the spot where the parachuted capsule will touch ground. It locates the impact point and transmits very precise coordinates on an ordinance survey map to the ground recovery vehicles. In the case of difficulty, it remains on the spot and guides the vehicles by sight.

For several years this procedure has yielded a 100 percent recovery rate. Applied to the BRAZIL field trip in 1973, it gave the same results.

The only difficult problem is that of recovery in the mountains or at sea, for which the C. N. E. S. is not equipped. Agreements have been drawn up with the army and the police force so that helicopters and patrol craft belonging to these bodies can be used if necessary (2 to 3 times per year).

#### 5. CONCLUSION

After 12 years of existence, the C. N. E. S. Stratospheric Balloon Launching Center may be considered one of the most effective tools in French space research, and also international research. The economical nature of balloon flights makes them escape the budgetary restrictions of other space research. As the number of clients does not seem to be about to decline, it seems that we may be very confident of the future.

## Updating Free Balloon Technology

J. R. Nelson  
Winzen Research Inc.  
South Saint Paul, Minnesota

### Abstract

Balloon sizes continue to increase with fabrication of two balloons in excess of 50 million cubic feet. Dynamic launch of heavier payloads in the range of 5000 to over 6000 pounds has progressed in the operations field. A review of size and performance data since the last AFCRL Symposium is presented. While the size of balloons and payloads have increased, a new method of launching for heavier payloads and larger balloons has proceeded further toward successful development. This reefing sleeve vertical inflation procedure was reported in the earlier phases of development at the Seventh AFCRL Symposium and has now been used at NCAR and AFCRL. Updated results will be reported.

Preceding page blank

When we talk about improving free balloons we are talking about three basic objectives which are to increase altitude, load capacity and flight duration. In achieving these objectives the three areas of design, manufacturing, and field operations must be considered with their interrelationships. Open end objectives may sometimes be nebulous or fuzzy, so it is important to set some goals that are very difficult, but not impossible to achieve. With this in mind this paper will set some goals to achieve the above objectives, update the current technology, and suggest some reasonable approach to achieving or exceeding the goals.

Increasing altitude requires larger balloons \* lighter material. A reasonable goal to set for an objective is considered to be lifting a scientific package of 200 pounds to 180,000 feet. While it looked as if this objective was being approached rapidly with the performance of the 47.8 million cubic foot balloon of 0.35 mil Strat-o-Film® that took 350 pounds to 170,000 feet at AFCL, Chico, in 1972, it has yet to be achieved. Significant advances in the last few years at Winzen Research Inc. in thin film extrusion, in improved sealing machines and in multi-cap sealing techniques and design indicate that this altitude objective can currently be reached. Figure 1 shows altitudes by years. The maximum altitudes attained were progressively higher each year with 146,000 feet in 1967, 158,000 in 1968 and 161,000 in 1969. However, in 1970 no flights exceeded 150,000 feet. Altitudes up to 160,000 in 1971 and 170,000 in 1972 were achieved. Maximum altitudes in 1973 and 1974 were under 160,000 feet, but more balloons with significantly larger payloads were flown. In the category of thin film balloons of 0.6 mil down to 0.35 mil, the average payload has increased from 400 pounds in 1965 to 1900 pounds in 1974 while the average altitude has decreased 4000 feet. The average balloon volume has doubled since 1965. From these aver-

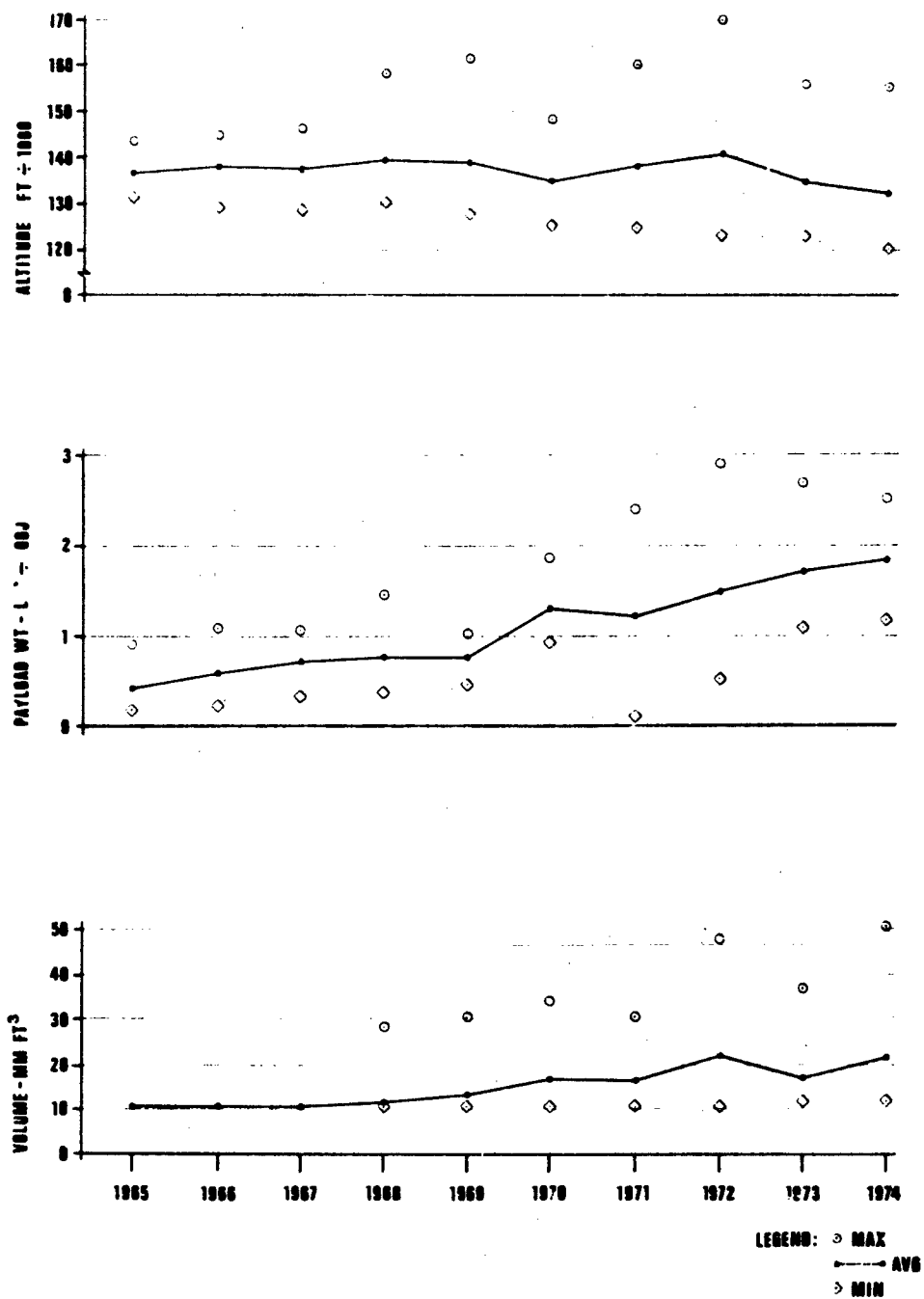


Figure 1. Summary of Balloon Flights With Volume Greater Than 10 mm ft<sup>3</sup> and Film Gauge of 0.6 Mils or less.

age values it would seem that heavier payloads to an altitude around 130,000 is the main objective. This, however, requires basically the same development thrust as does extreme altitude performance. Both require larger balloons with higher strength to weight ratio materials.

Heavy Load: A reasonable goal for heavy payload is considered to be lifting 20,000 pounds to 100,000 feet. There have been at least 35 payloads in excess of 4000 pounds successfully flown in the last five years on StratoFilm® balloons. The heaviest loads of 8,379 and 9,040 pounds were flown on 6.87 million cubic foot tandem balloons of 1.8 mil StratoFilm® with two 1.8 mil StratoFilm® caps to 84,000 feet. The launch balloons were of mylar scrim material. A third balloon of this size tandem model, but with a StratoFilm® launch balloon has not yet been flown. The third largest payload of 7,424 pounds flown on StratoFilm® had a main balloon volume of 18.9 million cubic feet and flew to 106,000 feet. It was constructed of 1.5 mil StratoFilm® with a 2 mil cap and used a launch balloon of 323,000 cubic feet made from 2 mil double-wall StratoFilm®. Other smaller loads of 3500 and 3800 pounds were flown on 27.5 million cubic feet StratoFilm® balloons in a tandem configuration with mylar scrim launch balloons to 125,000 feet.

Most significant advances in operations techniques have resulted in seven or eight flights with loads in the 5000 and 6000 lb. range using a dynamic launch. The heaviest payloads ever launched with a dynamic type launch were 6321 and 6300 pounds by NCAR and AFCRL. These 6.68 million cubic foot balloons of 1 mil StratoFilm® and 1 mil plus 1.5 mil caps flew to 92,000 feet. Close behind these heavy load dynamic launches was 6155 pounds flown on a 19.76 million cubic foot balloon of 1.0 mil StratoFilm® with two 1.5 mil caps. The balloon was flown by NCAR to an altitude of 112,000 feet for 14 hours.



Figure 2 shows performance data for heavy loads flown in the last 10 years. Despite these impressive performances by operations crews, it is felt that this is close to the maximum stresses that a plastic balloon can withstand in the indeterminate conditions sustained in a dynamic launch. As reported in the Seventh AFCRL Scientific Balloon Symposium, September 1972, a development program, sponsored by the Office of Naval Research, was in progress to achieve a launch system for vertical inflation of giant balloons. We have every confidence that this system when fully developed will enable achievement of the goal to take 20,000 pounds to 100,000 feet. Since last reported a successful flight was conducted with an 0.5 mil StratoFilm®, 0.25 million cubic foot balloon using the reefing sleeve design to protect against the ground winds of 5 - 8 knots. Three ground inflations of 2 million cubic foot balloons were made by NCAR and AFCRL for training and continuing development purposes. Several required modifications were evident after these development test operations. The reefing sleeve closure, required to protect the balloon during excursions or sweep across the ground during erection of the inflating bubble, was accomplished by reefing lines restrained by lanyard-released pin fittings. These pins were pulled as the reefed balloon left the ground. It was decided that this procedure was too complicated and could be performed adequately by using a plastic tear panel such as has been successfully used on hundreds of large balloons with current design reefing sleeves. It was also decided that the cables required to operate the restraint line cutters and the cutters themselves could be contained within the reefing sleeve. There would thus be no external lines, wires or hardware to snag on ground objects, or be abraded due to sliding.

Currently there are three balloons equipped with a fabric reefing sleeve for the vertical inflation launch that are awaiting flight

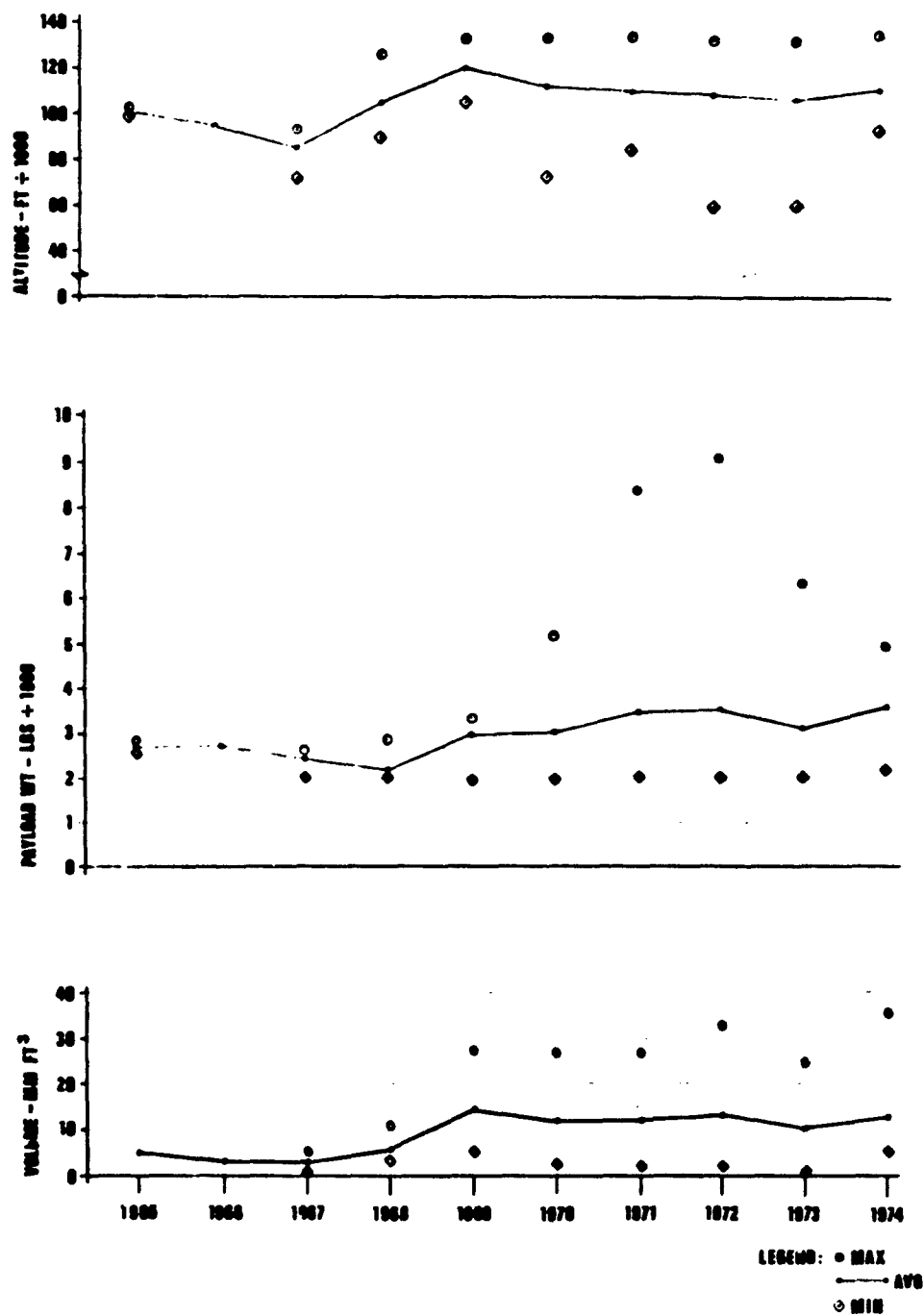


Figure 2. Summary of Balloon Flights With Payloads Greater Than 2,000 lbs.

test. The design payloads are 5000, 7500 and 10,000 pounds. The intermediate load balloon of 6.45 million cubic feet is an ONR balloon at NCAR for test flight, and the 4.38 and 32.1 million cubic feet balloons are at AFCL.

A program to achieve the stated objective for heavy load flight might be first to fly at least two more two-million cubic foot balloons at each operation facility to evaluate the mentioned modifications and to familiarize flight crews more thoroughly with the launch operations technique. Then the larger balloons should be flown--or modified if necessary, and flown. With a successful 10,000 pound flight completed, additional balloons designed for payloads increasing in 2000 pound increments to meet the objective should be fabricated and flown. If the balloon can be inflated and started on its flight in the ascent attitude without the trauma of rapidly shifting stresses and snapping of plastic, the assurance of a successful flight is tremendously improved.

Long Duration: The optimum balloon for long duration flight is a superpressure balloon, which permits the pressure instead of volume to change because of temperature variation caused by sunset and sunrise, cloud cover or other factors. With the improved geopolitical situation and the improved technology of world-wide data retrieval, development of a large circumnavigating balloon is a high priority scientific requirement. A reasonable goal at this time is to develop a superpressure plastic balloon that will float 700 pounds at an altitude of 140,000 feet for a period of two months or to circumnavigate the earth.

Some progress has been made toward this goal using primarily small mylar laminate balloons. The GHOST program by NCAR has been circumnavigating the earth many times for several years with small balloons. In 1968 a 66 foot diameter StratoFilm® balloon with no

supporting tapes flew from England to Canada with 5 kilograms at 10 mb. In March 1973 a mylar balloon of 137,000 cubic feet flew around the earth twice with a payload of 50 kilograms at 30 mb and was recovered within 15 kilometers of the launch site.

The limiting factor on an unsupported film such as polyethylene or polyester is the material strength below the elastic limit required for supporting the payload plus the superpressure stresses. This stress for a given payload, balloon weight and altitude is directly proportional to the balloon diameter or radius of curvature of the shell. If, however, a network of strong tapes or lines are used to support the gas barrier, the stress in the film will be proportional to the local radius of curvature of the film in each panel rather than to the total spheroid radius. This concept, dating back to the very beginning of ballooning, was presented to NASA, Manned Spacecraft Center in 1969 as a means to use an economical material such as StratoFilm® in superpressure balloon construction. StratoFilm® is many times more economical as a material for manufacturing large balloons due not only to lower material costs but to faster manufacturing processes that can be used. It further has the ability in large structures to equalize high stress irregularities without ultimate failure.

After a number of ground inflation tests and two flight tests with rectangular panels formed by load tapes, the program was redirected toward the old fashioned diamond or triangular shaped panels. Two ground test balloons of this configuration with panel areas comparable to a full size superpressure balloon were tested to 2.4 inches of water pressure. At 140,000 feet the pressure differential across these 15 square foot panels would be approximately 0.0056 inches of water, so the test was far in excess of flight requirements. The structural meridional and circumferential tapes and lines would

provide strength to take the payload and superpressure stresses at this altitude which are generated as a function of the superpressure and balloon radius plus payload.

A viable program for achieving the long duration objective with StratoFilm® balloons would be to resume the program started under NASA MSC sponsorship by optimizing structure of the lines, tapes and panel shapes using larger ground inflation balloons of about 60 feet in diameter. It is recognized that an improved StratoFilm® with better abrasion resistance may be necessary and work toward this end has been initiated by Winzen Research. Progression to flight operations with this size balloon and then implementing flights with increasingly larger balloons to meet the final objective should be programmed.

## **Session 4 Balloon-Borne Experiments**

**NOTE:** All papers from Session 4 are contained in the  
Main Volume, AFRL-TR-74-0393, dated 21 August 74.

**Alvin H. Howell, Chairman  
Tufts University**

**Session 5**  
**Special Applications**

**James A. Winkler, Chairman**  
**Raven Industries**

**Preceding page blank**

**- 271 -**

#### Contents

1. Introduction	273
2. Thermal Efficiency and Hot Airship Usefulness	274
3. The Hydrodynamic Approach to Airship Shape	278
4. Boundary Layer Calculations	282
5. Heat Transfer Calculations	285
6. The Influence of Fineness Ratio	287
7. Computer Program Overview	292
8. Closure	292
References	295
Appendix A	297
Appendix B	299
Appendix C	301
Appendix D	303

## Pressure Hot Airship Design and Performance

James B. Hebel  
650 Robbins Ave., Apt. 30  
Dorset, Mass. 01826, and  
John F. Hebel  
P.O. Box 246  
Barnesville, New York 13304  
(Buoyant Flight Systems)

### Abstract

Some unique design problems and characteristics of pressure hot airships are identified and discussed. Computation study results are provided. The conclusion is drawn that hot airships are useful in performing certain missions. An appendix of significant equations is also provided.

### 1. INTRODUCTION

The information provided in this paper is the result of about three years of private study by the authors. The result, beyond this paper, is the ongoing development of a hot airship and an IBM 370/155 FORTRAN program for pressure hot airship design. The purposes of this hot airship are twofold; collection and



verification of research and development data; exhibition and advertising flights to promote more interest and activity with the hot airship vehicle itself. The work is being funded by private sponsors.

## 2. THERMAL EFFICIENCY AND HOT AIRSHIP USEFULNESS

Thermal efficiency, as defined as  $\frac{\text{work out}}{\text{heat added}}$ , is a common and useful index of the merit of a work producing system. It is useful to divide the hot airship problem into two parts: air expansion and hot gas preservation. Theoretical or ideal thermal efficiencies can often be calculated. The efficiency of inflation will be addressed first.

### 2.1 Thermal Efficiency

The ideal work done in expanding the gas which inflates the lighter-than-air vehicle envelope is  $\Delta W = mR(T_{\text{hot}} - T_{\text{cold}})$  since it is an isobaric process. The ideal heat added to  $m$  is  $\Delta Q = mC_p(T_{\text{hot}} - T_{\text{cold}})$ , hence  $\eta$ , the efficiency =  $\Delta W / \Delta Q = R / C_p$ . For air this becomes  $C_p - C_v / C_p = .286$ . This efficiency is not closely approached by currently used heating systems (burners) which have either large flue losses (red flame) or large radiation losses (blue flame). Things can be done to improve the situation. Specifically, a much larger percent of excess air should be supplied, thereby cooling the blue flame. Further, radiant heat photons not impinging in the envelope should be redirected into the envelope with reflectors. There is also the exciting possibility of using this hot air expansion cycle as an extension of an Otto or perhaps Brayton cycle to further improve overall efficiency.

### 2.2 Heat Loss

The examination of this last aspect of improving thermal efficiency leads to the clear cut desirability of an insulated envelope. The average hot air sport balloon of about 1700 cubic meters volume has an energy loss on the order of .4 KW/M<sup>2</sup> due to natural thermal convection and air leakage due to fabric porosity and needle holes. The convective heat transfer coefficient, for forced convection can rise an order in magnitude above this. Because of this, the cost and weight of insulation in the envelope is not the question. The use of insulation determines whether or not a hot airship is feasible. The use of dead air space is an attractive way to insulate a hot airship because of its low weight. Envelope fabric weights can be altered by sharing the stress between layers of fabric so that the overall envelope weight increase is held below two by the use of dead air space. A theoretical investigation has been completed. Further details of the mathematical

models used and details of results are provided in Sections 4 and 5 below and in the appendices.

### 2.3 Hot Airship Characteristics

The characteristics of airships that use gas for buoyancy<sup>1</sup> have been cussed and discussed many times in many places by airship aficionados. The characteristics of the newly developing airships that use hot air for buoyancy have not been so widely discussed so an initial estimation of these characteristics is of interest.

(1) The cost of inflation of similar volume airship envelopes with helium as compared with hot air is larger for helium by a factor of 4000 to 5000;

(2) The specific lift of helium is about 3 times higher than hot air (for standard atmospheric conditions with the hot air at 250°F as is typically possible with a NYLON\* envelope);

(3) The cost of construction of pressure envelopes (and ballonets) to contain helium compared with hot air is approximately 5 to 15 times more expensive for helium;

(4) The cost of maintaining inflation is quite different between the two types of airships. Pressure hot airships consume fuel to maintain buoyancy at a rate determined by the effectiveness of their insulation, burner ventilation losses and envelope leakage. Gas airships consume helium at a rate determined by the leakage, diffusion, trim adjustment losses, gross buoyancy adjustment losses and occasionally by exceeding pressure altitude. However, carefully designed hot airships can utilize propulsion engine exhaust heat solely for maintaining buoyancy in a cruise condition;

(5) The detrimental effects to flight caused by reduction of atmospheric density in conditions above standard day temperatures and/or altitudes affect gas airships, airplanes, helicopters, ornithopters and hot airships equally;

(6) Pressure hot airships, unlike gas airships, can be economically and quickly deflated for storage and, if necessary, for surface transportation;

(7) Pressure hot airships are lighter, for a given volume, than gas airships thus facilitating their handling for storage and surface transportation;

(8) A pressure hot airship of up to about 4000 cubic meters of volume can be immediately stored in an automobile garage-sized building worth about \$5000 while an equal volume gas airship\*\* requires a full-sized hanger that is hundreds of times more expensive;

---

\*DuPont Tradename

\*\*The author's reference is to a fully-inflated gas airship. Temporary storage on an inexpensive mooring mast is also possible. (Ed. Note)

(9) The hot airship can hover and/or loiter in the presence of atmospheric temperature<sup>2</sup> change without valving gas or dropping ballast as necessary in a gas airship;

(10) The hot airship can hover to discharge or pick-up loads without the noisy downwash from rotors/propellers (downwash produces dust and flying debris) as found on advanced gas airships (or helicopters);

(11) The hot airship's lift is very significantly improved when it is operated in cold environments (arctic regions). For example, under standard day conditions (50°F outside) a NYLON envelope hot airship at 250°F inside has a lift of about 20 lbs/1000 cubic feet. A NYLON envelope operating at 250°F inside and at -20°F outside has a lift of about 38.5 lbs/1000 cubic feet. Use of a material in the envelope with higher operating temperature limits further improves performance. A hot airship with a KEVLAR\* envelope operating at 391°F inside on a standard day at sea level has a lift of about 30 lbs/1000 cubic feet, while at -20°F outside it has a lift of 43 lbs/1000 cubic feet. (Typically, helium lifts 62 lbs/1000 cubic feet.);

(12) The increase in lift of a hot airship in cold climates is not accompanied by a proportional increase in drag, i. e., its lift over drag ratio improves. This may be seen from the following:

$$\frac{L}{D} = \frac{\rho \Psi \left(1 - \frac{T_{\text{outside}}}{T_{\text{inside}}}\right)}{(1/2) \rho v^2 A C_d} \text{ where}$$

L = lift

D = Drag

$\rho$  = Density of atmosphere

$\Psi$  = Volume of envelope

T = Temperature (absolute)

A = Characteristic area

$C_d$  = Coefficient of drag

v = Velocity

Notice that the density divides out. As  $T_{\text{outside}}$  becomes smaller, the numerator becomes larger, the L/D ratio improves. Consequently, the L/D ratio of a NYLON hot airship is improved by 90 percent when it is operated with the outside air at -20°F compared to standard day conditions. Changing to KEVLAR will improve the L/D ratio by 115 percent at -20°F. Finally, as a corollary,

flight in cold climates will use less fuel to heat the envelope if the gross weight of standard conditions is retained.

(13) A low-heat-loss hot airship can utilize propulsion engine exhaust heat solely for maintaining buoyancy in cruise condition. However, for a given airspeed and gross weight, the hot airship's propulsion engines are larger than on a gas airship due to the higher drag of the larger envelope;

(14) If a hot airship is designed to fly at the same speed as an equal volume gas airship it will be identical in mass, and approximately equal in horsepower. The equal volume and same airspeed conditions basically provide for equal dynamic lifts from their envelopes. The equality of mass of the two airships indicates that they will have:

- (a) An equal radius of turn,
- (b) equal acceleration in straight flight, and
- (c) equal capability for termination of a climb or descent.

(15) A hot airship may be driven up or down by stormy air currents without the irretrievable loss of lifting gas and ballast that a gas airship experiences. Thus, the gas airship's problem of crashing out of control in a storm due to unwillingly exceeding pressure altitude a few times and associated exhaustion is not at all present in a hot airship.

Other significant points will undoubtedly be added to the above list as hot airships become operational.

#### **2.4 Missions for Hot Airships**

A first listing of missions especially suited to accomplishment with hot airships is provided below:

- Aerial Exhibitions for Advertising**
- Aerial Photography**
- Air Quality Sampling**
- Antenna Pattern Measurements**
- Arctic Operations**
- Border Patrol**
- Communications Relay Platform**
- Construction Site Surveys**
- Disaster Relief**
- Fish Surveillance**
- Flight Training**
- Fog Dispersal Study/Operations**
- Forestry Management**
- Geological Surveys**

- Harbor Surveillance
- Hunting Party Support
- Large Airship In-Flight Simulation for Pilot and Crew Training
- Leaflet Distribution
- News Collection
- Ocean Surveillance
- Pipeline/Power Line Surveillance
- Police Surveillance
- Public Address
- Sport Flying
- Traffic Surveillance
- VIP Short Haul Transportation
- Wildlife Management

### 3. THE HYDRODYNAMIC APPROACH TO AIRSHIP SHAPE

The advantage of using the mathematical apparatus of hydrodynamics in establishing airship envelope shape is that the coordinates of the profile and its velocity distribution are given in an analytic form. Further, it is an easy step to find the pressure distribution and one important envelope stress parameter, the longitudinal radius of curvature.

The disadvantage of this description of the flow is that it is an ideal one (inviscid) not accounting for the boundary layer. However, if additional calculations are made to approximate boundary layer effects, then an essentially complete solution of the envelope shape and pressure problem has been found. One previous disadvantage of this hydrodynamic approach was the formidable amount of arithmetic. The advent of electronic computation removed this difficulty.

#### 3.1 The Stream Function

The notion of the hydrodynamic stream function, its definition, properties and the conditions of its existence are given in the common works on this topic, Lamb<sup>3</sup> etc. For this investigation a stream function  $\Psi$  defined for axisymmetric, three-dimensional flow was made up by the superposition of flows from a linearly varying line source, a linearly varying sink and a uniform flow. The cylindrical coordinate system is shown in Figure 1. The coordinates are  $X$ ,  $R$ . (The function is degenerate in  $\Phi$ .) The source/sink configuration adapted was chosen from among those suggested in Burgess.<sup>4</sup> Derivation of the stream function integral for a constant line source or sink may be found in Valentine.<sup>5</sup> Appended to this paper

is a brief derivation of the general expression for a linearly varying source. Any of the Burgess configurations may be obtained by superposition of this function. For mathematic simplicity the configuration illustrated in Figure 2 was chosen.

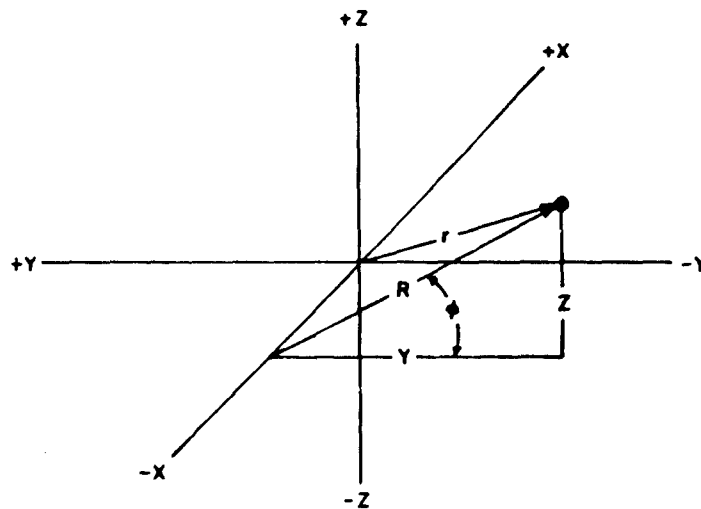


Figure 1. The Envelope Coordinate System. Cartesian  $X, Y, Z$ , Cylindrical,  $r, R, \phi$

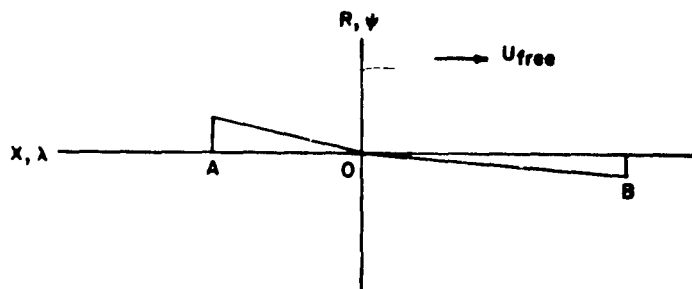


Figure 2. The Source-Sink Configuration

The airship stream function for this configuration is:

$$\begin{aligned} \psi(X, R) = & \frac{-2Q}{A^2} \left\{ \frac{R^2}{2} \ln \left[ \frac{\sqrt{(X-A)^2 + R^2} - (X-A)}{\sqrt{X^2 + R^2} - X} \right] - \left[ \sqrt{(X-A)^2 + R^2} \left( \frac{X+A}{2} \right) - \sqrt{X^2 + R^2} \left( \frac{X}{2} \right) \right] \right\} \\ & + \frac{2Q}{B^2} \left\{ \frac{R^2}{2} \ln \left[ \frac{\sqrt{(X-B)^2 + R^2} - (X-B)}{\sqrt{X^2 + R^2} - X} \right] - \left[ \sqrt{(X-B)^2 + R^2} \left( \frac{X+B}{2} \right) - \sqrt{X^2 + R^2} \left( \frac{X}{2} \right) \right] \right\} \\ & + \frac{1}{2} U_{\text{free}} R^2 \end{aligned}$$

### 3.2 Velocity

Since the velocity components for axisymmetric flow are

$$V_X = \frac{1}{R} \frac{\partial \psi}{\partial R}, \quad V_R = -\frac{1}{R} \frac{\partial \psi}{\partial X}.$$

The velocity profile is given by

$$\begin{aligned} V_X = & + \frac{1}{R} \frac{\partial \psi}{\partial R} = \frac{-Q}{A^2} \left\{ R \left( \frac{\sin \theta_A}{(r_A - X + A)} - \frac{\sin \theta}{(r - X)} \right) + 2 \ln \left( \frac{r_A - X + A}{(r - X)} \right) \right. \\ & \left. - \left( \frac{X + A}{R} \right) \sin \theta_A + \frac{X}{R} \sin \theta \right\} \\ & + \frac{Q}{B^2} \left\{ R \left( \frac{\sin \theta_B}{(r_B - X + B)} - \frac{\sin \theta}{(r - X)} \right) + 2 \ln \left( \frac{r_B - X + B}{(r - X)} \right) \right. \\ & \left. - \left( \frac{X + B}{R} \right) \sin \theta_B + \frac{X}{R} \sin \theta \right\} \\ & + U_{\text{free}}, \text{ and} \end{aligned}$$

$$\begin{aligned}
v_R = -\frac{1}{R} \frac{\partial \psi}{\partial X} = \frac{-Q}{B^2} & \left\{ R \left( \frac{(\cos \theta_B)^{-1}}{(r_B - X + B)} - \frac{\cos \theta - 1}{(r - X)} \right) - \frac{r_B}{R} - \frac{(X+B)}{R} \cos \theta_B \right. \\
& + \frac{r}{R} + \frac{X}{R} \cos \theta \left. \right\} \\
& + \frac{Q}{A^2} \left\{ R \left( \frac{(\cos \theta_A)^{-1}}{(r_A - X + A)} - \frac{\cos \theta - 1}{(r - X)} \right) - \frac{r_A}{R} - \frac{(X+A)}{R} \cos \theta_A \right. \\
& + \frac{r}{R} - \frac{X}{R} \cos \theta \left. \right\}
\end{aligned}$$

where

$$r = \sqrt{R^2 + X^2}; \quad r_A = \sqrt{(X-A)^2 + R^2}; \quad r_B = \sqrt{(X+B)^2 + R^2}$$

and

$$\frac{X}{r} = \cos \theta; \quad \frac{R}{r} = \sin \theta$$

$$\frac{X-A}{r_A} = \cos \theta_A; \quad \frac{R}{r_A} = \sin \theta_A$$

$$\frac{X-B}{r_B} = \cos \theta_B; \quad \frac{R}{r_B} = \sin \theta_B$$

### 3.3 Longitudinal Radius of Curvature

The longitudinal radius of curvature for purpose of finding stresses can be derived for a hydrodynamic shape. The correct<sup>6</sup> expression for the total second derivative of R with respect to X when they are related by a function  $\psi(X, R) = 0$  is:

$$\frac{d^2 R}{dX^2} = - \frac{\frac{\partial^2 \psi}{\partial X^2} \left( \frac{\partial \psi}{\partial R} \right)^2 - 2 \frac{\partial^2 \psi}{\partial X \partial R} \cdot \frac{\partial \psi}{\partial X} \cdot \frac{\partial \psi}{\partial R} + \frac{\partial^2 \psi}{\partial R^2} \left( \frac{\partial \psi}{\partial X} \right)^2}{\left( \frac{\partial \psi}{\partial R} \right)^3}$$



Remembering the hydrodynamic relations:

$$V_x = \frac{1}{R} \frac{\partial \psi}{\partial R} \text{ and } V_R = -\frac{1}{R} \frac{\partial \psi}{\partial X}$$

and substituting them into the above\*,

$$\frac{d^2 R}{dX^2} = \frac{\psi_{XX} V_x^2 - 2\psi_{XR} V_x V_R + \psi_{RR} V_R^2}{R V_x^3}$$

The curvature is given by

$$K = \frac{\left| \frac{d^2 R}{dX^2} \right|}{\left[ 1 + \left( \frac{dR}{dX} \right)^2 \right]^{3/2}} = \frac{d\alpha}{dS}$$

Of course  $d\alpha/dS$  is radians of direction change per unit of path length. The radius of curvature is  $R_c = 1/K$ . The analytic expressions in addition to  $V_R$  and  $V_X$  that are needed are  $\psi_{XX}$ ,  $\psi_{RR}$  and  $\psi_{XR}$ . These second partial derivatives must be found for the specific stream function being used.

The usefulness of hydrodynamics is brought to an end with the above information. Now it is necessary to look at the effects of viscosity.

#### 4. BOUNDARY LAYER CALCULATIONS

Elegant empirical solutions and excellent numerical techniques have been developed to deal with boundary layer effects.<sup>7</sup> However, since that inquiry is not the main focus of this study, rather liberal approximations were made. The mathematical model employed utilizes a one-dimensional, energy oriented technique.

The primary assumption of this model is that since the longitudinal radius of curvature of the vehicle is large compared with the boundary layer thickness, the layer may be handled as a piece-wise smooth flat plate. It is further assumed that the energy profile for the flow is one degraded by the energy dissipated by the skin friction determined by the hydrodynamic velocity distribution. Hence the expected pressure recovery of the hydrodynamic case is not realized.

\*This may be done just in case it can be shown that  $\psi_{X,R} = \psi_{R,X}$

When the dissipation integral rises to the value of the local dynamic pressure, it is assumed that the boundary layer has separated and the local pressure has returned to the atmospheric pressure.

The skin temperature used is provided by the solution of the thermal circuit of the vehicle wall.

Admittedly, this model is an optimistic, isentropic one; consequently the pressure drag found is somewhat low. This slightly low value of pressure drag is compensated for by a slightly high skin friction. Disturbances<sup>8</sup> caused by the empennage are lumped into the overall drag.

#### 4.1 Skin Friction

The local Reynolds Number was calculated at each integration step of air stream path along the ship from nose to tail. The number was found using the hydrodynamic velocity distribution. Since this distribution provides higher velocities than found in a real gas, skin friction predicted using it will be pessimistic, i.e., larger than actually encountered. Since there are always fittings, seams and other protrusions which increase the drag, and since the above model has mathematical simplicity, it was used. The local skin friction coefficient was obtained using the Prandtl-Schlichting skin friction formula for a smooth flat plate at zero incidence.<sup>9</sup>

#### 4.2 Pressure Drag

An integration of the force against the vehicle due to the revised pressure distribution leads to a pressure drag. Since the vehicle entrains a wake of air moving with it which has a momentum change equivalent to the drag force, it is possible to find a new non-closing hydrodynamic shape which possesses the non-recovering pressure distribution\*. Ordinarily the total source flow is equal to the total sink flow in the hydrodynamic equations. The non-closing shape has a total source flow greater than the total sink flow. The uniform flow velocity and the airspeed used for drag calculations should be the same. The source flow is made equal to the sink flow plus the flow entrained by drag. See Figure 3.

---

\*This could be done after the pattern coordinate is found from the closing source/sink configuration.

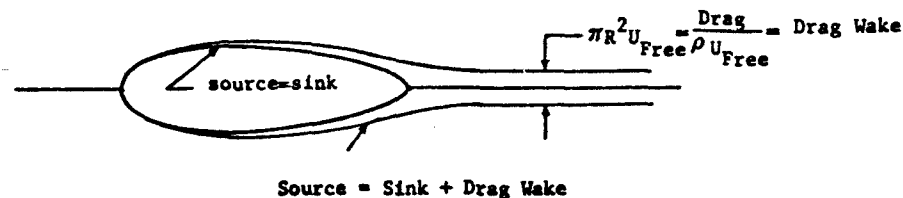


Figure 3. The Non-Recovering Pressure Distribution

#### 4.3 Convective Heat Transfer Coefficients

The physics of the convective heat transfer coefficients are discussed below. Means for calculating their values are referenced as well.

##### 4.3.1 FREE OR THERMAL CONVECTION ON THE INTERIOR ENVELOPE SURFACE

There are two distinct modes of circulation inside a hot air lifting compartment characterized by whether or not the burner is being operated. The air currents caused during the burn drive a form of quasi-forced convection. See Figure 4. In the relaxation time between burns, the flow path is similar but much milder. If the wall is insulated, then, because the inner wall is almost as warm as the enveloped air, the internal thermal boundary becomes quite thick and laminar enhancing the already good thermal resistance of the wall. Thus, violent air currents during the addition of heat must be "designed out".

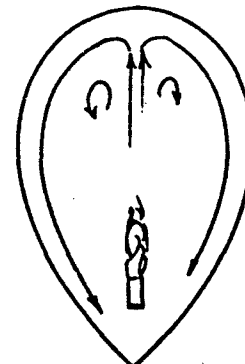


Figure 4. Air Current Paths

The theoretical value for the internal convective coefficient may be calculated from equations offered in Appendix C. If those expressions are used to find the heat loss by a typical sport balloon, they may appear low. Actually, more than half of the fuel's energy for that class of vehicle is lost via leakage (porosity and needle holes), radiation and in many cases due to excessive flue losses (poor combustion).

##### 4.3.2 FORCED CONVECTION ON THE EXTERIOR ENVELOPE SURFACE

The equations used in the computer program study are given in Appendix D.

Both the skin friction coefficient and the convective heat transfer coefficient are functions of the Reynolds number. The influence of a heated skin upon air drag and heat loss can be determined by a brief examination of the functions used. The kinematic viscosity is a rapidly increasing function of temperature for air.

The Reynolds number  $Re_X = \frac{VX}{\nu}$ , therefore, is depressed by an increase in skin temperature. This, in turn, causes the local friction to increase.

## 5. HEAT TRANSFER CALCULATIONS

The subject of the convective heat transfer coefficients is dealt with above in the discussion of the boundary layer effects. The effects of the envelope side wall are addressed below.

### 5.1 Thermal Circuit of the Envelope Wall

Actually, using the concept of a thermal circuit, the boundary layer for the exterior is but one of several components in a series of heat transferring media. The premise on which this argument is founded is summarized here. The envelope wall is assumed to be a surface sufficiently flat and subject to sufficiently mild temperature gradients as to allow the local element of the wall to be analysed one-dimensionally. For the envelope, the surface integral may be performed so as to find an overall surface resistance. In analogy with Ohms law, the heat flow is to a current as the temperature difference is to the electrical voltage, hence if  $\dot{Q}_{TX} = U \cdot A \cdot \Delta T$  then  $1/UA = \mathcal{R}$ , the "thermal resistance".

#### 5.1.1 POSSIBLE CIRCUIT COMPONENTS

The minimum circuit components would be those of a single layer vehicle namely,

- (a) The inner thermally convective boundary layer.

$$\bar{h}_c = \text{approximately } \frac{4 \text{ Watts}}{\text{Meter}^2 \text{ } ^\circ\text{K}}$$

- (b) The fabric material forming the surface.

$$k/t = \text{approximately } \frac{500 \text{ Watts}}{\text{Meter}^2 \text{ } ^\circ\text{K}}$$

- (c) The outer forced convective boundary layer

$$\bar{h}_c = \frac{3-3/4 \text{ Watts}}{\text{Meter}^2 \text{ } ^\circ\text{K}} \text{ to } \frac{50 \text{ Watts}}{\text{Meter}^2 \text{ } ^\circ\text{K}}$$

(The value 3-3/4 is for free ballooning, i.e., no air speed.)

When dead air spaces are incorporated within the envelope walls their conductivity is about 2.84 Watt Centimeters/ Meter<sup>2</sup> °K for each centimeter of space thickness.

### 5.1.2 TYPICALLY EXPECTED THERMAL RESISTANCE

Obtaining an overall heat transfer coefficient in the vicinity of .2 Watts/ Meter<sup>2</sup> °K for a pressure hot airship does not present a large technical problem. Such a vehicle having a surface of 2000 Meters<sup>2</sup> would present a thermal resistance of 2.5°K/KW power.

### 5.2 Wall Temperature Profile

The temperature distribution through the wall can be found from the simultaneous solution of the heat transfer equations for the circuit components. Proceeding from the inner boundary layer to the outer one they are:

$$\frac{\dot{Q}}{A} = (\bar{h}_c)_{\substack{\text{inner} \\ \text{skin}}} (T_{\text{inner}} - T_1)$$

$$\frac{\dot{Q}}{A} = \left(\frac{k}{t}\right)_1 \cdot (T_1 - T_{i+1}) \dots \dots$$

$$\frac{\dot{Q}}{A} = \left(\frac{k}{t}\right)_n \cdot (T_n - T_{\text{skin}})$$

$$\frac{\dot{Q}}{A} = (\bar{h}_c)_{\substack{\text{outer} \\ \text{skin}}} (T_{\text{skin}} - T_{\text{outer}})$$

for  $i = 1, 2 \dots$  for  $n$  wall components, where:

$\bar{h}_c$  = Average convective heat transfer coefficient in  $\frac{\text{Watts}}{\text{Meter}^2 \text{ } ^\circ\text{K}}$  ;

$(T_k$  = Temperature in degrees Kelvin);

$k_i$  = Conductivity for the  $i$ -th component in  $\frac{\text{Watt Centimeters}}{\text{Meter}^2 \text{ } ^\circ\text{K}}$

$t_i$  = Wall thickness for the  $i$ -th component in centimeters;

$T_i$  = Kelvin temperature of the inside wall of  $i$ -th component;

$A$  = Surface of wall normal to the heat path in Meters<sup>2</sup>; and,

$\dot{Q}$  = Heating power in Watts and finally,

$$1 \text{ BTU/Hour} = .2928757 \text{ Watts}$$

or

$$1 \text{ Megawatt} = 3.414418 \text{ million BTU/Hour.}$$

## 6. THE INFLUENCE OF FINENESS RATIO

The subject of fineness ratio (Fr) in airship design has been quite controversial. The approach taken to selection of Fr for hot airships in this study was to run the design program (See Section 7) at a number of values of Fr, keeping volume constant. Drag and mass were affected. The results are graphically presented. They indicate that an optimum value of Fr is possible and, for the particular design, its value.

As discussed in Section 4, the drag is composed of skin friction and pressure induced components. These components are described below for a specific hot airship of a volume of 4000 cubic meters, operating at an altitude of 1000 meters at 20 meters/second, resulting in a dynamic pressure of 2.102 millibars.

### 6.1 Drag as a Function of Fineness Ratio

Figure 5 provides the drag components and their total for a specific hot airship under the stated conditions. The skin drag increases as Fr increases due to the added surface area of the envelope. The pressure drag decreases as Fr increases due to a larger percentage of pressure recovery. The total drag of the bare envelope is the summation of the components. Notice the sharp change of slope in the total drag force in kilograms near FR = 3.5. This fact along suggests Fr of 3.5 be considered a minimum acceptable value since the drag at Fr = 3.5 is about 56 percent less than the drag at Fr = 2.5. However, the effect of increasing Fr on drag is offset by the increase in airship weight as described next.

### 6.2 Mass as a Function of Fineness Ratio

Figure 6 provides the significant mass components and their total affecting hot airship mass for the same conditions described above regarding drag. These components are envelope mass and engine mass. The envelope mass increases as Fr increases principally because more fabric is needed to enclose the constant, specified volume. The engine mass, assuming a fixed horsepower to weight ratio and fixed propulsion efficiencies, decreases as Fr increases because the total drag behaves as shown previously in Figure 5.

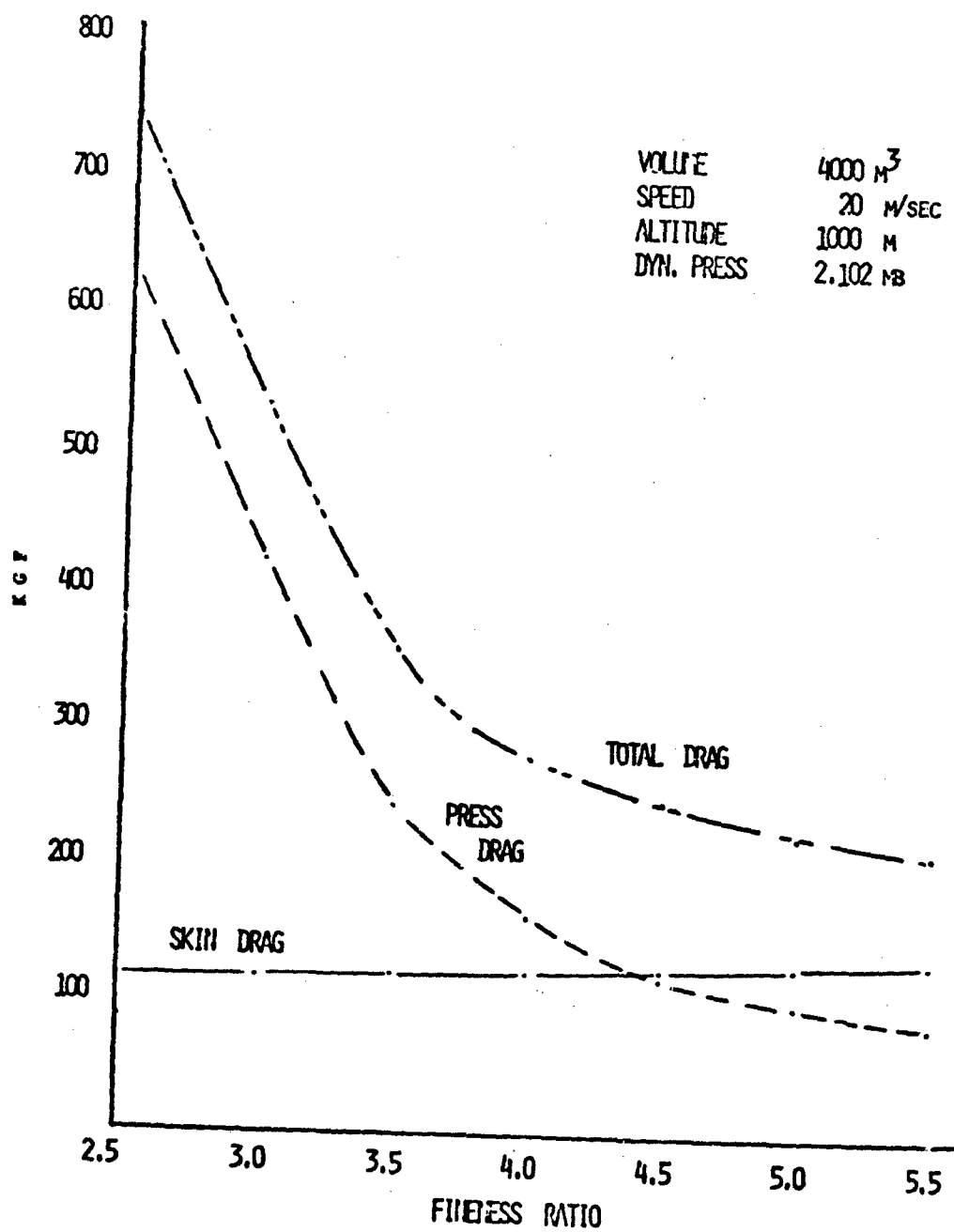


Figure 5. Drag Versus Fineness Ratio

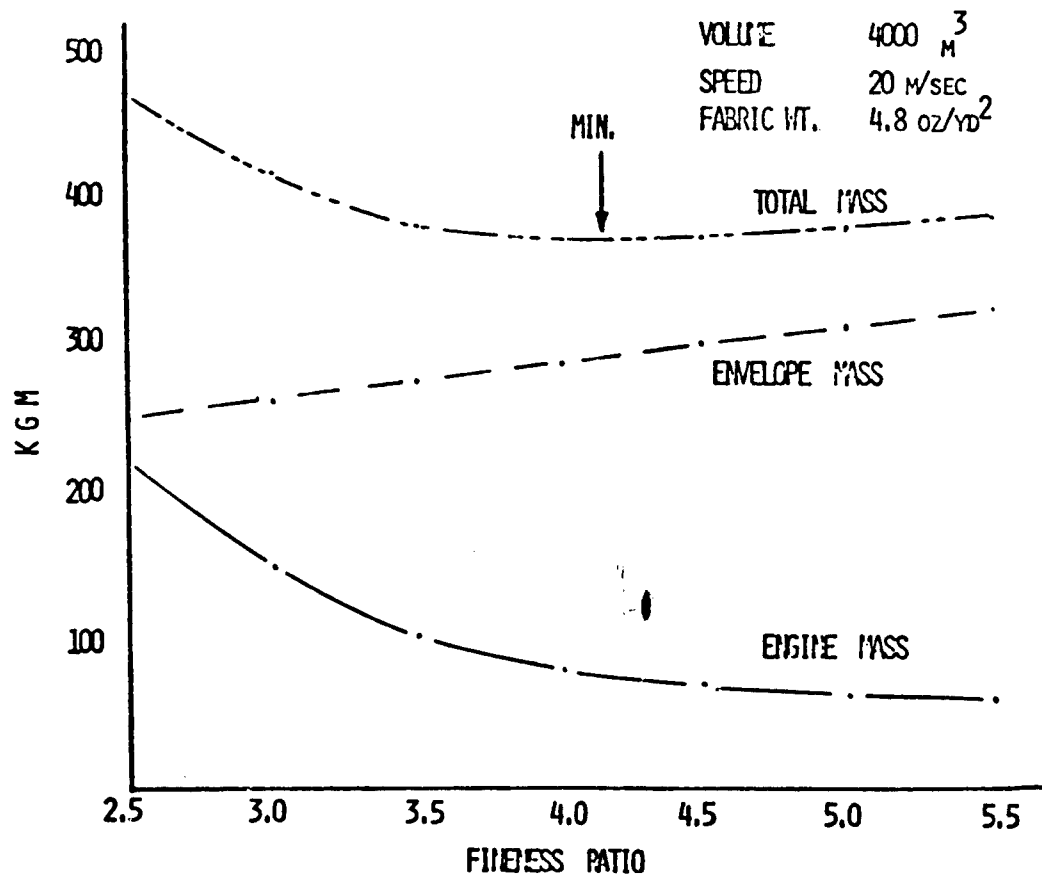


Figure 6. Mass Versus Fineness Ratio

### 6.3 Optimum Fineness Ratio

The significant point is that in respect to the total mass that there exists a minimum at an Fr of approximately 4.1. This minimum in total mass is, of course, desired because it means a better overall performance and for a given performance, a lower cost to operate. Moreover, since the specific lift of hot air is about 1/3 of that of helium, attention to Fr effects in hot airships is well worthwhile.

### 6.4 Envelope Shape Coefficients

A table of shape coefficients of the hot airship envelopes used in the Fr study described above is provided. (See table 1.) The hydrodynamic parameters A, B and Q that were used with  $U_{free}$  to produce these coefficients are included.



Table 1. Envelope Shape Coefficients

Fineness Ratio	Max. Diam.	Length	Cyl. Coef.	A	B	Q
2.5	14.691	36.890	.63979018	-13.002	19.239	1728.7
3.0	13.723	41.329	.65447557	-16.598	24.730	1408.4
3.5	13.005	45.702	.65904427	-18.541	27.161	1215.1
4.0	12.424	49.880	.66121596	-19.622	28.438	1079.5
4.5	11.940	53.922	.66257012	-21.704	30.710	978.1
5.0	11.524	57.810	.66348195	-23.615	32.911	898.1

Vol = 4000 m<sup>3</sup>      Speed = 20 m/sec  
 q<sub>∞</sub> = 2.101 mb      Alt = 1000 m  
 U<sub>free</sub> = 100 m/sec

The units associated with the source end A and the sink end B are meters from a point which for convenience is the origin. The strength of the source (and sink) is Q in meters<sup>3</sup>/second. The length and maximum diameter are in meters. The cylindrical coefficient is without dimension. It represents the airship's fraction of the volume of a cylinder that just encloses the envelope. This coefficient is useful for estimating volume, length, maximum diameter relationships when other sizes of envelopes are being considered.

#### 6.5 Envelope Coordinates

A table of envelope coordinates (table 2) is presented. At the level of detail presented "artists conception" type of information on the shape may be obtained. Actual design and pattern information is much more detailed in the program in use.

The values of X are in meters representing stations along the length of the envelope. The corresponding values of R, radii, are in meters. The program as designed did not produce stations on round number locations. The addition of a constant,  $\delta$ , completes the station location information. Notice that the closure of the nose and tail is not indicated. These locations may be obtained for graphical use by drawing fair lines.

Table 2. Envelope Coordinates

Fr = 2.5 X+δ	3.0 R	3.5 R	4.0 R	4.5 R	5.0 R
0	1.74	.97	1.23	1.26	1.71
2	3.93	3.31	3.11	2.89	2.93
4	5.11	4.44	4.11	3.80	3.70
6	5.91	5.22	4.81	4.45	4.27
8	6.49	5.79	5.34	4.95	4.72
10	6.89	6.20	5.74	5.34	5.07
12	7.15	6.50	6.04	5.64	5.35
14	7.30	6.71	6.26	5.86	5.57
16	7.35	6.82	6.40	6.03	5.74
18	7.30	6.86	6.48	6.14	5.86
20	7.16	6.84	6.50	6.20	5.93
22	6.94	6.75	6.48	6.21	5.97
24	6.62	6.60	6.40	6.19	5.97
26	6.19	6.39	6.29	6.13	5.94
28	5.64	6.12	6.12	6.03	5.88
30	4.91	5.77	5.91	5.90	5.79
32	3.92	5.34	5.65	5.73	5.67
34	2.35	4.79	5.33	5.52	5.52
36	0.08	4.09	4.93	5.26	5.34
38		3.14	4.45	4.96	5.12
40		1.52	3.85	4.59	4.96
42			3.05	4.14	4.56
44			1.81	3.60	4.19
46				2.88	3.76
48				1.81	3.21
50					2.50
52					1.37
54					2.33
56					1.27

2.5		.44		.56
3.0		.16		.84
For Fr = 3.5	add following δ to X,	.35	add following δ to X	.65
4.0	[ for X before and in-	.44	[ for X after maxi-	.56
4.5	cluding maximum R	.96	imum R ] .	.04
5.0	(radius)].	.91		.09

**EXAMPLE**

22 → 22.65  
For Fr = 3.5

## 7. COMPUTER PROGRAM OVERVIEW

A block diagram of the computer program under development is provided. (See Figure 7.) This program has reached the stage in development that enables it to generate the load, shear, moment and stress table for axisymmetric flight as shown in the block in the center of sheet 2 of Figure 7.

### 7.1 Objectives

An objective of writing this IBM 370/155 FORTRAN H Program has been the development of an understanding of the characteristics of pressure hot airships. An additional objective is to provide an easy base for custom-tailored pressure hot airship designs.

### 7.2 Program Flow

The input design information includes such requirements as envelope volume, elongation, position of maximum diameter, range, speed, payload, altitude, material properties, etc. On the basis of these inputs, the size of the vehicle is found. A pass along the ship, using the air stream path (gore position) as step points, is made. Computation of pattern strike up marks, and heat transfer information is made. After the hydrodynamic and geometric profile of the shape has been calculated and stored, the boundary layer calculations are made. Some of the activity is redundant however, the step points are now longitudinal abscissae rather than gore positions. Finally, weight, balance and stability are determined.

## 8. CLOSURE

The work which enabled preparation of this paper is yet to be completed. However, at this point, conclusions may be drawn as follows:

- (1) A well designed pressure hot airship may be expected to perform useful missions in "standard" atmospheric conditions.
- (2) The gross lift and dynamic lift of a hot airship in arctic regions is greatly improved over standard conditions.
- (3) A pressure hot airship is more airworthy in storm conditions than a gas airship due to absence of the pressure altitude limitation of a gas airship.
- (4) A pressure hot airship is much less expensive to build, inflate and store than a similar volume gas airship.
- (5) A pressure hot airship has less lift but more maneuverability for a given envelope volume and airspeed than a gas airship.

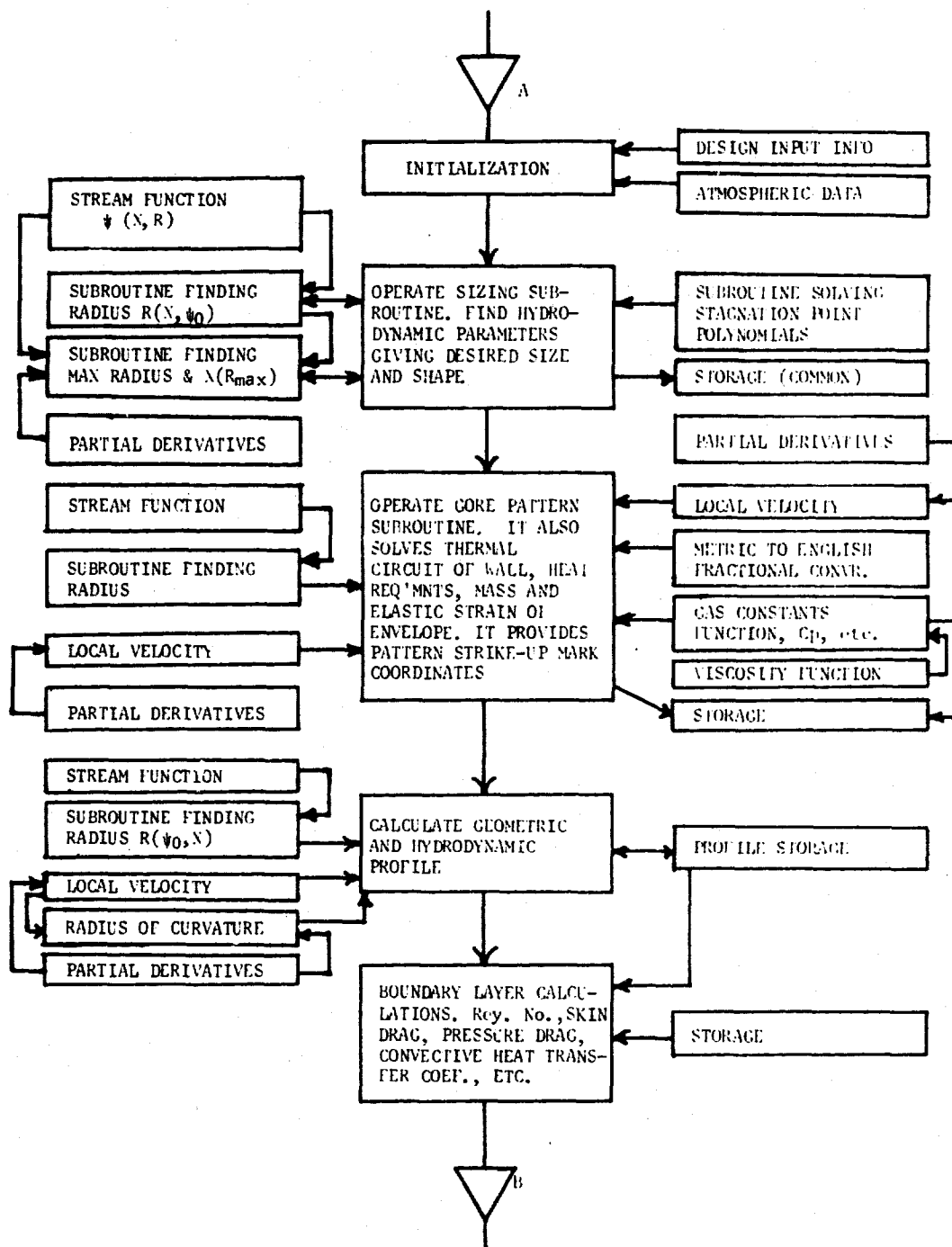


Figure 7. Computer Program Block Diagram (Sheet 1 of 2)

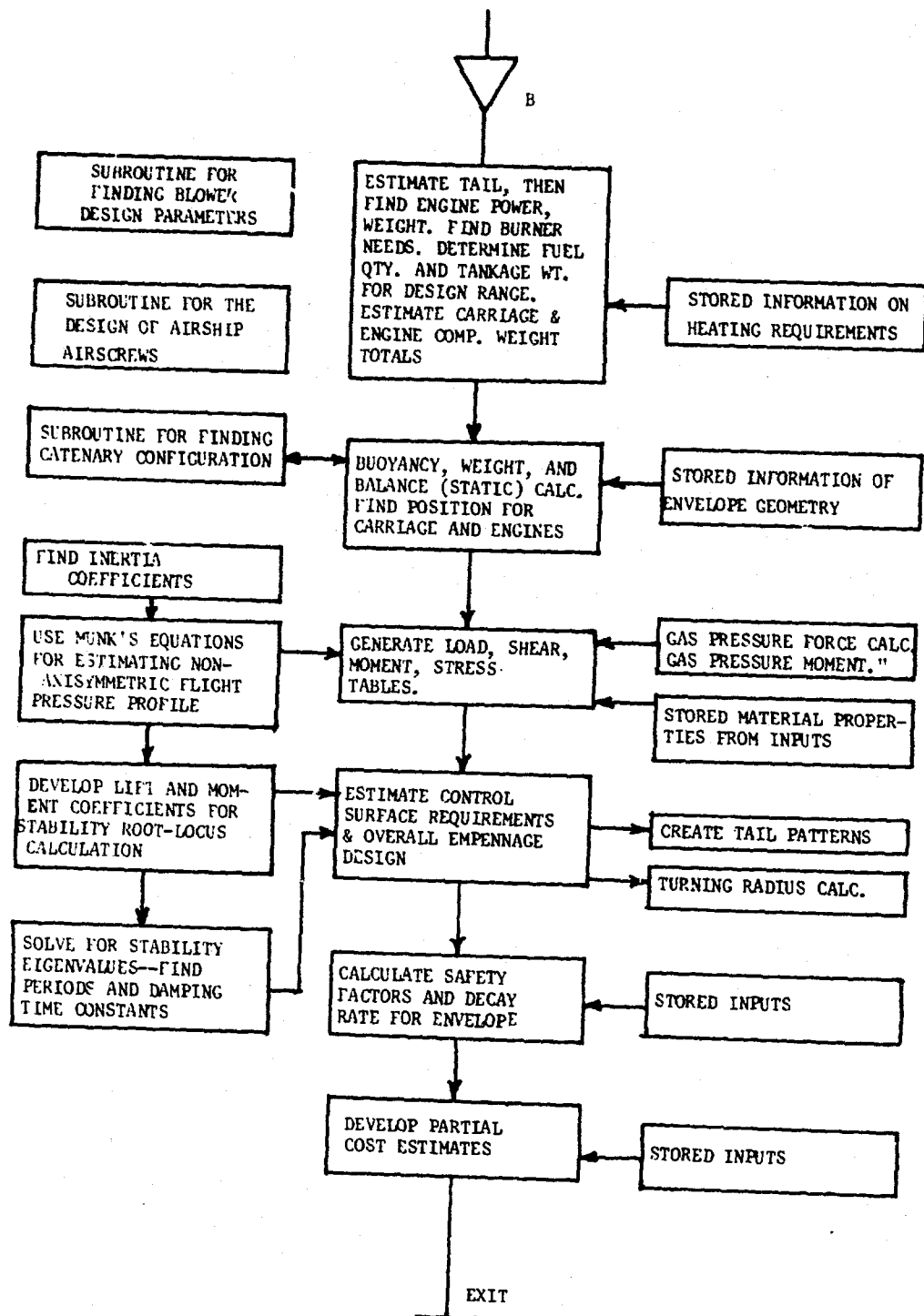


Figure 7. Computer Program Block Diagram (Sheet 2 of 2)

- (6) The hot airship can pick-up or unload weight while hovering without the ballast changes necessary in a gas airship.
- (7) The hot airship can pick-up or unload weight while hovering without the undesirable side effects associated with rotor downwash of a helicopter.
- (8) The need to burn fuel to maintain buoyancy in a hot airship causes storage of the ship during idle periods to be attractive rather than mooring or hanging. Storage is practical because reinflation is cheap and the storage space required is small.
- (9) A hot airship cruising entirely on propulsion engine thrust and exhaust heat is an efficient machine deserving further study in our present energy oriented environment.
- (10) The maximum range and duration of a current design gas airship exceed those of a current design hot airship of equal volume.
- (11) When the envelope weight of a hot airship becomes too great for a ground crew of three or four men to deploy or store a useful upper limit in pressure hot airship size has probably been attained. This limit may be 4000 to 5000 cubic meters of volume.
- (12) There is no good reason to construct a rigid airship utilizing hot air alone for buoyancy. The virtue of rapid and easy, low cost storage found in a pressure hot airship clearly influences selection of this basic design over that of a rigid structure.

#### 8.1 Future Tasks

The technical development of practical hot airships will be speeded as certain subjects receive more attention. At present, these subjects appear to be:

- (1) Burner development (lower weight and noise and higher combustion and mixing efficiencies are needed);
- (2) Lower heat loss envelope designs;
- (3) Less expensive joining methods for fabric structures; and,
- (4) Further improvements in fabric characteristics, specifically better resistance to high temperatures and to ultraviolet radiation degradation.

## References

- 1. Blakemore, T. L., and Pagon, W.W.P. (1927), Pressure Airships, Part I and II, Ronald Press Co., N.Y.
- 2. Prandtl, L. and Tietjens, O.G. (1934) Fundamentals of Hydro and Aero-mechanics, Dover Publications, Inc., N.Y.

3. Lamb, H. (1932) Hydrodynamics, Cambridge.
4. Burgess (1927) Airship Design, Ronald Press, Page 75.
5. Valentine, H.R. (1967) Applied Hydrodynamics, 2nd ed., Plenum Press, N.Y. p. 243.
6. Soklinkov and Redheffer (1958) Mathematics of Physics and Modern Engineering, McGraw Hill, N.Y. p. 236.
7. Keller, H.B., and Cebeci, T. (1972) Accurate Numerical Methods for Boundary-Layer Flow. II: Two-Dimensional Turbulent Flows, AIAA Journal, Vol. 10, No. 9, Page 193.
8. Hoerner, S.F. (1965) Fluid-Dynamic Drag, Page 14-1.
9. Schlichting, P. (1968) Boundary Layer Theory, 6th ed., McGraw-Hill, N.Y. Page 602, footnote.

## Appendix A

### The Stream Function

The stream function of a point source located at  $\lambda$  on the  $X, \lambda$  axis has the form

$$\psi = \frac{-Q}{4\pi} \frac{X - \lambda}{\sqrt{R^2 + (X - \lambda)^2}} .$$

When this point source becomes an infinitesimal segment  $d\lambda$  along a line source, then the expression for its contribution to the flow at the space point  $X, R$  is  $d\psi = Q'd \cos \theta$ . See Figure A1.

More generally,  $Q'$  is a function of  $\lambda$ , and, in fact, the source strength is modulated by  $Q'(\lambda)$ .

$$\frac{dQ}{d\lambda} = Q'(\lambda)$$

This amplitude function has the property that

$$\int_E^F Q'_1(\lambda) d\lambda = Q_1^* \quad \text{hence} \quad Q'_1(\lambda) = \frac{2Q}{(F-E)} \cdot \frac{(\lambda-E)}{(F-E)}$$

---


$$* \sum_i Q_i = 0$$



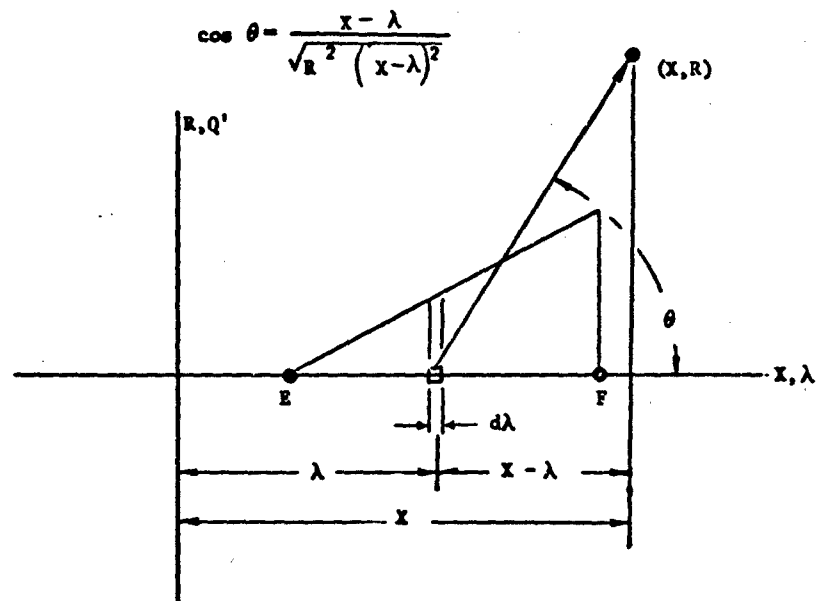


Figure A1. Geometry of Stream Function

and therefore

$$d\psi_i = \frac{-2Q_i}{(F-E)^2} \cdot \frac{(\lambda-E) \cdot (X-\lambda)}{\sqrt{R^2 + (X-\lambda)^2}} d\lambda$$

Integration of this yields

$$\psi = \frac{2Q_i}{(F-E)^2} \left\{ \sqrt{(X-\lambda)^2 + R^2} \left( \frac{X+\lambda}{2} + E \right) - \frac{R^2}{2} \ln \left[ \frac{R_\lambda}{R_\lambda - X - \lambda} \right] \right\} \bigg|_{\lambda=E}^{\lambda=F}$$

## Appendix B

### The Coefficient of Local Skin Friction

Following H. Schlichting<sup>1</sup>, this coefficient is

$$c'_{fs} = \left[ 2 \log Re_s - .65 \right]^{-2.3}$$

for turbulent flow. (See the footnote on p. 602 of his book, Boundary Layer Theory.)  
For laminar flow ( $Re > 50,000$ ),

$$c'_{fs} = .664 / \sqrt{Re} \text{ was used.}$$

The Friction Drag Integrand

$$\Delta D_i = c'_{fs} \left( \frac{1}{2} \rho V_{\text{mean}_i}^2 \right) \left( 2 \pi R_{\text{mean}_i} \right) \Delta S$$

$$V_{\text{mean}} \text{ and } R_{\text{mean}} \text{ are } R_i \frac{(X_i + X_{i+1})}{2}, \psi_o$$

$$V_i \frac{(X_i + X_{i+1})}{2}, \psi_o$$

### The Pressure Drag Integrand

$$\Delta D_i = \pi(R_{i+1}^2 - R_i^2) P_{\text{local}};$$

$$P_{\text{local}} = P_{\text{atm}} + \left[ \frac{1}{2} \rho V_{\infty}^2 - \int_0^{S_i} C_f \frac{1}{2} \rho V_i^2 ds \right] \left[ 1 - \frac{V_i}{V_{\infty}} \right]^2$$

See Figure B1.

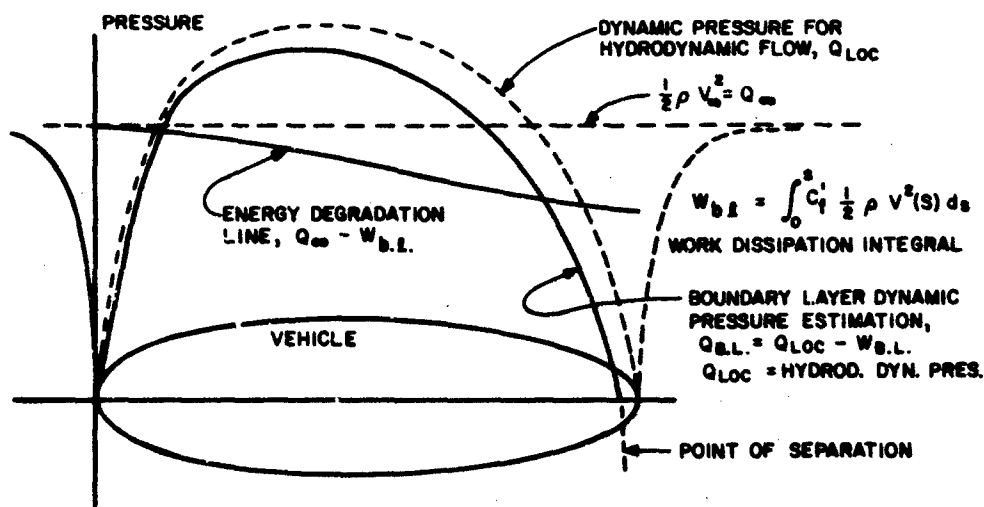


Figure B1

### Reference

1. Schlichting (1968) Boundary Layer Theory, 6th ed., McGraw-Hill, N.Y. Page 602, footnote.

## Appendix C

### The Convective Heat Transfer Coefficient for Free or Thermal Convection on the Interior

The Grashof<sup>1</sup> modulus for the vehicle should be found using the local envelope height for the characteristic length,  $L$

$$Gr = \frac{gL^3}{\nu^2} \left| \frac{T_{skin}}{T_{\infty}} - 1 \right|$$

$T_{\infty}$  = Kelvin temperature well away from the wall.

$\nu$  = kinematic viscosity.

$g$  = acceleration of gravity.

The Prandtl number for air used for current thermally buoyant vehicles is .72.

The Nusselt modulus is found for turbulent flow from the equation<sup>1</sup>

$$\overline{Nu} = .0210 (Gr Pr)^{.4}$$

and from the equation

$$\overline{Nu} = .555 (Gr Pr)^{.25}$$

for laminar flow ( $Gr Pr < 10^9$ )

The convective heat transfer coefficient is a factor in the Nusselt modulus,

$$\overline{Nu} = \frac{h_c L}{k}$$

$k$  = conductivity of boundary layer air.

If  $Gr Pr$  is well above  $10^{10}$ , the McAdam's relation

$$h_c = .13 k \left[ \frac{.72g}{\nu^2} \left| \frac{T_{skin}}{T_\infty} - 1 \right| \right]^{1/3} \quad \text{may prove a simplification.}$$

### Reference

1. Kreith, F. (1965) Principles of Heat Transfer, International Textbook Co., Scranton, Pa. Page 313, 333 and Figure 7-4, page 335.

## Appendix D

### The Convective Heat Transfer Coefficient for Forced Convection on the Exterior of the Airship

The local Reynolds number,  $\frac{VS}{\nu} = Re_s$  may be used to find the local Nusselt modulus along the flow path.

$$Nu_s = .332 \sqrt{Re_s} Pr^{1/3} \text{ for laminar flow}^1 \text{ and}$$

$$Nu_s = .0288 Pr^{1/3} (Re_s)^{.8} \text{ for turbulent flow}^2$$

The critical  $Re_s = 5 \times 10^5$  in this case.

$V$  = local hydrodynamic velocity

$S$  = path length from nose to local point

$\nu$  = kinematic viscosity

## References

1. Gledt, W.H. (1957) Principles of Engineering Heat Transfer, D. Van Nostrand Co., Inc., Princeton, N.J. page 149.
2. Kreith, F. (1965) Principles of Heat Transfer, International Textbook Co., Scranton, Pa. Page 313, 333 and Figure 7-4, Page 335.